NEXT GENERATION ELECTRIC VEHICLE ENERGY MODELING IN TRANSPORTATION NETWORKS

A Dissertation
Presented to
The Academic Faculty

by

Xiaodan Xu

In Partial Fulfillment
of the Requirements for the Degree
Doctor of Philosophy in the
School of Civil and Environmental Engineering

Georgia Institute of Technology
December 2019

NEXT GENERATION ELECTRIC VEHICLE ENERGY MODELING IN TRANSPORTATION NETWORKS

Approved by:

Dr. Randall Guensler, Advisor
School of Civil and Environmental Engineering
Georgia Institute of Technology

Dr. Patricia Mokhtarian
School of Civil and Environmental Engineering
Georgia Institute of Technology

Dr. Michael Rodgers
School of Civil and Environmental Engineering
Georgia Institute of Technology

Dr. Yajun Mei
School of Industrial and Systems Engineering
Georgia Institute of Technology

Dr. Husain Aziz
School of Civil Engineering
Kansas State University

Date Approved: Sep 15, 2019

ACKNOWLEDGEMENTS

First of all, I would like to express my deepest appreciation to my advisor, Dr. Randall Guensler for his supervision, encouragement, and patience over the past five years. Without his support, I wouldn't have been able to finish this long journey and accomplish this dissertation. I would also like to extend my deepest gratitude to my mentor Dr. Husain Aziz, for inviting me to Oak Ridge National Laboratory and initiating this dissertation research. I have also learned a great deal from him on how to plan research work and collaborate with others during my two internships.

I am deeply grateful to my committee members, Dr. Michael Rodgers, Dr. Patricia Mokhtarian, and Dr. Yajun Mei, for their valuable feedbacks on this dissertation, as well as teaching me the basic research skills through their excellent classes. I have learned plenty of energy/emissions modeling from Dr. Rodgers, travel behavior analysis from Dr. Mokhtarian, and statistics from Dr. Mei, which makes me well prepared for this dissertation work. In addition, I would like to appreciate Dr. Guensler and Dr. Mokhtarian for being volunteers and contributing their vehicle operation data to this dissertation. I am also thankful for other faculty members for helping me in the past five years, including Dr. Laval, Dr. Hunter, Dr. Watkins, Dr. Amekudzi-Kennedy, and Dr. Pendyala. Thank you all for bringing me to this department; I feel so lucky to have had this wonderful experience in my lifetime.

I am also grateful to many friends that works or worked with me at Georgia Tech, including Haobing, Ann & Cody, Daejin, Hongyu, Zixiu, Alper, Alice, etc. It has been my great pleasure to work with you, learn from you, and share moments of happiness and sorrow. I am also thankful to Dr. Ann Xu, for guiding me on the Fuel and Emissions Calculator and supporting me all the time. I would also like to express my gratitude to our awesome administrator, Marjorie, for

providing endless support whenever needed and sharing hilarious Corgi memes. I very much appreciate other friends I met at Georgia Tech, including Fangru, Shuqi, Xinyi, Tu, Abhilasha, Atiyya, Ali, Sunghoo, April, etc. Thank you all for being part of this enjoyable experience.

Many thanks to those friends I get to know at ORNL, including Lin, Lingcheng, Zhonghua, Manqing, Kevin, Prof. Sun, Yiling, Yaoping, etc. It was a great experience to study with you and hang out with you during the nice summers in Oak Ridge, and learn about the environment energy, science, and computing. Thank you for sharing tons of memes as well! Special thanks also to some inspiring artists that bright my life every sleepless (working) night, including Aimer, Hiroyuki Sawano, Arashi, and Owl City. Thank you for keeping me energized and motivated.

Finally, I would like to thank my parents, who gave me greatest support in my life and the freedom to pursue the graduate study abroad. I feel so proud to be your daughter. Last but not the least, I am extremely grateful to my husband Dr. Muyuan Chen for being the most supportive person in this world. Without him, I wouldn't enter the acedemic field and know how big the world is. I am also thankful to our lovely fluffy girl, Kasia, for always being a sweet friend.

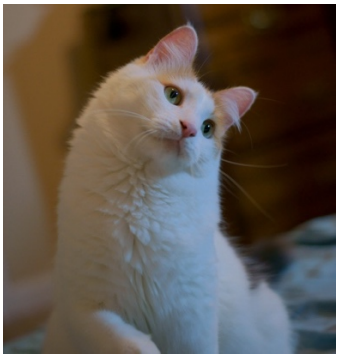

Figure 0. Appreciation to my cat

TABLE OF CONTENTS

LIST OF TABLES

LIST OF FIGURES

LIST OF SYMBOLS AND ABBREVIATIONS

ABM	Activity-based (travel demand) model
ADVISOR	Advanced Vehicle Simulator
AER	All-electric range
ANL	Argonne National Laboratory
API	Application Programming Interface
ARC	Atlanta Regional Commission
BEV	Battery electric vehicle
Btu	British thermal unit
CART	The classification and regression tree
CH_4	Methane
CD	Charging depleting
CO	Carbon monoxide
CI	Compression ignition
CS	Charging sustaining
CO_2	Carbon dioxide
CO_2e	CO_2 equivalent
DEM	Digital Elevation Model
eGRID	Emissions and Generation Resource Integrated Database
EV	Electric vehicle
FASTSim	Future automotive systems technology simulator
FCEV	Fuel cell electric vehicle
FHWA	Federal Highway Administration, USDOT
GDOT	Georgia Department of Transportation
Georgia Tech	Georgia Institute of Technology
GIS	Geographic information system
GPS	Global positioning system
GREET®	Greenhouse Gases, Regulated Emissions, and Energy Use in Transportation
GHG	Greenhouse gas
HD-UDDS	Heavy-Duty Urban Dynamometer Driving Schedule
HDV	Heavy-duty vehicle
HEV	Hybrid electric vehicle
hp	Horsepower
Hz	Hertz (frequency, cycles per second)
HPMS	Highway Performance Monitoring System
HSD	Hybrid Synergy Drive
HTBR	Hierarchical tree-based regression
HVAC	Heating, ventilation, and air conditioning
ICE	Internal combustion engine
ICEV	Internal combustion engine vehicle
IEEE	Institute of Electrical and Electronics Engineers
IM	Inspection and maintenance
IPCC	The Intergovernmental Panel on Climate Change

KDE	Kernel density estimation
kg	Kilogram
kJ	Kilojoules
kW	Kilowatt
kWh	Kilowatt-hour
LCA	Life-cycle assessment
LDV	Light-duty vehicle
LOESS	Locally estimated scatterplot smoothing
LOWESS	Locally weighted scatterplot smoothing
MARTA	Metropolitan Atlanta Rapid Transit Authority
MAF	Mass air flow
MOVES	MOtor Vehicle Emissions Simulator
MLE	Maximum likelihood estimation
MSE	Mean-square error
mmBtu	Million Btu
mph	Miles per hour
MPGe	Miles per gallon of gasoline equivalent
MPO	Metropolitan Planning Organization
MWh	Megawatt-hour
NA	Not applicable
N_2O	Nitrous oxide
NO_x	Oxides of nitrogen
NPMRDS	National Performance Management Research Data Set
NREL	National Renewable Energy Laboratory
OBD	On-board diagnostic
O-D	Origin to destination
O&M	Operation and maintenance
opMode	Operating mode
ORNL	Oak Ridge National Laboratory
PFCEV	Plug-in fuel cell electric vehicle
PHEV	Plug-in hybrid electric vehicle
PM_{10}	Particulate matter with a mean aerodynamic diameter of 10 μm
$PM_{2.5}$	Particulate matter with a mean aerodynamic diameter of 2.5 μm
PPS	Peak power source
PSAT	Powertrain System Analysis Toolkit (precursor to Autonomie)
PTW	Pump-to-wheel
RMSE	Root-mean-square error
R&D	Research and development
SA	Sensitivity analysis
SI	Spark ignition
SIP	State implementation plan
SRTA	Georgia State Road and Tollway Authority
STP	Scaled tractive power
SOC	State of charge (battery)
SO_2	Sulfur dioxide
SO_x	Oxides of sulfur

FEC	Fuel and Emissions Calculator
TDM	Travel demand model
TRB	Transportation Research Board
USDOT	United States Department of Transportation
USEIA	United States Energy Information Administration
USEPA	United States Environmental Protection Agency
VOCs	Volatile organic compounds
VPC	Vehicle propulsion controller
VMT	Vehicle mile travelled
VSP	Vehicle-specific power
Wh	Watt-hour
WTP	Well-to-pump
WTW	Well-to-wheel (includes WTP and PTW)

SUMMARY

Electric vehicles (EVs) will play a central role in future energy-efficient and sustainable transportation systems. Estimating energy consumption of EVs is essential to assessing changes in fuel use and overall cost savings associated with EV use. Traditional modeling methodologies for estimating real-world EV energy consumption depend either on numerical analysis of laboratory or on-road vehicle test data, or on the use of full-system vehicle simulation tools. Unfortunately, available real-world data may not be comprehensive enough to include all relevant driving and state of charge conditions, and full-system simulation tools suffer from scaling problems in the context of large transportation networks. Hence, new approaches that support large transportation network projections of modal EV operations and applicable modal energy use rates (energy use for various on-road modes of operation) are needed to predict EV energy consumption.

The major objective of this dissertation is to propose an analytical framework for estimating energy use from electric vehicles that operates within large-scale transportation networks. With this framework, the operation, energy, and cost impacts of adopting EV can be assessed at the aggregate-level for dynamic transportation networks and at the individual-level for households, persons, or businesses that use the transportation network for their daily travel routines. In this research, a modal-based modeling approach previously applied to conventional internal combustion engine vehicles (ICEVs) was employed to estimate EV energy use as a function of on-road driving conditions. The modal-based approach considers the variance of vehicle operating conditions and supports energy estimation for large-scale transportation networks.

The Department of Energy's (DOE's) full-system vehicle simulation tool, known as Autonomie, was used to generate energy consumption rates for specific on-road simulations. Autonomie was used to simulate a wide range of operating conditions and generate energy use rates for selected EV types. Classification and regression tree (CART) analysis was applied to the simulation output data to generate energy consumption rates under distinct on-road modal operating conditions, as represented by combinations of vehicle speed, acceleration rate, and battery state of charge (SOC). Outputs from the regional travel demand model for the Atlanta, GA metropolitan area, were coupled with a variety of EV market penetration scenarios to generate vehicle activity by electric and conventional vehicles. The CART energy consumption rates were then applied to the model-predicted link-by-link on-road conditions to estimate fleet energy consumption. The modeling framework employed MOVES-embedded driving cycles to represent on-road operations for average speed operating conditions and random initial SOC levels as model inputs. The results of the initial model suggest that if a 50% Plug-in Hybrid Electric Vehicle (PHEV) market share can be achieved, more than 30% energy saving can be achieved compared to no PHEV scenario, without significantly adding to regional electricity load.

Network-level energy use predictions derived from this first modeling approach can be used for a variety of transportation studies, such as evaluating transportation improvement plans, assessing the net impact on the electric grid, and forecasting the potential benefits of electrifying shared-autonomous vehicles under future scenarios. However, the diversity of EV models (and their individual EV control strategies) expected to enter the fleet over time may not be well-represented by the current tree branches generated by CART methods employed in these analyses. These CART analyses need to be continuously updated as new technologies enter the fleet (i.e., tree branches may become too thin). Hence, in a mixed EV fleet future, sufficient on-road

performance data will need to be collected and analyzed as these new vehicle technologies (and embedded powertrain control strategies) enter the fleet.

Using the same general modeling framework but replacing the CART method with an advanced activity-based modal modeling approach, the second model predicts EV energy consumption as a function of different modal operating conditions. The activity-based modal modeling approach employs a structure that is consistent with the modal modeling for internal combustion engine vehicles. The full-system high-fidelity vehicle simulation tool (Autonomie) was employed to simulate energy consumption under these modal operating conditions, and three preliminary steps were used to develop the activity-based approach for EVs. First, sample EV models were configured in Autonomie for battery-electric, fuel-cell electric, hybrid-electric, and plug-in hybrid-electric vehicles. Energy use data for selected vehicles were generated by simulating a wide range of operating conditions with different average speeds, driving styles, road grades, and air conditioning load. Second, the energy consumption models were established for various types of EVs using a simulation inference design, which combines the physical knowledge of vehicle operation (how engine, motor, battery works together) with data-driven inference. The upper-level vehicle control mode (e.g., engine operation, electric motor operation, and electricity generation for recharging) were modeled as a function of vehicle driving conditions using generalized linear models. The lower-level energy consumption was simulated under distinct control mode from upper-level model using linear regression. The instantaneous energy use is the expected value calculated by summing up the energy use by control modes multiplied by the probability of those control modes. Finally, the proposed EV energy models were verified using a separate testing dataset developed from Autonomie simulation results of a different set of driving profiles.

The modeling results suggested that the proposed modal model is able to predict the energy use predictions of the full-vehicle simulator at relatively high accuracy. In addition, the real-world observed operations and energy use data were collected from select EV models using on-board diagnostic (OBD) devices to verify the energy prediction from the proposed model. The verification results suggested that the proposed model can predict energy use patterns under specific driving conditions. The resulting model accuracy depends on the quality of underlying Autonomie simulation and the accuracy of collected operation data from OBD devices.

After developing and verifying the EV energy model, new methodologies are presented for estimating aggregate energy consumption (total energy use from all vehicles) for large-scale transportation networks using link-level inputs. Scatter plots of energy rates under different link-level inputs (e.g., link average speed, road grade, initial SOC) illustrate the variation of energy rates under different operating conditions, and show potential non-linear relationship between energy use and operating parameters. Variance-based sensitivity analysis (using the "Sobol method") quantifies the contributions of different factors and interactions among factors on the variance of energy rate results. After demonstrating the relationship between on-road operating conditions and corresponding energy rates, the network-level energy use is estimated using link-level traffic information, including traffic volumes and average speeds from network links, current market share vehicle types, and randomized initial SOC levels. The link-level energy consumption for given EV penetration rates are generated for each roadway link, for each hour of operation, and compared to the baseline no-EV scenario (an EV fleet penetration rate of zero) to assess energy savings. This approach can generate network-level EV energy consumption for a variety of transportation studies. For example, the vehicle-to-grid integration can be analyzed by refining the initial SOC distributions by time of day under real-world charging patterns and splitting the

energy supply between fuel and electricity with higher accuracy. Eco-driving and eco-routing benefits can also be analyzed using high-resolution vehicle traces. The life-cycle energy use, carbon footprint, and cost- savings analysis can also be performed given the fuel-cycle and vehicle-cycle energy, emissions, and cost elements for EVs.

Using the EV energy model framework, energy consumption, and cost savings of adopting EVs can also be quantified at the household-level, individual-level, or business-level using travel demand model outputs or monitored business activity data. In this study, the household travel routines from a typical workday generated by the regional travel demand model (TDM) were used to estimate the energy use, driving range and cost using alternative EVs. The Directions Application Programming Interface (API) for Google Maps® was adopted to generate network-level traffic information using modeled departure time and origin-destination pairs provided by the TDM. The link-level energy estimation method was applied to each trip performed by each driver in the household to estimate energy use, driving range, and operating cost under different EV adoption scenarios, ranging from insufficient battery charge (the relatively worst scenarios) to scenarios where battery charge was sufficient for each trip. The cost savings of using different kinds of EVs compared to conventional ICEVs can be assessed for a variety of households with diverse travel patterns. The research efforts in this dissertation can be further expanded to address pressing EV research questions, such as estimating the available range of EVs under distinctive operation scenarios, assessing how charger station location can extend daily vehicle range, assessing the return-of-investment of using EVs for daily travel, and optimizing EV operations.

CHAPTER 1. INTRODUCTION

1.1 Background

The transportation system consumes large amounts of energy every year and is a major contributor to greenhouse gas (GHG) emissions. Globally, the transportation sector accounted for 27% of final energy use and 6.7 $GtCO_2$ direct emissions in 2010, with baseline CO_2 emissions projected to increase to 9.3 to 12 $GtCO_2$/year in 2050 (IPCC, 2014). In United States, the transportation sector accounted for about 28.7% of the total energy use, and 36.3% of total greenhouse gas (GHG) emissions in 2016 (Davis and Boundy, 2019). Such a heavy reliance on petroleum fuel causes both energy security and environmental problems (Kromer, 2007). Within the transportation sector (car, trucks, rail, aviation, etc.), the 245 million total light-duty vehicles, including cars and light-duty trucks, accounted for 90% of the vehicle-mile traveled and contributed to 59% of U.S. transportation energy use in 2016 (Davis and Boundy, 2019). Given the high uncertainty of future fuel supply and growing demand from transportation sectors, it is necessary to take actions aimed at reducing the energy use and GHG emissions in transportation system, especially from light-duty vehicles (LDVs).

1.1.1 EV Significance

Vehicle electrification is the current focus to shift petroleum fuel to alternative energy in transportation system (Zhang and Mi, 2011). Electric vehicles (EVs), including battery electric vehicles (BEVs), hybrid-electric vehicles (HEVs), plug-in hybrid-electric vehicles (PHEVs), and fuel-cell electric vehicles (FCEVs), use electricity from on-board resources (e.g., engine, fuel-cell and battery pack) or off-network charging (plug into grid) either as their energy source or to improve the efficiency of conventional vehicle designs (U.S. Department of Energy, 2014). The

major benefits of EVs can be categorized into four categories (Sperling, 2018), which are introduced below.

1. **Environmental benefits.** EVs operate partly or entirely on electricity that can be generated from local, renewable, and less carbon intensive energy sources than gasoline (Karabasoglu and Michalek, 2013). The life-cycle benefits of using EVs compared to other alternative fuel vehicles and baseline conventional gasoline vehicles are shown in Figure 1 (U.S. Department of Transportation, 2010), and EVs can save about 30%-90% of life-cycle GHG emissions compare to a conventional gasoline vehicle. In this case, adopting EVs essentially reduces the dependence on petroleum fuels, even under the consideration of the whole life-cycle.

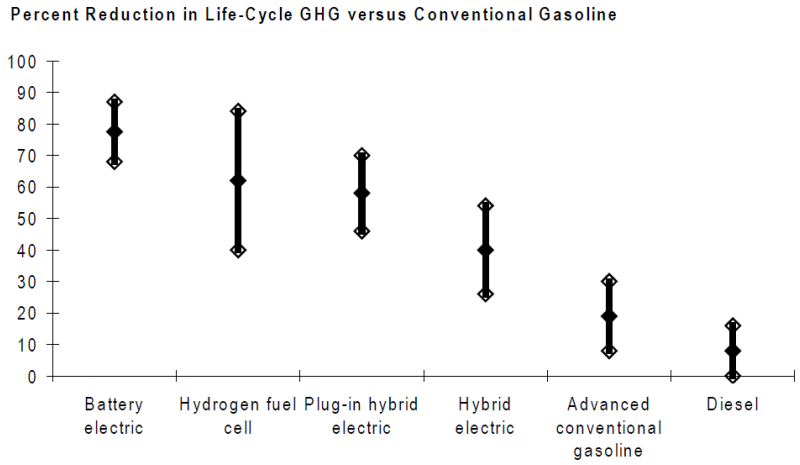

Figure 1. Percentage reduction in life-cycle GHG of alternative fuel vs. conventional gasoline *(U.S. Department of Transportation, 2010)*

2. **Technological benefits.** EVs use complex management systems to control power flow in vehicles, and the powertrain control strategies are optimized to reduce energy consumption (Zhang and Mi, 2011). With such technological benefit, EVs often achieve much higher fuel economies than conventional vehicles. The fuel economy data of BEVs, HEVs and PHEVs from fueleconomy.gov are illustrated in the **Figure 2** below. Most EV technologies can meet the fuel economy standard. The most energy efficient electric cars have fuel economy up to

140 mpg and the most energy efficient electric light-duty trucks have fuel economy around 90 mpg.

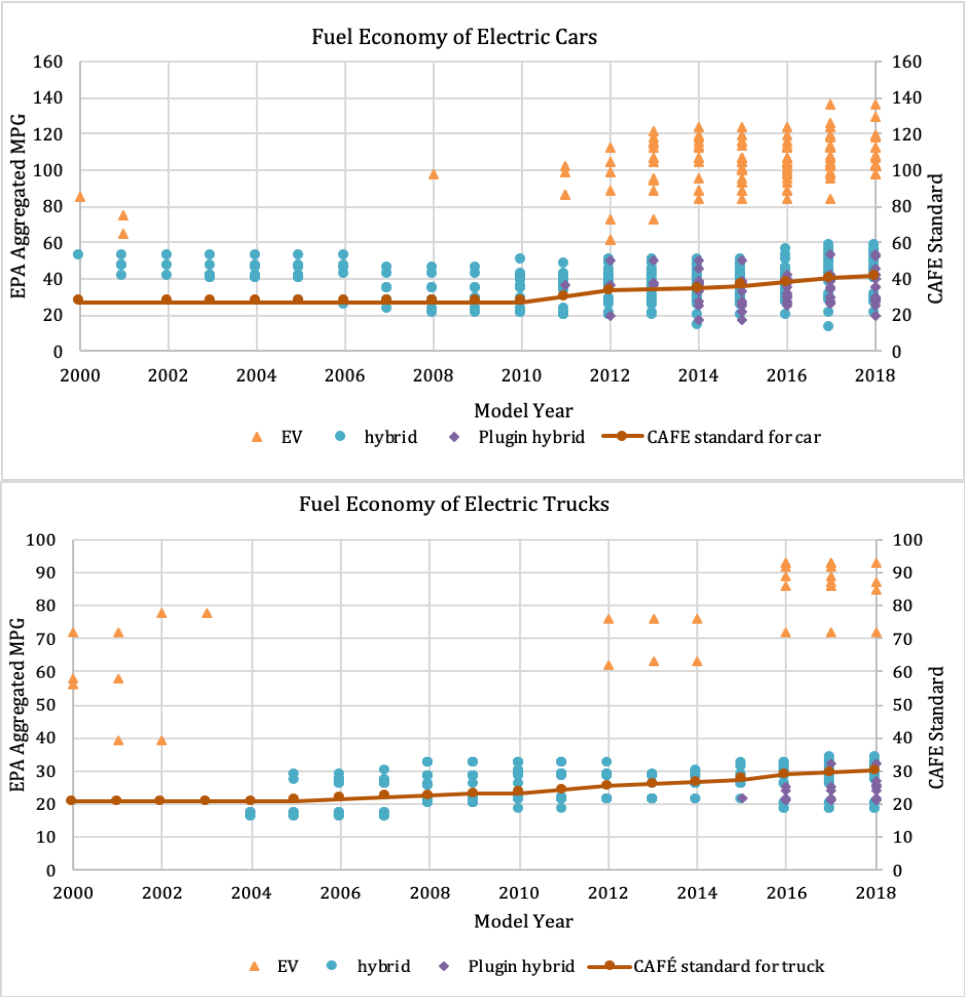

Figure 2. Fuel economy of BEV, HEV and PHEV

3. **Vehicle design benefits.** EVs offer great opportunities for improving vehicle design (Sperling, 2018). The car is more stable with batteries being placed in and under the vehicle frame, and this provide engineers with new opportunities to redesign the vehicle chassis and enhance vehicle performance and safety.
4. **Reliability and cost savings.** Adopting EVs is essentially beneficial for consumers in reducing operation cost, becoming less vulnerable to fuel prices, driving quieter and more

smoothly (Sperling, 2018). In this case, EVs can provide an attractive alternative to reduce the energy consumption during on-road operations through replacing fuel with electricity and significant vehicle efficiency improvements, and also helps customers with advanced vehicle design and driving experience.

1.1.2 Challenges in EV Adoption

To make a significant impact on reducing urban energy use, air pollution and climate change, EVs need to capture a notable market share (Hardman et al., 2018). However, innovations take a long time from invention to widespread adoption (Rogers, 1995), so do EVs. Until now, EVs still capture a relatively small market share in the petroleum-fuel dominant vehicle market, despite the large benefits they offer to the customers. About 97% of vehicles sold in 2017 still use conventional combustion engines, while the HEV market share has grown from 0.1% in 2000 to 2.2% in 2017, and the plug-in vehicle (BEV and PHEV) market share has grown from near 0% in 2000 to 1.2% in 2017 (Davis and Boundy, 2019). In terms of the future fleet, leading economic forecasters and demographers believe that a total of 9% of EV market share (BEV, PHEV and FCEV) can be achieved by 2025 under the assumptions of known technology development and economic and demographic trends (U.S. Energy Information Administration, 2017). Another study suggests that conventional technologies are likely to continue to dominate the in-use vehicle fleet, based on the speed of technology improvements and market growth over the coming several decades (Kromer, 2007). In the foreseeable future, the transportation system is likely to be predominantly ICEVs, with some uncertain fraction of EVs. However, the energy impacts associated with EV purchases are likely to become more and more significant over the next decade. The energy impact under possible EV adoption scenarios needs to be analyzed to understand the system and guide future policy making processes, given certain assumptions and methodologies.

Policy makers and auto manufacturers need system-level knowledge to make the right decisions, such as the local/regional market share, fleet composition, and cost savings of providing EV incentives to public. However, the system-level impacts are largely controlled by individual vehicle purchase choice. The actual benefits and cost of using EV compared to their conventional counterpart could largely depend on individual's travel patterns, on-road traffic conditions, and relative electricity price compared to fuel price. In this case, a bottom-up approach, which derives system-level knowledge by accumulating results from individuals, is needed to mitigate the gap between system-level policy making and individual-level decision process.

Given the above discussion, the major objective of this study is to build the activity-based bottom-up EV energy consumption model as a function of vehicle characteristics, the users' travel patterns in large-scale transportation network, and on-road operating conditions. The energy model will be able to handle individual-level travel inputs, such as travel distance, speeds, and vehicle type to estimate energy use, while also accounting for driving range and cost. The model will also be designed for large-scale network application by aggregating individual-vehicle energy consumption. The models also need to be capable of quantifying the energy impact of different EV policy scenarios that may affect fleet penetration rates and on-road travel decisions in a large-scale transportation network. The approach would define the key elements considered in EV adoption and application, with necessary assumptions made for other system elements using the best available domain knowledge.

1.2 Problem Statement

As stated above, the major objective of this dissertation is to propose an activity-based bottom-up approach for estimating system-level energy consumption based on household-attributes (and/or person-attributes) and vehicle fleet composition. To develop the modeling approach for estimating

system-level energy use, it is essential to build the connections among electric vehicles, system users, and the transportation network. The connection is established using a data-driven approach, which defines the relationships based on real-world observed data or high-fidelity simulation data. The diagram of this data-driven development framework is illustrated in **Figure 3** below.

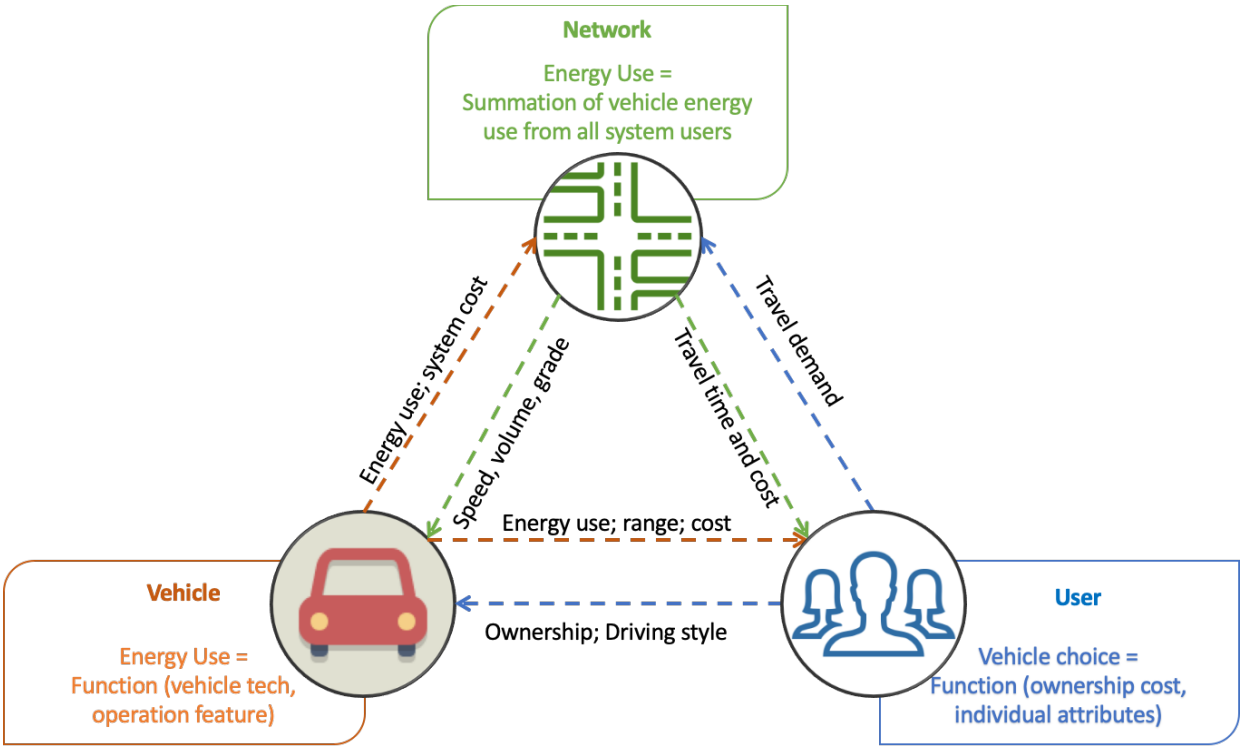

Figure 3. Conceptual framework of energy modeling using vehicle, user, and transportation network Information

The connections among vehicle, network and users demonstrated in diagram above are further split into four research questions, which are introduced below:

1. **Data availability:** Due to the low market penetration of EVs (except in the State of California) and reluctance of manufacturers to share user data, EV operations and energy use patterns are largely unclear. Existing studies are often performed as case studies, so the energy use and user preference results are often not comparable, due to different sets of variables, research context, and assumptions made. A representative data set (in time and geographic space) is

needed, with consistent attributes for all kinds of vehicle technologies including driving patterns, road grade, and energy use profiles. The individuals travel pattern is also needed travel need to describe EV adoption and predict future market share under the local context.

2. **Vehicle energy modeling:** EV energy use is affected by vehicle powertrain and control system design, operation characteristics, driving environment, and vehicle age and system deterioration, etc. Those attributes may or may not be measurable in the transportation system, and analyzing each aspect explicitly is cumbersome, hampers scalability, and increases the level of knowledge needed to perform such studies. Using average values, such as fuel economy ratings, and average energy/emission rates lowers the hurdles for large-scale application. However, the results are not sensitive to key factors that interest drivers and policy makers, such as energy impacts of speed/acceleration, road grade, and charging frequency. Developing a methodology which is scalable for local/regional network but still keep reasonable-level of complexity is a key task in this dissertation.
3. **Projection to transportation network:** The transportation network is a highly dynamic and complex system and is difficult to model. It is almost impossible to analyze or model all of the aspects in the network, but it is also not necessary for most purposes to do so. From a network-level perspective, only the key attributes that significantly affect energy use needs to be considered in this study, such as average speed (represented by a driving cycle), link length, and road grade. The effect of other attributes, such as signal timing, lane changing, road pricing, will be assumed to be fixed or represented by the factors in the model (e.g., the impact of signal timing is inherent in the vehicle speed profiles). On the other hand, such simplifications ignore some key factors that may affect electric vehicle energy consumption, such as the current state of battery charge in an EV. The methodology of generating those attributes is needed. Also,

the input features in different EV energy models should be consistent so that the energy results are comparable.

4. **User's travel pattern:** The cost savings of adopting EVs varies greatly due to different characteristics of system users and local contexts. Different users have different travel needs and preferences, which may be best-served by a specific vehicle type, or a combination of several vehicles. It is essential to assess the cost savings of potential customers using different vehicles based on their travel needs under a local context and to propose locally-optimized vehicle adoption strategies based on estimated results and household constraints.

1.3 Major Research Tasks

Based on the four major research needs introduced above, an activity-based bottom-up approach is selected to model the system-level energy use based on individual's behavior and choice. There are four major tasks to achieve this approach in this dissertation: 1) collecting and post-processing data, 2) developing and testing the EV energy model framework, 3) linking the EV energy model and transportation network model, and 4) assessing energy use and cost savings of different energy adoption scenarios.

1.3.1 Data Collection and Post-processing

The key problem to resolve before performing any analysis is to assemble a standardized dataset collected under the same context, containing consistent response and factors, and using the same assumptions for all electric vehicle technologies. The two major data source including on-board vehicle measurement data and full-system vehicle simulations. Under the latest development of sensor technologies and latest vehicle diagnostic standard, data available from vehicle on-board diagnostic (OBD) system often contain high time-resolution operating conditions (speed, acceleration, state-of-charge), vehicle control commands (engine on/off, battery charging or

discharging), energy and emission rates. In addition, the OBD data can be merged with GPS data given time-series information, to look up the roadway information such as road type and grade. While the field measurement data are great representations of real-world vehicle operating conditions, the collection process is expensive, and its quality is usually limited by adopted measurement technologies and sensor reliability. Additionally, data collected from field-measurement are limited by the low adoption rate in the current market and not likely to cover all available EV models (especially hydrogen fuel-cell vehicles).

The full-system vehicle simulation tools, on the other hand, are able to generate vehicle energy use for a variety of latest vehicle technologies under almost all operating conditions. Those models often take the vehicle operating conditions to generate vehicle tractive load, assign the load to different power converter (engine, motor, etc.), account for transmission and conversion loss, and finally derive the energy consumption. In this case, the full-system vehicle simulators are suitable to take real-world operation data as input, to expand the depth and precision of the energy use data and assess all vehicle technologies. However, as the simulation tool can take almost all input combinations, it is inevitable that some of those combinations are actually not available in the real-world and need to be exempted from actual analysis. Also, the model could be significantly biased if not calibrated with real-world data. It is essential to feed in real-world data and assess the model performance before using the generated dataset.

In this study, one full-system simulation tool, called Autonomie, will be used to generate energy consumption of all kinds of EVs with inputs from vehicle manufacturing information and real-world operation conditions. The real-world driving cycles will be put in the simulation tool for vehicle physical and control parameters (such as engine speed, torque, engine/motor temperature, etc.), fuel and electricity consumption, and battery state-of-charge (SOC). On the

other hand, the on-board measurement data from existing electric-drive fleet will still be collected and applied to verify the full-system simulation model for downstream analysis. The goodness-of-fit measurement of the simulation model compared to real-world energy use data will be used as a major metric to verify and adjust the model and ensure the quality of generated dataset.

1.3.2 Vehicle Energy Consumption Model Development

The design of energy model is based on the major purpose of its engineering application. In this case, the model development is constraint by following considerations on its application:

- **Models only measurable factors:** there are many factors that could affect vehicle energy consumption, such as vehicle powertrain design, ambient environment, driving conditions and quality of the fuels. However, not all of the factors are measurable from a transportation system, and adding more variables significantly increase the difficulty of performing such analysis. In this case, only measurable factors that have significant impact on vehicle energy use are included.
- **Model interpretability and scalability:** as the model is used for engineering practice, the interpretability is a key attribute for users to judge the reliability of the model. The coefficients of regression analysis are often good indicators of factors' impact on responses. In this case, the parametric regression-based model is selected instead of high-dimensionality learning tools with low interpretabilities such as neural network model, random forest model and support vector machines. Also, as the model is ultimately used for large-scale application, the simplicity and scalability are key considerations in model development. In this case, a parametric model with factors, coefficients and response fit in matrix form is a great option for large-scale application. Although interpretability and scalability are different model attributes,

they end up require the same model structure, which is the family of parametric regression-based models.

- **High temporal resolution**: transportation network is a highly dynamic system, with driving conditions change almost instantaneously. There are large variances during daily vehicle operation, as the speed, acceleration, road grade and vehicle control strategies keep changing during the driving period. So, it is desired to have a high temporal resolution, such as second-by-second, in the modeling framework. Also, as discussed above, the model only needs measurable operation conditions as input, so it is possible to prepare limited data inputs in high temporal resolution.

Based on the above constraints, a data-driven, parametric modeling framework is needed. The **modeled responses** (denoted by E_{fuel} and E_{elec}), including fuel and electricity consumption, with separate energy models trained for fuel and electricity separately due to different work domain of fuel converter and electric machines. The **objective function** (loss function) is to minimize the root-mean-square error (RMSE) of modeled fuel and electricity consumption (denoted by R_{fuel} and R_{elec}). The **candidate factors** include variables from vehicle architecture and control, driving conditions and roadway conditions. The dataset is split into training and validating set, and the parametric model is established using **regression analysis**. The on-board measurement data serve as the testing set for measuring the accuracy and validity of final model.

1.3.3 Linkage between EV Energy Model and Large-scale Transportation Network

The energy model developed in previous step is designed for individual vehicles, and individual vehicle energy use needs to be accumulated to obtain the system-level energy and cost. Two sets of information need to be extracted from a transportation network: data sets for model prediction

and data sets to predict the impact across the vehicle fleet. The network attributes, such as link average speed and road grade, will be used to predict unit energy consumption per vehicle for each roadway link using predefined energy model. The magnitude attributes, such as hourly link traffic volume and link fleet composition, will be used to project unit energy consumption to total energy use in the network. In addition, it is likely that some energy model inputs are not available from the transportation network, such as battery SOC, so a randomized mechanism will be adopted to generate those inputs and measure its impact.

With energy consumption estimated at the link-level during different time period, the fuel and electricity demand can be determined both spatially and temporally. The cost of adopting EV can be further estimated as a function of energy use. Given the linkage above, there will be a framework which is able to take the travel attributes as input and generate a composite travel cost (include the travel time, energy cost and other induced cost). Also, given individuals travel information (e.g., origin, destination, and vehicle), it is able to generate the energy use and cost profile for their daily travel, by estimating energy use from traversed roadway links.

1.3.4 Energy Use Variability under Different User Characteristics

Given the energy saving and potential cost recovery during EV operation, it is possible that people could use EVs to serve certain travel needs to achieve largest energy saving and cost saving benefits. However, the cost-benefits of choosing different kinds of EVs have large uncertainty due to individual's attributes such as travel needs and preferences. In this case, a representative resident sample is needed to study those attributes, and how those attributes would affect their EV relative cost savings. In this step, the energy use and cost savings compared to their current vehicles serves as the response, and individual attributes and travel demand serves as the factors. The variance of EV energy use is generated under a variety of adoption scenarios for understanding

the potentials of energy saving under different conditions, such as range reduction under hot/cold weather, energy recovery with sufficient charging availability and changing fuel/electricity prices. A summary of proposed research tasks is illustrated in **Figure 4** below.

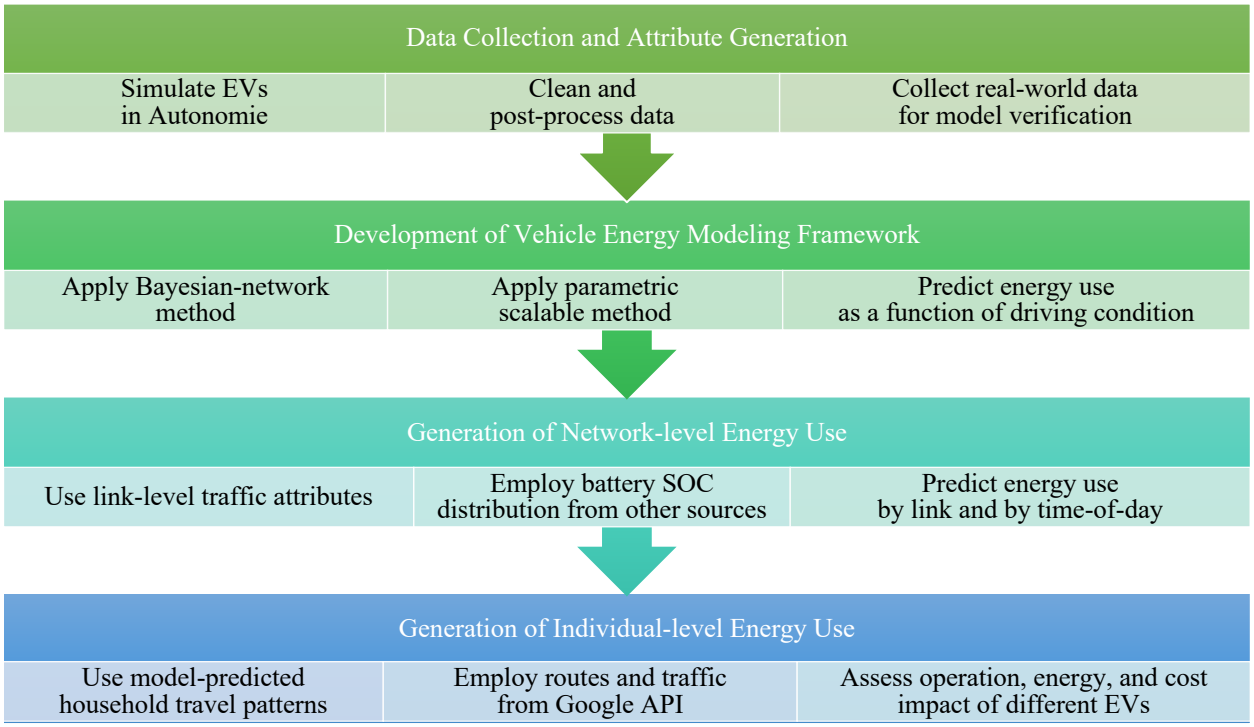

Figure 4. Workflow of EV energy modeling framework

1.4 Expected Outcomes

The major contributions from this dissertation include following items:

- **Data contributions:** both real-world operation data and vehicle simulation data from high-performance models are collected and processed for this study. The data will account for current and potential future conditions. The protocol of data generation and verification will be documented to prepare the data for energy and emission analysis purpose at any time and serve as a helpful resource for future research projects.

- **EV energy modeling contributions.** In this dissertation, an energy analysis framework using Bayesian Network methods is developed for electric vehicle fleets, including BEVs, PHEVs, HEVs and FCEVs. The analysis framework is trained using a rich supply of full-system vehicle simulation data and can be applied to large-scale network-level energy analysis efficiently. With this tool, we can assess the impact of various transportation-related attributes on energy use.
- **Contributions on identifying important system features for energy analysis**. The energy analysis framework connects to the regional travel demand model, and energy estimation is responsive to variations in system features. Energy use sensitivity analysis, using descriptive (scatter plots) and quantitative (variance-based sensitivity analysis) methods helps identify the system features that have significant impact on energy use. The conclusions from this paper will inform traffic engineers, planners, and policy makers on data needs for energy analysis.
- **Contributions on establishing an analytical approach for EV energy modeling with selected network and user features.** Given that some of the system elements could have a significant impact on total network-level energy consumption, it is important to propose an energy analysis approach that can support the detailed specification of those features. The proposed modeling approach is able to help researchers use travel activity and choice data sets to predict the energy profile for their travel routines and investigate the EV cost-benefits including driving range, energy use, charging demand and cost savings. In this case, the effectiveness of potential strategies on encouraging EV adoption and optimizing operations can be analyzed to inform the policy making and transportation planning process.

The proposed model framework can be employed to support of the following policy analyses:

- Assessing the regional energy impacts of EV policy and legislation, such as EV purchase incentives and providing EVs with managed lane priority use (e.g., using a managed lane) or parking preferences, where the travel demand model predicts the change in travel behavior.
- Assessing the regional energy impacts of EV infrastructure planning and design, such as construction and location of charging stations, providing home charging facilities, and adding new power sources, where travel demand model data are post-processed to incorporate range constraints.
- Assessing the energy and cost reduction benefits associated with new EV technology applications, such as implementing eco-driving and eco-routing strategies, adopting the autonomous driving systems, and using improved sensor technology (e.g., integration of GPS and driving cycle prediction).
- Assessing the impact of EVs on the electricity grid and identifying the peak charging requirements based on daily EV use patterns.
- Providing EV operations information for use in predicting criteria pollutant (NOx, VOC, PM, etc.) emissions, including engine starts and engine soak time distributions.
- Providing insight into regenerative braking activity for use in predicting brake wear emissions.

1.5 Dissertation Outline

Due to the workload required, and connection among tasks, the four major tasks are presented in five chapters, with the data collection efforts covered in each chapter. The research efforts in this dissertation will be introduced as follows:

- **Chapter 2 provides a comprehensive literature review** that summarizes the fundamentals of vehicle design and operations, latest research efforts on EV energy analysis and potential influential factors, EV model development, and EV benefits assessment. The current research gaps are identified at the end of literature review. The attributes with significant impacts on EV energy use are identified for data collection and model development tasks.
- **Chapter 3 proposes an analytical framework on EV energy modeling** as a function of vehicle operation patterns within large-scale transportation network. The classification and regression tree (CART) method is adopted to partition a PHEV operating conditions into a finite number of bins, where each bin contains specific fuel/electricity rates. The proposed method is tested using a regional-level case study to demonstrate its scalability and sensitivity to on-road operating conditions.
- **Chapter 4 proposes an enhanced energy modeling approach using a Bayesian Network model.** The Bayesian Network model adopts a simulation-inference design, which combines the vehicle physical knowledge from the research domain via simulation modeling and a parametric form that enables the data-driven inference. The methodology is verified using a separate test set and verified using real-world OBD data.

- **Chapter 5 applies the developed energy modeling framework to quantifying network-level energy use** with pre-defined EV market share. First, the sensitivities of EV energy rates under different operating conditions are explored using scatter plots for each type of EVs. The contribution of various factors on link-level energy use is assessed using a variance-based sensitivity analysis (also known as "Sobol method"). Then, the significant factors were extracted from the regional-level travel demand model to estimate link-level fuel and electricity use for a typical travel day under different EV market shares. The energy saving benefits by replacing a fraction of conventional vehicles with EVs are assessed spatially and temporally for the entire region. The energy savings by facility type and speed bin are also examined to identify the roadway facilities with the largest energy saving potentials after EV adoption.
- **Chapter 6 applies developed energy modeling framework to estimation of individual-level energy use** using EVs based on household travel patterns and potential adoption scenarios. The household travel data in a typical travel day is provided by the regional travel demand model, with shortest-path (i.e., shortest travel time) route and on-road link speeds generated by the Google direction API. The energy use of selecting different vehicle alternatives were estimated under a variety of adoption scenarios from relatively pessimistic to relatively optimistic. The operation, energy, and cost impacts of choosing different kinds of EVs are assessed to examine the cost-effectiveness of different EVs under different travel patterns and adoption scenarios.
- **Chapter 7 provides the summary of this dissertation** and highlights the major findings from this work. This chapter summarizes the major tasks performed in this dissertation and the research questions answered by this study, then identifies potential applications of

this work. This chapter also plans the potential future work given the limitations of the current study and possible future development in this field.

CHAPTER 2. LITERATURE REVIEW

The major purpose of the literature review is to provide an overview of EV design and operation, as well as examine how EV energy use relates to different network and user factors. In this study, the significant factors will be selected, and key assumptions will be based upon the latest research findings and engineering considerations.

2.1 Fundamentals of Vehicle Design and Operation

A vehicle, consisting of thousands of components, is a complex system (Ehsani et al., 2018). A simple-structured mathematical model with reasonable level of uncertainty is needed to represent the design of the vehicles and how they operate under various driving conditions. All kinds of vehicles, regardless of fuel and powertrain, are designed to convert on-board energy storage (gasoline, diesel, electricity, etc.) into kinetic energy to provide work against a load. The vehicle load includes friction resistance, uphill and downhill load due to road grade, and resistance from surrounding environment such as wind and rain (Mi et al., 2011). From previous research findings, a widely used vehicle load definition is provided below (Ehsani et al., 2018):

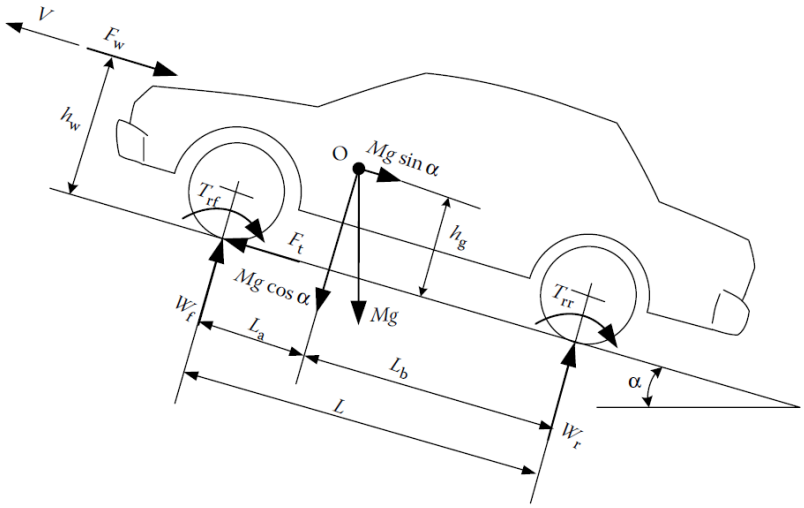

Figure 5. Conceptual representation of vehicle driving load

In this graph, we have all the vehicle driving loads defined as following:

T_r, - rolling resistance of front tires (T_{rf}) and rear tires (T_{rr})

F_w - aerodynamic drag

$F_g = Mgsin(\alpha)$ - gravity force

Also, the vehicle and road characteristics are defined as following:

α – road grade (rad)

M – Vehicle mass (kg)

g - standard acceleration due to gravity (9.8 m/s^2)

The vehicle tractive power is the product of tractive force and instantaneous speed, where vehicle tractive force F_T is often simplified and represented as follows (Zhang and Mi, 2011):

$$\boldsymbol{F_T = Ma + F_R} \quad \textbf{(1)}$$

Where,

a is the acceleration (m/s^2);

F_R is the force that must be delivered by the powertrain to perform the required work, which is often simplified and represented by the sum of forces required to overcome aerodynamic drag F_w, rolling resistance T_r and work against gravity. Each element in vehicle traction force can be approximated by vehicle driving parameters, including speed, acceleration, and road grade:

$$\boldsymbol{F_T = Ma + F_R = Ma + F_w + T_r + F_g =}$$

$$\boldsymbol{M(a) + \frac{1}{2}(\rho)(v^2)(A)(C_d) + c_r(M)(g)cos(\alpha) + M(g)sin(\alpha)} \qquad \textbf{(2)}$$

Where,

ρ - density of the air (kg/m^3)

V - vehicle speed (m/s)

A - vehicle frontal area (m^2)

C_d - coefficient of drag

c_r - coefficient of rolling resistance

In this case, the **vehicle tractive power $\boldsymbol{P_T}$** is hence represented as:

$$\boldsymbol{P_T = F_T v = Mav + \frac{1}{2}\rho v^3 AC_d + c_r Mgvcos(\alpha) + Mgvsin(\alpha)} \quad \textbf{(3)}$$

Vehicle-specific Power (VSP), which equals the tractive power divided by vehicle mass (Jimenez-Palacios, 1999) is widely accepted for defining and comparing tractive power among same types of vehicles. In this study, VSP will represent the power demand level. The VSP absorbs the effect of vehicle specifications and operating conditions. However, it is not enough to solely rely on tractive power, as distinct driving conditions can fall into the same power level (e.g., low-speed hard-acceleration and high-speed cruising can have the same power demand). In this case, the original speed, acceleration, and road grade information are still useful for energy analysis and will also be employed in this research.

Given the input vehicle tractive power demand, the vehicle control system calculates the total energy required, which may split among different power sources (i.e., in hybrid vehicles) under specific driving conditions (Zhang and Mi, 2011). The characteristics of the vehicle as an energy provider can be represented by its powertrain, which includes the energy source and the

energy converter of that power source (Ehsani et al., 2018). Using the powertrain characteristics, the following vehicle types can be described as following:

- **Internal combustion engine vehicles (ICEVs)** use the internal combustion engine powered by gasoline, diesel, natural gas or other fuel for propulsion (Zhang and Mi, 2011).
- **BEVs** use one or more electric motor(s) for traction with batteries as the energy resource; they do not employ an ICE (Ehsani et al., 2018).
- **HEVs** have two or more powertrains, with an ICE and one or more electric motor(s) to power the vehicles (Ehsani et al., 2018).
- **PHEVs** are hybrid electric vehicles usually equipped with a large rechargeable battery pack (>4Kwh), that can be driven solely on electricity for at least 10 miles (IEEE-USA, 2007) and can be recharged via an external connection to a land-side electricity source.
- **FCEVs** use only an electric motor for propulsion power, with a hydrogen fuel cell as the primary energy resource to power the battery packs. Vehicles powered solely by fuel cells usually suffer from some disadvantages, such as a heavy power unit, long start-up time, low energy efficiency under extreme driving conditions, and slow power response (Ehsani et al., 2018). Hybridization of the fuel cell powertrain helps enhance vehicle performance. FCEVs can be treated as HEVs, where the ICE is replaced by the fuel cell system.

For all kinds of vehicles using different powertrains, a conceptual vehicle structure can be represented as illustrated in Figure 6 (Ehsani et al., 2018). Powertrain 1 has the unidirectional power supply to both final drive and Powertrain 2, while Powertrain 2 has bidirectional power flow, which both supplies the final drive and recovers energy from regenerative vehicle braking

and receives energy from Powertrain 1. Internal combustion engine vehicles (ICEVs) only have Powertrain 1. BEVs only have Powertrain 2, and the energy recovery is enabled solely from regenerative braking. PHEVs, HEVs and FCEVs have two or more powertrains on-board and a coupler to join the power between the powertrains. PHEVs can be treated as a HEV with larger battery storage (and an off-network recharge capability). A FCEV can be treated as a HEV where the ICE is replaced by a fuel cell and electric motor. Hybridized FCEVs enable energy recovery from braking and smooth operation under severe weather conditions (Ehsani et al., 2018). The different types of hybrid configurations can be defined by the device(s) used for power coupling. The power coupling can be achieved through an electric coupler (mostly in series hybrid), a mechanical coupler (mostly in parallel hybrid), or both (mostly in series-parallel hybrid). For EVs that only have the electric motor powertrain (Powertrain 2), the goal is often set to minimize energy use. For vehicles equipped with both powertrains, it is important to optimize fuel economy while maintaining the state-of-charge (SOC) of the battery at a desired level to ensure efficient operations over a wide range of driving conditions (Zhang and Mi, 2011).

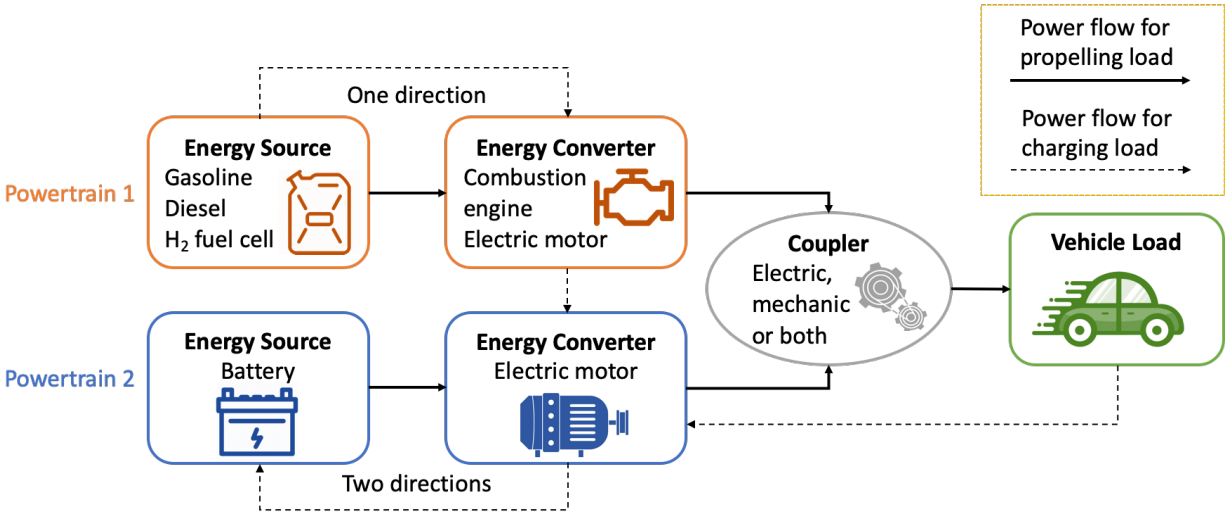

Figure 6. Conceptual structure of electric vehicles

In this case, the **objective** of the **vehicles with one powertrain** option is to provide sufficient energy supply under vehicle propelling load L_p. The **objective** of **vehicles with two powertrains** is to provide energy for vehicle propelling load L_p plus battery recharge L_c. The propelling load, as introduced above, is a function of vehicle characteristics, driving conditions and road grade. The charging load is decided by vehicle control system. Under most condition, it is a function of current battery SOC and propelling load.

How the loads are split among powertrains depend on the selection of different energy source, energy converter and power coupler (Ehsani et al., 2018). The different types of hybrid configurations can be defined by device(s) used for power coupling. The power coupling can be achieved through an electric coupler (mostly in series hybrid), a mechanical coupler (mostly in parallel hybrid) or both (mostly in series-parallel hybrid).

- **Series hybrid:** The key feature of this configuration is that the **electric power coupler** (a controllable electronic power converter) controls the **electric power** flows from the batteries and from the motor generator powered by internal combustion engine (ICE). The two electrical supplies can be added together in the power converter and delivered to the tractive motor, or the power from the motor can be sent to charge the batteries. The fuel tank, the IC engine, and the generator constitute the primary energy supply and the batteries function as the energy bumper (Ehsani et al., 2018).
- **Parallel hybrid:** The key of this configuration is that two **mechanical powers** are added together through a **mechanical coupler** (torque coupler or speed coupler). The IC engine is the primary power plant, and the batteries and electric motor drive constitute the energy bumper (Ehsani et al., 2018).

- **Series-parallel hybrid:** The key feature of this configuration is the employment of both **mechanical and electrical coupler**. In this case, this design is the combination of series and parallel structures and have more operation modes than those of the series or parallel structure alone (Ehsani et al., 2018).
- **Complex hybrid:** The sole difference is that the electric coupling function is moved from the power converter to the batteries and one more power converter is added between the motor/generator and the batteries (Ehsani et al., 2018). As this design is not common in the current market, it will not be employed in the research and model design in this study.

For an ICE, common fuel options include gasoline, diesel, electricity, hydrogen, natural gas, ethanol, etc. However, in the U.S., about 96.9% of light-duty vehicle energy consumption in 2015 came from gasoline (Davis and Boundy, 2019). Hence, this research will assume that all the vehicles equipped with internal combustion engine use gasoline as primary fuel option. For FCEVs, hydrogen is the primary fuel. For BEVs, electricity is the primary fuel.

The vehicle operating modes are classified based on the control mode of Powertrain 1 and Powertrain 2. In general, Powertrain 1 (gasoline-engine, or hydrogen fuel cell) can be either on or off, and Powertrain 2 (battery-tractive motor) can be either charging or discharging, also known as operating in charging sustaining (CS) and charging depleting (CD) modes. As the battery is often used to supply vehicle controllers and auxiliary devices during operation (Emadi et al., 2008), it is very rare to have Powertrain 2 totally off in real-world cases. So, Powertrain 2 in the off mode is combined with the discharging mode. The range of battery power under discharging is [0, max battery power]. The combination of Powertrain 1 status and Powertrain 2 status define the four operating modes, as illustrated in Figure 6 below.

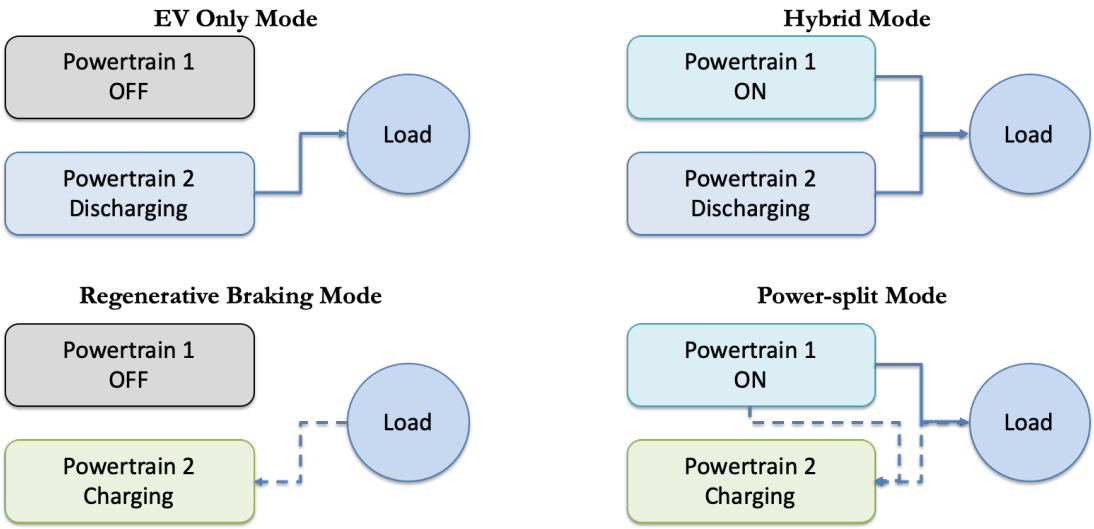

Figure 7. EV operating mode classification

- **EV only mode:** The engine/fuel cell is off, and the battery-motor powertrain provides all of the propelling power to the final drive
- **Regenerative braking mode:** The battery receives electricity from regenerative braking recovered during braking events
- **Hybrid mode:** Powertrain 1 and Powertrain 2 both supply propelling power to the final drive
- **Power-split mode:** Powertrain 1 supplies power to the final drive as well as to the batteries via the generator (battery recharge).

By assigning the proper modes under various operation conditions, the vehicle are likely to operate under the optimal fuel economy, driving performance and emissions (Ehsani et al., 2018). It is critical to define the control modes in the modeling process under each driving condition.

2.2 EV Energy Consumption

The mechanism of EVs have been introduced above, as well as key attributes which affect the energy use. In general, the fuel consumption of LDVs is affected by the fuel delivery system, engine design, transmission, and hybridization (Frey, 2018). However, the variables such as tractive power and engine design are not directly measurable in most cases and need to be derived from other measurable factors. In this case, we need to identify the measurable factors from transportation studies and find potential treatment for unmeasurable factors in this study. Numerous studies have investigated the system-level factors that have significant impacts on EV energy use. Table 1 below presents a brief summary of latest studies, the research samples and methods, and major findings and limitations.

Table 1. Summary of studies on EV energy modeling

Study	EV Type	Sample	Method	Major Findings	Limitation
Gonder et al., 2007	PHEVs and HEVs	Simulate one ICEV, one HEV and two PHEVs over 227 days of real-world data	• Collect real-world driving data • Simulation on energy use with 4 vehicles in ADVISOR	• The results demonstrated that using PHEV and HEV can significantly improve vehicle fuel efficiency.	• Travel diary data are expensive to collect • Limited vehicle models
Lee et al., 2011	PHEVs	181 real-world trips from 9 drivers	• Collect real-world data from local drivers • Vehicle simulation in PSAT	• PHEV energy consumption simulated in PSAT was significantly impacted by real-world cycles, vehicle arrivals and parked time	• Limited vehicle models • Parking information is often not available in traffic studies
Doucette and McCulloch, 2011	BEV and PHEV	Simulated ICEV, BEV and PHEV with New European Drive Cycle (NEDC)	• Simulate vehicle control and energy use with a backwards–forwards simulator OVEM (Oxford VEhicle Model). • Embedded battery and auxiliary power simulation • EV CO2 derived on-road energy use and power generation mix	• PHEVs can potentially generate less on-road CO2 emissions over their entire range than both a similar EV and ICEV.	• Focus on small samples and specific powertrains • Needs full-system vehicle information for energy model
Holdstock et al., 2012	BEVs	Four EVs with three types of transmissions over two driving cycles	• Vehicle operation and energy use simulation with physical models • Optimize transmission parameters	• The four-speed vehicles reduce energy use over standard driving cycles against single- and double-speed variants	• Limited sample size • Drivetrain info not available in most other studies
Shankar and Marco, 2013	BEVs and PHEVs	One PHEV drove 1691 micro trips	• Field trip measurement • Neural network for EV trip classification • Calculate energy using micro-trip information	• The energy consumption of EVs would vary under different micro-trip groups representing varying road type and congestion levels.	• Limited vehicle types • Need battery info for energy calculation
Xie et al., 2012	BEV	Simulated network with different fractions of EVs	• Using PARAMICS to simulate a small transportation network • Using MOVES to obtain energy and emission rates with traffic inputs from PARAMICS and different EV fractions	• Results indicated that BEVs can greatly reduce the emission rates of SO2, CO2, and energy consumption for passenger cars.	• MOVES not capable of estimating HEVs.

Table 1 continued

Study	EV Type	Sample	Method	Major Findings	Limitation
Wu and Aliprantis, 2013	PEV (BEV and PHEV)	N/A	• National level energy use analysis with different LDV electrification levels • Ensemble four different energy models • HEV energy model based on lab-tested average value	• By introducing PEVs and renewable energy, the total cost from transportation systems can be reduced by 5% over 40 years. • The annual LDV gasoline use can be greatly reduced at a cost of higher annual electricity demand.	• Energy model not sensitive to traffic operation parameters other the daily VMT
Lorf et al., 2013	BEV, PHEV and HEV	26 BEVs, four PHEVs, four HEVs and six ICEVs drive a 91.94 km route	• Collect real-world OBD and GPS data	• Vehicle powertrain has the largest impact on energy use • Driving behavior and regenerative braking impact energy use • Energy use are not sensitive under medium speeds.	• Small sample size • Limited driving condition
Neubauer and Wood, 2014	BEV	Three cities; 317 trips	• Field measurement of driving cycles • Vehicle & battery simulation	• Increasing driver aggression, hot climate and key-on cabin HVAC reduce driving range • Driver aggression has minimal effect on battery wear, while cold climate has low impact on driving range and battery wear	• Only consider 3 cities • Only consider BEV
Mohd Zulkefli et al., 2014	Power-split HEV	Simulated vehicles from 6-mile and 15-mile VISSIM models	• Microscopic trajectory prediction • Build a physical model on HEV energy use • Constraint vehicle control optimization methods	• Accurate driving cycle prediction strategy show 7-9.6% average fuel economy improvements achieved compared to rule-based control • Prediction-with-error cases show smaller gains for average MPG	• Only applicable for this specific powertrain
Wu et al., 2015	BEV	169 trips from one converted EV	• Field collected trajectory and CAN BUS data • Developed an energy model to predict EV energy use • Validated energy model with collected real-world data	• Speed, acceleration, and road grade have significant impact on vehicle power demand • A physical model can predict trip energy use with low level of errors.	• Limited sample size • Need motor and battery features to calculate energy

Table 1 continued

Study	EV Type	Sample	Method	Major Findings	Limitation
Zhang and Yao, 2015	BEV	On-road operation of one BEV on all road types in a month	• Collect real-world OBD and GPS data • Predict energy consumption rate using physical knowledge • Calibrate parameters under different driving modes with real-world data	• Real-world energy use is different from lab test result • EV driving behavior and powertrain characteristics are critical for energy estimation • The regression-based energy model cannot be applied without checking multi-collinearity, heteroskedasticity and serial correlation	• Data collected from non-peak traffic • Range of speed and acceleration is low • Cruising and idling errors seems to be high
Asher et al., 2017	HEV	N/A	• Literature review	• Sensor technology could enable eco-driving and route predicting at different levels • Large predict error and short predict windows would decrease vehicle fuel economy	• Benefits of installing new sensor and signal technologies are not quantified
Thomas et al., 2017	HEV	One HEV and one ICEV	• Energy modeling base on physical formulas and chassis dynamometer experimental comparisons.	• Regenerative braking limitations could help improve HEV fuel economy variation under the range of standardized drive cycles. • Aggressive driving would increase fuel consumption	• Small vehicle sample size • Limited driving conditions considered
K. Liu et al., 2017	EVs (without specification)	GPS data from 68 sample EVs	• Regression modeling of energy use as a function of operating conditions	• higher road grade will cause energy use increase linearly • EVs have higher energy efficiency than conventional vehicles especially in mountainous areas	• Fleet information is not included • Energy model seems more suitable for trip-level than link-level analysis
Qi et al., 2018	BEV	A BEV with 100 hours of driving	• Collected real-world OBD and GPS data • Energy use model with regression and neural network built based on field data	• Using kinetic energy can improve energy prediction compared to using average speed, acceleration, and road type • Neural network can predict non-linear relations between energy use and operation parameters	• Neural network does not seem to be better than regression analysis with carefully selected factors

The major research findings presented in the table above were typically derived from real-world vehicle measurements or full-system vehicle simulators. Studies that have used real-world energy measurement data, such as on-board diagnostic (OBD) data, have revealed that the most important factors affecting EV energy use and range include: vehicle powertrain design (Lorf et al., 2013; Zhang and Yao, 2015), driving behavior (Lorf et al., 2013; Qi et al., 2018; Wu et al., 2015; Zhang and Yao, 2015), roadway characteristics (Qi et al., 2018; Wu et al., 2015), battery state-of-charge (SOC) (Zhang and Yao, 2015), and ambient environmental conditions (Yuksel and Michalek, 2015). For studies that used full-system vehicle simulation tools, such as Autonomie developed by Argonne National Laboratory (ANL) (Rousseau, 2015) and FASTSim developed by National Renewable Energy Laboratory (NREL) (Brooker et al., 2015), the conclusions are generally aligned with field measurement results (Gonder et al., 2007; Lee et al., 2011; Mohd Zulkefli et al., 2014; Neubauer and Wood, 2014). In addition, the control strategies to minimize vehicle energy use were also identified in those studies with the flexibility provided by those simulation tools (Holdstock et al., 2012; Mohd Zulkefli et al., 2014; Shankar et al., 2012). Table 2 below summarizes the major factors that affect EV energy consumption:

Table 2. Major factors that affect EV energy consumption

Factor Category	Factors	Mechanism	Source (selected)
Vehicle and powertrain design	Vehicle class and body style	Affect vehicle load such as aerodynamic drag	Ehsani et al., 2018; Mi et al., 2011; Zhang & Mi, 2011
	Vehicle (plus cargo) weight	Affect vehicle load, such as uphill work against gravity and friction forces	Ehsani et al., 2018; Mi et al., 2011; Zhang & Mi, 2011
	Powertrain design	Better drivetrain design increases the range of the available torques under various speeds and enables operations under higher efficiency	Ehsani et al., 2018; Holdstock et al., 2012; Lorf et al., 2013; Mi et al., 2011; Zhang and Mi, 2011
	Control system design	Accurate driving prediction and optimal control strategy leads to most efficient energy use	Asher et al., 2017; Mohd Zulkefli et al., 2014
	Battery size	Larger batteries add fuel replacement and add more weight	Wu and Aliprantis, 2013
	Sensor and signal technology	Facilitate eco-driving and driving cycle forecast	Asher et al., 2017
Vehicle operation characteristics	Driving cycle	The speed and acceleration affect vehicle load and energy recovery from braking	Doucette and McCulloch, 2011; Ehsani et al., 2018; Mi et al., 2011; Zhang and Mi, 2011
	Driving distance	Affect total energy use and fraction of time under discharging	Gonder et al., 2007
	Road grade	Affect vehicle uphill load	Brooker et al., 2015; Doucette and McCulloch, 2011; Lee et al., 2011; K. Liu et al., 2017; Shankar et al., 2012
	State-of-charge (SOC)	Lower SOC increases battery impedance and power loss	Ehsani et al., 2018; Mi et al., 2011; Zhang and Yao, 2015; Zhang and Mi, 2011
	Hours of parking	Affect charging hours hence affect SOC	Lee et al., 2011
Environment	Temperature and solar load	Affect energy by affecting auxiliary load in all vehicles and affecting chemical reaction in batteries and fuel cells in EVs	Ehsani et al., 2018
	Humidity	Humidity affect auxiliary load and affect fuel cell performance	Ehsani et al., 2018
Other	Fuel efficiency standard	More stringent standard promotes implementation of energy saving technology	Ehsani et al., 2018
	Fuel property	Better fuel quality can better serve combustion engine and improve fuel economy	National Research Council, 2011

Some factors above can be linked to existing network-level analysis and user-level analysis. Other factors not linked with existing studies are separated as other factors. The sources of various factors are described below:

- **Network-level attributes**: traffic volume, vehicle speed, and traffic density are three fundamental elements in traffic flow and were modeled extensively in previous traffic studies (Roess et al., 2011). In this case, the average speed, VMT, and total number of vehicles for EV energy models can be extracted from most network-level analysis. Also, the road grade (and interactions between road grade and on-road speed/acceleration profiles) can be generated from existing network (Liu et al., 2018), to integrate the impacts of uphill and downhill load effects.
- **User-level attributes**: A common approach adopted in modelling EV use patterns is to collect information from national, regional or metropolitan travel surveys (Daina et al., 2017). The travel patterns may include travel schedules, O-D pairs, selected mode, recharging information, and miles travelled. More detailed EV use patterns that imply the vehicle trajectories can be employed when travel diaries and GPS data are collected (Daina et al., 2017). Another popular approach is to use activity-based travel demand models to predict daily travel schedules from synthesized households (trips and tours generated, destinations visited, and paths selected).
- **Other attributes**: Some additional variables that must be accounted for include environmental factors (temperature and humidity) that which affect vehicle performance and accessory loads, vehicle/fuel standards, and inspection and maintenance programs. Those variables are mostly fixed in the following analysis or being modeling only as the additional cost during post-processing.

However, few applications have quantified the energy impact on EV at the network level (Agrawal et al., 2016; Auld et al., 2018; Xie et al., 2012), and those existing studies considered only a subset of EV fleets and/or lack an affordable and transferrable approach for other regions. The major issues on the aforementioned findings on a large-scale transportation network can be summarized as follows:

1) **Data availability issues:** due to the low EV adoption rate (Daina et al., 2017) and lack of open data from manufacturers, most studies only covered one or two EV types at a time (*e.g.*, Gonder et al., 2007; Lorf et al., 2013; Thomas et al., 2017). The energy results from different studies are not directly comparable due to different level of uncertainties in those studies. An EV energy analysis framework that includes all common EV types is highly desirable for future applications.
2) **Vehicle specification (input data availability) issues:** the vehicle simulation tools or methods from those studies require vehicle powertrain specifications as inputs (*e.g.*, Holdstock et al., 2012; Mohd Zulkefli et al., 2014; Shankar et al., 2012). Those powertrain parameters, such as engine size, battery size and control strategies, are not directly observable in the current transportation systems. An EV energy analysis framework that uses measurable fleet information as inputs and powertrain configurations as hidden variables is preferable for network-level applications.
3) **Network scalability issues:** the scales of most studies were limited to case studies and the tested scenarios often cover only a subset of operation conditions within a highly-dynamic transportation network (*e.g.*, Gonder et al., 2007; Qi et al., 2018; Wu et al., 2015). A scalable EV energy model should be able to predict the energy use pattern under a wide

range of operating conditions and account for potential system-level changes over time, such as the operation improvements introduced by shared and autonomous vehicles.

4) **User issues:** the tested scenarios usually do not reflect actual user travel patterns. Real-world users can drive at extreme high speed, low speed, or aggressive conditions, depending on surrounding traffic condition and individual driving habits.

2.3 EV Energy Modeling

The key questions for estimating EV energy consumption is to answer the total energy required at given operating conditions and to answer how the energy demand is split among different power sources (Zhang and Mi, 2011). Given the low EV market share in the current transportation network, it is not practical to collect sufficient energy data under all possible real-world operating conditions to answer those key questions. In this case, the vehicle simulation tools can be a viable alternative to collect the energy use data for this study. An overview of state-of-art vehicle simulation tools is provided below.

2.3.1 Autonomie

Autonomie is a powerful and robust simulation tool for vehicle energy consumption and performance analysis. Autonomie, previously known as PSAT, was developed by Argonne National Laboratory (ANL) in collaboration with General Motors (Argonne National Laboratory, 2014). The simulator is a MATLAB®-based software environment and framework for automotive control-system design, simulation, and analysis. Autonomie is the primary vehicle simulation tool selected by DOE to support its U.S. DRIVE Program and Vehicle Technologies Office (VTO). The Autonomie is a commercial software package which costs $2,000 for one educational license.

Autonomie uses two parts of inputs for generating energy consumption and assessing vehicle's performance: the vehicle model and the operation process that the vehicle is running. For the vehicle model, a vehicle is defined by its architecture (like hardware) and control system (like software). The vehicle architecture includes all vehicle physical components, including chassis, wheels, engine, motor, battery, gearbox, auxiliary units, etc. The vehicle control system is defined by key control strategy parameters, including engine/motor map, regenerative braking availability, battery level for stopping, etc. The vehicle architecture and control system calculate how much energy is required to move the vehicle and how much energy to supply from fuel/battery given a specific operating condition. The vehicle process, on the other hand, defines the instantaneous operating conditions for the vehicle. The vehicle process includes second-by-second speeds, road grade and key-on/key-off time.

2.3.2 FASTSim

The Future Automotive Systems Technology Simulator (FASTSim) is a high-level advanced vehicle powertrain systems analysis tool developed by National Renewable Energy Laboratory (NREL) (Brooker, et al., 2015). FASTSim provides a quick and simple approach to compare powertrains and estimate the impact of technology improvements on light- and heavy-duty vehicle efficiency, performance, cost, and battery life. FASTSim models the energy and performance of conventional vehicles, hybrid electric vehicles, plug-in hybrid electric vehicles, all-electric vehicles, compressed natural gas vehicles, and fuel cell vehicles. FASTSim simulates the vehicle and its components using speed-versus-time drive cycles. At each time step, FASTSim accounts for drag, acceleration, ascent, rolling resistance, each powertrain component's efficiency and power limits, and regenerative braking. FASTSim is currently supported as an Excel spreadsheet tool and as Python tool.

2.3.3 MOtor Vehicle Emission Simulator (MOVES)

The MOtor Vehicle Emission Simulator (MOVES) model was developed by the U.S. Environmental Protection Agency (USEPA) to estimate emissions from on-road and off-road vehicles in the United States. In the MOVES model, emissions are defined as a function of speed and vehicle-specific power (VSP) for light-duty vehicles, or speed and scaled tractive power (STP) for heavy-duty vehicles, which better reflects acceleration and speed impacts on work and engine load (U.S. Environmental Protection Agency, 2016). The U.S. EPA's MOVES model employs a "binning" approach in modeling emissions for different on-road fleets and operating conditions, where on-road activities that falls into the same operating mode bin are assigned the same emission rate for a given vehicle type and set of environmental conditions. In MOVES, driving cycles (speed-acceleration activity) can be decomposed into operating mode bins and modeled as a function of time spent operating in each bin. This design enables MOVES to provide common emission rates for all modeling scales (macroscale, mesoscale, and microscale). The current version of MOVES includes ICEV and BEV models. Energy and emission rates from HEVs, PHEVs, and FCEVs are not available in the latest release.

In previous studies, MOVES has proven to have great scalability and has been applied for various transportation studies at both local- and regional- level (Alam et al., 2014; District Department of Transportation, 2012; Fincher et al., 2010; Liu et al., 2019; Lv and Zhang, 2012; Xu et al., 2018a). The major advantages of MOVES include: (a) it is highly data-driven, capable of deploying on-board energy and emission measurement data, and (b) it is scalable to large transportation network (Aziz and Ukkusuri, 2018; Bachman et al., 2000; Barth et al., 1996; Frey et al., 2006; Xu et al., 2019). Nevertheless, the simplified binning architecture of MOVES (U.S. Environmental Protection Agency, 2015a) which outputs average energy use and emission rates

for an array of vehicle-specific power and average speed bins, may not be directly applicable to advanced fuel and powertrain vehicles. A previous study (Xie et al., 2012) integrated MOVES with a microscopic traffic simulation model to assess emission variation under different fractions of electric vehicles. However, the Xie, et al. (2012) assessment did not contain any hybrid electric vehicles because MOVES did not contain the HEV module.

2.3.4 The Fuel and Emissions Calculator (FEC)

The Fuel and Emissions Calculator (FEC) is an operating-mode-based, life-cycle energy and emissions modeling tool developed by Georgia Institute of Technology researchers (Xu et al., 2018b, 2015). The FEC was originally designed to assist transit agencies in evaluating the purchase of new transit bus and rail technologies (Li et al., 2014), but has been expanded overtime to other on-road vehicle classes. The primary purpose of the FEC is to assist fleet owners and managers, regulatory agencies, and policy analysts in assessing the energy and emissions impacts of fleet alternatives. The open platform allows users to see all input data and every calculation, which makes the model transparent and accessible for most users.

For on-road vehicles (bus, car, truck, etc.), users can choose from ICEVs, HEVs (parallel or series), PHEVs, BEVs and FCEVs. The FEC's modeling approach estimates emissions as a function of engine load, which in turn is a function of vehicle operating parameters, allowing modelers to account for local on-road operating mode conditions as model inputs. The driving cycles of various vehicles were used to generate vehicle tractive power, and then match with specific operating mode bins for estimating energy and emissions. The operating mode bin distributions were post-processed for alternative powertrain vehicles to obtain their energy and emissions. Emissions associated with fuel production and transmission (well-to-pump) are

estimated with energy and emission rates from the GREET® (Greenhouse Gases, Regulated Emissions, and Energy Use in Transportation) model, developed by Argonne National Laboratory (Wang et al., 2018). Upstream emission rates for electric vehicle are from the Emissions and Generation Resource Integrated Database (eGRID), developed by the U.S.EPA (U.S. Environmental Protection Agency, 2018). The aggregated modeling results has been supported by empirical fuel economy data (Xu et al., 2015). However, the tool adopts transit vehicle specifications and is not directly scalable to other classes of EVs. It is highly desired to customize the modal-based approach for EVs, which both serves the purposes of predicting energy use for large transportation network and maintain a reasonable level of accuracy.

In this research effort, all potential vehicle simulation tools used for estimating vehicle energy are classified into three categories: full-system simulation, data-driven aggregate models, and simulation inference models. A full simulation model, such as Autonomie and FASTSim, can predict the power flow within a vehicle with built-in engine maps and power transmission rules (Rousseau, 2015). The model requires detailed engine specifications as input and often hard to apply for large transportation network due to cost and effort limitations (Xu and Aziz, 2019). Aggregate models, such as the MOtor Vehicle Emissions Simulator (MOVES) developed by the US Environmental Protection Agency (US EPA), have been widely used for calculating mobile source emissions (U.S. Environmental Protection Agency, 2015b). In this approach, the emission inventories were calculated by multiplying emission rates as a function of operating condition with corresponding travel activity, and then summing up the emissions from all sources in a given region (U.S. Environmental Protection Agency, 2016). These models are typically highly data-driven, integrating on-board energy and emission measurement data, and are scalable to large transportation networks (Aziz and Ukkusuri, 2018; Xu and Aziz, 2019). However, these models

also typically incorporate energy and emissions binning approaches to manage calculations. For example, the MOVES model provides emission rates by vehicle-specific power an average speed bin, providing average emission rates for a vehicle type for a range of operating conditions that tend to have similar emission rates. Aggregate models tend to over-simplify the impacts of drivetrain and emissions control systems in fleets, so they are rarely applied to advanced fuel and powertrain vehicles. Thus, both full-simulation and aggregate models have significant limitations in estimating energy use of EVs, especially combined-powertrain EVs. Therefore, an advanced modeling approach for EVs is needed.

2.4 System-level EV Cost Savings

Sustainable transportation systems are designed to efficiently satisfy most of the natural- and reasonable travel demands with lowest social-, economic-, environmental-, and resource cost, and achieve harmonious development with other social- and economic sectors (Hu et al., 2010). As the key element of achieving sustainable transportation, the adoption of EVs is highly related to the current and future travel demand, and how well the functionalities of EVs can be aligned with person's need for mobility.

As discussed in Section 1.1.2, EVs only took around 3% of total U.S. vehicle market share in 2017. The major findings from recent consumer studies have been summarized in Table 3 below. The factors affecting EV purchase and use decisions can be classified as internal factors that raised by the characteristics of EVs and external factors that associated with the outside environment and consumer characteristics (Coffman et al., 2017) and are summarized in Table 4 and Table 5 below.

Consumer behavior and attitudes towards EV adoption have been widely examined in previous studies through stated-preference surveys, meta-analysis, and literature reviews. The

customers, individuals or groups, are reluctant to purchasing EV as there are key concerns of EV have not been addressed especially the high ownership cost and limited range (Bonges and Lusk, 2016; Coffman et al., 2017; Hardman et al., 2018; International Energy Agency, 2018; National Renewable Energy Laboratory, 2016). Other limitations include lack of charging availability (Bonges and Lusk, 2016; Coffman et al., 2017; Hardman et al., 2018), insufficient incentives (Aasness and Odeck, 2015; Coffman et al., 2017) and limited models from which to choose (Coffman et al., 2017; National Renewable Energy Laboratory, 2016). Most of the factors are related to current EV performance, as discussed above, and their impacts vary under different operating conditions. The actual cost-benefits of EVs could vary given different powertrain designs, operation conditions, and various charging strategies. Quantifying the EV cost of ownership and allowed range as a function of the operation patterns is the key to address the consumer's concerns discussed above.

Table 3. Summary of EV adoption studies

Study	EV type	Sample Size	Location	Methodology	Major Findings	Major Limitations
Wang et al., 2016	HEV	433 respondents	China	Interview survey in Auto shops	• Consumers' attitude, subjective norm and perceived behavior control significantly affect adoption intention	• A biased sample could be collected
National Renewable Energy Laboratory, 2016	BEVs and PHEVs	1008 respondents	U.S.	RDD survey; weighted results to represent US population	• Major reasons for using PEV include environment, cost (operation), energy, performance, and technology considerations • Major barriers include technology, unavailability, cost (purchasing) and performance (range)	• Analysis performed mostly use descriptive information; not enough explanatory studies
Bonges and Lusk, 2016	BEVs and PHEVs	N/A	U.S.	Meta-analysis	• the major reason for low EV sales is range anxiety. • The lack of public compatible charging stations constrains the PEV target market • Improvements on charging station design and policies have the potential to relief range anxiety	• The proposed strategies not fully verified in the real-world
Nicholas, Michael A., Gil Tal, 2016	BEVs and PHEVs	10,000+ PEV owners for email survey; 264 PEV households for field data	California	Survey and field measurement	• PEVs accounted for more than 50% of household VMT except Nissan Leaf • Greater electric range encourages more charging activities • PEVs are preferred than ICEVs for household travel	• Only descriptive statistics available from the current report

Table 3 continued

Study	EV type	Sample Size	Location	Methodology	Major Findings	Major Limitations
Coffman et al., 2017	BEVs and PHEVs	N/A	Worldwide	Literature review	• Significant internal factors include vehicle ownership costs, driving range, and charging time • Significant external factors include fuel prices, consumer characteristics, availability of charging stations, and public visibility/social norms. • Available policies to support EV include financial and non-financial incentives, add charging infrastructure, and raising awareness.	• Significance of each factor depends greatly on author's judgement
Hardman and Tal, 2018	FCEV and BEV	470 FCEV owners + 1550 BEV owners =2020 samples	California	Email survey+ statistical test on results	• FCEV early adopters are mostly male, highly educated, have high household incomes, of middle to later age, have higher number of household vehicles • FCEV adopters are similar to BEV adopters	• No comparison to ICEV owner; • Only sampling CA users
International Energy Agency, 2018	All EVs	N/A	Worldwide	Literature review + meta-analysis	• Over 1 million electric cars were sold in 2017 • The high cost of ownership is largely contributed by battery cost and limit EV adoption • The policies that aim at reducing EV upfront cost are most effective	• Conclusions draw globally, not under local context • Limited number of scenarios considered
Hardman et al., 2018	BEVs and PHEVs	56 studies between 2011and 2017	Worldwide	Literature review, meta-analysis	• Availability of home charging is the biggest positive factor for EV adoption • Other positive factors include charging availability, low operation cost, interoperability of charging and number of charging • Current EV development is unlikely to affect grid	• Over sampling CA in USA

Table 4. Internal factors on EV adoption

Category	Factors	Impact	Source (selected)
Availability	Number of vehicle models on market	(-) limited number of EV models	National Renewable Energy Laboratory, 2016
Cost	Operation cost	(+) lower operation cost of EV	National Renewable Energy Laboratory, 2016
	Capital cost	(-) high Purchase cost of EV	Coffman et al., 2017; International Energy Agency, 2018; National Renewable Energy Laboratory, 2016
Battery performance	Driving range	(-) low driving range of current EV	Coffman et al., 2017; National Renewable Energy Laboratory, 2016
	Charging time	(-) long charging time of current EVs	Coffman et al., 2017

*(+ sign for positive effect on EV adoption, - sign for negative effect on EV adoption)

Table 5. External factors on EV adoption

Category	Factors	Impact	Source (selected)
Facility	Charging location	(+) higher availability (+) more charging facilities (+) high interoperability	Coffman et al., 2017; Hardman et al., 2018
Consumer characteristics	Vehicle purchasing frequency	(+) higher frequency of buying new vehicles	Nicholas, Michael A., Gil Tal, 2016
	Income	Vary by studies	Coffman et al., 2017; Nicholas, Michael A., Gil Tal, 2016
	Vehicle ownership	Vary by studies	Coffman et al., 2017; Nicholas, Michael A., Gil Tal, 2016
	Education	(+) higher education	Coffman et al., 2017
	Personal attitude	(+) concerns about environment (+) technology enthusiasm	Coffman et al., 2017; Wang et al., 2016
	Personal moral norm	(+) higher personal moral norm	Coffman et al., 2017; Wang et al., 2016
Other	Relative fuel cost	(+) higher fuel cost	Coffman et al., 2017

*(+ sign for positive effect on EV adoption, - sign for negative effect on EV adoption)

The impacts of EV cost and range have been well examined in previous studies (Elgowainy et al., 2013; Karabasoglu and Michalek, 2013; Khan and Kockelman, 2012; Liu and Lin, 2017; Needell et al., 2016; Pearre et al., 2011; Propfe et al., 2012; Zhang et al., 2013) without looking intensively into energy use and cost associated with specific travel activity and on-road operating conditions. In terms of EV cost, Propfe et al. (Propfe et al., 2012) found that a typical BEV costs 4,000 euros more than an ICEV, using energy rates from a typical driving cycle. Their results also suggested that HEVs and PHEVs can save about 2,000 euros of total ownership cost compared to an ICEV using the distance-based energy rates. Elgowainy et al. (Elgowainy et al., 2013) found that the longer range of EVs and PHEVs would have higher life-cycle vehicle and fuel costs, but most of the EVs will have similar vehicle ownership cost as ICEVs by 2035 with medium successful research and development scenarios. Energy and cost are typically estimated using average MPG, assumed annual VMT, and various development scenarios of different vehicles. Zhang et al. (Zhang et al., 2013) estimated $3.50 to $7.50/100 miles of cost saving of PHEV compared to a normal HEV baseline using pre-defined MPG and AER of EVs. In terms of range issue, it has been found that a 100-mile BEV can serve about 50% of one-vehicle households and 80% of multiple-vehicle households (Khan and Kockelman, 2012) on aggregated level under relative optimistic assumptions. Another study found the 100-mile BEV would meet the needs of 9%-32% of drivers with different levels of EV adaptations (Pearre et al., 2011). In any cases, EVs were predicted to be able to serve a much larger fraction of populations than the current market share, given the operational and cost benefits offered and limited impact of ranges issues. The actual impacts need to be analyzed at individual-level to help identify EV adoption issues under the combined effects of cost, range, and other operational characteristics.

The individual-level energy and operating cost assessment of EVs, however, remains a challenge for transportation modelers, due to the lack of connection between complex EV powertrain design and network/user factors. Needell, et al., demonstrated that an existing, affordable electric vehicle can meet the energy requirements of 87% of vehicle-days using second-by-second GPS data and NHTS travel data (Needell et al., 2016). Karabasoglu and Michalek (Karabasoglu and Michalek, 2013) found that the energy and cost saving of HEVs and PHEVs are much greater on urban streets driving condition and almost vanished on freeway conditions, with vehicle simulation performed in PSAT (the previous verion of Autonomie) under handful of driving cycles. Wu and Aliprantis (Wu and Aliprantis, 2013) calculated PHEV energy using average PHEV fuel economy, tractive energy (travel pattern) and consistent transmission efficiency for long-term national transportation planning. The proposed method suggested that the annual LDV gasoline consumption can be reduced by 66% at the end of the 40-year planning horizon, at a price of 800 Trillion Wh/year of additional electricity demand. This method is not sensitive to the potential changes in operation patterns during the entire planning period, which are likely to occur. He et al. (He et al., 2012) integrated a driving-cycle optimization algorithm into a forward-look vehicle model that is built in MATLAB®/Simulink with control parameters come from Toyota Prius PHEV. The results suggested that about 115% energy efficiency improvements can be achieved by optimizing the driving cycle. However, as the vehicle control parameters can be hard to achieve or observe in the real-world, the proposed method is hard to be applied to other cases. Khan and Kockelman (Khan and Kockelman, 2012) discussed potential miles can be electrified by a 40-mile AER PHEVs, with 80% of miles can be electrified for single-vehicle household and 50-70% of miles can be electrified for households with multiple vehicles, based on assumed 23-mile daily VMT. The conclusions were based on the average travel patterns

of a household, and the vehicle ranges are subject to change for different households and different driving patterns. Auld et al. (Auld et al., 2018) linked Autonomie with an agent-based model to estimate energy use from EV fleet in Metropolitan Detroit Region. Their study found that energy saving was about 30% by utilizing advanced powertrain technologies. However, since Autonomie is a commercial software, predicting energy use with this tool generally requires high cost and administrative permissions, which may not applicable for other research groups.

So far, assessing EV energy, emissions, and costs under the context of actual travel behavior remains a challenging task. All of the aforementioned studies suffer at least one of the following limitations:

- The EV energy use and cost have been rarely linked to full-spectrum travel behavior or customers' choice towards EV. There is no comparison among different kinds of EVs in terms of energy savings, costs, and range anxiety under the context of household travel patterns and habits (including variation of charging, driving, parking behavior). Also, there is rarely a feedback loop of sending EV utility back to users' choice side for updating trip making results.
- The EV energy model inputs and parameters often contain factors or attributes that are often not observable or available in transportation studies, including detailed powertrain specifications, control parameters, and battery capacity. To use the current model, users essentially ensure the EV fleet is the same as modeled one or post-process output from transportation studies (e.g., processing license plate, vehicle make and model, etc.), which may not be applicable in all studies.
- Many of the EV models are not scalable and compatible with high-performance computing resources. Many energy models are MATLAB®/Simulink based, which

may only be available on limited platforms and come with high cost for distributed computing.

Partial solutions to above existing challenges are proposed in this dissertation, under the constraints and limitation of current data and analytical resources. Many of the transportation models for network modeling/simulation, including travel demand models, microscopic simulation models, and dynamic traffic assignment models, are already computational intensive and may not contain all the energy-sensitive parameters (Saleem et al., 2018; Song et al., 2017; Wang et al., 2018; Zhou et al., 2015), the computational resources for calculating vehicle energy, emissions, and cost are often limited. Also, the potential development of new technologies such as shared autonomous vehicle, shared mobility, connected vehicles, internet of things will bring a variety of transportation scenarios to analyze (Chen et al., 2016; Hermawan and Regan, 2017; Rodier, 2017). A scalable and sensitive EV energy model should be able to predict the energy use patterns under a wide range of operating conditions and account for potential system-level changes in the future, such as the operation improvements introduced by shared and autonomous mobility systems. The energy model needs to be sensitive to different aspects of travel behavior (VMT, speed, aggressiveness, etc.) and on-road operation characteristics (road grade, volume, fleet composition, etc.). The model also needs to be scalable, to support the linkage with various transportation analysis tools, including activity-based models, agent-based models, micro-simulation models, and dynamic traffic assignment models.

2.5 Chapter Summary

This chapter reviewed the fundamentals of electric vehicle powertrain design and power management. The conceptual framework of EV powertrains and simplified representations of

power flow were provided as the basis for EV energy modeling. Next, the latest research efforts addressing EV energy consumption under different conditions were examined. The key attributes from transportation network and user characteristics that are linked with EV energy use were summarized. Then, the state-of-the-art modeling tools were reviewed, with pros and cons of model functionalities summarized. Finally, the current methods of quantifying EV utilities in terms of energy use and costs were presented, and outstanding research needs were identified for large-scale individual-level energy and cost analysis. This Chapter identified several research gaps, which will be partially addressed in this dissertation:

- Model scalability and accuracy are not balanced in current research efforts. Detailed EV powertrain models in general have good accuracy but are hard to apply to large-scale systems. EV fuel economy (distance-based rate) models can be applied in any scale of analysis but are not sensitive to operation patterns. A model that balances scalability and accuracy will provide dynamic energy predictions at relatively low computational costs.
- The uncertainty associated with modeling different kinds of EVs need to be compared under combined effects of network and users. Previous studies mostly focused on a subset of factors and powertrain alternatives, which only suggested partial effect of those factors on selected EV energy use/cost. These factors and vehicle alternatives need to be analyzed altogether in order to examine the global sensitivity and uncertainty and help provide the decision making process with more comprehensive information.
- The proper procedures for linking network factors, user factors, energy use, and costs need to be determined to help modelers and policy makers. Currently, various modeling approaches are used in different studies, under different context and assumptions. The results from different studies are not directly comparable, and the potential bias and errors

in the conclusions depend upon the methodology adopted and data sources employed in each study. A standardized approach, with guidance provided for specifications of inputs and uncertainty on outputs to users, would generate comparable conclusions across scenarios.

CHAPTER 3. AN ANALYTICAL FRAMEWORK FOR EV ENERGY MODELING

This chapter establishes the analytical framework for estimating EV energy and builds the linkages among EV powertrain characteristics, operation patterns, and corresponding energy use. The objectives of developing the analytical framework include: 1) identifying the strategies to properly simulate and post-process the combination of different factors, 2) selecting the important factors that affects EV energy use, 3) assessing the performance of selected statistical learning tools on modeling EV energy use, and 4) evaluating the accuracy and scalability of developed energy model for network-level applications.

3.1 Methodology Overview

Vehicle powertrain control systems focus on providing desired driver performance while also managing energy use (and emissions). Unlike the control system in an ICE vehicle, which focuses on minimizing engine fuel use, the control system for an EV optimizes fuel economy while maintaining the state of charge (SOC) of the battery at a desired level to ensure efficient operations over a wide range of driving conditions. Estimating EV energy consumption involves simulating the high-level vehicle control strategy that determines the total energy required and the corresponding split among different power sources under a specific driving condition (Zhang and Mi, 2011). Furthermore, the vehicle optimization control strategy is also constrained by physical configurations of the vehicle, such as powertrain design (*e.g.*, series-hybrid, parallel-hybrid, power-split hybrid, and all-electric) and the maximum output of each component (*e.g.*, maximum engine/motor power, battery capacity, voltage, etc.). In this case, the energy supply and its split

among different energy sources can be treated as a function of vehicle specifications, driving conditions, and instantaneous SOC.

Only a few full-system simulation tools exist that can simulate the energy consumption from vehicles with advanced powertrain and sophisticated control strategies under various driving conditions. For instance, simulation tools including Autonomie and FASTSim can predict the power flow within a vehicle with build-in engine maps and power transmission rules (Brooker et al., 2015; Rousseau, 2015). In this study, one full-system simulation tool, called Autonomie, will be used to generate energy consumption of all kinds of EVs with inputs from vehicle manufacturing information and real-world operation conditions. Compared with the other full-system simulation tool FASTSim, Autonomie has more explicit powertrain specifications and higher flexibility to configure the vehicle components and corresponding parameters. A screenshot of a typical power-split hybrid electric vehicle configuration used in Autonomie is given in Figure 8 as an example of vehicle configuration in the tool.

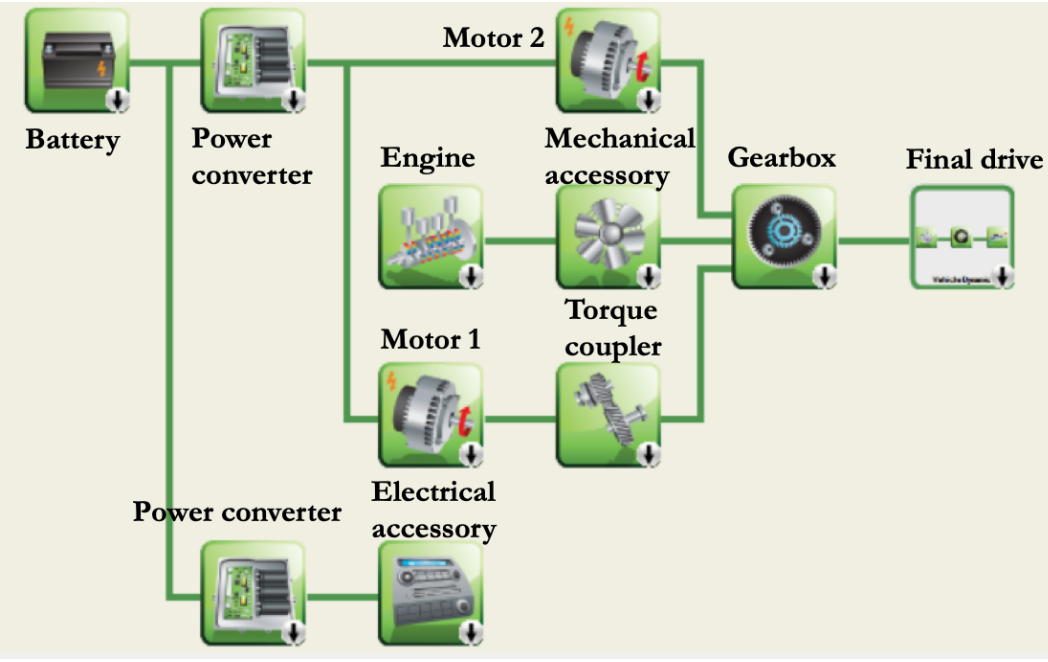

Figure 8. An example of vehicle configuration in Autonomie

However, it is challenging to directly apply such full-system simulation tools for large transportation network due to the gap between high fidelity requirements of those tools and the collected data from most transportation studies. A recent survey investigating how Metropolitan Planning Organizations (MPOs) preparing transportation inputs for emission modeling suggested that most MPOs used vehicle registration data for fleet information, used traffic volumes and average speeds (by facility type) from their regional travel demand model, and typically did not generate their own operating condition compositions (Fincher et al., 2010). From a transportation system perspective, the level of details from common transportation studies is insufficient for these full-system simulation tools. From the vehicle-level perspective, the optimizations are often achieved using standardized cycles and iterative offline runs for best solution (Hu et al., 2016; Mohd Zulkefli et al., 2014; Salmasi, 2007), while feeding in large data will greatly slow down the process. In this study, to take advantage of such tool but iterate through comprehensive traffic conditions, a trade-off between model complexity and scalability needs to be made for large scale application, with different considerations given to measurable and unmeasurable factors from transportation studies.

In this preliminary study, to simplify the modeling process but keep a reasonable level of accuracy, the researchers categorized the energy modeling factors into direct factors that can be linked to specific network attributes and indirect factors that need to be collected from other resources. The indirect inputs, including vehicle powertrain architecture and control system, are assumed hard to achieve in most transportation studies, and are modeled using predefined vehicles. The direct variables, including vehicle driving conditions and battery SOC, are assumed to be achievable in transportation projects and are simulated under a wide range of possible conditions. Both types of inputs are feed into Autonomie, to generate near-ground-truth energy consumption.

To demonstrate the effectiveness of the modeling framework, the classification and regression tree (CART) method (also known as modal-based approach) is selected to define relationship among vehicle energy consumption, driving conditions and SOC for any kind of EV and generate a finite number of clusters by different operating conditions. The CART method has been widely adopted to generate the energy and emission rates for application in various vehicle simulation tools including MOVES (Frey et al., 2002; Washington et al., 1997; Wolf et al., 1998). With this approach, the network-level EV energy use can be defined by matching the driving conditions from the network and the energy rate defined in the CART bin results. The workflow of generating data for CART analysis, implementing and verifying CART results and applying generated EV models to large-scale transportation network is provided in **Figure 9**.

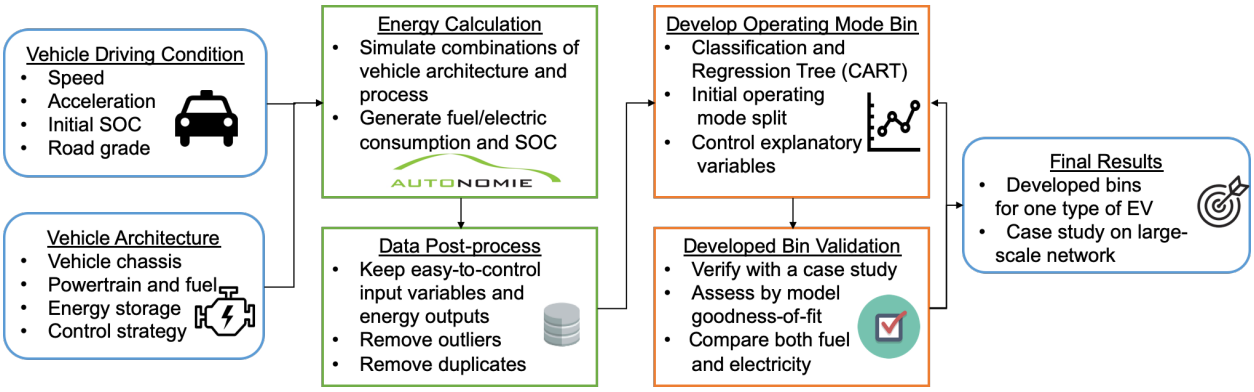

Figure 9. Workflow on developing modal-based approach for estimating EV energy consumption

As the flow chart indicated, the first step is to prepare a relatively represented input sets, including vehicle specification inputs and operational inputs. Next, the large number of simulation runs are performed in Autonomie with prepared input data sets. The simulation results are post-processed to remove erroneous data, remove duplicates and keep useful information. After post-processing, the relationship between energy consumption and driving conditions are defined within a statistical model framework using the cleaned dataset. The initial operating conditions

are separated using prior engineering and physics knowledge. The CART method is used to further classify the operating conditions into smaller distinct clusters or so-called "bins" based on different levels of energy and electricity use in on-road operations. The developed clusters are verified and consolidated where practicable by comparing the energy use calculated from the CART results and energy use from Autonomie based on real-world trips. Finally, a network-level energy model is performed using validated CART results, under various EV market share scenarios. The model performance will be assessed based on its interpretability, accuracy at different aggregation levels and sensitivity to network attributes.

3.2 Input Preparation

For the vehicle configuration attributes, we chose a Toyota Prius Prime plug-in hybrid-electric vehicle (PHEV) with 20 miles of all-electric range (AER) as a typical EV. The Toyota Prius Prime, which adopts a series-parallel hybrid powertrain design with one engine and two generator motors, are equipped with both torque coupling and speed coupling devices (Ehsani et al., 2018) and a rechargeable battery. This design provides high flexibility (high degree-of-freedom) in energy output, across different control modes (engine-alone, motor-alone, hybrid with speed-coupling, hybrid with torque coupling, etc.). The simulated Toyota Prius Prime uses the same Toyota powertrain design ("Hybrid Synergy Drive (HSD)") as various other popular EV models including Toyota Prius, Toyota Camry hybrid, Toyota Mirai, Nissan Altima hybrid and Lexus hybrid (Wikipedia, 2019). In 2017, the models with HSD powertrain accounted for about 50% of HEV sales and about 10% of PEV (PHEV+BEV) sales (U.S. DOE Alternative Fuels Data Center, 2019a). The full-system simulation model developed in Autonomie has been previously calibrated using vehicle testing data by Argonne National Lab and has the prediction errors within 5% under most test cases (Jeong et al., 2019). We used the default Autonomie model "PHEV20 Power Split

Midsize Gasoline with One-way Clutch". The maximum engine power is 97.7 kW. The maximum power of first motor is 68.3 kW and the maximum power of second motor is 56.6 kW. The battery capacity is 37.6 Ah (8.11 kWh). The vehicle chassis is 1712 kg, with 2.372 m^2 frontal area and 0.311 drag coefficient. In this model, the coefficient of rolling resistance is assumed to be a function of speed, with $c_r = 0.008 + 0.00012\mathrm{v}$ (where v is speed). For vehicle control strategy, the vehicle uses the power-split control with target SOC set as 0.3, maximum SOC as 0.9 and minimum SOC as 0.1.

For the vehicle driving conditions, wide-ranges of speed, acceleration and SOC combinations are considered in this study. The actual driving condition collected from real-world measurement or simulation is expected to be a subset of the simulated conditions. The initial SOC levels are set from 10% to 90%, in 5% increments. The speed and acceleration data come from the 18 default driving cycles used in MOVES, with average speeds ranging from 2.5 mph to 76 mph. The speed and acceleration distribution are represented in Figure 10 below. Each cycle is simulated at different initial SOC levels and repeated five times to allow the SOC to stabilize around the target SOC level. Autonomie uses second-by-second cycles and initial SOC as inputs and generates linear splined cycles at 0.1s resolution (Argonne National Laboratory., 2014).

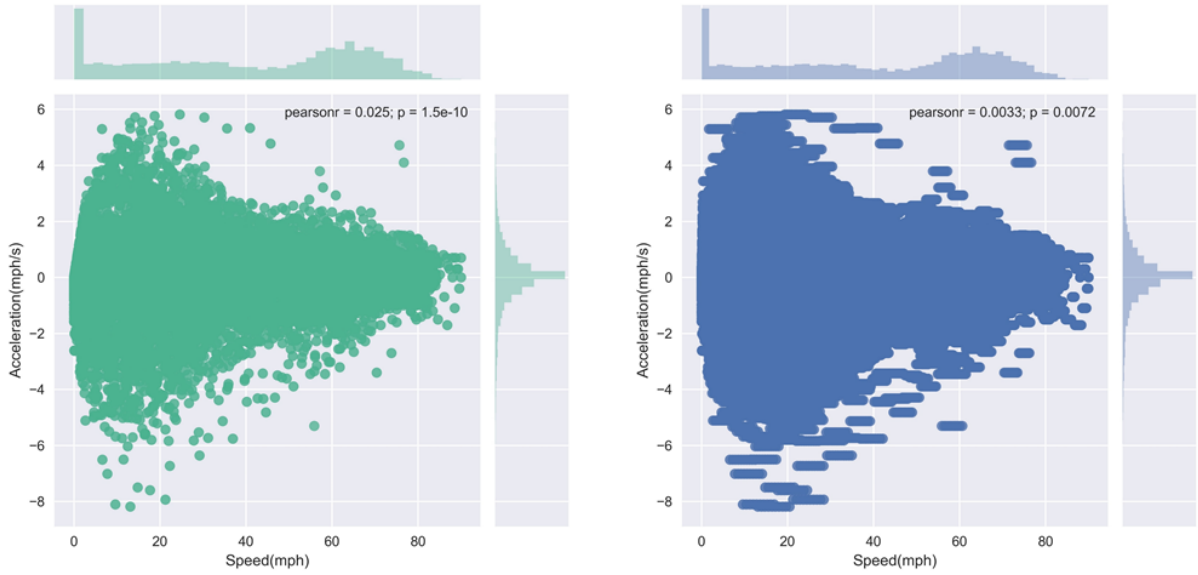

Figure 10. Speed and acceleration distributions of input cycles (left) and Autonomie splined cycles (right)

Moreover, the vehicle characteristics and on-road operating conditions both affect power demand, which can be quantified using the equation presented earlier (Ehsani et al., 2018; Mi et al., 2011; Zhang and Mi, 2011) from Fundamentals of Vehicle Design and Operation:

$$P_T = F_T v = Mav + \frac{1}{2}\rho\, v3AC_d + c_r Mgvcos(\alpha) + Mgvsin(\alpha) \quad (3)$$

However, it is not enough to solely rely on tractive power, as distinct driving conditions can fall into the same power level (e.g., low-speed hard-acceleration and high-speed cruising can have the same power demand). In this case, the speed and acceleration information are kept for the following analysis, while the vehicle configurations are covered by vehicle tractive power. The correlation matrix is provided here to support this conclusion.

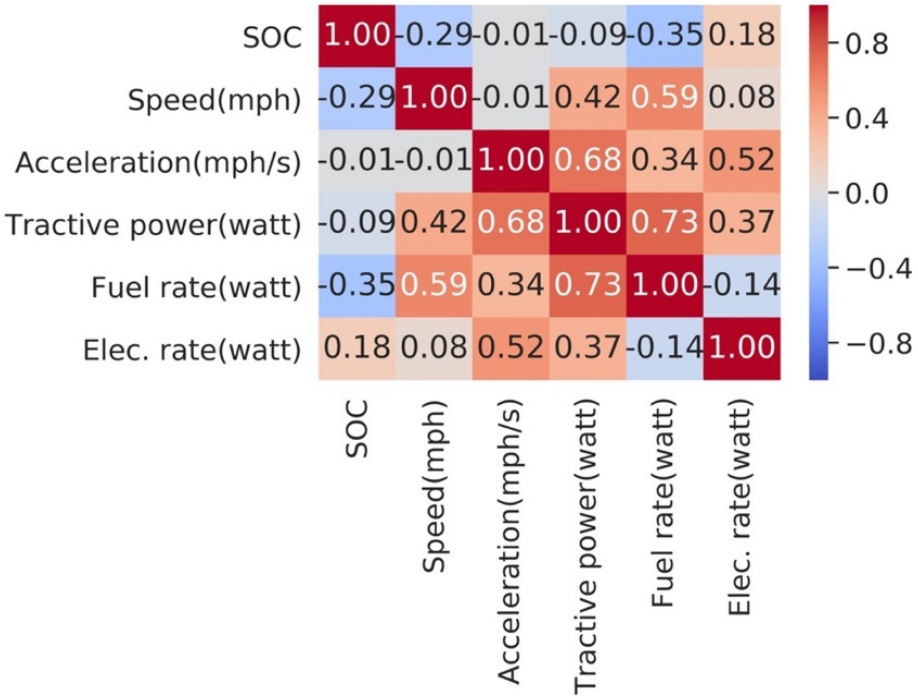

Figure 11. Pearson's correlation matrix of variables

3.3 Autonomie Simulation and Post-processing of Results

In Autonomie, the Vehicle Propulsion Controller (VPC) allocates propulsion and braking demand among components at vehicle level using the given vehicle model and driving cycle (Argonne National Laboratory., 2014). The low-level controls use inputs from the VPC and powertrain components to coordinate the tasks of components (engine, clutch, gearbox, motor) during transient processes. After assigning tasks within the vehicle, the fuel and electricity supply can be determined using demand signals and energy conversion efficiency. For the fuel rate, given a requested torque from the powertrain controller, the engine model provides the torque at certain engine speed and determines the fuel rate. For the electric rate, the battery pack is modeled as a charge reservoir and an equivalent circuit whose parameters are a function of the remaining charge in the reservoir. The positive/negative signs in the electric rate output indicate if the battery is charging (charging sustaining, CS) or discharging (charging depleting, CD), and the electricity

consumption is the discharging energy subtracted by charging energy (from the fuel or regenerative braking).

After simulating input combinations, Autonomie generates hundreds of output attributes, with only a few attributes are measurable or estimable in the engineering practice. In this case, only **vehicle speed, acceleration, SOC, tractive power and fuel/electric rates** are kept for preliminary studies. Also, the fuel rate and tractive power could be unreasonably high given extreme input conditions which go beyond vehicle physical constraints (e.g., combinations of high speed, hard acceleration and low SOC). Such erroneous data are removed if they are significantly higher than 99 percentiles of the training set, and 1% of data were removed from this step. Finally, there are many duplicated records in the output data as the input cycles are executed recursively. The duplicated data are removed to accelerate the analysis process.

3.4 Statistical Analysis with CART

With the cleaned dataset, a statistical model framework is established to delineate and simplify the relationship between energy consumption and operating conditions. CART analysis (Frey et al., 2002; Hastie et al., 2009; Washington et al., 1997; Wolf et al., 1998), also known as hierarchical tree-based regression (HTBR), is primarily used in this framework to classify operating conditions into smaller and homogeneous clusters, while the clusters are further applied to develop the discrete fuel consumption and electricity use rates in operating mode bins. The key advantages of the tree compared to other statistical categorization methods (e.g., K-nearest neighbor, support vector machine and neural network) are the interpretability and simplicity of its results (Hastie et al., 2009). The method is non-parametric, which is easier to calibrate and transfer. The model has a low sensitivity to outliers in the data. This method is also highly data-driven and well suited for distributed computing resources (Frey et al., 2002; Liu et al., 2019). The primary consideration in

statistical model development is the objective and bias-variance trade-off, which suggests the model cannot achieve high prediction accuracy and keep a simple structure at the same time (Chen, 2014). In this case, several supporting techniques are taken to balance the model interpretability and accuracy:

- Previous engineering practice and physical knowledge is introduced for the initial split within the entire dataset into operating modes to reduce the variance.
- No more than three levels of tree depths were used for developing the cluster to maintain the result interpretability.
- The final clusters are limited within 30 nodes for fuel and electricity use respectively to reduce complexity and prevent overfitting.

3.4.1 Initial Operating Mode Split

For determining the final tree structure, the authors realized that finding the best binary partition in terms of minimum sum of squares is generally computationally infeasible (Hastie et al., 2009). In this case, a final tree structure with equivalent goodness-of-fit as other trees but is more superior in terms of interpretability is preferred in this study. The operating modes employed in MOVES (U.S. Environmental Protection Agency, 2015a) are used to the split dataset into six initial operating modes, where each operating mode may be accommodated with a specific control strategy:

- **Braking**: instantaneous acceleration ≤ -2.0 mph/s or acceleration < -1 mph/s for three continuous seconds.
- **Idling** (stand-by): vehicle speed <= 1 mph.
- **Coasting**: vehicle is not braking nor idling, with tractive power < 0 watt, speed <= 50mph.

- **Low-speed propelling:** vehicle is not braking nor idling, with tractive power >= 0 watts, and speed between 1 mph and 25 mph.
- **Medium-speed propelling:** vehicle is not braking nor idling, with tractive power >= 0 watts, and speed between 25 mph and 50 mph.
- **High-speed propelling:** vehicle is not braking nor idling, with speed > 50 mph.

3.4.2 CART Clustering

After initial driving condition partitioning, the CART model is applied to individual operating modes to further split on-road operating conditions based upon their energy use. The CART model predicts value with respect to a region (or leaf node) instead of individual points (Hastie et al., 2009). The model iteratively selects the best set of features and the partitioning those features into smaller regions (intervals) to minimize the variability of dependent variables within each region. In this study, the fuel consumption and electricity consumption were predicted in separate CART models as a function of instantaneous vehicle tractive power, SOC, speed and acceleration. The CART regression model can be represented as follows:

$$\boldsymbol{f(x) = \sum_{m=1}^{M} \omega_m I\{x \in R_m\}} \quad \textbf{(4)}$$

Where

R_m - the mth region (leaf node)

M - the total number of regions

ω_m - the coefficient (score) for the region

It is computationally infeasible to search all regions and try all splitting depths, as there is an infinite number of potential trees. In this case, the maximum splitting depth is set as three and maximum leaf nodes are set as eight to maintain the interpretability of the results. The function

goal to achieve the best-split tree in this case is to minimize the tree structure score, which is defined as following (Chen, 2014):

$$\boldsymbol{Obj} = \sum_{n=1}^{N} \boldsymbol{l}(\boldsymbol{y}, \hat{\boldsymbol{y}}) + \boldsymbol{\Omega}(\boldsymbol{f}) \quad \textbf{(5)}$$

Where, $l(y, \hat{y})$ is the loss function and $\Omega(f)$ is the complexity of the grown tree. In this study, the quadratic form of loss function, or mean-square-error (MSE) is used. The tree complexity is the weighted total of tree nodes and the sum of score squares in each node. The loss function and complexity function are listed below:

$$\boldsymbol{l}(\boldsymbol{y}, \hat{\boldsymbol{y}}) = (\boldsymbol{y} - \hat{\boldsymbol{y}})^{\boldsymbol{2}} \quad \textbf{(6)}$$

$$\boldsymbol{\Omega}(\boldsymbol{f}) = \boldsymbol{\gamma M} + \frac{\boldsymbol{\lambda}}{\boldsymbol{2}} \sum_{\boldsymbol{m=1}}^{\boldsymbol{M}} \boldsymbol{\omega_m}^{\boldsymbol{2}} \quad \textbf{(7)}$$

Where γ and λ are coefficients for regularization terms. In our case, since M is fixed, $\gamma = 0$ is used. The $\lambda = 1$ based on previous engineering practice.

CART clusters are generated for fuel and electricity consumption, respectively. This is important because fuel may be used to provide tractive power or to recharge batteries, and electricity may be used at higher rates to provide acceleration under certain conditions. If the clusters are the same for fuel consumption and electricity use, it means the fuel and electricity follow a similar pattern and the clusters can be shared for both energy sources. The initial model specification and final condensed model, and improvements resulting from consolidation will be discussed in the next section.

3.5 Application of CART Results to the Atlanta, GA Network

Using the CART results, the energy consumption for EVs can be estimated for a wide range of operating conditions. In this study, a separate set of driving profiles for the same vehicle

technology was used to test the cluster performance and to adjust the pre-determined clusters. The operation data for cluster assessment come from the light-duty vehicle real-world driving dataset from the Atlanta Household and Activity Travel Survey in a 20-County Region of Metro Atlanta (Atlanta Regional Commission, 2011; Liu et al., 2019, 2018). The test data consist of 150 second-by-second sample trips collected for multiple conventional vehicles under a wide range of operating speeds and facility types. These test trips are simulated in Autonomie with random initial SOC to predict energy consumption. The clusters developed in the CART analysis from the training data set are then used to predict energy consumption. The goodness-of-fit statistics from testing results are used to merge clusters when there is no significant loss in prediction accuracy. The performance of the final set of clusters will be assessed (a) by simplicity and interpretability, (b) by the accuracy of prediction, and (c) sensitivity to network attributes. The verification also serves as an illustration of how the clusters can be adopted from different transportation inputs. The initial model specification (dependent and independent variables) and modeling results will be presented in the next section.

Finally, a network-level case study is performed using the Atlanta Regional Commission's 2015 Activity-based Model (ABM15) model (Atlanta Regional Commission, 2012) for metropolitan Atlanta, GA, with a population of 5.68 million people, 2.19 million household and 4.16 million vehicles. The ABM15 modeled transportation network contains 73,822 roadway links and predicts 19.9 million trips per day in the region. Regional energy consumption was generated from previous studies with the assumption that the entire on-road fleet is composed of conventional vehicles (Xu et al., 2018a). In this study, the energy consumption with different market shares of EV is estimated using link-level traffic attributes (average speed, road type, link length and volume) and a hypothetical distribution for average SOC. For each link, and each scenario run, a portion

of the on-road fleet vehicles is assumed to be PHEVs (pre-assumed market shares). Then, the corresponding driving cycles were randomly selected from real-world driving data collected in the Atlanta travel survey (Atlanta Regional Commission, 2011) for all the PHEVs on the same link based on link road type and link average speed. The average SOC for each vehicle on that link is drawn from an assumed uniform distribution from 20% to 90%. The driving cycle and average SOC levels serve as inputs to calculate the power demand using equation (1) and then used to match with CART energy rates and adjusted by link length. After calculating the energy consumption per PHEV and per link, the total energy consumption for the network is calculated by summarizing the energy use contributions from PHEVs and conventional vehicles across all of the links. The network-level and aggregated results are provided for assessing the sensitivity of the CART method to various network attributes, such as volume, EV market share and average speed.

3.6 Results and Discussions

In this section, the methodology introduced in the previous section has been applied to classify the operating conditions into an initial finite number of clusters, consolidate the clusters, and then apply the final model to a case study. First, the CART clusters were introduced and assessed for its interpretability using prior engineering knowledge. Second, the CART clusters were assessed using a test data set prepared by vehicle operation data from real-world measurements. Clusters were consolidated based upon the verification test results to facilitate faster modeling. Finally, a large-scale network case study is performed using the CART results and tested driving profiles. The sensitivity of modeled energy use to various network attributes, including EV market share, traffic volume and traffic speed are assessed using the modeling results.

3.6.1 CART Classification Results

After making an initial operating mode allocation, the CART method is applied to classify driving modes under each condition for fuel and electricity consumption, respectively. The fuel consumption rates and electricity consumption rates were predicted as a function of instantaneous vehicle speed, acceleration, vehicle tractive power and SOC. The definitions of clusters were summarized in Table 6 and

Bin ID	Category	Speed (mph)	Acceleration (mph/s)	Tractive Power (watts)	SOC	Energy rates (Watts)	Energy use scenario
0	Braking	Any	a<-2 or a<-1 for three continuous seconds	Any	Any	609	-
1	Idling	<=1 mph	Not braking	Any	>0.29	70	L
2					<=0.29	68,753	H
10	Coasting	<=50 mph	Not braking	<0	>0.29	400	L
11					<=0.29	44,225	H
12	Low speed	1mph-25mph	Not braking	0-12,000	>0.3	1,827	VL
13				12,000-29,000	>0.31	2,096	L
14				0-12,000	0.29-0.30	12,679	ML
15				12,000-23,000	<=0.31	41,364	SL
16				0-12,000	0.28-0.29	51,639	SH
17				>29,000	>0.31	66,511	MH
18				>23,000	<=0.31	75,214	H
19				0-12,000	<=0.28	87,134	VH
22	Medium speed	25-50mph	Not braking	0-10,000	>0.305	1,264	VL
23				10,000-21,000	>0.305	9,338	L
24				0-9,000	<=0.305	14,449	ML
25				21,000-30,000	>0.31	25,876	SL
26				9,000-21,000	<=0.305	42,728	SH
27				21,000-30,000	<=0.31	70,573	MH
28				>30,000	>0.3	86,816	H
29				>30,000	<=0.3	104,208	VH
31	High speed	>50 mph	<=-0.4	<=20,000	>0.29	16,717	VL
32			>-0.4	<=20,000	>0.3	21,616	L
33			<=-0.4	<=20,000	<=0.29	42,491	ML
34			Not braking	20,000-30,000	>0.3	49,217	SL

35			>-0.4	<=20,000	<=0.3	55,962	SH
36			Not braking	20,000-30,000	<=0.3	85,989	MH
37			Not braking	>30,000	>0.29	108,574	H
38			Not braking	>30,000	<=0.29	142,424	VH
Final range		[0, 90]	[-8.18, 5.82]	[-60,000, 60,000]	[0, 0.902]	[70, 142,424]	

Table 7 (electricity) below. The energy use scenarios among each operation category are represented by low (L) to high (H) levels, which may contain up to 8 levels ordered from very low (VL), low (L), moderate low (ML) and slightly low (SL), to slightly high (SH), moderate high (MH), high (H) and very high (VH).

Table 6. CART fuel clusters

Bin ID	Category	Speed (mph)	Acceleration (mph/s)	Tractive Power (watts)	SOC	Energy rates (Watts)	Energy use scenario
0	Braking	Any	a<-2 or a<-1 for three continuous seconds	Any	Any	609	-
1	Idling	<=1 mph	Not braking	Any	>0.29	70	L
2					<=0.29	68,753	H
10	Coasting	<=50 mph	Not braking	<0	>0.29	400	L
11					<=0.29	44,225	H
12	Low speed	1mph-25mph	Not braking	0-12,000	>0.3	1,827	VL
13				12,000-29,000	>0.31	2,096	L
14				0-12,000	0.29-0.30	12,679	ML
15				12,000-23,000	<=0.31	41,364	SL
16				0-12,000	0.28-0.29	51,639	SH
17				>29,000	>0.31	66,511	MH
18				>23,000	<=0.31	75,214	H
19				0-12,000	<=0.28	87,134	VH
22	Medium speed	25-50mph	Not braking	0-10,000	>0.305	1,264	VL
23				10,000-21,000	>0.305	9,338	L
24				0-9,000	<=0.305	14,449	ML
25				21,000-30,000	>0.31	25,876	SL
26				9,000-21,000	<=0.305	42,728	SH
27				21,000-30,000	<=0.31	70,573	MH
28				>30,000	>0.3	86,816	H
29				>30,000	<=0.3	104,208	VH
31	High speed	>50 mph	<=-0.4	<=20,000	>0.29	16,717	VL
32			>-0.4	<=20,000	>0.3	21,616	L
33			<=-0.4	<=20,000	<=0.29	42,491	ML
34			Not braking	20,000-30,000	>0.3	49,217	SL
35			>-0.4	<=20,000	<=0.3	55,962	SH
36			Not braking	20,000-30,000	<=0.3	85,989	MH
37			Not braking	>30,000	>0.29	108,574	H
38			Not braking	>30,000	<=0.29	142,424	VH
Final range		[0, 90]	[-8.18, 5.82]	[-60,000, 60,000]	[0, 0.902]	[70, 142,424]	

Table 7. CART electricity clusters

Bin ID	Category	Speed (mph)	Acceleration (mph/s)	Tractive Power (Watts)	SOC	Energy rates (Watts)	Energy use scenario
-4	Regenerative braking	Any	a<-2 or a<-1 for three continuous seconds	<=-28,000	Any	-25,156	VL
-3				<=-17,000 and > -28,000	Any	-15,185	L
-2				<=-7,000 and >-17,000	Any	-8,392	H
-1				>-7,000	Any	-1,874	VH
1	Idling	<=1 mph	Not braking	Any	>0.29	300	L
2					<=0.29	-17,425	H
10	Coasting	<=50 mph	Not braking	<=-6,000	Any	-7,213	L
11				>-6,000 and <0	Any	-1,429	H
12	Low speed	1mph-25mph	Not braking	0-3,000	<=0.29	-16,492	VL
13				3,000-8,000	<=0.29	-16,126	L
14				>8,000	<=0.29	-15,265	ML
15				0-3,000	>0.29	1,747	SL
16				3,000-8,000	>0.29	5,922	SH
17				>8,000	<=0.31	4,131	MH
18				8,000-17,000	>0.3	13,119	H
19				>17,000	>0.3	19,225	VH
22	Medium speed	25-50mph	Not braking	>0	<=0.28	-19,324	VL
23			Not braking	>0	0.28-0.29	-8,642	L
24			Not braking	>0	0.29-0.3	1,979	ML
25			Not braking	0-5,000	>0.305	3,363	SL
26			Not braking	>0	0.3-0.305	4,432	SH
27			>2.4	>11,000	>0.305	8,258	MH
28			Not braking	5,000-11,000	>0.305	9,138	H
29			<=2.4	>11,000	>0.305	17,827	VH
31	High speed	50-80 mph	Not braking	Any	<=0.3	958	VL
33				Any	>0.3	11,321	L
35	Super high speed	>80 mph	Not braking	<=20,000	Any	14,357	H
37				>20,000	Any	30,814	VH
Final range		[0, 90]	[-8.18, 5.82]	[-60,000, 60,000]	[0, 0.902]	[-25,156, 30,814]	

A. **Braking:** during braking, the engine is generally turned off, so there was one cluster used for fuel. The battery can be charged during regenerative braking, and the charged energy

depends on the braking aggressiveness (captured by negative tractive power). In this case, the braking for electricity was divided into four distinct clusters based on tractive power.

B. **Idling:** during vehicle idling, engine and motor are mostly standby unless a low battery level present. The engine will be turned on to charge the battery once the SOC is low. So, two clusters were split for both fuel and electricity based on SOC level.

C. **Coasting:** the status of the engine during coasting can be generally split into two cases. While SOC is high, the engine is likely running at low power output. While SOC is low, the engine needs to provide additional power to supply the battery. On the other hand, the energy can be charged into the battery depend primarily on the tractive power according to CART results. The charged energy is higher with much lower tractive power demand.

D. **Low-speed propelling**: the major determinants for energy use under low-speed propelling are tractive power and SOC. With high SOC and low power demand, the vehicles are more likely on electric-drive mode with high electricity consumption (Zhang and Mi, 2011). While in low SOC and modest power demand, the vehicles are more likely on power-split mode, with engine turned on to propel the vehicle and charge the battery. For other conditions, the work is split between engine and motor, with both fuel and electricity consumption presented.

E. **Medium-speed propelling**: the energy consumption under medium speed propelling follows a similar pattern as low-speed, except the acceleration is introduced to further split electricity consumption. The vehicles are likely operating in hybrid mode during acceleration with both fuel and electricity supply (Zhang and Mi, 2011). The level of electricity supply depends on the aggressiveness of acceleration according to CART results.

F. **High-speed propelling**: the significant difference under high-speed operation is that the battery is less likely to be sufficiently charged as a larger portion of engine power is used to provide propulsion efforts. The motor is more likely to standby or under low power output. Also, under significant high speed (> 80 mph), the motor is requested to work together with engine. For the fuel consumption part, the energy consumption increases drastically with larger acceleration, larger power demand and lower SOC level.

The energy rate distribution for each cluster was displayed in the following box plots (Figure 12), with lower bound, first quartile, median, third quartile and upper bound marked on the box, respectively. It can be observed that the energy rates under each CART clusters are relatively distinct from each other and covers a wide range of energy consumption. However, some clusters have a significantly larger variance than others, due to the limited number of clusters specified in the model. As introduced above, the high variance is the price to be paid for estimating a simple, tree-based structure due to the objective and bias-variance trade-off (Chen, 2014; Hastie et al., 2009). For reducing variance in estimation, more complex statistical methods or more vehicle system-level knowledge needs to be introduced.

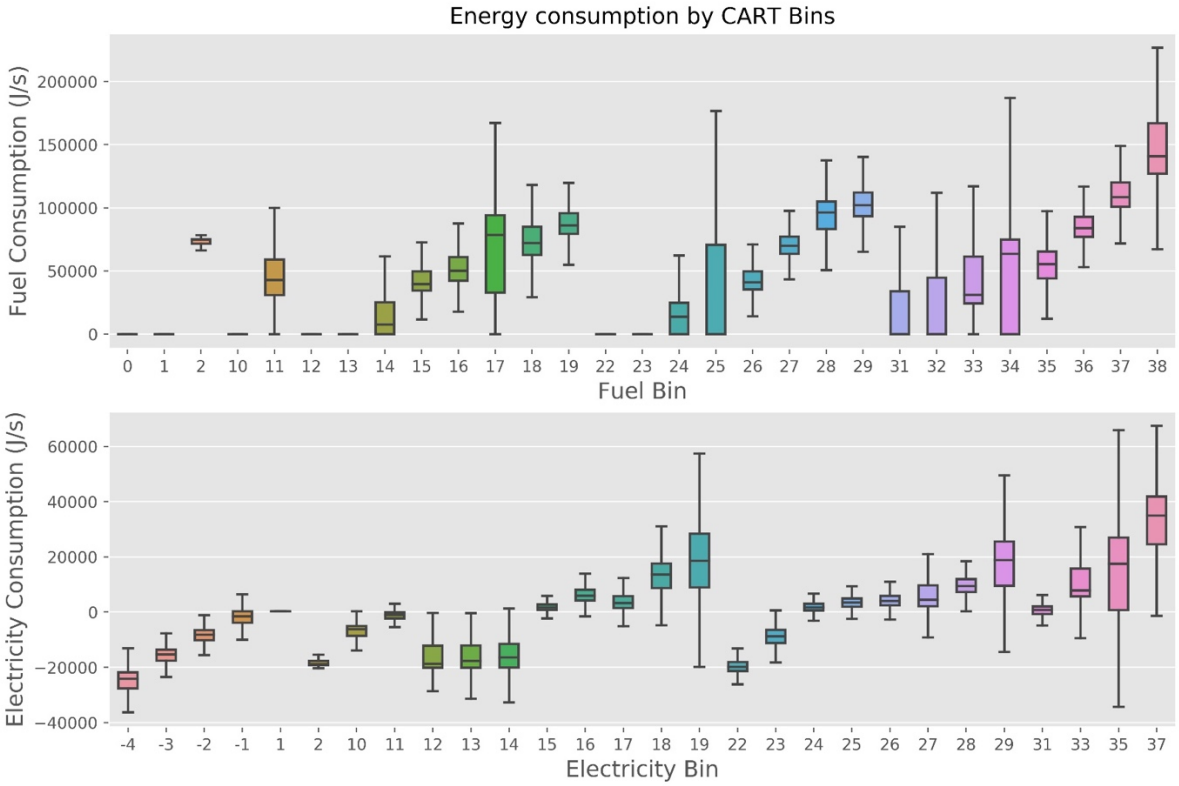

Figure 12. Energy rate distribution for CART fuel clusters and electricity clusters

3.6.2 CART Cluster Verification

The performance of CART classified clusters was tested using a case study with input data from real-world trips (monitored second-by-second). The speed and acceleration distributions of input testing cycles and Autonomie splined testing cycles are shown in the figure below. The testing represents a wide range of real-world operating conditions. The input cycles (Figure 13) were processed with the same PHEV in Autonomie to obtain the energy consumption and processed with the initial proposed CART clusters to predict energy consumption and electricity use.

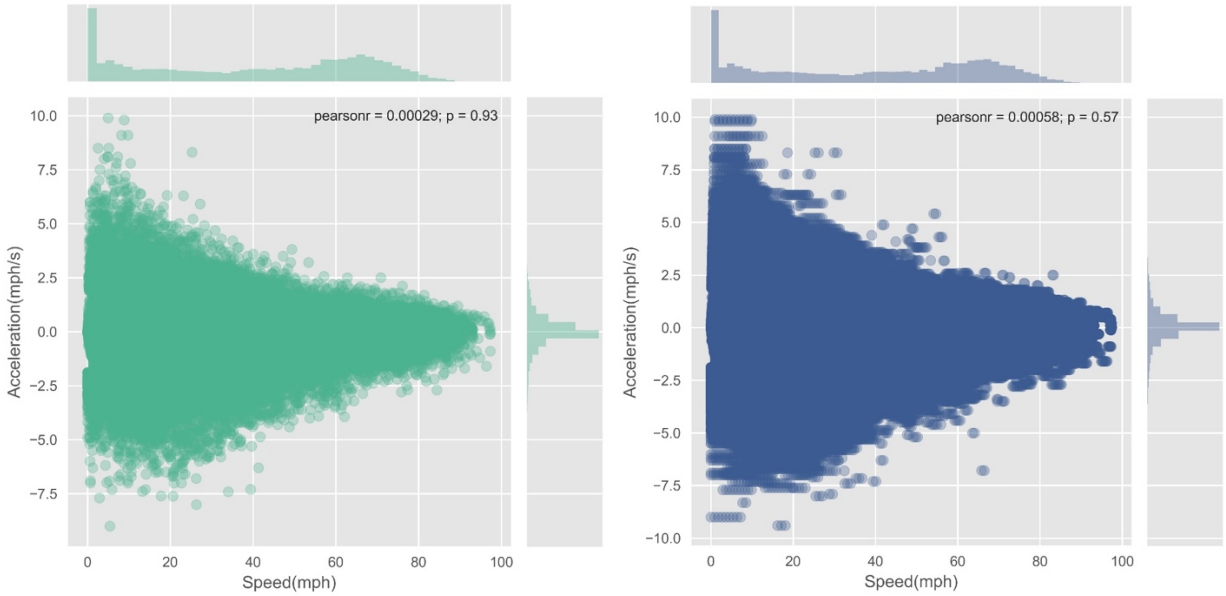

Figure 13. Speed-acceleration distribution for input testing cycles (left)

The performance of CART clusters was assessed at trip-level and instantaneous-level. For trip-level results, the total energy consumption by trip generated from Autonomie and CART clusters were compared using an ordinary linear regression as indicated in Figure 14 below. The R^2 value and standard error of the coefficient is also provided as indicators of model performance. For both fuel and electricity consumption, the predicted energy consumption is close to the ground-truth energy consumption with low prediction variance (represented by the shaded area). The R^2 of both fuel and electricity use predictions are above 0.95, indicating that the CART-based model application replicates the Autonomie simulation results fairly well.

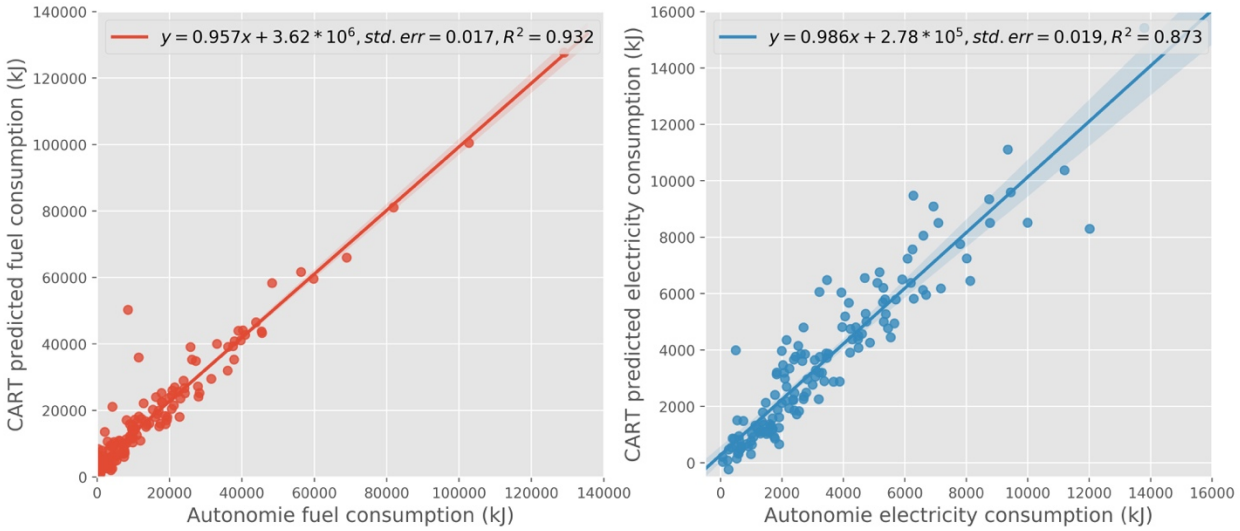

Figure 14. Trip-level CART cluster energy prediction VS. Autonomie energy results

The instantaneous energy prediction from CART versus Autonomie generated energy were then further compared at a disaggregate level (Figure 15). Autonomie generated energy consumption is continuous and sensitive to the fluctuation of speed and SOC, while the CART-predicted energy consumption still follows a similar trend as Autonomie results but eliminated the small oscillations. For fuel consumption, the CART may predict positive energy consumption while the engine is off. It suggests the control strategy within a certain cluster (certain driving condition) actually differs, and further split on vehicle conditions can be made based on different control response.

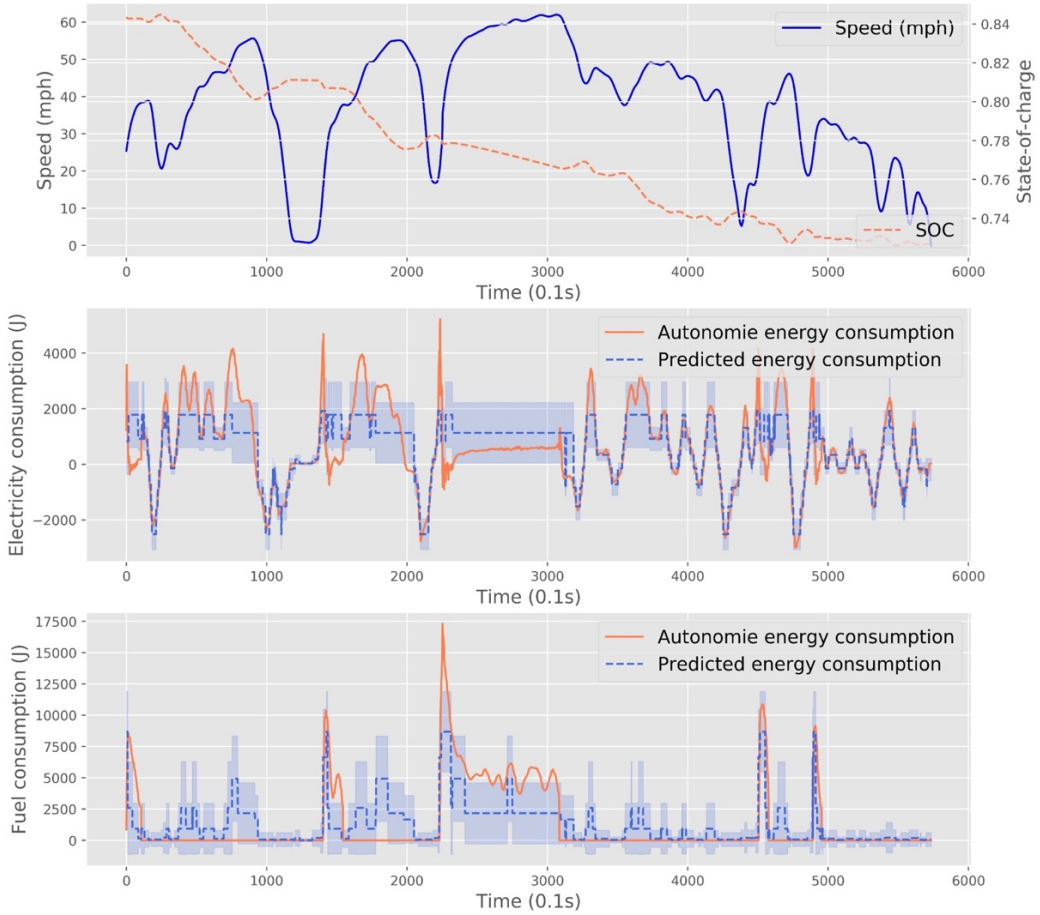

Figure 15. Instantaneous energy prediction VS. Autonomie energy results

Overall, the CART classified cluster system can predict Autonomie simulated energy consumption with reasonable accuracy. Limited by the statistical method applied and the maximum number of clusters, the variance of prediction is still large under certain conditions and can be further improved by introducing more advanced methods and more variables into consideration (e.g., control strategy).

3.7 Large-Scale Transportation Network Case Study

A case study with the Metropolitan Atlanta network is performed by applying the CART results and real-world driving cycles applied in the model testing chapter. First, link-level traffic attributes (traffic volume, average speed, etc.) and energy use from ICEVs were generated by the

regional travel demand model developed by the Atlanta Regional Commission (Atlanta Regional Commission, 2012; Xu et al., 2018a). The activity-based model (ABM) transportation network is composed of 74,505 roadway links and predits 17.7 million personal vehicle trips per day in the region for 2024. The predicted travel speeds by time of day were calibrated and verified by the planning agency using FHWA's National Performance Management Research Data Set (NPMRDS), and the daily VMT derived from traffic volume on links were verified by the agency using GDOT HPMS data (Atlanta Regional Commission, 2016a). The road type and traffic volume from 8:00 a.m. to 9:00 a.m. are displayed in Figure 16.

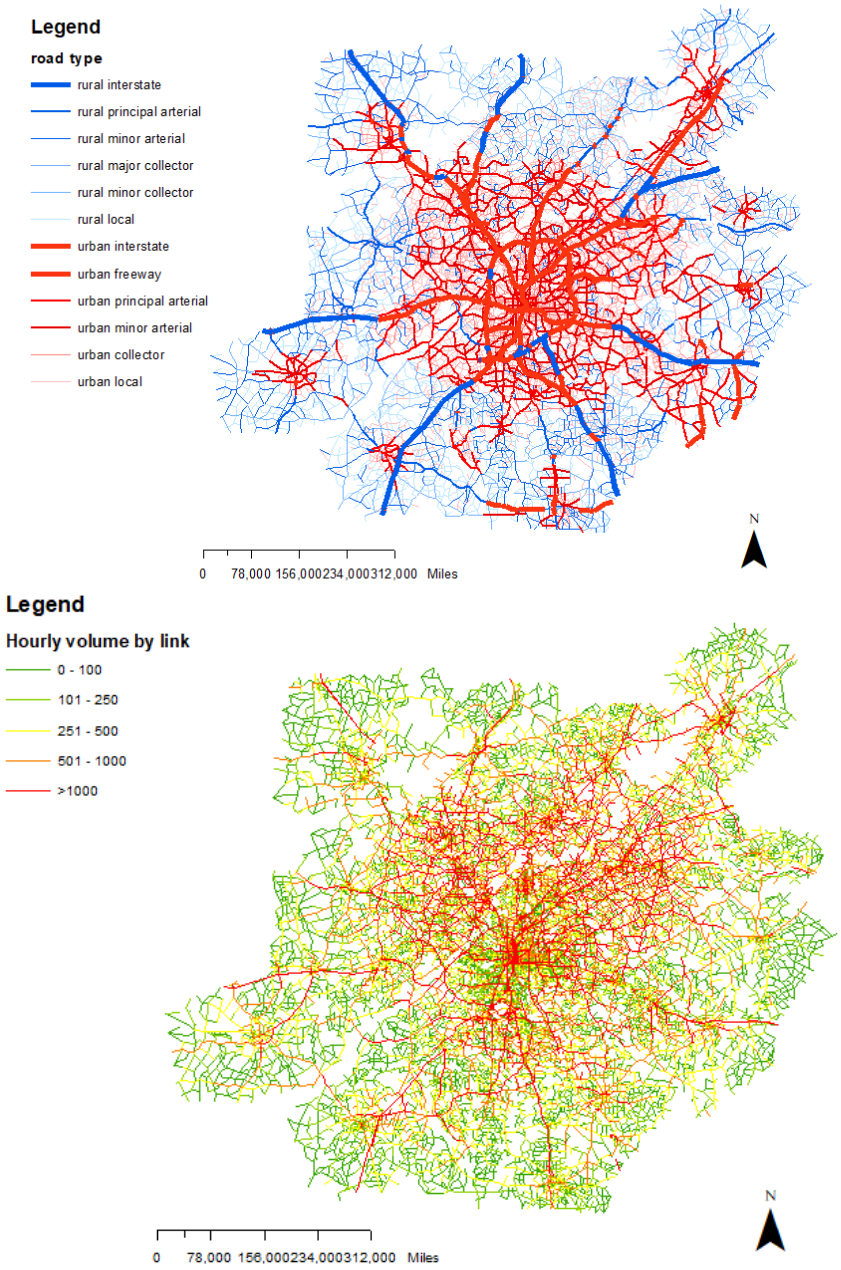

Figure 16. Road type (up) and traffic volume (down) of Atlanta network

Regional energy consumption is generated using MOVES-Matrix methodology outlined in previous studies (Xu et al., 2018a) with the baseline assumption that the on-road fleet is composed of 100% conventional vehicles. The energy consumption rates for ICEVs came from MOVES-Matrix, a multidimensional array of MOVES2014a energy and emission rates (Guensler et al., 2018). Next, the CART method developed in previous section is adopted to predict EV energy

use for certain fleet penetration fractions of 20-mile all-electric range PHEVs. The energy saving of entire network and energy saving by roadway segments are discussed in the results section. Using these case study results, the scalability of proposed CART energy rates can be demonstrated, and the energy saving benefits can be quantified under given fraction of PHEV fleet and assumed operating conditions.

3.7.1 Methodology of Estimating ICEV Energy Use

The energy estimation method of ICEVs is based on general procedures adopted in transportation conformity analysis (U.S. Environmental Protection Agency, 2015b), where transportation conformity ensures that federal funding and approval are given to highway and transit projects that are consistent with ("conform to") the air quality goals established by a state air quality implementation plan (SIP). The MOVES model is the approved regulatory emission model that must be applied to all current emissions inventory development and transportation conformity analysis (unless a project-level conformity screening tool has been approved for use in the region). A recent survey of nearly 80 transportation and air quality agencies indicated that more than half of agencies already applied MOVES in SIP or conformity study, and most of the other agencies were switching to, or planning to apply, MOVES (S. Fincher, 2015).

There are basically two approaches to apply MOVES for a conformity study, which include the inventory approach and emission rate approach (U.S. Environmental Protection Agency, 2015b). By adopting the inventory approach, mass emissions are estimated using total vehicle mile traveled (VMT), a speed bin distribution, and other supplemental input files. By adopting the emission rate approach, emissions rates for running emissions and engine starts, etc. are estimated independently. Using this approach, emissions estimates are derived by matching the travel activities with corresponding emission rates under specific speed, road type, and fleet composition

conditions. Regardless of which approach applied, the same group of input files are required (S. Fincher, 2015):

- **Fleet composition**, including MOVES vehicle source type and model year distributions;
- **Regional travel activity data**, including VMT, month, day, and hour VMT adjustment factors, road type, ramp fraction, daily vehicle starts and average speeds;
- **Scenario inputs**, including meteorology, inspection & maintenance (I/M) program data, and fuel specifications.

Adopting the emission rate approach can help address several limitations of using inventory approach and provide modelers with great flexibility in model development at the cost of increasing complexity. Using this approach, users have to prepare fewer MOVES runs, but each run requires more supporting data. This approach achieves a more detailed emission output, generally at the link or travel analysis zone (TAZ) level. This approach normally requires the user to initially estimate emission rates using MOVES under selected scenarios, then match the travel activity information (VMT by road type, speed bin, source type and model year) with applicable emission rates for that specific road type, speed bin, source type and model year (U.S. Environmental Protection Agency, 2015b). The link-level or TAZ-level emission output can be mapped to visualize the spatial distribution of pollutants, and further applied for air quality assessment. However, there are no standardized public domain connections with MOVES to post-process emission rates into link-level or TAZ-level emissions and developing such a connection requires a considerable understanding of MOVES modeling structure and regional activity features to avoid estimation errors.

In this study, a link-based emission modeling approach is described for regional emission analysis by using MOVES-Matrix instead of MOVES. In MOVES-Matrix, MOVES 2014a is run 146,853 times for Atlanta area, iterating across all combinations of vehicle source-type, fuel, environmental, operating mode bins, and other parameters, and the modeled emission rate outputs are stored in a huge multi-dimensional array so that the emission rates can be used in other analyses without re-running MOVES (Liu et al., 2019). With proper scripting, users can extract MOVES emission rates from MOVES-Matrix and obtain the exact same emission results as MOVES. In the advanced emissions modeling approach, activity estimates are derived from the regional travel demand model and properly processed using the recommended modeling approaches provided by USEPA (U.S. Environmental Protection Agency, 2016, 2015b). This approach bypasses the time-consuming process of running MOVES to generate applicable emission rates, and the uniform format helps to simplify the assessment for both inventory model and emission rate models, while achieving the same results. (H. Liu et al., 2017; Liu et al., 2019).

3.7.2 Network Specification

Travel demand models (TDMs) are typically developed by a metropolitan planning organization (MPO) to output hourly traffic volumes and applicable on-road operating conditions, generally through post processing the model results. Here we describe a modeling process, currently being implemented, for coupling a typical TDM output and MOVES-Matrix emission rates.

In this approach, an analytical boundary (time, location, and duration) is designated first for running the TDM and MOVES-Matrix, and all the analysis are conducted within this domain. The methodology includes three preliminary steps: 1) preparing regional inputs within the TDM modeling domain; 2) generating MOVES-Matrix energy use and emission rate matrices for all possible model input combinations; and 3) matching regional TDM model activity outputs at link-

level with applicable emission rates from MOVES-Matrix (Liu et al., 2019; Xu et al., 2018a). The workflow diagram is shown in Figure 17 below. Due to the scope of this dissertation, only on-road energy consumption and emissions are considered.

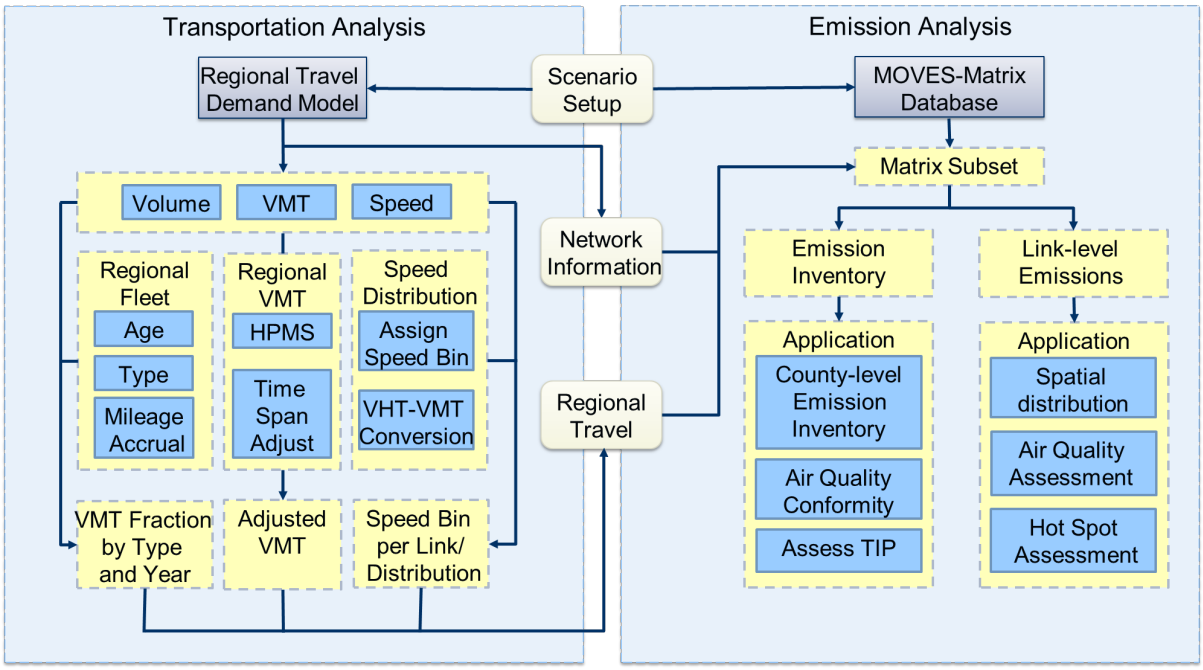

Figure 17. Analytical workflow of linking MOVES-Matrix and TDM

As discussed above, three different inputs are required for a MOVES-based regional emission analysis, which include regional fleet composition, travel activities, and other scenario inputs. According to conformity study requirements, the input data should be prepared for a single investigated year, aggregated by hours, and applied to all possible fuel-vehicle type combinations (U.S. Environmental Protection Agency, 2016). For on-road emissions, the emission inventory is derived as the product of hourly VMT and corresponding emission rates for that specific road type, source type, model year and speed bin where the VMT is generated. The methodology of preparing input files under conformity study requirements is introduced in the following sections.

a. Fleet Composition

Vehicle fleet features were represented in MOVES using 13 vehicle source type and 31 applicable model years (age 0~30 from investigated calendar year) (U.S. Environmental Protection Agency, 2016). Agencies can prepare the vehicle composition with data from the MOVES default database, from state motor vehicle registration data (e.g., motorcycles, passenger cars, passenger trucks, light commercial trucks), or from other possible resources like local transit agencies, bus companies, and refuse haulers (U.S. Environmental Protection Agency, 2015b). In this study, vehicle compositions by road type were prepared for investigated counties. For each road type, the vehicle type distribution was represented by a three-dimensional matrix, with source type, model year, and fraction of population as the three axes.

Different vehicle types and model years may have significantly different probabilities of being present on the roadway network due to vehicle owner's use preferences. In this case, the on-road vehicle population distributions are usually not equivalent to the VMT fraction by vehicle types and model years. Mileage accrual rates for different vehicle types and model years should be considered in projecting the vehicle population distribution into VMT distribution for post-processing TDM output. In MOVES, VMT is represented by HPMS vehicle type. A relative mileage accumulation rate (RMAR), in combination with source type populations and age distributions, is used to distribute the total annual miles driven by each Highway Performance Monitoring System (HPMS) vehicle type to each source type and age group. This rate only varies by calendar year. The VMT data are assigned to different source types and model years by multiplying RMAR factors within a HMPS vehicle type (U.S. Environmental Protection Agency, 2016). The final VMT by source type and model year is calculated using the following equation:

$$\boldsymbol{VMT_{t,a}} = \frac{\boldsymbol{f_{t,a}^{POP} \times RMAR_{t,a}}}{\sum_{t \in C_h} \boldsymbol{f_{t,a}^{POP} \times RMAR_{t,a}}} \boldsymbol{VMT_h} \quad \textbf{(8)}$$

Where,

t is source type

a is model year

h is HMPS vehicle type

C_h is the set of source types included in HMPS vehicle type h

$RMAR_{t,a}$ is relative mileage accumulation rate for source type t and model year a

$f_{t,a}^{POP}$ is population fraction of source type t and model year a

For link-level emission analysis, the VMT variables in equation above can be replaced by set VMT fractions for each link type to speed-up the emissions calculation process. In this case, the VMT fraction by source type and model year are used to obtain aggregate fleet average emission rates, which are multiplied by hourly VMT for that specific link under the specific average speed and road type.

b. Regional-level Travel Activity

The TDM outputs include three components for conventional vehicle analysis, which include hourly VMT, road type, and average speed. However, this information cannot be directly used as emission model inputs for two reasons: 1) the TDM is usually run for an annual average day or weekday condition, while high emission often occurs during one season and under high congestion level (e.g. the highest NO_X emissions often occur hot summer afternoons); and 2) the VMT in most TDM outputs is populated by theoretical models, which may be different from actual on-road conditions. In this case, specific time-span and VMT adjustments are usually applied to model-

predicted VMT outputs. Average speeds are also usually post-processed so that speed bin distributions better match field observations and corresponding emission rates are selected from MOVES. The roadway facility type from TDM outputs should also be assigned with a MOVES road type ID, and where applicable, the ramps in the modeled network are differentiated from the highway segments.

The TDM outputs are post-processed to prepare link-level emission model inputs, in MOVES formats, for emissions modeling. Each has a MOVES road type, VMT, and average speed with adjustment factors applied directly to the individual links.

c. Other Settings

Other inputs used for on-road energy/emission estimation include fuel, I/M program, retrofit data, and meteorological data. For meteorology data, a 24-hour temperature and humidity profiles are defined for each investigated month. The MOVES default I/M, fuel and retrofit data were applied for the remaining inputs.

After preparing the input, the MOVES-Matrix emission rate array was prepared using the MOVES default scenario and EPA-approved I/M program and fuel specifications across all possible meteorology inputs by taking the advantage of the powerful computational ability of a computer cluster at Georgia Tech (Liu et al., 2019). Because MOVES has been run for all possible model input iterations that apply to the region, the user can call for the applicable MOVES emission rate in the MOVES-Matrix array for use in other operations and obtain the exactly the same emission output that MOVES provides without ever having to launch MOVES again or transfer MOVES outputs into the analyses.

With the emission rate for each speed bin, road type, and source type, the emissions can be estimated by linking regional activities with applicable emission rates. The average speed bins and road types (e.g. arterial vs. freeway) are exported as operational data from the TDM for use as emissions modeling inputs. The fleet mix can come from multiple sources as discussed above. To calculate emissions, users need only link their regional travel data, including facility type, link average speed, and fleet composition, with the applicable MOVES-Matrix emission rates.

3.7.3 ICEV Energy and Emission Modeling

The ARC Travel Demand Model generates regional travels by using an activity-based model for the 20-county non-attainment area (Atlanta Regional Commission, 2016b). Coordinated Travel-Regional Activity-Based Modeling Platform (CT-RAMP) is implemented in the travel demand model system to facilitate the regional activity forecasting with 30-minute resolution. The TDM-generated activities are sub-divided into trips based on the origin and stop information and allocated to links within the local transportation networks during five different time periods (early morning, morning peak, mid-of-day, PM peak and evening). These activity estimates are used as the basis for estimating emissions on the network through a linkage to emission estimation tools.

In this study, the ARC TDM model was used as a case study to estimate on-road energy and emissions with the proposed method. The link-level TDM network output was used for obtaining link-level emissions and analyzing the spatial and temporal distribution of emissions within the entire 20-county non-attainment area. First, the fleet average energy/emission rates by speed bin and road type were calculated by aggregating emission rates by speed bin, road type, source type, and model year, and VMT fraction by source type and model year. The equation for calculating this aggregate emission rates $\boldsymbol{e_{agg}}$ is shown below.

$$e_{agg} = \sum_{all\ t,a} f_h^{VMT} \times \frac{f_{t,a}^{POP} \times RMAR_{t,a}}{\sum_{t \in C_h} f_{t,a}^{POP} \times RMAR_{t,a}} \times e_{t,a,v,r} \quad (9)$$

Where f_h^{VMT} is the VMT fraction by HPMS types prepared for each road type respectively. The VMT fraction by HMPS types is partitioned into VMT fraction by source type and model year by deploying the relative mileage accumulation rate (RMAR) factors. Next, the monthly adjustment factors for road type r was also calculated by aggregating the VMT fractions by source type and model year, and the monthly adjustment factors by source type f_m^{VMT}:

$$f_r^{VMT} = \sum_{all\ t,a} f_h^{VMT} \times \frac{f_{t,a}^{POP} \times RMAR_{t,a}}{\sum_{t \in C_h} f_{t,a}^{POP} \times RMAR_{t,a}} \times f_{m\ for\ all\ a\ and\ all\ r}^{VMT} \quad (10)$$

The aggregate fleet average emission rates were populated for different counties and road types and stored in separate lookup tables. Next, the hourly VMT were prepared by applying MOVES default hour adjustment factors as the ARC TDM divided a simulated day into five time periods. Finally, as the TDM link-level outputs are generated from a typical weekday, the day adjustment factors were not applied in this model.

For each hour of operation, the link-level inputs were screened individually, with VMT under specific, time period, road type and average speed was distributions chosen and then multiplied by adjustment factors an aggregated emission rate. The link-level emissions were populated for the TDM network, and then aggregated results by TAZ for the AM peak period. The sample regional-level results for a typical workday in July are shown in Figure 18 below (The link-level energy results are provided in Figure 19 for comparison). The total computation time for a

24-hour period, 20-county area network with 73,730 links and four selected pollutants was 5.4 minutes.

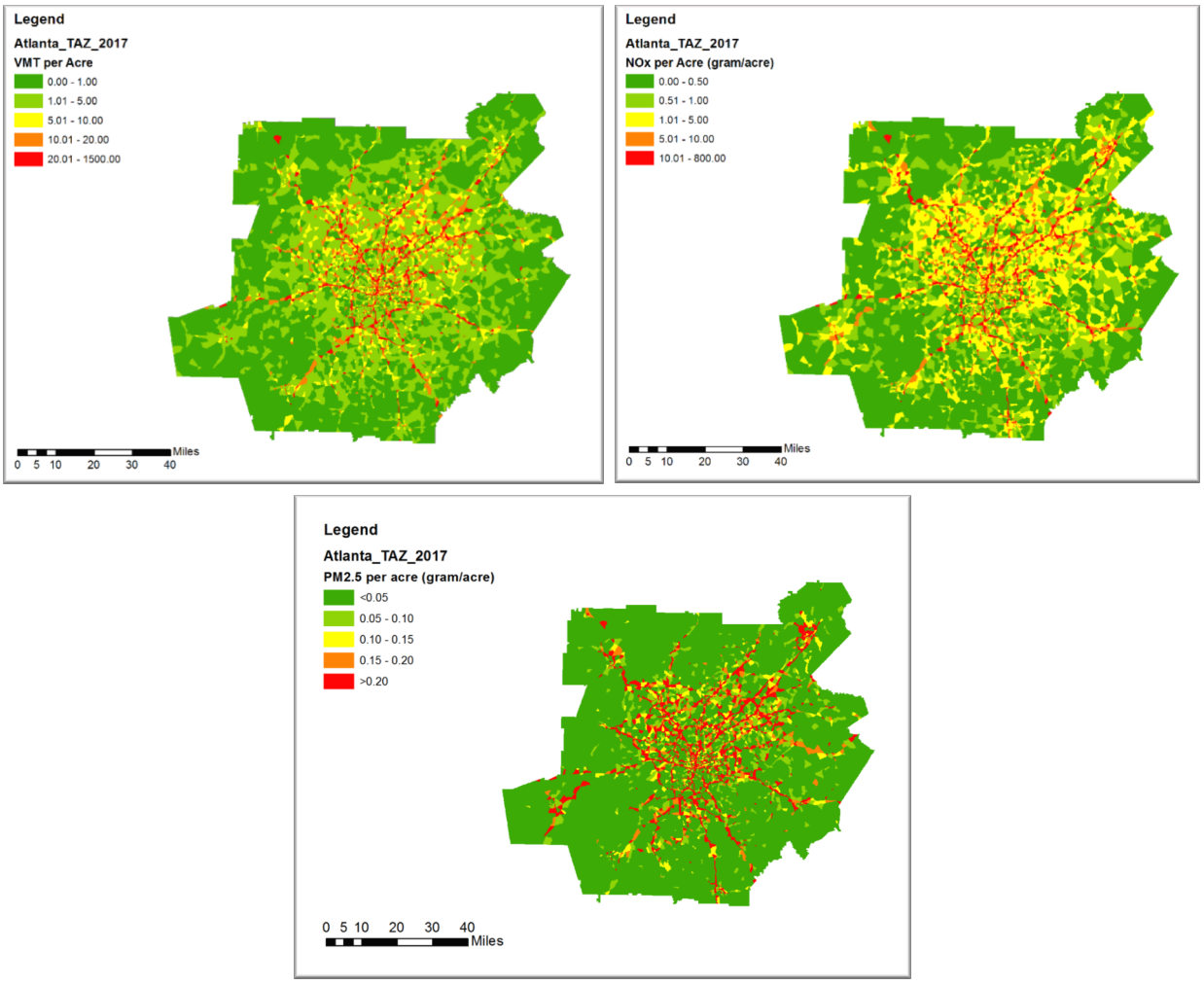

Figure 18. VMT, NO_X and $PM_{2.5}$ emissions per acre by TAZ (8:00 AM – 9:00 AM)

The linkage of these models can assist researchers in obtaining emission distribution throughout the region and are beneficial for further air quality analysis. For example, MOVES-Matrix can be connected with both TDMs and dispersion models and all the processes can be automated. A high-performance dispersion modeling system based on MOVES-Matrix and distributed computing cluster (Liu et al., 2019) produced receptor modeling results more than two

orders of magnitude faster than the normal procedures based on MOVES Graphical User Interface (GUI), with both CALINE4 and AERMOD microscale dispersion models.

3.7.4 PHEV Energy Modeling

Using the CART method described in previous sections, and traffic attributes for the morning peak, the network-level energy consumption under 0%, 10%, 20%, 30%, 40% and 50% EV market share is generated. In this analysis, the modeling approach assumes that the EVs will continue to follow the use patterns of the conventional vehicles that they replace (which is a limitation of the analysis, but not a major concern for these HEVs). The CART model was applied to Atlanta network using following procedures:

a. **Generate the energy rate:** a driving profile for a given road type and average speed is selected from the 150 driving samples. The fuel and electricity use are generated using the CART method from given driving profile (second-by-second speed for about 5-10 minutes of driving), looping loop through all possible initial SOC level with 1% SOC increment. The energy consumption rate per mile at a given average speed (2-80 mph), road type and initial SOC equals to the total fuel and electricity consumption divided by the distance of the driving profile. Since the highway operations missing low speed operation data (<8 mph), the local low speed energy rates are used to fill the gap.
b. **Generate the EV VMT:** at the pre-defined EV market share, the EV volume on each link is derived by multiplying the total traffic volume with the market share. The link-level EV VMT is then derived by multiplying the EV volume and the link length.
c. **Generate the EV Energy Use:** using the energy rate per mile from step a and the VMT from step b, the total energy per link is the product of EV VMT and energy rates under link average speed, link type and random initial SOC.

The link-level analysis was performed for each hour of the loaded network, and the 24-hour network energy profiles were generated under each market share scenario. Energy use by transportation link with 0% EV market share and 40% EV market share are provided in Figure 19 below. When 40% of the total on-road fleet is replaced by EVs, energy use drops significantly, especially in the urbanized areas with higher traffic volumes.

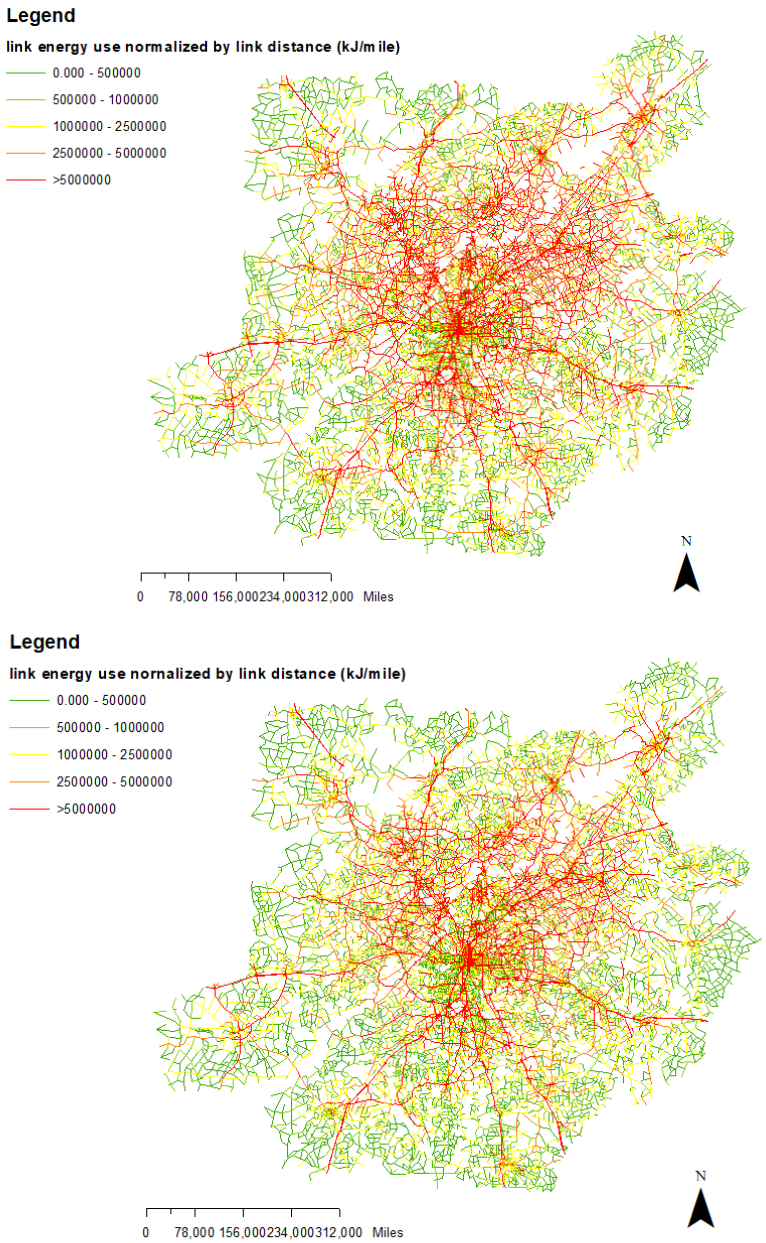

Figure 19. The link-level energy use with 0% EV share (up) and 40% EV share (down)

The variation of predicted energy use is also analyzed under different market shares (Figure 20). The network-level total energy consumption for 50% EV market share is about 68.5% of the energy use for that of the 0% EV market share (about a 31.5% reduction in energy use). The energy savings provided by EVs are largely contributed by efficiency improvements of advanced powertrain design. Further energy savings can be achieved by adopting alternative fuel power plants (e.g., CNG, hydrogen) to produce the electricity. The results suggest that with a growing PHEV share, the energy saving benefits will be large. Given that this change is a relatively small share of overall energy use in the region (8.8% of daily electricity use per household based on 2016 residential electricity consumption per household in Georgia) (U.S. Energy Information Administration, 2019a), and with the implementation of off-peak charging, any negative impact on the electricity grid will likely be limited.

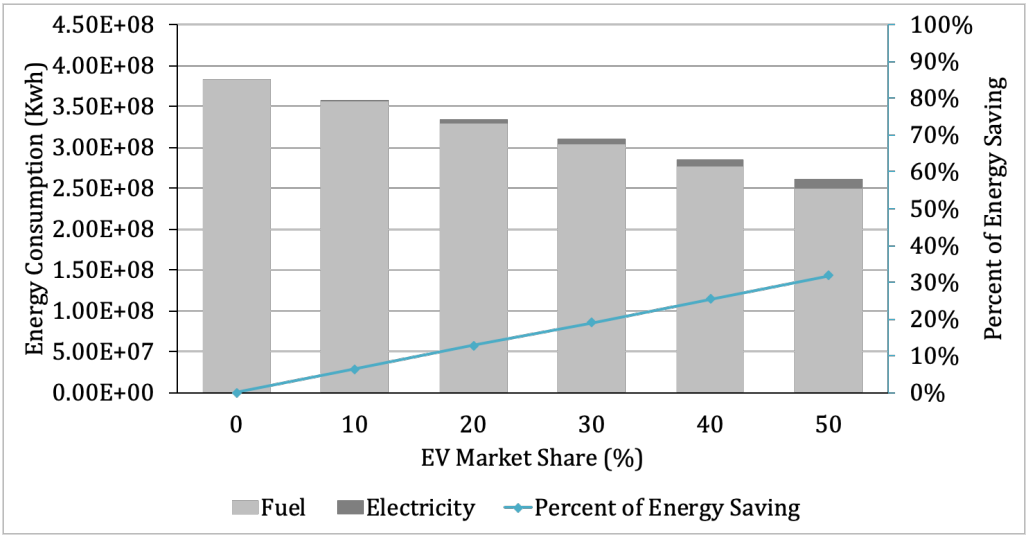

Figure 20. Predicted daily energy use under different market share

The network total fuel consumption aggregated by different facility type and different speeds are also plotted in Figure 21. For facility type, the fuel consumption was aggregated by unrestricted road (arterials) and unrestricted roads (highways). For link average speeds, the fuel

consumption was aggregated from 2.5 mph to 65 mph by 5-mph increment interval, with mean average speed represented in Figure 21 below. On arterials, the vehicle energy savings increase rapidly as average speeds increase from 2.5 mph to 25 mph and begin decrease again at higher speeds. On highways, the energy savings would be greater during medium-high speed (30 mph - 60 mph) and is maximized around 60 mph (where the vehicles operate mostly under cruising). Also, mitigating congestion and increasing average speeds will further increase the fuel economy, and such benefits are amplified with a larger share of EVs.

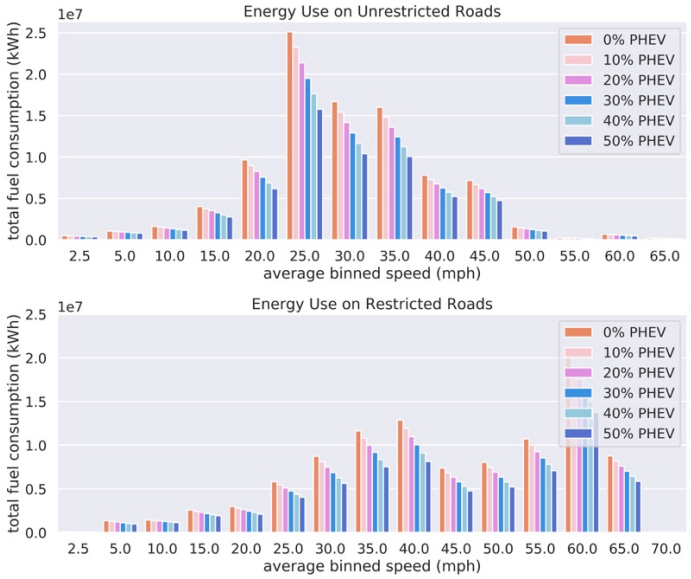

(a) Fuel Use

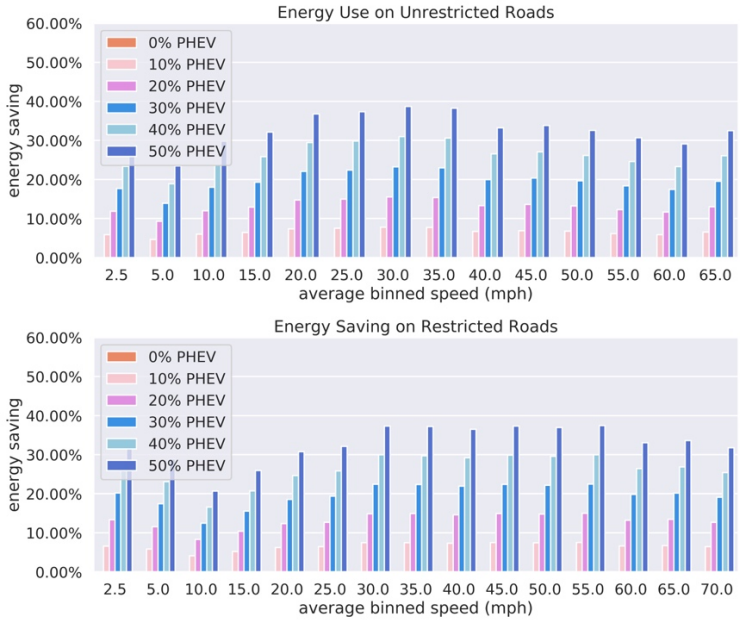

(b) Fuel saving (%)

Figure 21. Predicted daily (a) fuel consumption and (b) fuel saving by market share and average speeds

3.8 Chapter Summary

The research efforts presented in this study yielded a new modeling framework that can be used to predict energy consumption from EV subfleets operating in large-scale transportation networks. A statistically-based energy use model, derived from the Autonomie full-system simulator, is used to link applicable energy use rates with predicted on-road vehicle operating conditions. The model can be applied to link-by-link vehicle operations to assess EV energy use model and spatially and temporally aggregated to obtain regional results. The modal-based approach used in this framework, allows analysts to easily derive network-level EV energy use by matching on-road operating conditions with corresponding CART energy consumption rate clusters. The model is applied to the Metropolitan Atlanta transportation network to predict the energy use under various EV adoption scenarios. The results suggest that a 50% PHEV market share can achieve more than a 30% reduction in the energy savings, without adding significantly to overall electricity demand.

Also, at network-level, both the arterials and highways with medium average speeds (20 mph – 40 mph) earned the largest energy saving benefits under higher EV market shares.

With the results from this preliminary study, an analytical framework has been demonstrated for its sensitivity to operation patterns and scalability for regional-level network. However, there are several remain tasks identified in this study:

Improving the training set for the statistical model: as demonstrated in

1. Table 6 and Table 7, the acceleration of training dataset ranges from -8.18mph/s to 5.82 mph/s, which is smaller than the acceleration range that actually occurred during real-world operations (-10 mph/s to 10mph/s from Figure 13). Using the driving cycles from MOVES may under-represent the operations under aggressive driving (high acceleration and deceleration), and the training set should be improved to incorporate driving data from such type of operations.
2. **Addressing the simulation of vehicle control mode:** as demonstrated in Figure 15, the black-box CART model cannot effectively differentiate the vehicle control mode, which causes the energy results can be significantly different from actual energy use under certain cases. A modeling tool that is able to incorporate the prediction of vehicle control mode is highly desirable for improving the goodness-of-fit of the energy model.
3. **Applying to other EV models:** it will be a challenge task to apply the CART methods for different kinds of EVs if the tree branches cannot be shared by all kinds of EV (which is highly possible). The CART results for a single vehicle contains about 60 energy rates for fuel and electricity, and the result matrix would be huge if considering different EV types and various GHGs and pollutants. Also, it will be cumbersome to apply different mode-split methods for all kinds of EV and interpreting results. A more consistent model design is needed to account for the heterogeneity within EV fleet.
4. **Refining network-level inputs:** the primary question answered by this preliminary study is that whether the method is scalable for regional-level transportation network. The activity inputs, including speed, acceleration and SOC, may or may not be representative for EV fleets within the region. Also, there are other significant factors, such as roadway characteristics and ambient environment, that are not included in current study but will

impact the EV energy use. The methodology of preparing proper regional-level activity inputs for energy modeling needs to be proposed in following analysis.

CHAPTER 4. EV ENERGY MODEL DEVELOPMENT AND VERIFICATION

In this chapter, the methodology of developing EV energy model system using the analytical framework proposed in Chapter 3 is introduced. A new, scalable, and transferrable approach for estimating the energy use of common EV fleets (including both fuel and electricity) will be developed for large-scale transportation networks. The proposed methodology needs to address the current model shortcomings: 1) support energy use modeling from all existing EV technologies, including BEVs, HEVs, PHEVs and FCEVs; 2) accept inputs that are directly measurable from transportation systems, treating factors such as powertrain specifications as hidden variables that are linked to measurable factors; and 3) predict energy use under a wide range of operating conditions where energy results are sensitive to on-road operating conditions, such as vehicle speeds, vehicle accelerations, and road types. Engineers, planners, and policy makers should be able to use the model to assess EV energy impacts under different transportation operation scenarios and assess potential system-level solutions to EV implementation questions. Those typical questions for EV adoption include optimizing electricity supply from the grid, promoting eco-routing and eco-driving designated for different vehicle types, and investigating the energy impact of vehicle electrification for shared and autonomous vehicles.

In this chapter, an activity-based, bottom-up approach is proposed for estimating EV energy consumption as a function of on-road operating conditions. The activity-based approach allows energy estimation for large-scale transportation networks, while accounting for the variability in on-road vehicle operating conditions. The designed energy modeling approach uses a simulation inference model development design, which combines prior knowledge of vehicle

design and a data-driven approach using simulation data for parameter estimation. The CART model used in Chapter 3 will be replaced with the simulation inference models developed in this chapter. The energy modeling framework developed in this study is activity-based, using measurable transportation system factors as inputs, such as vehicle types, on-road vehicle operating conditions, and roadway characteristics. The model generates fuel and electricity consumption at the disaggregate level, using single vehicle inputs, or at the aggregated level, given a fleet composition and operations.

The full-system vehicle simulation tool (Autonomie) was used to estimate energy consumption for various on-road driving conditions. Three analytical steps are undertaken to generate the energy models with cleaned energy output from Autonomie. First, sample EV models were configured in Autonomie for BEVs, HEVs, PHEVs and FCEVs. The energy use data for each selected vehicle option were generated by simulating a wide range of operating conditions with different average speeds, driving styles, and road grades. Autonomie simulation runs were then performed using second-by-second vehicle activity inputs, and post-processed to retain important features within reasonable ranges for the remaining analysis. Third, energy consumption models are established for various types of EVs using the outputs from the full vehicle simulation model using a simulation inference model design, which combines the physical knowledge of vehicle operation (how engine, motor, battery works together), and data-driven energy inferences. A Bayesian Network approach was adopted to simulate the power flow within EVs and the corresponding energy use. The model first estimates the likelihood that an EV is operating under specific control modes for the given driving conditions, and then the model calculates energy use as a function of chosen control strategy and operating conditions. The final energy model is verified using a separate trip set and real-world on-board diagnostic (OBD) data.

Finally, the verified modeling framework is applied in a regional-level network as a case study to demonstrate its scalability at network-level and sensitivity to operation characteristics. The final results demonstrate the energy saving potential of using EVs in Metropolitan Atlanta area under possible EV market development by 2024. Figure 22 illustrates overall modeling approach described above.

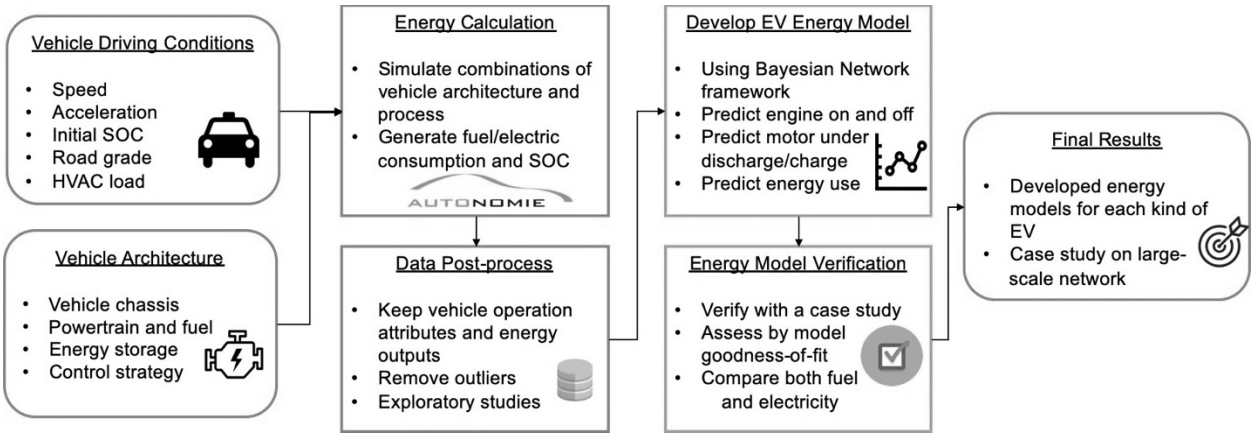

Figure 22. Workflow of the energy model framework development

4.1 Data Preparation

As introduced in **Section 2.2,** vehicle powertrain design, vehicle operations, roadway characteristics and ambient environment significantly impact EV energy use. It is critical to account for the impact of those factors using model variables that can be observed/measured in the real world. The key considerations in preparing data for use in the modeling processes are introduced in following sections.

4.1.1 Vehicle Powertrain Design

Vehicle powertrain specifications, including the power source and power converter information, cannot be discerned directly by observing the vehicle fleet (without real-time automated license plate recognition and processing). Hence, vehicle type information is typically used as a surrogate

for powertrain specifications, with accessible powertrain information reported by manufacturers assigned to selected vehicle types in modeling process. In this study, we selected seven typical EV models to represent commonly used EV fleet. The Toyota Prius and Toyota Prius Prime (39% of market share), Ford Fusion hybrid and similar models (15% of market share), Tesla series models (9% of market share), Chevrolet Volt and similar models (4% of market share), and Nissan Leaf (2% of market share), together account for nearly 70% of the total EV market (BEV+PHEV+HEV) in 2017 (U.S. DOE Alternative Fuels Data Center, 2019b, 2019a). The Toyota Mirai was selected as the base model for FCEVs as it is one of the few early commercialized FCEV models (Serov et al., 2018). The market share of the different kinds of EV is provided in Figure 23 below.

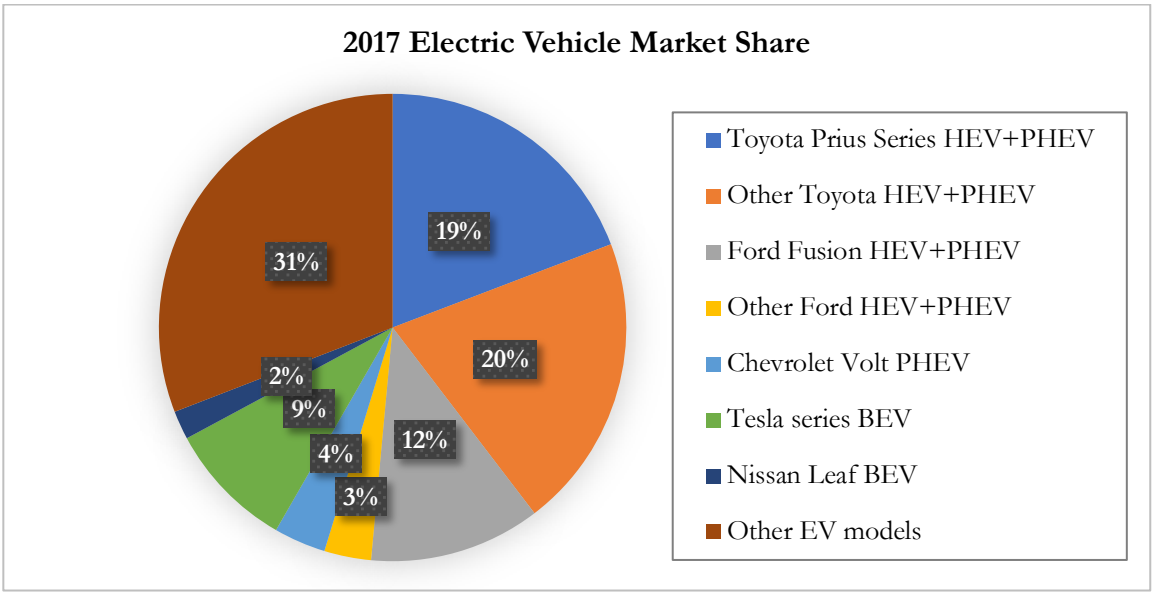

Figure 23. Electric vehicle market share in 2017 (U.S. DOE Alternative Fuels Data Center, 2019b, 2019a)

The drag coefficients, frontal areas, and other vehicle parameters used in Autonomie modeling for the seven vehicle types are summarized in Table 8 below. Notice that one control strategy is assigned to each vehicle type. Vehicle control parameters can be optimized based on

different operating scenarios and fuel economy can be improved as a consequence. A new set of energy models will likely be necessary over time to account for evolution of control strategies.

Table 8. Electric vehicle powertrain specifications

Vehicle Type ID	100mile BEV	300mile BEV	Fuel Cell EV	Parallel HEV	Power-split HEV	Power-split PHEV	Series PHEV
EV Type	BEV	BEV	FCEV	HEV	HEV	PHEV	PHEV
Base Model	2016 Nissan Leaf	2016 Tesla Model S	2016 Toyota Mirai	2015 Ford Fusion	2015 Toyota Prius	2017 Toyota Prius Prime	2016 Chevrolet Volt
Vehicle Weight (kg)	1659	2270	1760	1639.7	1669	1712	1893
Drag Coefficient	0.32	0.30	0.30	0.30	0.31	0.31	0.30
Frontal Area (m^2)	2.76	2.83	2.79	2.25	2.37	2.37	2.57
Maximum Motor Power (kW)	80	285	113	79	68	68	87
Maximum Motor2 Power (kW)	-	-	-	-	57	57	48
Battery Size (kWh)	30.41	101.18	1.82	1.46	1.26	8.11	14.89
Maximum SOC	0.99	0.99	0.70	0.90	0.90	0.90	0.90
Minimum SOC	0.14	0.04	0.40	0.10	0.10	0.10	0.10
Maximum Fuel Cell Power (kW)	-	-	114	-	-	-	-
Max engine power (kW)	-	-	-	105	90	98	75

4.1.2 Vehicle Operation and Roadway Characteristics

To define on-road vehicle operations and roadway characteristics, second-by-second speed, acceleration, and location information collected from GPS data is the most widely used data source to explicitly represent the driving conditions (Jun et al., 2006; Yoon et al., 2005). Even for vehicle

simulators that use average speeds and road types as indicators of operating conditions, the underlining distributions are typically derived from real-world driving traces (California Air Resources Board, 2018; U.S Environmental Protection Agency, 2016). In this case, the second-by-second speed and road grade profiles are selected as model inputs, using GPS traces collected during the Atlanta Household and Activity Travel Survey in a 20-County Region of Metro Atlanta (Atlanta Regional Commission, 2011; Liu et al., 2018; Liu, et al., 2019). The GPS traces contains second-by-second speeds, as well as the paired second-by-second road grade generated from the U.S. Geological Survey (USGS) digital elevation model (DEM), matched via latitude and longitude information (Liu et al., 2018). The sample trips that covered a wide range of possible operating conditions were selected from the GPS traces, and were split into two sets for model development: a training set (refers to training and validation set in machine learning) with 152 trips and a testing set with146 trips. Since the run time for a single vehicle and a single driving cycle take about 5 minutes to run in Autonomie, it is technically difficult to run use a larger sample in this analysis given the time limit. The current study can be further expanded by incorporating more driving cycles and more vehicle configurations with multiple Autonomie licenses and high-performance computing (HPC) resources. The vehicle speed-acceleration distribution and road grade distribution by different sets were provided in Figure 24 below.

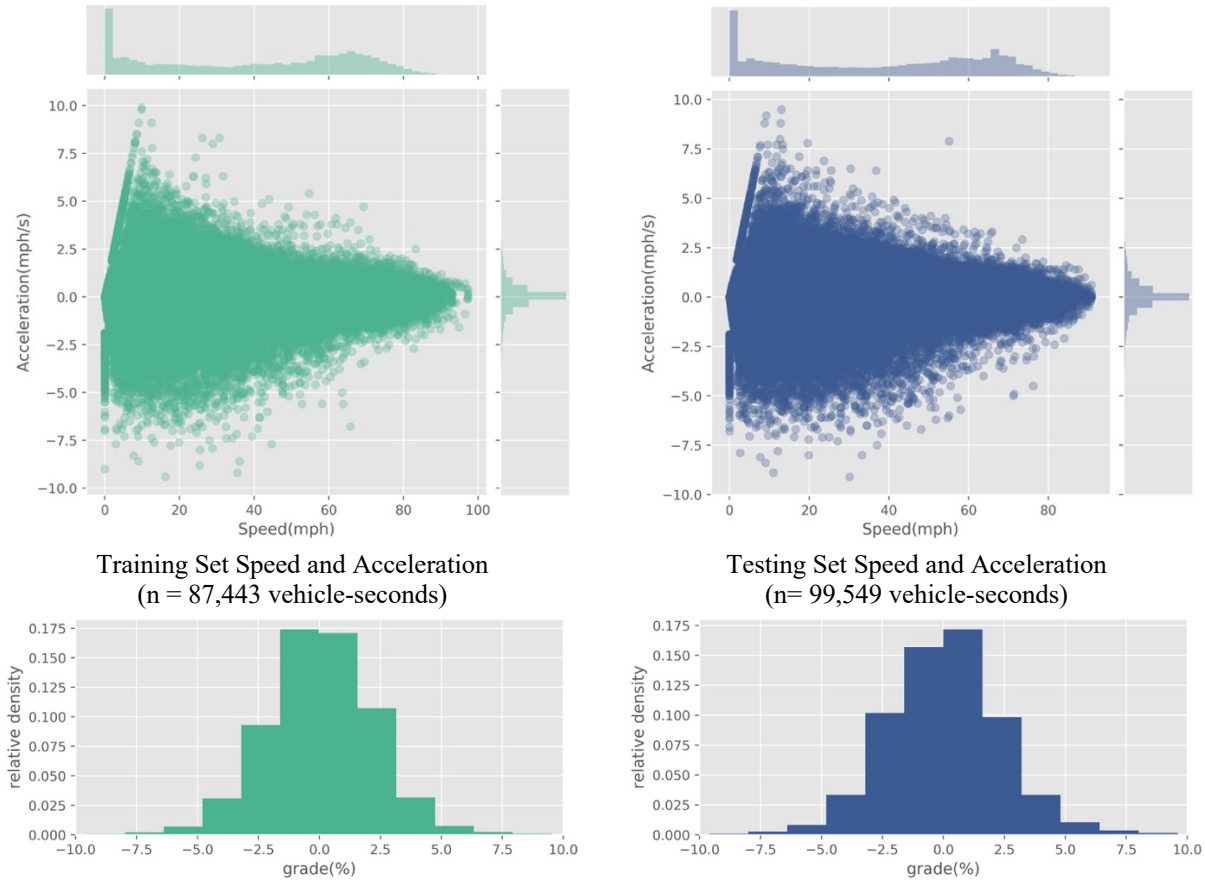

Training Set Speed and Acceleration
(n = 87,443 vehicle-seconds)

Testing Set Speed and Acceleration
(n= 99,549 vehicle-seconds)

Training Set Road Grade
(n = 87,443 vehicle-seconds)

Testing Set Road Grade
(n= 99,549 vehicle-seconds)

Figure 24. Vehicle operation input for training set and testing set

Although this is a relatively small sample of regional activity, the on-road driving profiles from 2011 household travel survey (Atlanta Regional Commission, 2011) are expected to represent the local driving patterns better than using MOVES default driving cycles. The speed-acceleration joint distributions of the local data versus MOVES default is provided in Figure 25 below. The local driving data have more high speed and high acceleration operations than MOVES default. Also, the 150 driving samples were purposefully selected to match the range of average speeds and road types from regional-level network. So, for each speed and each facility type of a specific link within the regional network, we can find at least one possible condition based on data from this region.

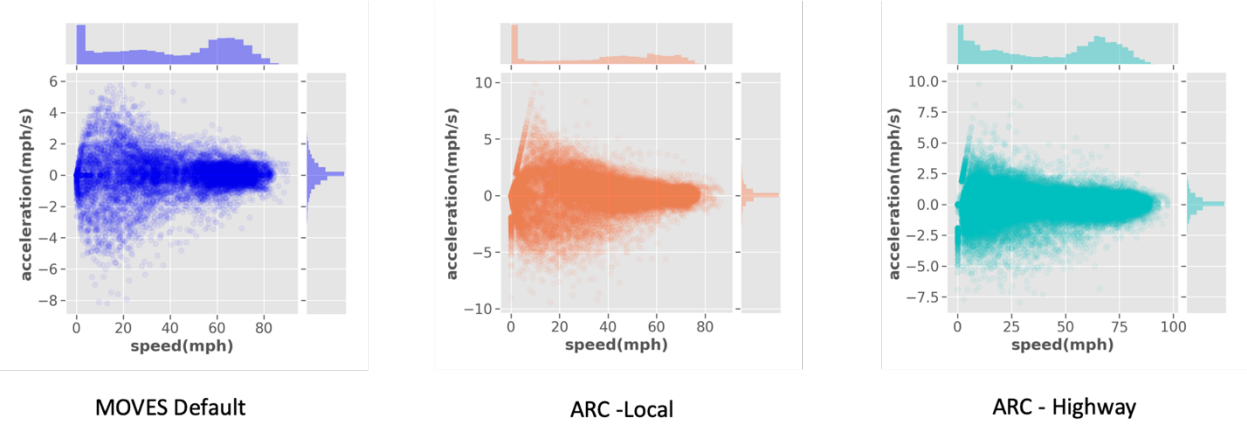

Figure 25. Comparison between MOVES default cycles and local driving data

4.1.3 Battery SOC

Battery SOC information has been particularly difficult to obtain in previous transportation energy analyses. Many previous studies assume vehicles operate in their all-electric range (AER) (Gonder et al., 2007), assume equal initial and final SOC levels (Kelly et al., 2012) or use additional parking and charging information (Lee et al., 2011). The link-level SOC distribution depends upon the vehicle characteristics and their on-road activity. The trip-start SOC, previous travel activities, vehicle control system design, and operating conditions of current link have a joint effect on the SOC level, and the potential optimal approach to quantify the SOC distribution should be collecting real-world operation data from the network or performing a comprehensive simulation with multi-day activity data.

In this study, the initial SOC is randomly generated using uniform distributions within the allowed SOC ranges for each vehicle, and each trip accounts for a wide range of operating conditions. The randomized scheme helps delineate the variation of energy use under various SOC levels. With better SOC information, users can match energy use under distinct SOC level from this study with SOC levels from the real-world to account for the local charging conditions.

4.1.4 Ambient Environment

During hot/cold weather conditions, the use of cabin climate control (e.g., air conditioning and heating) can contribute a significant amount of auxiliary load to the vehicle (Neubauer and Wood, 2014; Qi, 2014; Yuksel and Michalek, 2015). In this case, an additional heating, ventilation, and air conditioning (HVAC) load is assigned into the model process based on the severity of ambient temperature and humidity. The HVAC load is assumed constant during the trip to limit final model complexity, and the energy use under various HVAC loads was modeled separately using a smaller trip sample to reduce overall computational time. However, it will be relatively easy to re-run the models when more detailed HVAC load data (paired with on-road operating mode data) become available.

4.2 Vehicle Representation and Simulation

Vehicle powertrain systems are complex, consisting of thousands of components. Full-system simulation tools provide a great advantage, in that they explicitly model the complex relationships between various powertrain components (Argonne National Laboratory., 2014; Brooker et al., 2015). However, full vehicle simulators often generate hundreds of attributes, with high multi-collinearity among the generated results. In this case, a more simply structured mathematical model can be developed that retains only the key attributes that predominantly affect vehicle energy use. The modeling features (independent variables) were selected based on the fundamentals of vehicle design and operations introduced below.

4.2.1 Vehicle Power Demand

All vehicles are designed to convert on-board energy storage (gasoline, diesel, electricity, etc.) into kinetic energy that provide work to overcome friction resistance, uphill and downhill load due to road grade, aerodynamic wind resistance, rotational load, accessory load, etc. (Ehsani, et al., 2018;

Mi et al., 2011; Guensler, et al., 2005). Tractive power demand is often used as vehicle load parameter in energy modeling. In one form (Mi et al., 2011), vehicle tractive power can be simplified as:

$$\boldsymbol{P_T = F_T v = Mav + \frac{1}{2}\rho v^3 AC_d + c_r Mgvcos(\alpha) + Mgvsin(\alpha)} \quad (3)$$

Where,

ρ - density of the air (kg/m^3)

V - vehicle speed (m/s)

A - vehicle frontal area (m^2)

C_d - coefficient of drag

c_r - coefficient of rolling resistance

α – road grade (rad)

M – Vehicle mass (kg)

g - standard acceleration due to gravity (9.8 m/s^2)

In some models (Jimenez-Palacios, 1999; U.S. Environmental Protection Agency, 2015a), emissions are derived as a function of Vehicle Specific Power (VSP), which is the vehicle tractive power divided (standardized) by a standardized vehicle weight (metric tonnes). This analysis also uses VSP as an indicator of vehicle power demand (VSP values support comparisons across vehicle classes). VSP connects the vehicle energy demand with operating characteristics including speed, acceleration, and road grade. However, as the vehicle control strategies introduced in the

following sections can still use on-road operating conditions to develop control rules, vehicle speed, acceleration, and road grade were all retained for breakpoint detection in the modeling process.

The HVAC load also contributes to power demand. In this study, we assume the meteorology is constant during a trip, and will add a constant HVAC demand to the powertrain. Modeling a constant load within the regression model can raise singularity issues; hence, HVAC energy use is handled separately by post-processing the energy output, until HVAC load interactions with engine load become available in monitored drivetrain performance data streams for use in updated model development. This simplification may lead to potential inconsistent prediction errors associated with HVAC load in model application but is the best approach in the absence of an enhanced data stream.

4.2.2 Vehicle Power Supply

Given the input vehicle tractive power demand, the vehicle control system determines the total energy required and the split among different power sources under any specific driving condition (Zhang and Mi, 2011). The delivery of energy to the wheels is governed by characteristics of the entire powertrain system, from the power source, through the transmission and differential (torque-multiplication), to the diameter of the wheels (Guensler et al., 2005). The vehicle powertrain design and control mode were represented using proposed conceptual framework introduced in **Section 2.1** Fundamentals of Vehicle Design and Operation.

In Autonomie, the Vehicle Propulsion Controller (VPC) allocates power demand among components at the vehicle level, using the given vehicle model and driving cycle (Argonne National Laboratory., 2014). Based on the discussion above, the fuel consumption rate and electricity consumption rate (denoted by E_{fuel} and E_{elec}) were selected as dependent variables. The hidden vehicle control variables, including engine/fuel cell mode and battery

charging/discharging mode (denoted by C_1 and C_2), were also selected to represent control modes and split energy use by modes. The vehicle operation attributes (speed, acceleration, road grade, and VSP) and simulated SOC curves serve as independent variables for determining vehicle control and corresponding energy use. The HVAC load was applied during post-processing, as a scaling factor to account for the energy surcharge under high/low temperature conditions. In practice, the interactions will likely be much more complex, because the air conditioning compressor system that creates a power drag, and this compressor can be programmed by the manufacturer to cycle on and off as desired. All of the selected attributes described above were exported from Autonomie simulation results. The energy rates and VSP distributions can be unreasonably high or low, given extreme input conditions (e.g., specific combinations of high speed, hard acceleration, and low SOC) which go beyond a vehicle's physical operational constraints. The data that are out of Tukey fence were identified as non-relevant data points and removed from the analytical dataset (Tukey, 1977). Any simulation output that could not follow the input cycles (e.g., when a BEV runs out of battery power during the cycle) were also removed. The fraction of removed outliers ranges from 6% to 13% provided in Table 9 in the following section. The complete list of parameters kept for energy study is provided in Appendix B

4.3 Energy Model Development with the Bayesian Network Method

Simulation inference modeling will use a data-driven approach to develop a simplified model reflecting the powertrain performance knowledge derived from Autonomie full-vehicle simulation model outputs. Vehicle powertrain operation will be represented by a Bayesian Network graphical statistic model, also known as directional graph (Wasserman, 2013). The Bayesian Network is composed of nodes and arrows, where the nodes represent the probability distribution of variables that are either observable or hidden, and the arrows represent the dependence or even casual

relationship between variables. In this case, the Bayesian Network of the powertrain structure is illustrated in Figure 3, and the probability distribution of each variable can be inferenced using a statistical learning approach. Compared to a full-simulation model, the final structure of Bayesian Network is simpler and is easy to train. Compared to an aggregate model, the Bayesian Network integrates the domain knowledge from the simulations (which has been independently verified in a body of previous scientific work) and significantly reduces uncertainty in prediction associated with aggregation. The Bayesian Network is applied for fuel and electricity consumption, respectively. This is important because fuel may be used to provide tractive power or to recharge batteries, and electricity may be used at higher rates to provide acceleration under certain conditions.

The conceptual framework of a full hybrid electric vehicle powertrain provided earlier in Figure 6 is now represented by the directional graph in Figure 26 (BEV model is a special case of this framework). In this problem, the list of nodes is defined as $N = [C_1, C_2', C_2", E_{11}, E_{10}, E_{01}, E_{00}]$. The definition of each node is listed below:

$C_1 = \{^{1\ (powertrain\ 1\ on)}_{0\ (powertrain\ 1\ off)}$ is the mode of Powertrain 1

$C_2 = \{^{1\ (powertrain\ 2\ discharging)}_{0\ (powertrain\ 2\ charging)}$ is the mode of Powertrain 2

$C_2' = (C_2|C_1 = 1)$ is the mode of powertrain 2 given Powertrain 1 is on

$C_2" = (C_2|C_1 = 0)$ is the mode of powertrain 2 given Powertrain 1 is off

E is the energy consumption rate (kJ/sec).

$E_{11} = (E|C_2' = 1)$ – energy rate under hybrid mode

$E_{10} = (E|C_2' = 0)$ – energy rate under power-split mode

$E_{01} = (E|C_2" = 1)$ – energy rate under the EV only mode

$E_{00} = (E|C_2" = 0)$ – energy rate under regenerative braking mode

In this network, the mode of Powertrain 1 (on and off) is predicted first, based on the vehicle power demand. Then, the mode of Powertrain 2 (CS and CD) is predicted based on mode of Powertrain 1 and other parameters. The energy use conditioned as a function of vehicle control mode is estimated last. This is important, because the fuel use and electricity use depend predominantly on the combined powertrain mode, and then on operational variables within that combined mode. In a modern hybrid powertrains, the engines and fuel cells are often designed for steady power output, while the battery power often serves as the power damper to assist the engine or fuel cell (Ehsani et al., 2018).

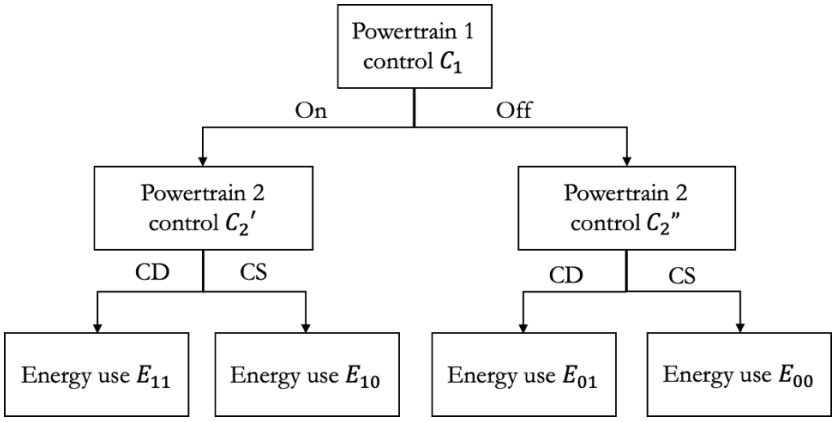

Figure 26. Conceptual structure of the Bayesian powertrain mode network

This model assumes that variables C_1, C_2' and $C_2"$ follow Bernoulli distributions, with probabilities $\pi_1, \pi_2', \pi_2" \in [0,1]$ respectively. For BEVs, $\pi_1 = 0$ (only an electric drivetrain is in operation). For FCEVs, we assume $\pi_1 = 1$. For other vehicle types, the operations probabilities range between 0 and 1. The model assumes that variables E_{11}, E_{10}, E_{01}, E_{00} follow normal distributions $N(\mu_i, \sigma_i^2)$ (i = 1,2,3,4). The instantaneous energy use by fuel and electricity can be

represented as the sum of conditional energy use by control mode, multiplied by the probability of given control mode:

$$\boldsymbol{E_{fuel}(E_{elec}) = \sum_{i=0,1}\sum_{j=0,1} E_{ij} P(C_2 = j | C_1 = i) P(C_1 = i)} \quad \textbf{(11)}$$

$$\boldsymbol{E_{fuel}(E_{elec}) = E_{11}\pi_1\pi_2' + E_{10}\pi_1(1-\pi_2') + E_{01}(1-\pi_1)\pi_2'' + E_{11}(1-\pi_1)(1-\pi_2'')} \quad \textbf{(12)}$$

The next step is to estimate the probabilities of each control mode and conditional energy consumption rates using common parametric statistical models. For motor control under Powertrain 1 off (C_2"), the vehicle operates as a BEV and it is almost sure that the Powertrain 2 is discharging while VSP >= 0 and is discharging while VSP < 0 (regenerative braking) (Ehsani et al., 2018). For control mode C_1 and C_2', the probability of control mode selection can be predicted by logistic regression in most cases using equations (13) and (14). Depending on the potential discontinuity of energy use in response to some input variables (i.e., energy use patterns differ with SOC above or below target SOC), the linear basis expansions are adopted to incorporate piecewise variables.

$$\boldsymbol{\pi_1(\pi_2') = \frac{1}{1+exp(-u)}} \quad \textbf{(13)}$$

$$\boldsymbol{u = h(X)\theta + \epsilon} \quad \textbf{(14)}$$

Where,

X – independent variables, $X \in \{Speed, Acceleration, VSP, SOC, Grade\}$

h(X) – potential linear expansion of X, such as polynomial, piecewise, and binned X

θ – model coefficients

ϵ – error term

However, some early EV models may use more simplistic rule-based power management strategies (Sabri, et al., 2016; Zhang and Mi, 2011), which assign distinct control modes under certain ranges of driving conditions. For example, the parallel HEV modeled in this study (a 2015 Ford Fusion) uses such a control algorithm and is not predicted very well by logistic regression. A simple alternative in those cases is to use a non-parametric decision tree method, which is easy to interpret and capable of predicting nonlinear relationships (Hastie et al., 2009). The probability of different control mode can be predicted using following equation:

$$\boldsymbol{\pi_1(\pi_2') = \sum_{m=1}^{M} \omega_m I\{X \in R_m\}} \quad \textbf{(15)}$$

Where,

X – independent variables, $X \in \{Speed, Acceleration, VSP, SOC, Grade\}$

R_m - the mth region (leaf node)

M - the total number of regions

ω_m - the probability for the predicted control mode in mth region.

The conditional fuel and electricity rates under each control mode were estimated via linear regression using equation (16) below:

$$\boldsymbol{E_{11}(E_{10}, E_{01}, E_{00}) = h(X)\beta + \varepsilon} \quad \textbf{(16)}$$

Where,

X – independent variables, $X \in \{Speed, Acceleration, vsp, SOC, grade\}$

$\mathrm{h(X)}$ – potential linear expansion of X, such as polynomial, piecewise, and binned X

β – model coefficients

ε – error term

The parameters were estimated using 80% of training samples and fine-tuned using the remaining 20% of training samples introduced in Figure 24 to reduce mean square error. The feature selection and parameter estimation procedures vary by vehicle type and powertrain configurations, and the specification for each kind of EV are introduced in the following sections.

4.3.1 BEV Modeling

The BEVs are only equipped with Powertrain 2, which suggested that the model structure would be simplest among all EVs. The energy models for BEVs only include electricity consumption, and there is no need to analyze the engine control strategies. In this case, only electricity needs to be modeled in response to various operating conditions.

The 300-mile BEV model is firstly used to develop the EV energy model. First, an exploratory study is performed to select the proper independent variables for electricity consumption. Pairwise plots of potential factors and electricity consumption are provided in Figure 27 below. It is clear that the VSP follows a fairly linear relationship with electricity consumption and is selected for modeling EV energy use.

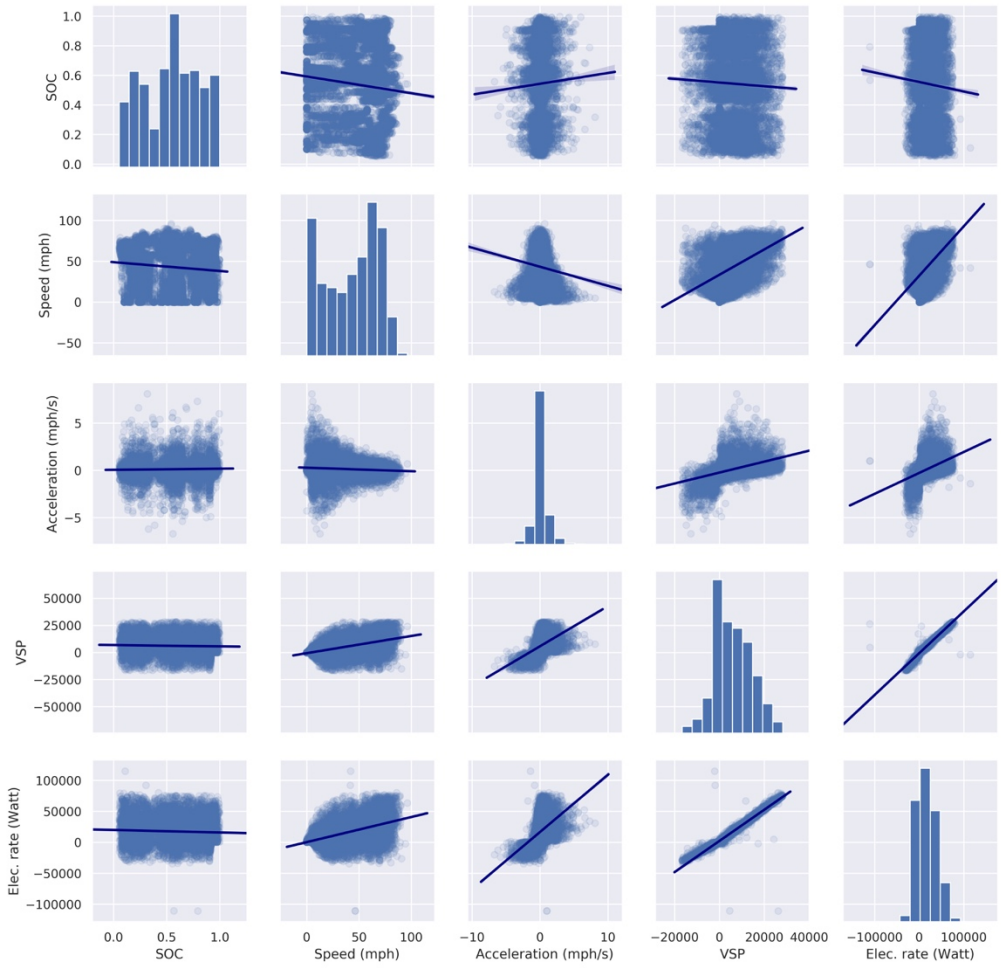

Figure 27. Pairwise plots of operation factors and 300-mile BEV electricity consumption

After selecting VSP for electricity modeling, the next step is to assess the Powertrain 2 control mode under different VSP values and the corresponding electricity use. As discussed above, it is almost sure that the Powertrain 2 of BEVs is discharging under positive kinetic energy (VSP>=0) and is charging under negative kinetic energy (VSP<0, regenerative braking) (Ehsani et al., 2018). In this case, VSP=0 is the model split point based on prior knowledge of vehicle operation, and a linear model is established for positive VSP and negative VSP, respectively. The relationship between electricity and VSP and fitted linear model are given in Figure 28 below. The R^2 value of the model for the 20% model verification set is 0.971, which indicates the model does a good job at explaining most of the variance in BEV electricity use.

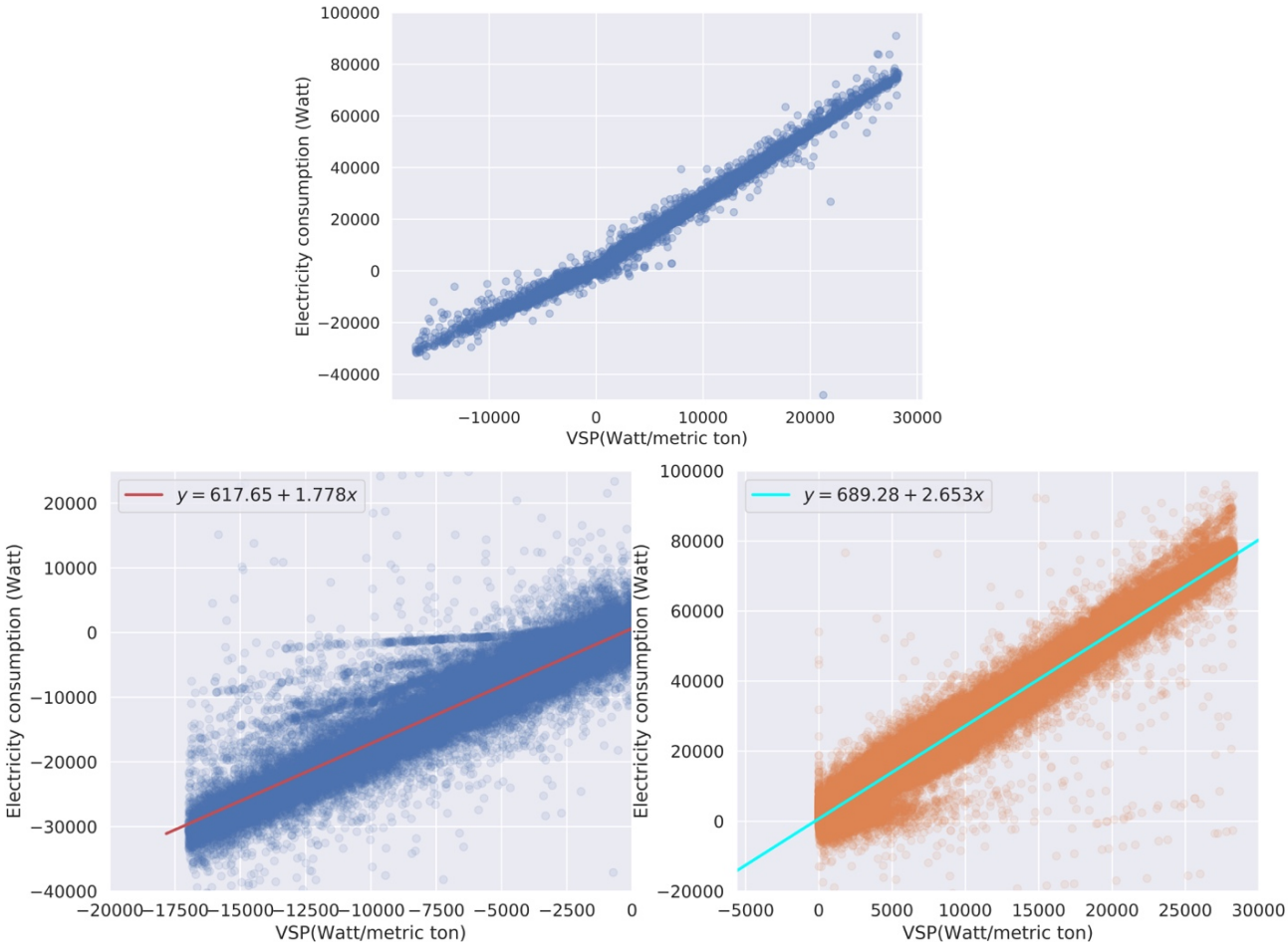

Figure 28. 300-mile BEV energy use vs. VSP

The modeling results of 100-mile BEV are similar to 300-mile BEV as the vehicle powertrains are similar, except for the battery size. The 100-mile BEV energy use model is illustrated in Figure 29 below. The R^2 value of the model using the 20% verification data set is 0.987, which indicates that this model explains most the variance of BEV electricity use.

.

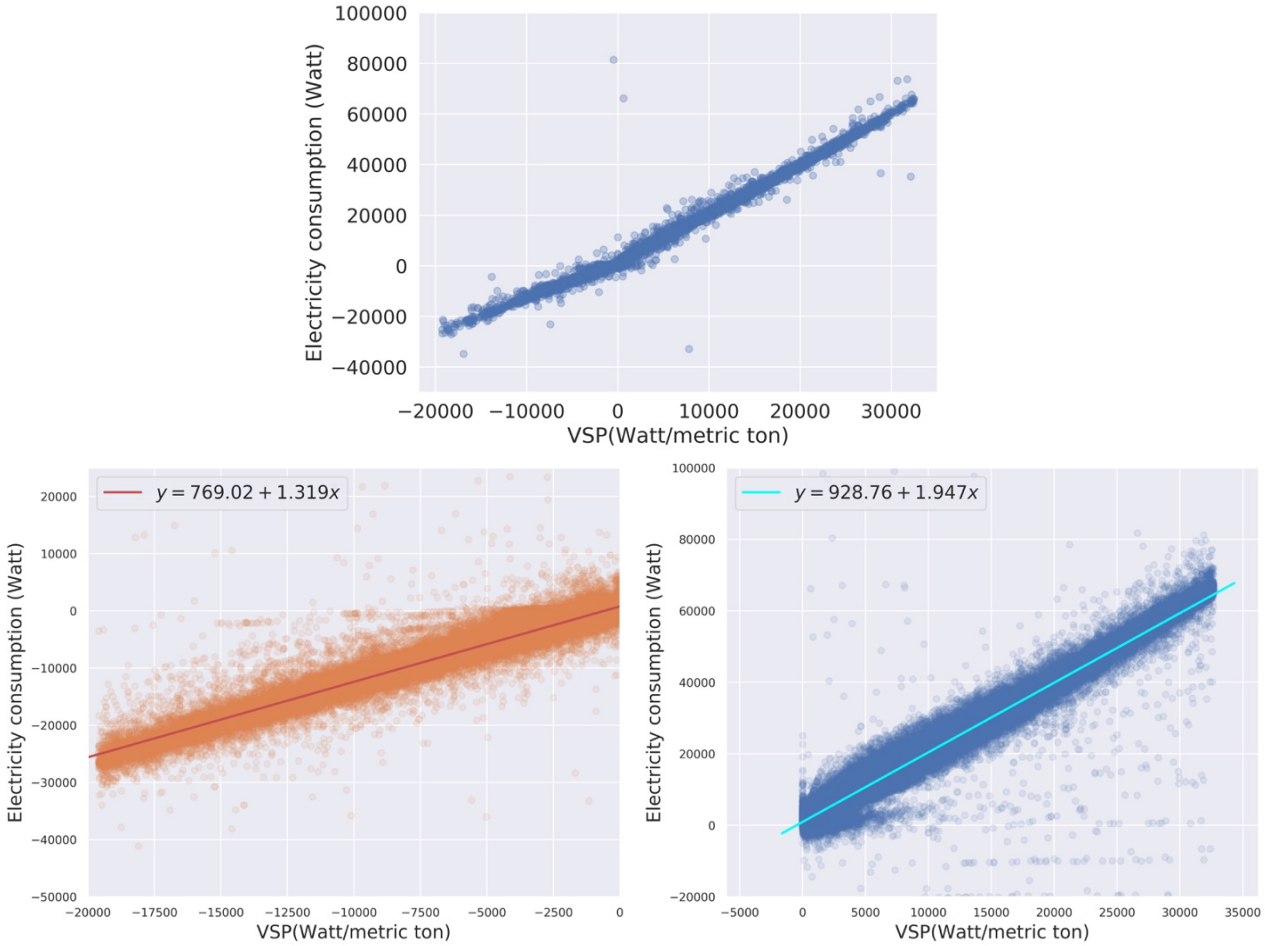

Figure 29. 100-mile BEV energy use vs. VSP

4.3.2 FCEV Modeling

The major difference between FCEV and BEV is that the fuel consumption needs to be modeled in addition to model electricity consumption. As introduced above, the FCEV is often designed with a series powertrain to overcome some limitations of using fuel cell alone and Powertrain 2 serves as a peak power source (PPS) (Ehsani et al., 2018). The PPS supplies the additional propulsion power under peak power demand and stores the energy during regenerative braking. In this case, the mode of PPS is clearly split by VSP=0 and is highly correlated with the power supply from the fuel cell. The power control of FCEV is different from normal HEV as there is no significant difference in efficiencies of the two powertrains. The correlation of potential factors

and fuel/electricity consumption are provided in Figure 30 below. The fuel cell is almost always on during the FCEV operations, so it is reasonable to assume that $\pi_1 = 1$. The fuel consumption is highly correlated with SOC and VSP, and electricity consumption depends on SOC, VSP and fuel consumption. Since predicting energy use of FCEV does not require prediction on fuel cell control mode, the energy modeling FCEV is essentially simpler than other hybrid vehicles.

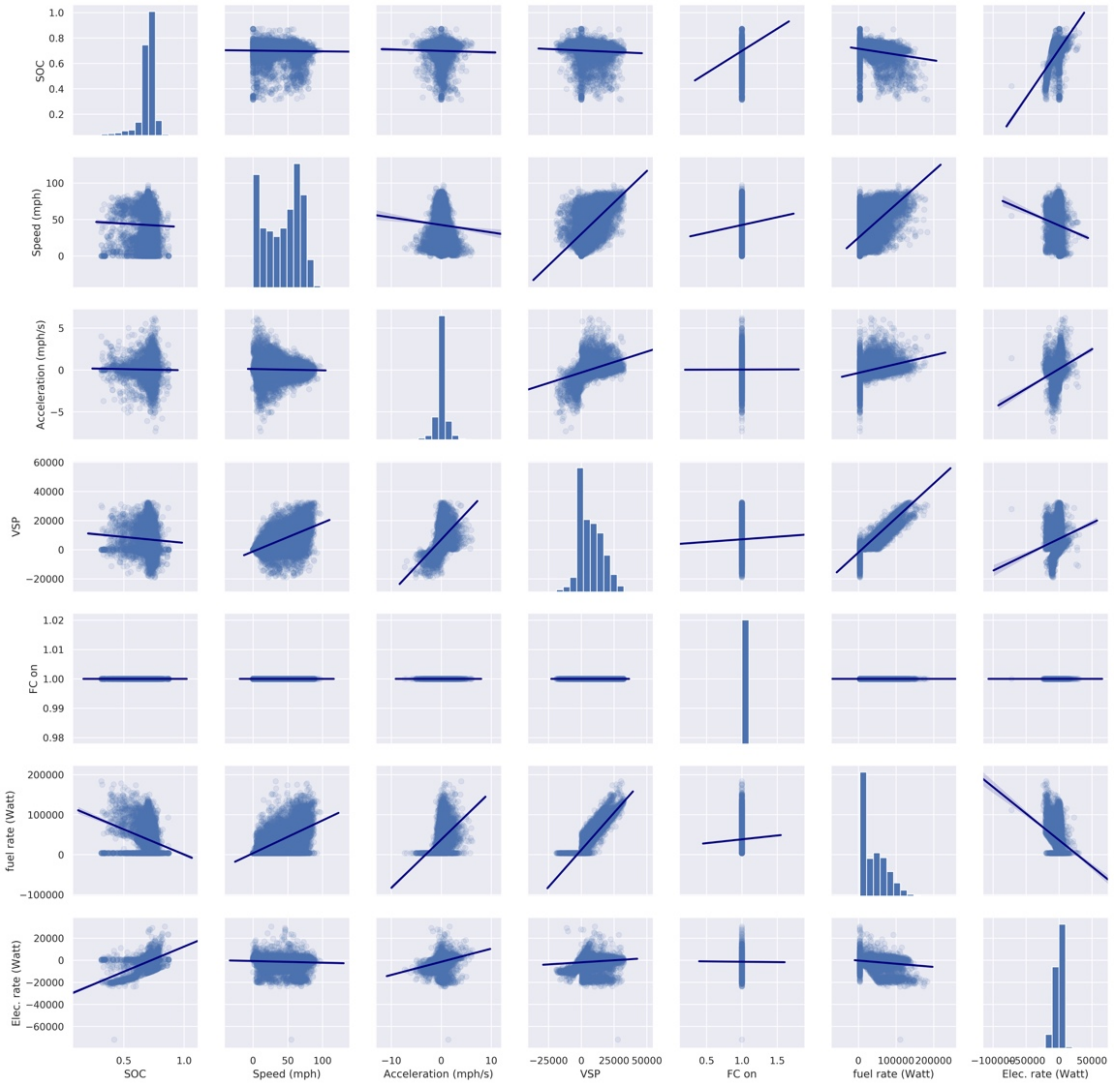

Figure 30. Pair plot of operation factors and FCEV fuel/electricity consumption

Predicting FCEV fuel use involves quantification of SOC, which requires an electricity consumption model to support the SOC prediction. As Figure 31 suggests, the Powertrain 2 is generally charging while VSP<0 and will be either under CS or CD depending on SOC when

VSP>=0. The electricity model can be predicted as following. The R^2 value of the model on 20% validation set is 0.85, which is lower than fuel model due to the discontinuity of the energy use pattern but still sufficient for model application.

$$\boldsymbol{E_{fuel}} = \begin{cases} \boldsymbol{-1.29 * 10^5 * SOC + 4.03 * vsp + 97,903.30} \ (\boldsymbol{vsp \geq 0}) \\ \boldsymbol{3892.00} \ (\boldsymbol{vsp < 0}) \end{cases} \quad \textbf{(17)}$$

Predicting FCEV fuel use involves quantification of SOC, which requires an electricity consumption model to support the SOC prediction. As Figure 31 suggested, the powertrain 2 is almost under charging while VSP<0 and will be either under CS or CD depending on SOC under VSP>=0. The electricity model can be predicted as following. The R^2 value of the model on 20% validation set is 0.85, which is lower than fuel model due to the discontinuity of the energy use pattern but still sufficient for model application.

$$\boldsymbol{E_{elec}} = \begin{cases} \boldsymbol{5.92 * 10^4 * SOC - 0.03528 * vsp - 42659.8} \ (\boldsymbol{vsp \geq 0}) \\ \boldsymbol{3.81 * 10^3 * SOC + 0.797 * vsp - 4204.68} \ (\boldsymbol{vsp < 0}) \end{cases} \quad \textbf{(18)}$$

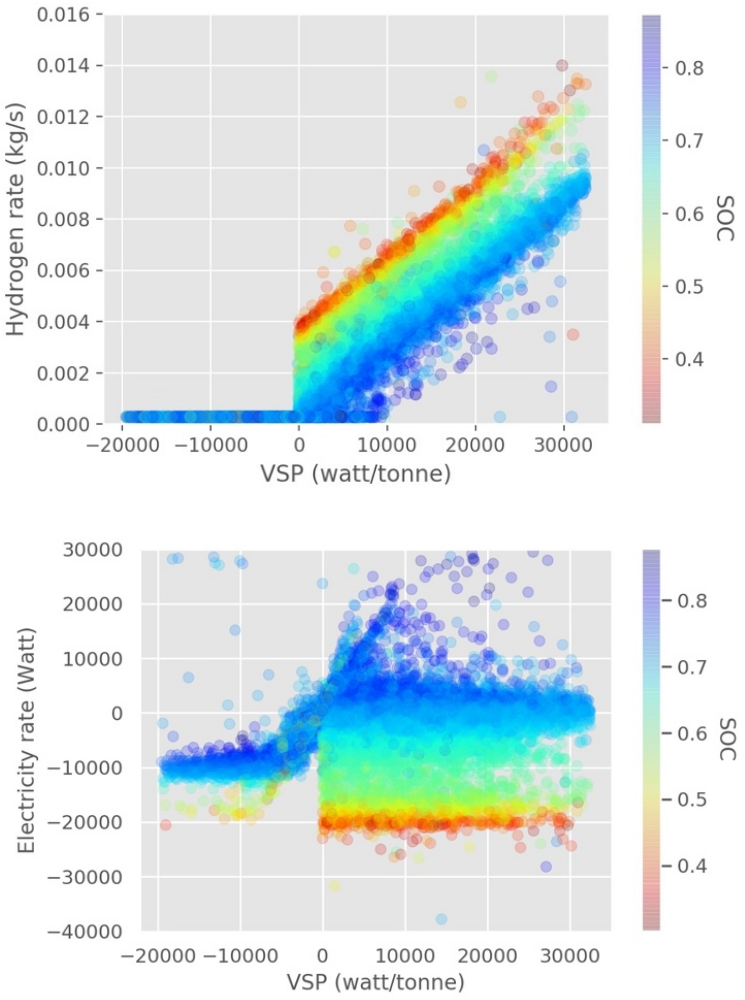

Figure 31. The fuel and electricity rate by VSP and SOC

4.3.3 Series PHEV Modeling

The initial motivation to develop a series-hybrid was to expand vehicle driving range by charging the batteries with the engine during vehicle operation (Ehsani et al., 2018; Mi et al., 2011). In a series PHEV, such as Chevrolet Volt, the vehicle is propelled by a traction motor, which is either powered by the battery or an engine/generator unit (Ehsani et al., 2018). A series PHEV has no direct mechanical linkage between the internal combustion engine and final drive. That is, the internal combustion engine and electric motor work in series. The battery is generally larger in a PHEV to provide sufficient power to the motor. A series PHEV has a variety of operation modes,

compared to the simpler control strategies of BEVs and FCEVs. Hence, a model needs to predict the series PHEV control mode and then the corresponding energy use. The relationship between engine control and motor control is shown in Figure 32 below. Motor 1 is the traction motor, which the control mode can be either charging or discharging regardless of engine control condition. Motor 2 is the motor-generator, and the operating mode of motor 2 is linked with the engine mode. When the engine is on, Motor 2 is almost always in charging mode to convert mechanical power from the engine to electricity. When the engine is off, Motor 2 is highly likely to be in an idle mode. In this case, only the engine control and Motor 1 control mode need to be modeled.

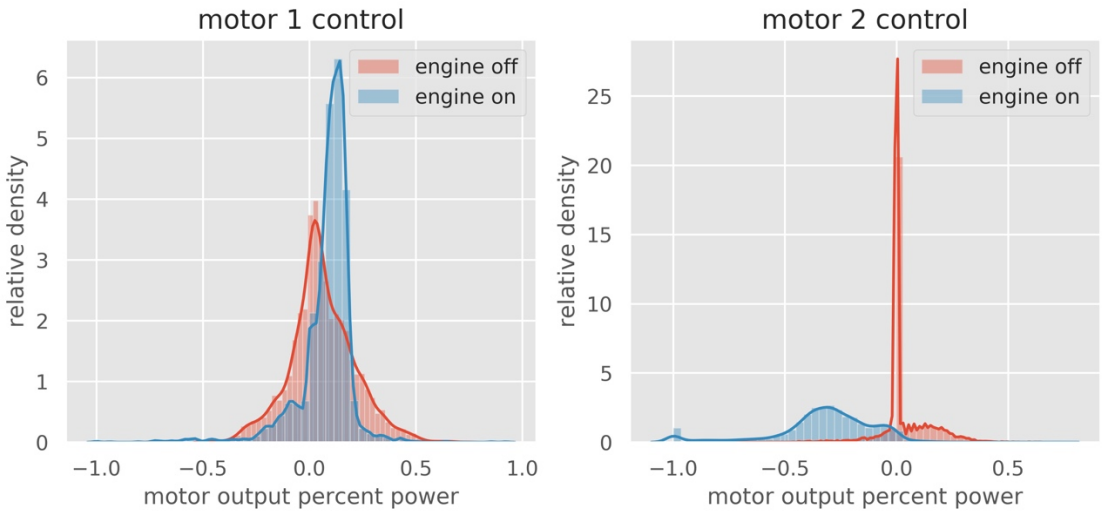

Figure 32. Series PHEV vehicle control

Next, the independent variables for fitting engine control, motor control, fuel consumption, and electricity consumption are identified using the Pearson correlation between factors and responses (the discrete variable cannot be well displayed in scatter plot). The Pearson correlation $\rho_{X,Y}$ measures the linear correlation between two variables X and Y, where $\rho_{X,Y}$ =1 means positive linear correlation, $\rho_{X,Y}$ = 0 means no linear correlation and $\rho_{X,Y}$ = -1 means negative linear correlation. The Pearson correlation matrix of the series hybrid is provided in Figure 33 below.

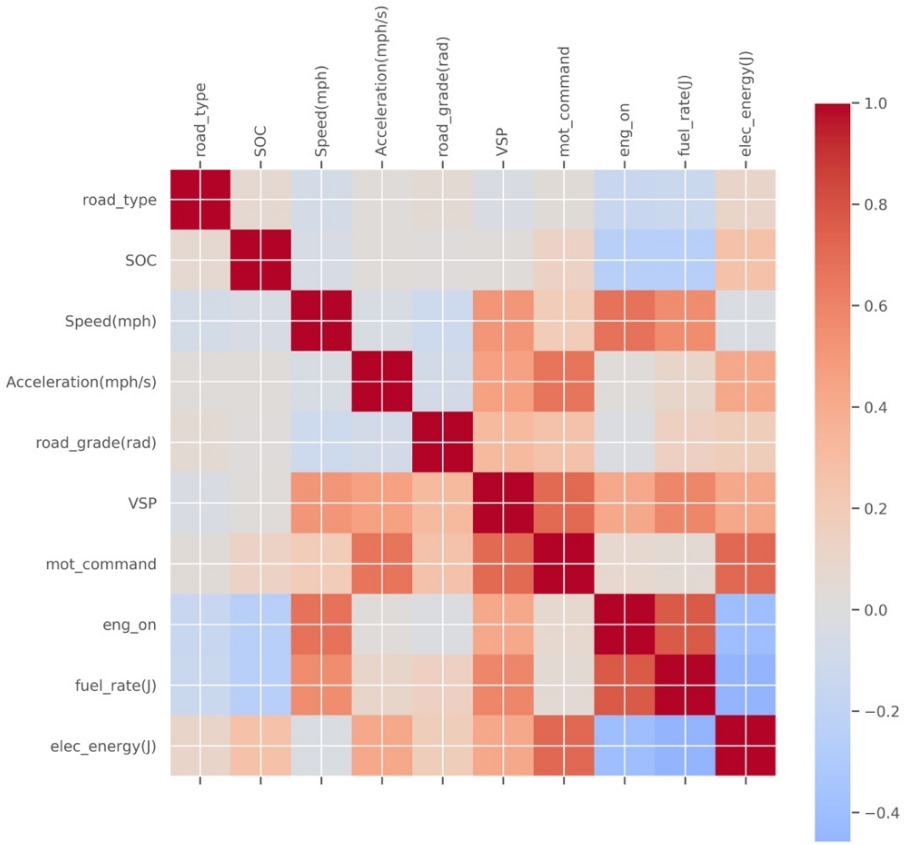

Figure 33. Pearson correlation between variables in series PHEV

As illustrated above, the engine control of the series PHEV is highly dependent upon SOC, speed, and VSP. The motor control is heavily dependent upon VSP and acceleration. The fuel consumption is highly correlated with SOC, speed, and VSP, and the electricity use depends on SOC, acceleration, and VSP. The variables above were therefore selected to model vehicle control and corresponding energy use. However, as VSP, acceleration, and speed are inter-correlated, they will only be added under rare cases when using VSP alone cannot achieve a high goodness-of-fit. The full list of parameters in the fitted model is provided in Appendix A. The R^2 value of the fuel model on 20% validation set is 0.833 and the, R^2 value of the electricity model on 20% validation set is 0.60. Overall, the model has decent performance, but the goodness-of-fit is limited due to the complexity and discontinuities in vehicle the control strategy.

4.3.4 Power-split PHEV Modeling

The major difference between power-split (series-parallel) PHEV from a standard series PHEV in powertrain configuration is the addition of a mechanical coupler to link engine output with final drive. The torque and speed coupler added in the power-split PHEV powertrain frees the engine from the drive wheels under specific torque and speed constraints (Ehsani et al., 2018), and the vehicle can be controlled with higher flexibility. The engine and (one of) two motors can be coupled to deliver the power to the wheel or engine can use one of the motors to charge the battery. The relationship between engine control and motor control is shown in Figure 34 below. Motor 1 (the tractive motor) is most likely to be in a charging mode when engine is on. In certain conditions (e.g., high power demand) the motor 1 and engine will both provide tractive power to final drive (hybrid mode). The motor 1 is often in discharge mode to propel the vehicle if engine is off. The motor 2 (the generator motor) is mostly under generating mode while engine is on. When engine is off, Motor 2 is highly likely to remain idling. In this case, only engine control and Motor 1 control mode need to be modeled.

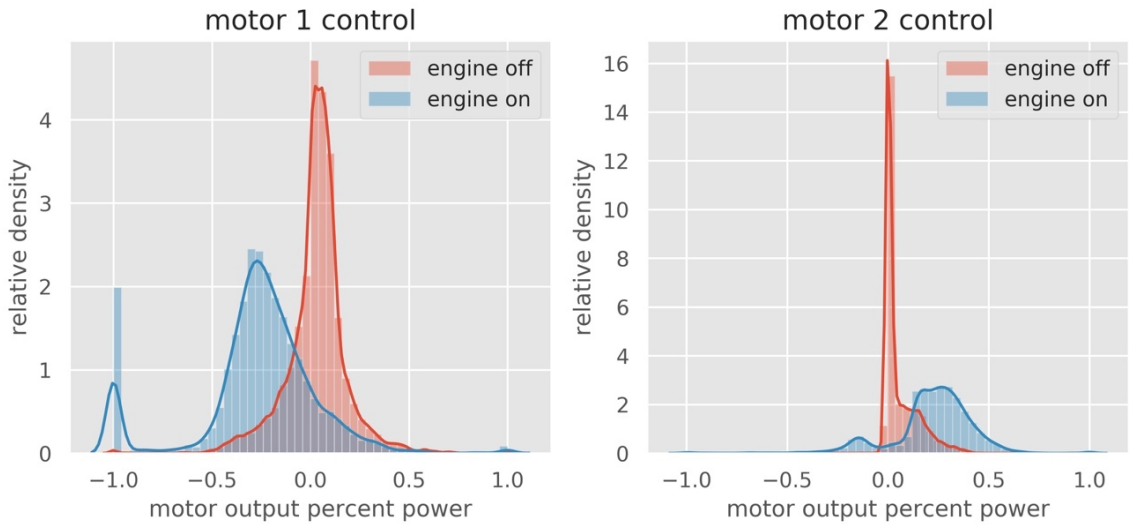

Figure 34. Power-split PHEV vehicle control

Next, the independent variables for fitting engine control, motor control, fuel consumption, and electricity consumption are still identified using the Pearson correlation between factors and responses. The correlation matrix is displayed in Figure 35 below.

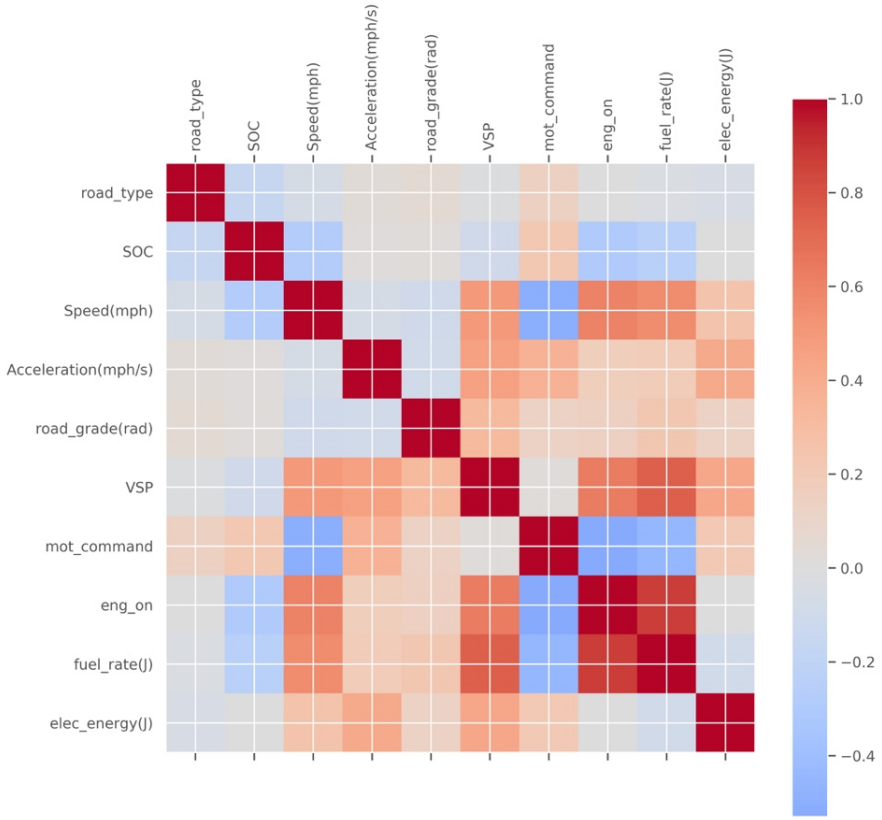

Figure 35. Pearson correlation between variables in power-split PHEV

As illustrated in the figure above, the engine control of the series PHEV is highly depending on SOC, speed and VSP. The motor control is heavily dependent upon speed and acceleration. The fuel consumption is highly correlated with SOC, speed, and VSP, and electricity use depends upon acceleration and VSP. The variables identified above were selected to fit the vehicle control and corresponding energy use. However, as VSP, acceleration, and speed are inter-correlated, they are only added under rare cases when solely using VSP cannot achieve high goodness-of-fit. The full list of fitted model is provided in Appendix A. The R^2 value of the fuel model on 20% validation set is 0.801 and the, R^2 value of the electricity model on 20% validation set is 0.69.

Overall, the model has decent performance, but the goodness-of-fit is limited due to control strategy complexity and discontinuities within the vehicle control strategy.

4.3.5 Power-split HEV Modeling

The power-split HEV has similar powertrain design to its PHEV version, except that battery size is much smaller. However, the battery maximum power is not a constant value as PHEV due to the limited battery size and the need to maintain SOC at a desired level. In this case, the battery output power (electricity consumption rate) in many cases is a function of battery SOC (Figure 36) and the model is necessarily different than that of a PHEV model. Besides updating parameters for SOC, the power-split model shares the similar structure to the PHEV model introduced above. The full list of fitted model is provided in the Appendix A. The R^2 value of the fuel model on 20% validation set is 0.957 and the, R^2 value of the electricity model on 20% validation set is 0.57. Overall, the model provides decent performance, but the goodness-of-fit of electricity use is limited due to the complexity of the powertrain control system and discontinuities in the powertrain control strategy.

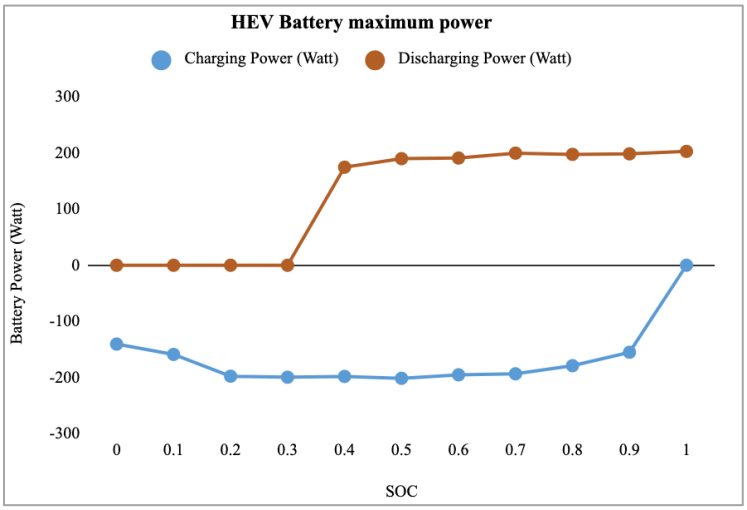

Figure 36. Maximum battery output power by SOC

4.3.6 Parallel HEV Modeling

In a parallel HEV, there is no electric coupler that converts engine power to electricity. The engine is linked with the final drive via a mechanical coupler and the work is split between the engine and one traction motor (Ehsani et al., 2018). For parallel HEVs, separate control models are developed for the engine and for the traction motor. The correlation matrix of all variables is provided below.

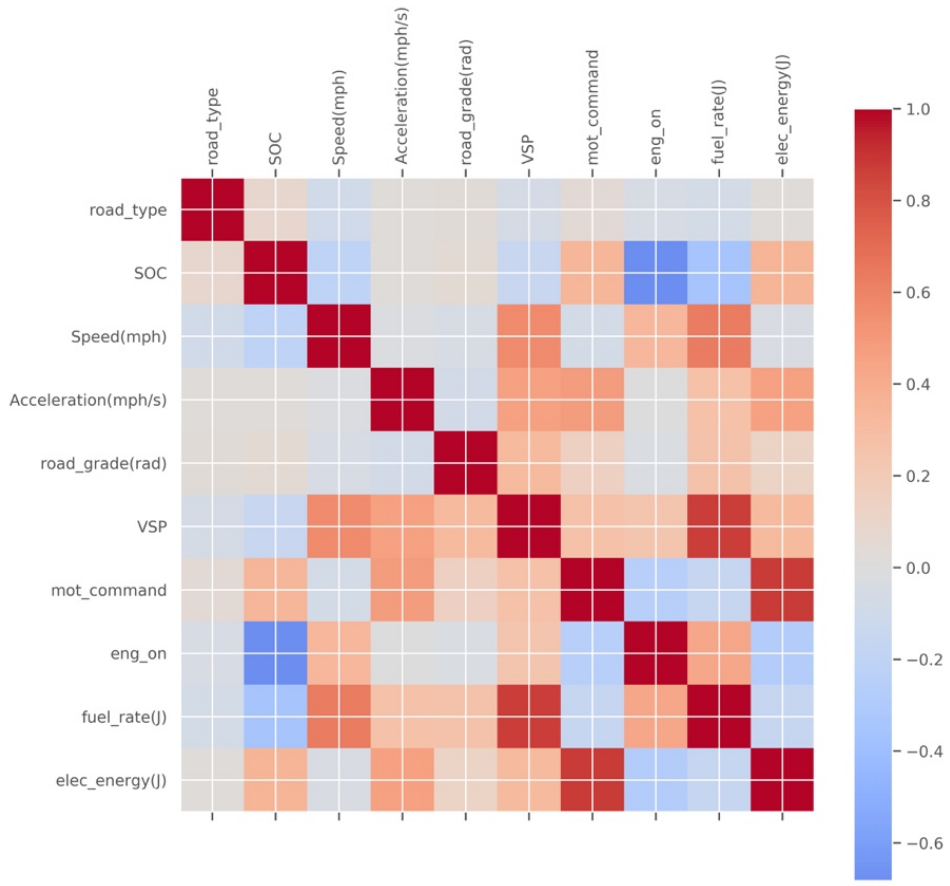

Figure 37. Pearson correlation between variables in parallel HEV

As illustrated in the figure above, the engine control of the series PHEV is highly dependent upon SOC, speed, and VSP. The motor control is heavily dependent upon SOC, acceleration, and VSP. The fuel consumption is highly correlated with SOC, speed, and VSP, and the electricity use depends on SOC, acceleration, and VSP. The variables identified above were selected to fit the vehicle control and corresponding energy use. However, as VSP, acceleration, and speed are

inter-correlated, they will only be added under rare cases, when using VSP alone cannot achieve a high goodness-of-fit. The full list of fitted model is provided in Appendix A. The R^2 value of the fuel model on 20% validation set is 0.921 and the, R^2 value of the electricity model on 20% validation set is 0.77. Overall, the model has good performance, but the goodness-of-fit of electricity use is limited due to control mode complexity and discontinuities present in the vehicle control strategy.

4.3.7 HVAC Loss and Charging Loss Adjustment

The conditional energy rates under vehicle heating and cooling is adjusted with a supplemental factor (λ). The adjustment factor is developed by running Autonomie simulation from 0.5 kW to 6.0 kW of auxiliary load under EPA standardized cycles for all EV types. The adjustment factors under distinct VSP level and control mode were defined using following equation:

$$\boldsymbol{\lambda}|_{\boldsymbol{vsp,control\ mode}} = \frac{(\boldsymbol{E_{HVAC\ load\ high}} - \boldsymbol{E_{HVAC\ load\ base}})}{\boldsymbol{\Delta_{HVAC\ load}}}|_{\boldsymbol{vsp,control\ mode}} \quad \textbf{(19)}$$

Where,

$E_{HVAC\ load\ high}$ - the energy rate under high HVAC load

$E_{HVAC\ load\ base}$ - the energy rate under baseline HVAC load (0.5 kW)

$\Delta_{HVAC\ load}$ - difference between high and low HVAC loads

In this case, the updated energy rates under given HVAC load can be calculated as following:

$$\boldsymbol{E_{HVAC\ load\ pred}}|_{\boldsymbol{vsp,control\ mode}} = [\boldsymbol{E_{HVAC\ load\ base}} + \boldsymbol{\lambda} * (\boldsymbol{HVAC\ load\ pred} - \boldsymbol{HVAC\ load\ base})]|_{\boldsymbol{vsp,control\ mode}} \quad \textbf{(20)}$$

The adjustment of HVAC load proposed in this study does not incorporate potential factors that may affect the auxiliary energy use, such as vehicle design and thermal management factors

(Qi, 2014; Yuksel and Michalek, 2015). However, the simple adjustment will not significantly add additional variance to final results and will maintain the robustness of the final trained model. Further research efforts should be conducted to further improve the accuracy of the model with respect to HVAC impacts by incorporating more detailed factors associated with HVAC operation and compressor control.

For BEVs and PHEVs, the electricity loss during transmission and charging is considered to calculate the final energy supply from the power plants. In this study, the transmission efficiency as 95.1% and charging efficiency as 85% from the Greenhouse gases, Regulated Emissions, and Energy use in Transportation Models (GREET®) is used for BEVs and PHEVs (Elgowainy et al., 2010; Kelly and Elgowainy, 2018), which leads to a combined 80.8% of energy efficiency from power plants to on-board electricity in State of Georgia.

4.3.8 Model Summary

The complete lists of parameters were provided in Appendix A. The model goodness-of-fit metrics, including R^2 and root-mean-square error (RMSE) on the validation set were listed in Table 9 below. Overall, the predicted fuel rates have R^2 greater than 0.80 and the predicted electricity rates have R^2 greater than 0.60. The goodness-of-fit metrics for electricity were generally lower than fuel, which may be caused by ignoring unmeasurable factors in electric motor operation, such as variation of internal impedance and battery state-of-health.

Table 9. Energy model performance summary

Vehicle Type ID	100mile BEV	300mile BEV	Fuel cell EV	Parallel HEV	Power-split HEV	Power-split PHEV	Series PHEV
Original sample size	BEV	BEV	FCEV	HEV	HEV	PHEV	PHEV
Final sample size	987,092	987,092	987,092	987,092	987,092	987,092	987,092
Percentage of Non-relevant Data	874,436	866,845	894,938	910,143	924320	873,137	860,727
Electricity Rate RMSE (Watts)	11%	12%	9%	8%	6%	12%	13%
Electricity Rate R^2	1,947.01	3,536.38	2,002.17	3,117.86	3490.9	8,210.25	7,303.31
Fuel Rate RMSE (Watts)	0.99	0.97	0.85	0.77	0.58	0.69	0.60
Fuel Rate R^2	-	-	7,102	10,485	7,808	22,014	16,036
Total Energy Rate RMSE (Watt)	-	-	0.957	0.921	0.957	0.801	0.833
Total Energy Rate R^2	1,947	3,536	7,412	8,496	7,181	12,143	14,489
Original sample size	0.987	0.971	0.952	0.947	0.965	0.908	0.895

4.4 Energy Model Verification

The energy model was externally verified using a separate set of 146 trips with speed, acceleration, and road grade distributions provided in Figure 24 above. The second-by-second speed, acceleration, road grade, a constant auxiliary load, and random initial battery state of charge level served as model inputs, with fuel rate, electricity rate and SOC level predicted using simulation inference method introduced above. The SOC level is updated continuously, using a constant battery capacity C (Table 8), available electricity E_0 at the beginning of the trip (initial SOC), and electricity consumption over time E_t using following equation:

$$\boldsymbol{SOC_t = \frac{E_0 - E_t}{C}} \quad \textbf{(21)}$$

Updating the SOC level every second tends to raise the accumulated SOC prediction error and increases energy prediction error along the time-series. Instead of updating SOC second-by-second, this modeling case study updates SOC once per minute of operation.

A sample trip prediction with EPA standardized driving cycle, 5.0 kW auxiliary load, and 90% initial SOC level as input is provided in Figure 38 below. While there are significant differences on a second-by-second basis for some on-road operating conditions, the predicted fuel use, electricity use, and decrease in SOC generally follow the general trends predicted by Autonomie. While the SOC predictions are close to Autonomie-generated SOC curve, the energy prediction errors are also much lower.

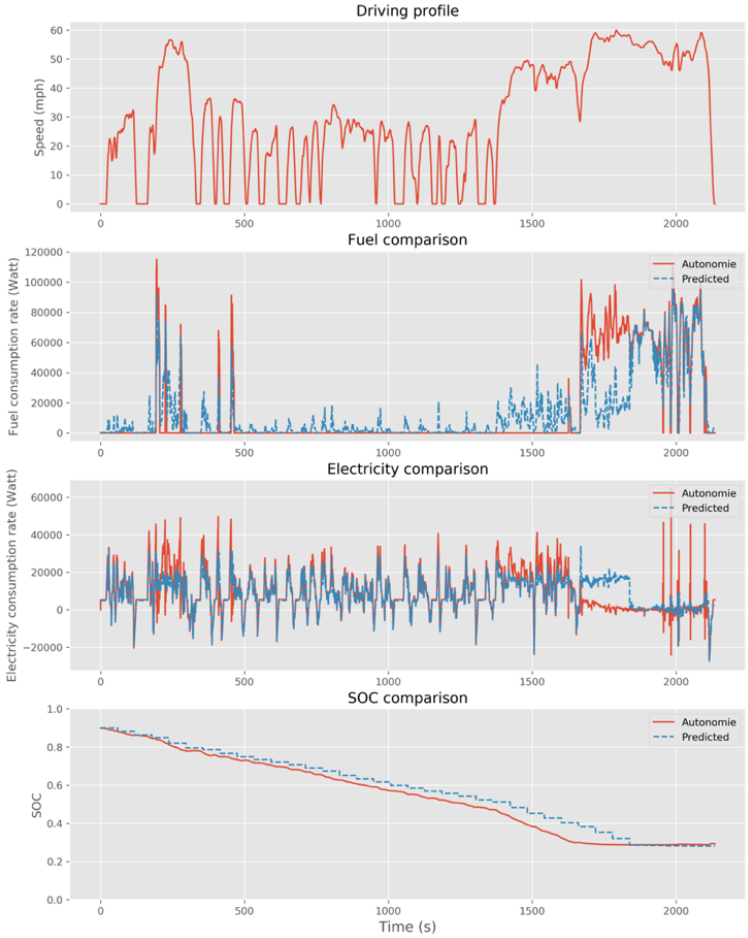

Figure 38. Energy prediction results under EPA combination cycles and 5kW HVAC load

For the 146 trips tested with random initial SOC and 0.5 kW auxiliary load, the trip-level energy prediction results are illustrated in Figure 39 below. The predicted energy use by fuel and electricity by the Bayesian Network model generally match with the energy consumption originally generated by Autonomie. The proposed model provides representative energy use profiles under a wide range of driving conditions and appears suitable for network-level applications applied to a given fraction of modeled EV fleets.

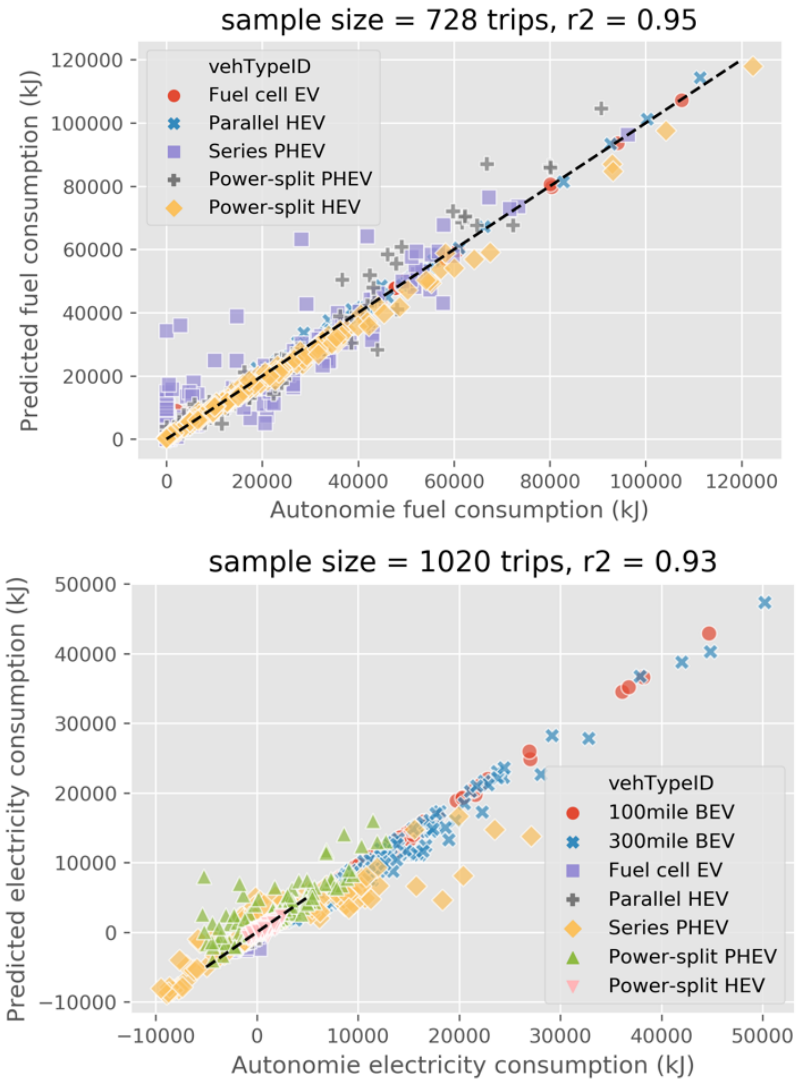

Figure 39. Trip-level energy results verification

4.5 Energy Model Verification Using Real-world Data

The energy model developed in this study is based on Autonomie-simulated vehicle models that were previously calibrated for certain EV models (Jeong et al., 2019; Kim et al., 2014; Wu et al., 2015). To demonstrate the effectiveness of applying such model to real-world EV fleet and identify potential future model applications to the transportation network, on-board diagnostic (OBD) devices have been used to collect observed EV operation and energy use data from a small set of EVs for model verification. The energy model developed in previous section is used to predict energy use from the observed operation data. The predicted trip-level energy use patterns were compared to the observed energy use to demonstrate whether: (1) the model can represent the energy use inventory of real-world fleet, and (2) the variation of predicted energy use is similar to the variation of actual energy use under different operation conditions.

4.5.1 OBD Data Collection

About one-week of EV operation and energy use data were collected from a small group of volunteer drivers from October 2018 to April 2019. Due to the limited number of EV ownership and limited usage of EV by each owner, the sample size of collected data is relatively small and is not representative of all kinds of operating conditions. However, the goal of the verification work is simply to demonstrate the energy model can provide reasonable predictions under certain operating conditions and for those vehicles tested, and to identify potential bias related to energy prediction.

Two OBD devices owned by the research group were used to collect data from EV fleet – the BlueDriver® OBDII scan tool and DAWN OBD Mini Logger™ (the later one is more expensive and was purchased in early 2019 but can guarantee stable data collection up to 50 HZ and directly incorporates GPS signals). Photos of the OBD devices are provided in Figure 40.

Figure 40. OBD data collection devices

Three volunteer drivers were recruited during the data collection (including the author). The OBD device was plug into the vehicle OBD portal and retrieving all the available parameters during vehicle operation. The availability and quality of collected attributes are subjected to sensors and control signals used in different vehicle models and may not necessarily be consistent among different vehicles. The summary of EV data is provided in **Table 10** below. Vehicle speeds, fuel consumption rates derived from MAF, and the battery SOC will be used in the analyses that follow, as they are included in the model inputs/outputs. Other attributes are retained for future model application and verification purposes.

Table 10. Summary of collected real-world OBD data

Vehicle	2017 Ford Fusion Hybrid	2015 Toyota Prius	2018 Prius Prime (25 mile AER)
Ownership	Rental car	Owned car	Owned car
Driver's occupation	Graduate student	Professor	Graduate student
Powertrain	Parallel hybrid	Power-split ("Synergy") hybrid	Power-split ("Synergy") plug-in hybrid
Primary trip purpose	Visiting and leisure	Daily commute	Daily commute
Data collection location	Denver, Colorado	Atlanta, Georgia	Atlanta, Georgia
Data collection time	Oct 6th – Oct 9th, 2018	Feb 8th – Feb 14th, 2019 Apr 9th – Apr 17th, 2019	Mar 4th – Mar 12th, 2019 Apr 25th, 2019
Data collection device	BlueDriver®	HEM data logger	HEM data logger
Original record	22761	25916	127731*
Record after removing idling	22761	20396	28785
Record after filling missing value	24634	20588	28942
Hours of operation	6.84	5.67	8.00
Average operation speed (mph)	24.49	19.22	23.69

*The driver forgot to unplug data logger and the device collected data overnight

For each vehicle at each second, the collected OBD data include at least the following attributes:

1. Date and time
2. Vehicle speed from the speed sensor on the wheel
3. Mass air flow (MAF) rate, which can be used to calculate a theoretical fuel consumption rate under normal combustion condition. Modern vehicles use the oxygen sensors to feedback data to the vehicle's electronic control module (ECM) and control the air to fuel ratio. The fuel consumption is calculated using the chemically ideal value of 14.7 grams of air to every gram of gasoline for a normal combustion engine.
4. Battery remaining power level (SOC)

5. Engine RPM: The current engine speed in revolutions per minute (RPM).
6. Calculated Engine Load Value (%): Indicates a percentage of peak available torque.
7. Absolute Load Value (%): This is the normalized value of air mass per intake stroke displayed as a percent.
8. Ambient temperature (°F)

The vehicle speeds, fuel consumption rates derived from MAF and the battery SOC will be used for following analysis as they are included in the model inputs/outputs. Other attributes are kept for future model application and verification purposes.

4.5.2 OBD Data Process and Energy Modeling

Due to the delay of data acquisition from the vehicle OBD portal, the OBD data output can drop one or two seconds of records from time to time. The OBD data need to be post-processed before they applied in the energy model. The data process and energy calculation are performed using the following procedures illustrated in Figure 41. As the diagram shows, the first step is to convert all of the time stamp in the raw data stream to local time, to reflect the vehicle operation by time of day. Then, the off-operation data (engine off, battery-level not decreasing, and speed = 0 mph) were removed, as the vehicle was likely being parked and not in use. The OBD data is then broken up into smaller trip sequences when there is a large time gap that would be difficult to reasonably infill. The key step in the OBD data process is using cubic spline for filling missing value along the time-series. The cubic spline can fit the data at given time stamp based on the trend of surrounding points. The sample splined data of selected attributes are shown in Figure 42.

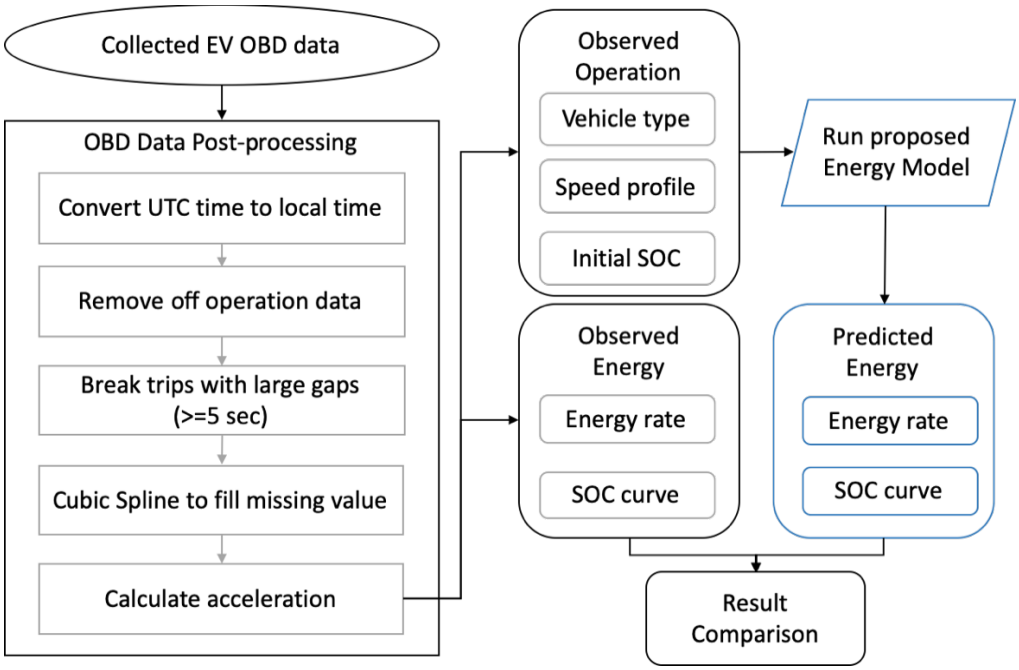

Figure 41. OBD data processing and energy calculation workflow

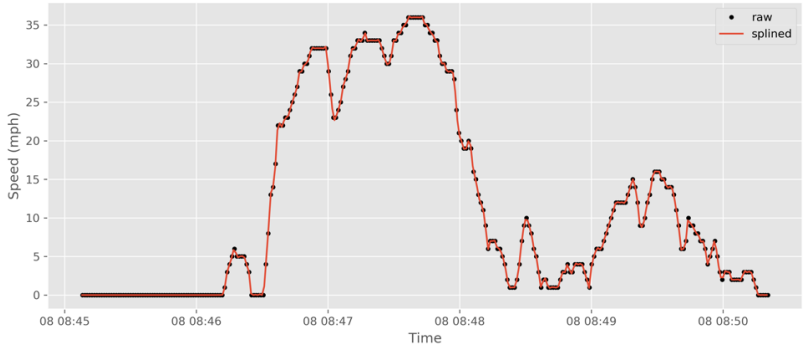

(a) Speed spline

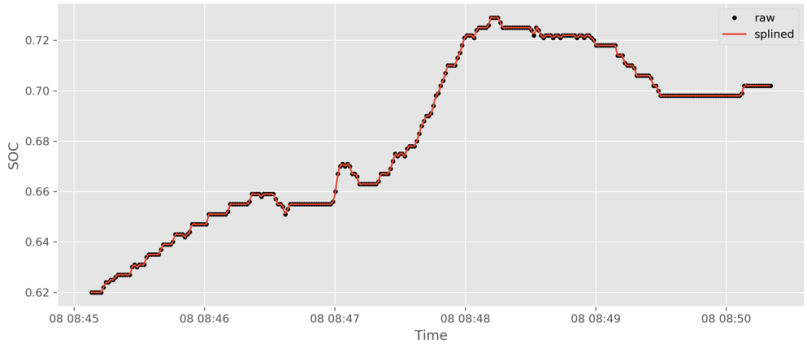

(b) SOC spline

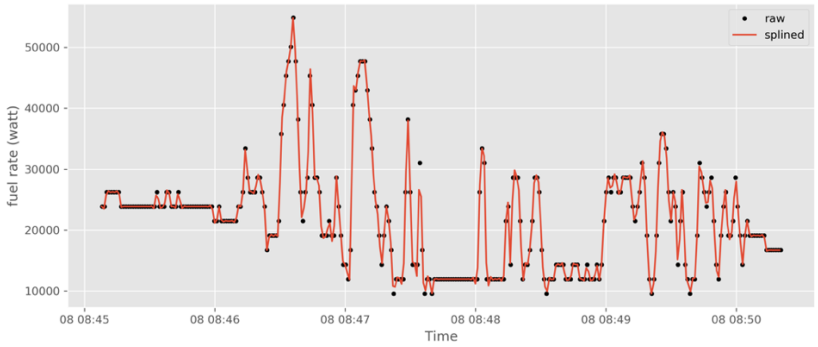

(c) Fuel rate spline

Figure 42. Sample cubic spline of OBD data

After filling missing data with cubic spline results, second-by-second speeds, SOCs, and fuel rates were exported. The acceleration rate is calculated by taking the derivative of the speed profile. The speed, acceleration, and initial SOC, from specific EVs are then used to calculate energy consumption using proposed model assuming flat terrain (which may lead to a slight estimation bias). The predicted energy use and SOC curve will be compared to the observed energy use and SOC curve for model verification.

4.5.3 EV Operation Data

About one week of vehicle operation and energy use data were collected from each vehicle. Due to the differences in travel routines of each driver, a limited number of operating conditions were observed in this study. These operations will not be representative of the entire population and are used for initial model verification only. The vehicle speed, SOC, and fuel consumption distribution of each vehicle are provided in Figure 43, Figure 44 and Figure 45 respectively.

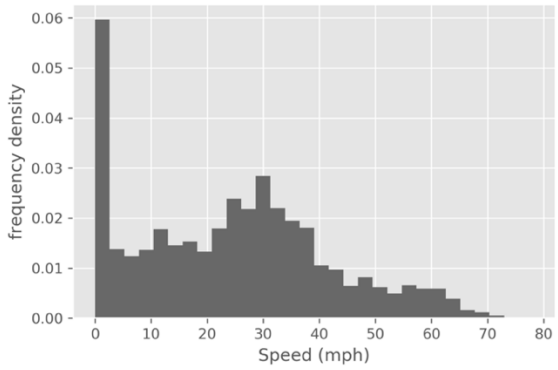

Speed distribution

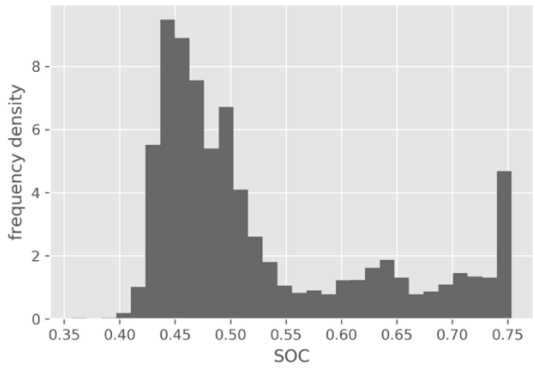

SOC distribution

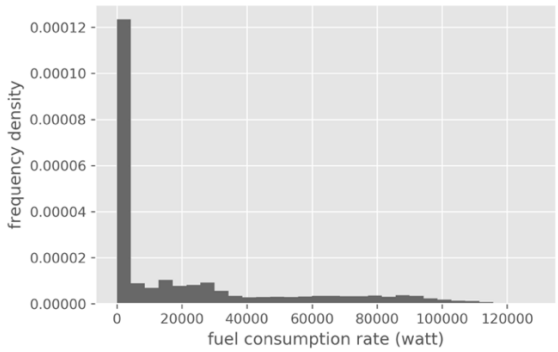

Fuel rate distribution

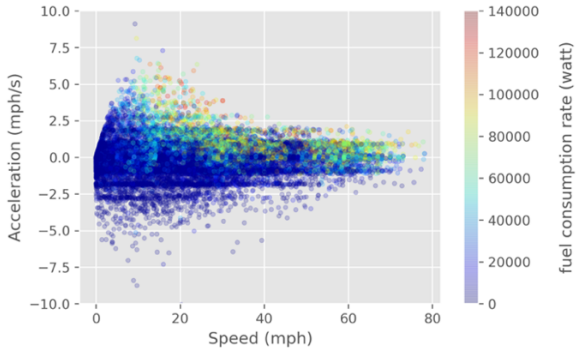

Fuel rate by operating condition

Figure 43. Operation and energy use of 2017 Ford Fusion

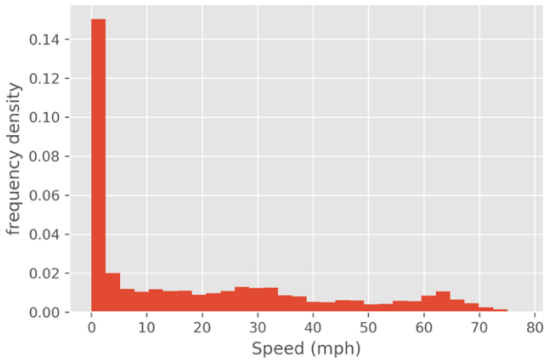

Speed distribution

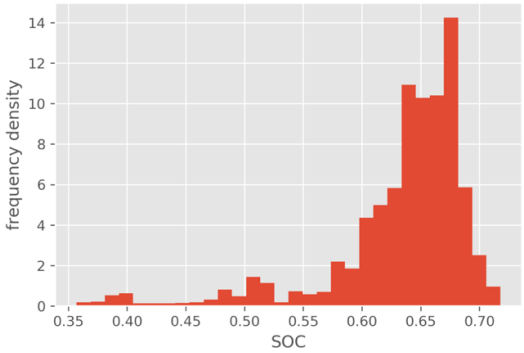

SOC distribution

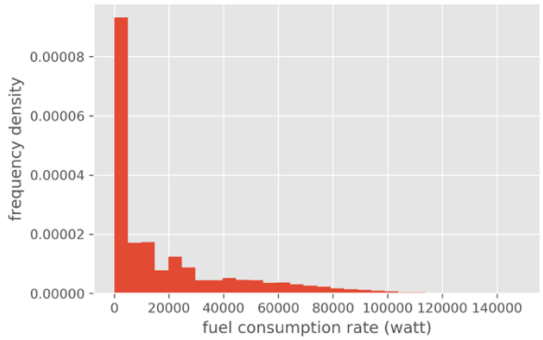

Fuel rate distribution

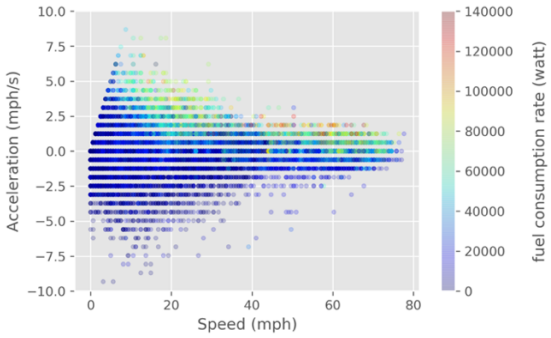

Fuel rate by operating condition

Figure 44. Operation and energy use of 2015 Toyota Prius

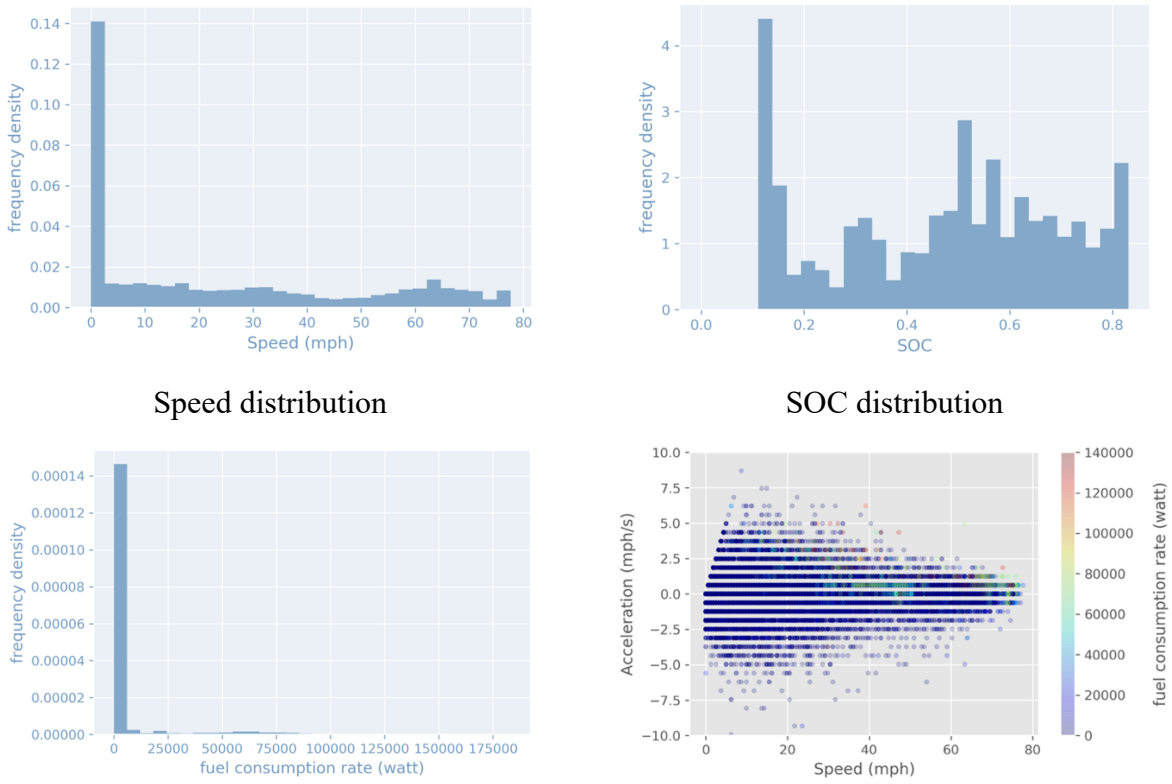

Speed distribution SOC distribution

Fuel rate distribution Fuel rate by operating condition

Figure 45. Operation and energy use of 2018 Toyota Prius Prime

In terms of operation characteristics, the vehicle operations across the three monitored EVs is dominated by lower speed operations and mild accelerations/decelerations (low aggressiveness) compared to the operations data used for model development in Figure 24. The SOC distributions of two HEVs are generally between 0.4 and 0.7, while the PHEV has a wider range of SOC from 0.1 to 0.8 (not up to fully charged). For HEVs, the SOC distributions are bell-shaped and skewed. For PHEVs, the SOC distributed around fully charged and fully depleted, with lower probability to be under medium-low battery level. In terms of energy use patterns, the high fuel consumption generally occurs under high-speed and high-acceleration operations for all three vehicles. The PHEV is usually sufficiently charged to meet all trips because the driver of that vehicle has a no-cost charging option available at their work destination, so the fuel consumption for this vehicle is around zero under most circumstances.

The operation data observed from real-world driving behavior represent some potential driving condition and the corresponding energy use represents potential energy inventory from an EV sub-fleet. In next section, the operation data will be used as model inputs to predict energy use with developed Bayesian Network model. The predicted energy use will be compared to observed energy use for model verification.

4.5.4 Energy Results Comparison

After running the EV energy model with second-by-second speed, initial SOC and given vehicle type (parallel hybrid, power-split hybrid and power-split PHEV), the trip-level fuel consumption results from observed data and model prediction is given in Figure 46 below.

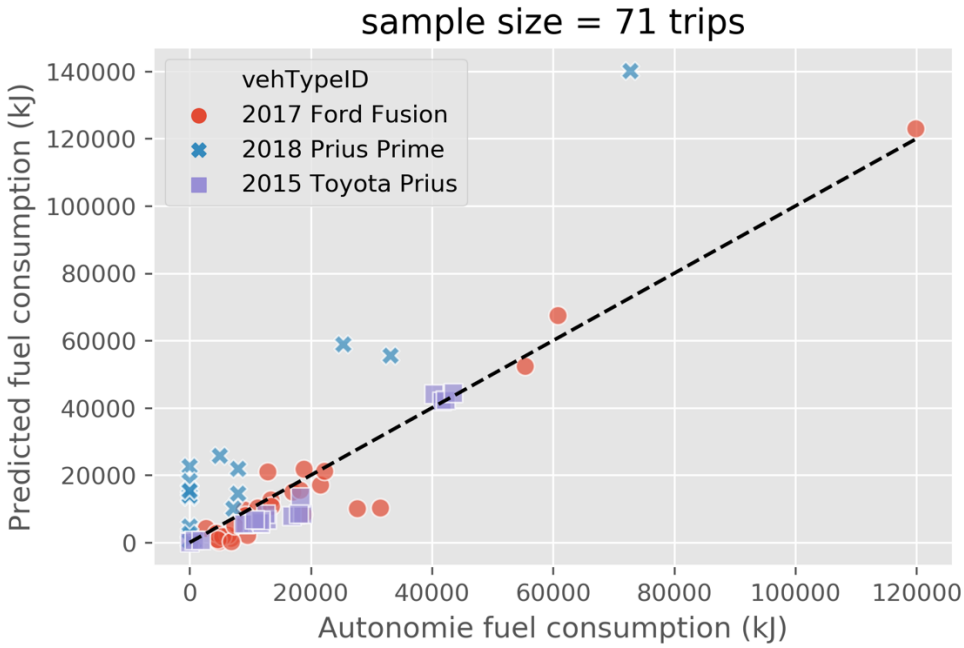

Figure 46. Comparison between observed and predicted EV fuel consumption

The above graph suggested that the predicted HEV energy use can generally follow the real-world energy use patterns of similar vehicle models. The observed fuel consumption of PHEV suggested a more fuel-conservative control strategy compared to predicted results, which may have

been introduced during the latest vehicle operating control system upgrade. Control models in the underlying Autonomie simulation model need to be updated and calibrated to reflect the latest vehicle model and control strategy development released with new EVs and in software upgrades in the existing fleet (such changes will need to be tracked). This also implies that simulation-derived models will likely need to be updated on a regular basis as manufacturers update software control strategies. Finally, the collected sample size is relatively small, and the conclusion may subject to change given more observation samples. Also, the effects of road grade and air condition load are excluded due to lack of grade information in the data stream and could lead to potential estimation biases. However, due to the time and budget limitation in this study, the verification is performed using the best dataset the author can acquire and the conclusions are drawn based on the best knowledge of the author.

Next, the second-by-second observed and predicted fuel consumption rates (Watts) were grouped and averaged by speed and SOC level to assess whether the model can predict the trend of energy consumption under varying operating conditions, as illustrated in Figure 47. Given the potential difference between the modeled vehicle and observed vehicle (especially in control strategy), the uncertainty of sensor accuracy, and uncertainty in temporal matching of on-road vs engine data, the residuals of second-by-second predictions are huge. However, the energy model aims to reflect the energy inventory across driving conditions, rather than predicting each second of data with high accuracy. The absolute difference between observed and predicted average fuel rates by speed and SOC bins were compared instead to verify if the model is able to predict the trend of energy use under different operating conditions.

The **Figure 47** suggested that the energy model can in general reflect the increase of fuel consumption under higher speeds and lower SOC for all three vehicles. The predictions are

generally more accurate under low-speed high-SOC range, potentially due to the same control strategies adopted in the Autonomie simulation as the actual vehicle. The absolute errors under higher speed and low SOC conditions are generally larger for all three vehicles. The fuel prediction of PHEV is much higher than observed fuel use potentially due to the different control strategies applied.

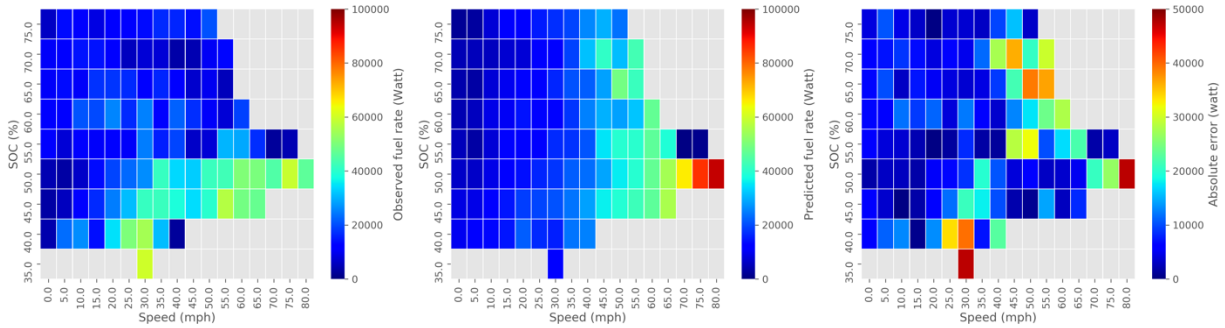

(a) 2017 Ford Fusion

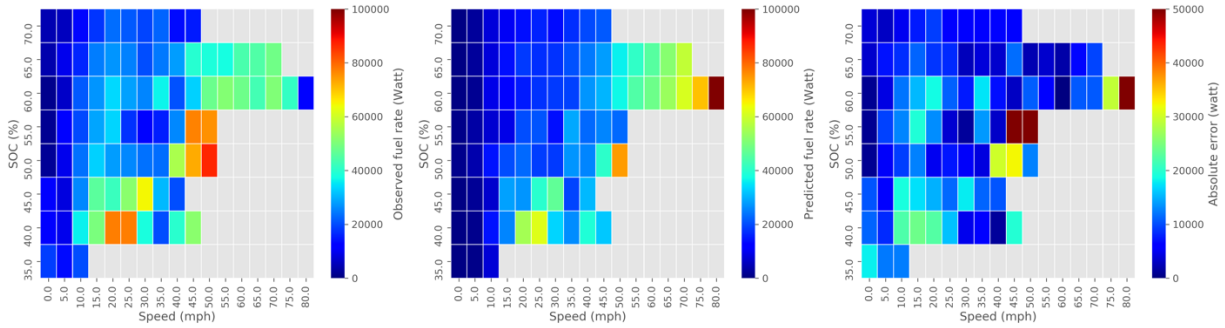

(b) 2015 Toyota Prius

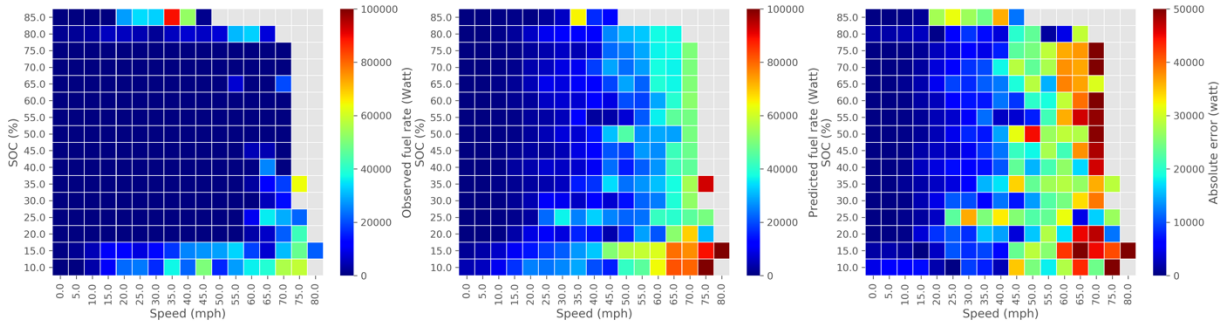

(c) 2018 Prius Prime (25 mile AER)

Figure 47. Energy consumption by instantaneous speed and SOC from (a) 2017 Ford Fusion, (b) 2015 Toyota Prius and (c) 2018 Prius Prime

Finally, the energy results from some selected driving profiles (one profile for highway and one profile for arterials) are provided in Figure 48 for model verification at instantaneous level. On both highway and arterials, the model can effectively identify potential engine-on periods, and the predicted range of energy rates is close to actual fuel rate. The predicted SOC variation is often more conservative compared to actual SOC in real-world fleet, which suggest potential improvements need to be made for predicting electricity use (e.g., updating effective battery capacity as a function of environmental conditions, during simulation instead of using constant capacity). The fuel use predicted by PHEV model is almost systematically higher than observed PHEV, which suggested the potential technology advance in latest PHEV model and the need for develop different EV energy models for the same vehicle type with different control strategies.

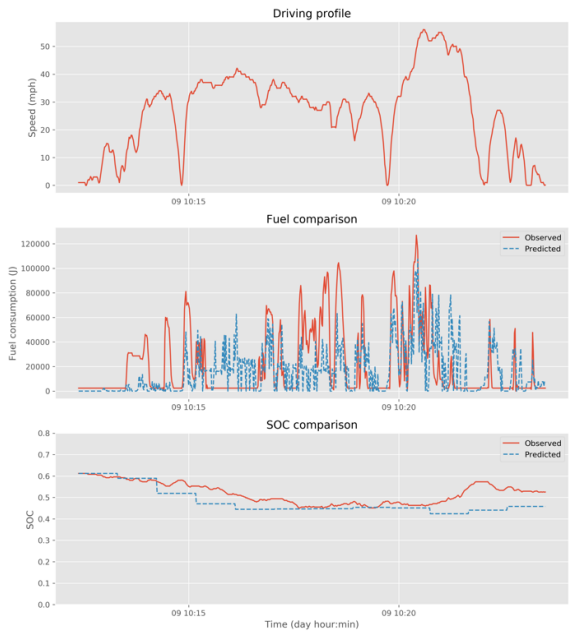

Fusion - Highways

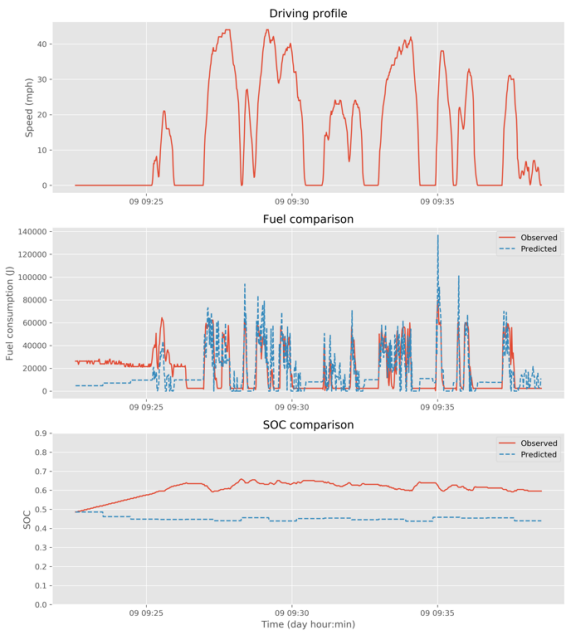

Fusion - Arterials

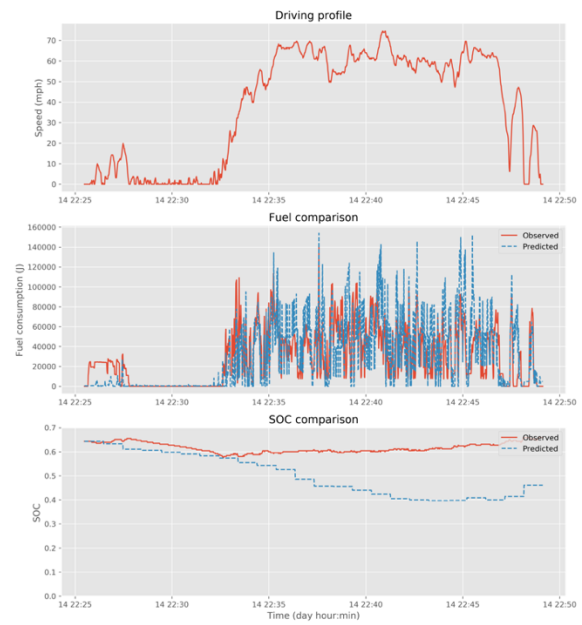

Prius - Highways

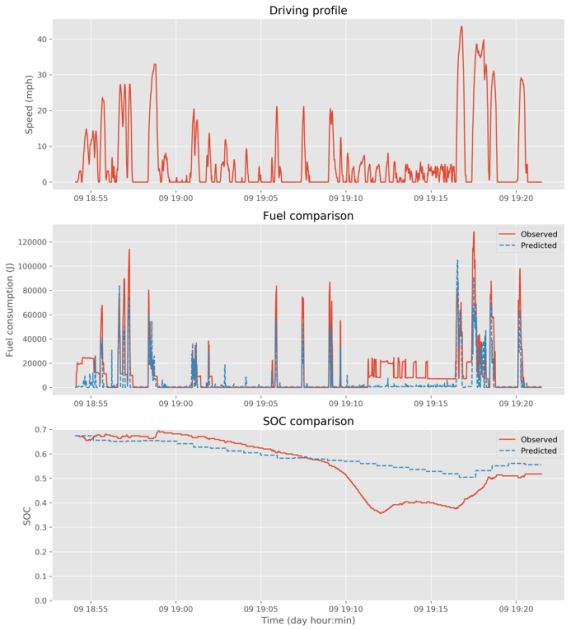

Prius - Arerials

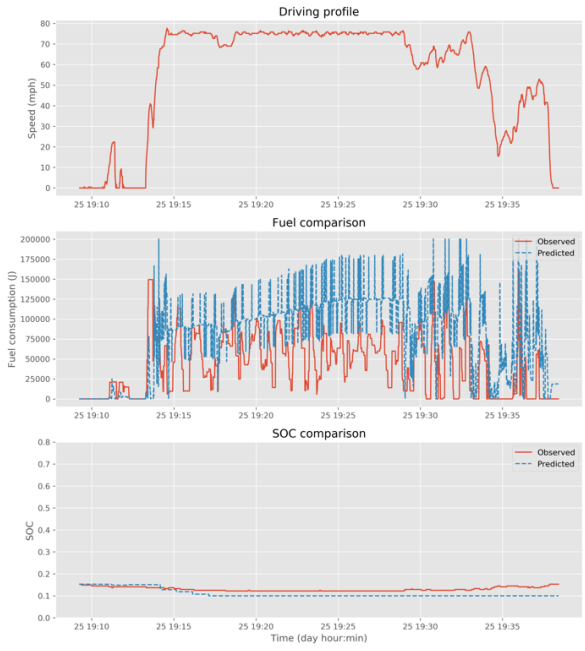

Prius Prime – Highways

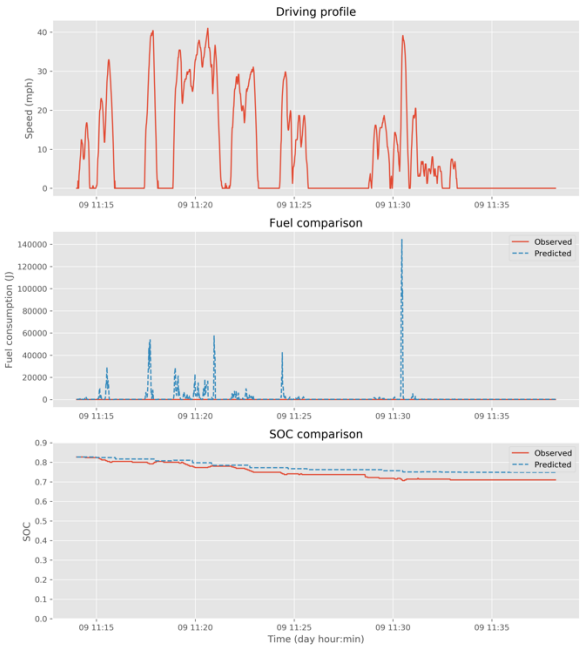

Prius Prime – Arterials

Figure 48. Vehicle speed, energy use and SOC variation of selected driving profiles

4.6 Chapter Summary

In this chapter, a simulation inference model is derived using outputs of the full-vehicle simulation Autonomie model using a Bayesian Network method. The model employs measurable factors for

vehicle type, on-road operation conditions, and ambient environmental conditions as model inputs and predicts EV fuel and electricity use for these different driving conditions. The model adopts a simplified powertrain framework into the structure, which is able to model most current EV designs within a consistent framework. The model results are parametric and incorporate only observable factors, which makes it scalable and amenable for integration into most transportation analyses. The model is verified using a separate development and testing data sets. Also, the real-world operation and energy use data were collected using OBD devices from a small sample of EV fleets. The results suggested that the developed energy model can predict the variation of energy use pattern under observed operation conditions, with different speed, aggressiveness, and battery SOC.

The EV modeling framework can be further improved based on the findings in this chapter and the identified future works are summarized below:

- **Enhancing the underlying Autonomie simulation model**. The Autonomie simulation model is calibrated and verified using a subset of the EV fleet and may or may not be representative of other EV vehicles, even those that share the same vehicle type and powertrain design, due to differences in control strategy and power management. The underlying Autonomie model needs to be calibrated for more EV models currently available in the market (and with forthcoming vehicle models) to allow the energy modeling fully representative to the real-world fleet.
- **Collecting more real-world operation data with higher accuracy.** Collecting real-world EV operation data plays a significant role in understanding EV control system performance and energy use patterns. For example, much more detailed information on

SOC is needed for these models. However, the current scale of data collection and insight into sensor and data accuracy are lacking. More stakeholders, including vehicle manufacturers, EV owners, transportation planners and engineers, need to be involved in the research efforts to collect high-fidelity data and perform analytic works.

- **Improving model training techniques for future application.** The current model is trained with limited factors and techniques. A highly-efficient parameter-tuning technique needs to be proposed in the future to train the model with a customized structure, so that the proposed modeling framework can be rapidly transferred to the remaining EV fleets.

CHAPTER 5. TRANSPORTATION NETWORK ENERGY USE

In this Chapter, the energy model developed in Chapter 4 is applied to the Atlanta Metropolitan Area as a case study to estimate the energy saving benefits of introducing EVs into the region across various fleet penetration rates. First, the methodology of estimating link-level energy use with proposed energy model is introduced as the primer for the analyses that follow. Then, a sensitivity analysis is performed using two approaches to investigate the impact of several operating factors on EV energy use. The first approach uses scatter plots of EV energy rates under different link-level inputs for each type of EV to show the relationship between operation conditions and energy results. The second approach adopts a variance-based method ("Sobol method") to investigate the quantitative impacts of input factors on energy results. The total variance of energy rates was decomposed by link-level input factors, and the Sobol indices were calculated as an indicator of impact from different inputs on the energy outputs. The sensitivity analysis (SA) is performed to demonstrate the sensitivity of model to various input factors, and to identify which factors may have the largest impact on result variability. Also, the SA will provide guidance on future work and help researchers better understand the uncertainty of energy outputs associated with different input factors. Finally, the link-level energy consumption is estimated using the simulation-informed statistical model developed in Chapter 4, using a mixed EV fleet of BEVs, PHEVs, HEVs and FCEVs with pre-defined fleet penetration fractions. The network-level results presented in this Chapter is an expansion of the energy modeling conducted in Chapter 3 to demonstrate the scalability of the proposed model.

5.1 Link-level Energy Rate Estimation

Similar to the study performed in Section 3.7.4, the network-level EV energy analysis in this chapter is performed using link-level traffic inputs. In this section, the energy consumption rates for fuel and electricity were estimated across the variety of link-level inputs to show the relationship between energy use and operation conditions. The initial SOC can be selected within the ranges provided in Table 8. Due to insufficient data to differentiate urban and rural driving conditions, the road type is represented by arterial or freeway for both rural and urban driving conditions. For each road type and each average speed, a representative driving cycle is drawn from regional GPS data as introduced in Section 3.7.4 to simulate the energy use for certain miles of operations. The speed and acceleration features of sample driving cycles by road type are provided in Figure 49 below.

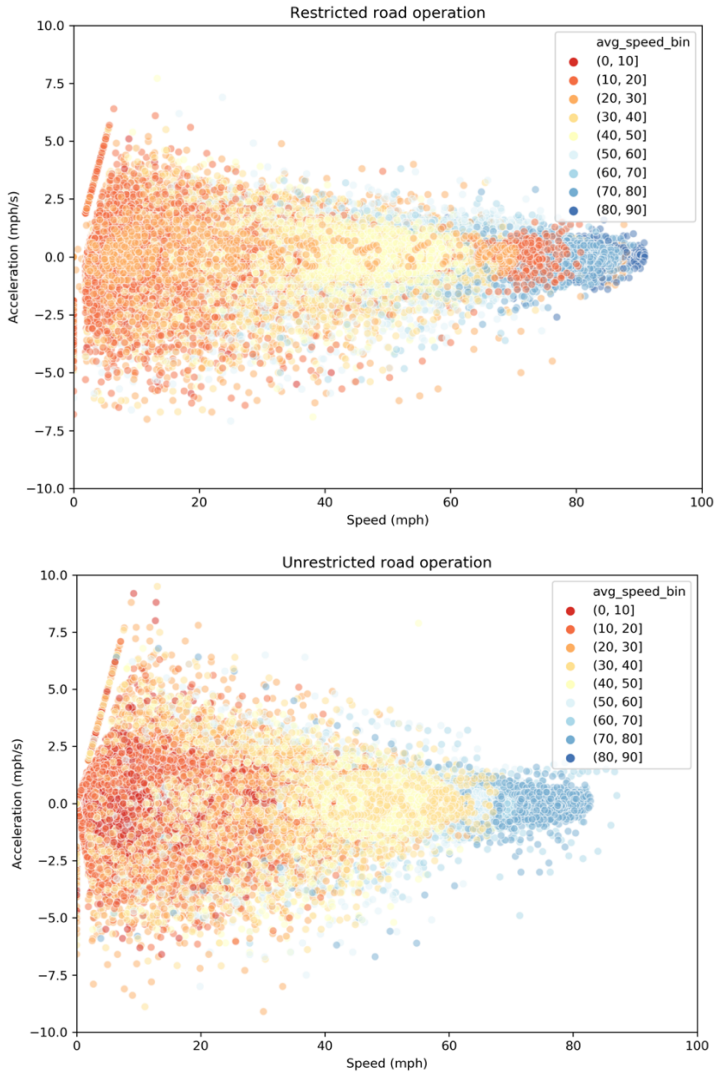

Figure 49. Speed-acceleration plots of selected driving cycles

As a majority of network links have road grade within ±5% suggested by Figure 24, the road grade is defined within the same range in the following network-level analysis. The HVAC load under extreme conditions can reach 4.0 kW or 4.5 kW depending on heating or cooling (Neubauer and Wood, 2014). In this case, the HVAC load is selected between 0.0 kW and 4.0 kW to represent the meteorology ranging from mild to severe. The sample input and output data are illustrated in Figure 50 below.

	Inputs					Outputs	
link_no	Avg. speed (mph)	SOC	Road type	Road grade (%)	HVAC load (Kw)	Elec. rate (Kj/mile)	Fuel rate (Kj/mile)
0	12	0.89	local	0	0.5	1000.26	0
1	17	0.89	local	0	0.5	850.04	0
2	33	0.88	local	0	0.5	1178.83	0
3	36	0.86	highway	0	0.5	1107.44	0
4	36	0.85	highway	0	0.5	1107.44	0
5	47	0.84	highway	0	0.5	1197.70	0
6	40	0.83	highway	0	0.5	817.47	0
7	41	0.89	highway	0	0.5	969.74	0
8	45	0.88	highway	0	0.5	1116.88	0
9	36	0.87	local	0	0.5	1107.44	0
10	37	0.85	local	0	0.5	1025.83	0

Figure 50. Sample link-level inputs and outputs

After preparing the input, the energy use rates on each link were estimated for each type of EV following the procedure illustrated in Figure 51 below using the energy model developed in Chapter 4. First, the link-level VMT and battery capacity by EV type, random initial SOC, driving cycle, road grade and environmental conditions on each link were prepared from ABM outputs. Next, the second-by-second inputs is post-processed for different EVs to obtain instantaneous VSP, available on-board electricity and HVAC load. Then, the proposed energy framework is applied to each type of EV with HVAC load, VSP, SOC, speed and acceleration as model inputs. Finally, the second-by-second control strategies, energy consumption, SOC drop and remaining range is generated for selected driving cycles and then projected to estimate the link-level energy inventory. The energy consumption from ICEVs were also adjusted based on updated VMT travelled and fleet composition. The total link-level energy use is generated by adding the energy use from ICEVs and EVs for each hour of operation.

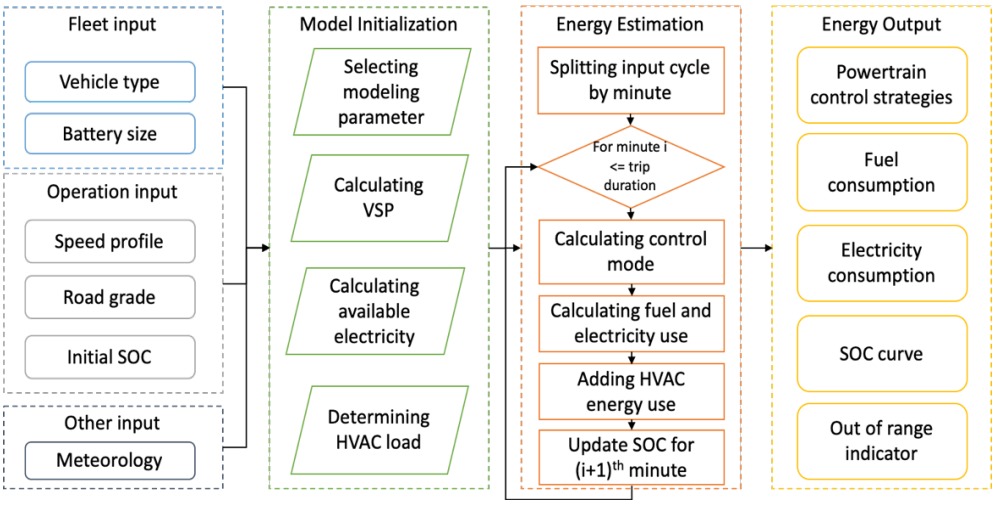

Figure 51. Energy processor for individual vehicles on each link

5.2 EV Energy Rate Sensitivity Visualization

For each vehicle type, 4,000 Monte Carlo samples were drawn to represent the combination of input operating conditions. The specification of Monte Carlo sample for each vehicle type is provided in Table 11 below.

Table 11. Range specifications of Monte Carlo sample

Variable	*100-mile BEV (2016 Nissan Leaf)*	*300-mile BEV (2016 Tesla Model S)*	*Series PHEV (2016 Chevrolet Volt)*	*Power-split PHEV (2017 Prius Prime)*	*Power-split HEV (2015 Toyota Prius)*	*Parallel HEV (2015 Ford Fusion)*
Road Type	Arterials vs. Freeway					
Average speed (mph)	5 mph – 75 mph					
Initial SOC	N/A	N/A	20% - 90%			
HVAC load	1 kW – 4 kW					
Road grade	-5% – 5%					

Using the energy rate estimation method introduced in Section 5.1, the link-level energy rates were estimated for the 4,000 Monte Carlo samples and for each type of EVs in Table 11. The scatter plots for BEVs, PHEVs and HEVs are provided in following sections.

5.2.1 BEV Results

First, the scatter plots were generated for two types of BEVs using the Monte Carlo samples. The results are provided in Figure 52 below. For all of the scatter plots, the average speeds are on the x-axis and the electricity rates are on the y-axis, with other variables being color-coded. The trend lines are generated using the Locally Weighted Scatterplot Smoothing (LOWESS) method (Kvam and Vidakovic, 2007). The results suggested that the electricity rates increase with increasing road grade and HVAC load, with road grade showing a larger impact on energy rates than HVAC load. The electricity rates are higher under low and high speeds, and not very sensitive to road type under the same average speeds.

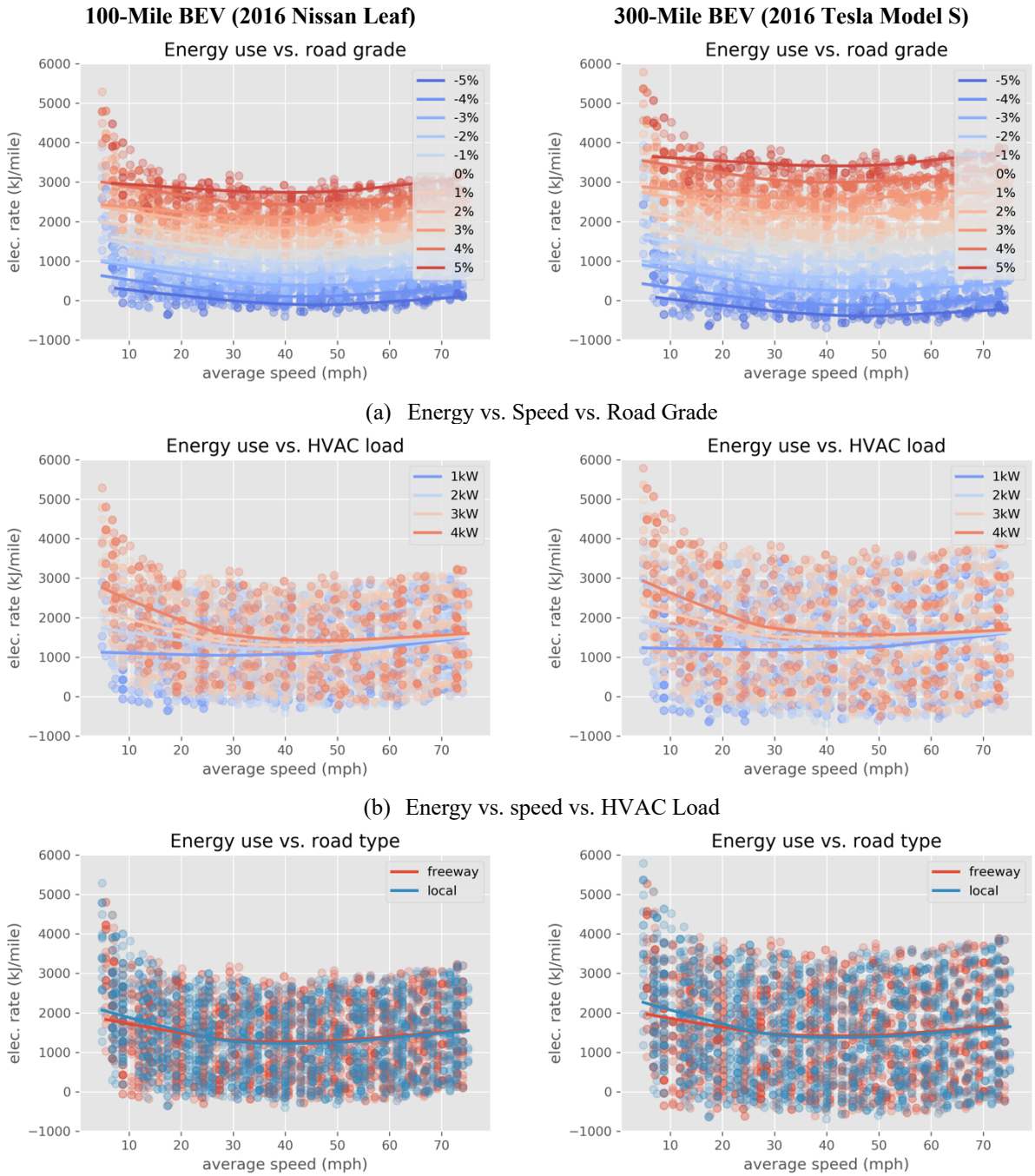

(a) Energy vs. Speed vs. Road Grade

(b) Energy vs. speed vs. HVAC Load

(c) Energy vs. speed vs. road type

Figure 52. BEV energy rates under different operating conditions

5.2.2 PHEV Results

The sensitivity of fuel rates and electricity rates for PHEVs are illustrated under various conditions for two types of PHEVs in Table 11. The scatter plots for the two PHEVs are provided in Figure

53 and Figure 54 below. The common feature shared by both types of PHEVs is that the fuel rates and electricity rates show opposite effects under different average speeds and SOC levels. An increase in average speed requires a greater vehicle power demand; hence, the fuel rates increase, and the electricity rates decrease. As the initial SOC level increases, the vehicle has more available electricity in power storage; hence, fuel rates will decrease, and electricity rates increase. An increase in HVAC load adds to both fuel and electricity use, with larger impact on electricity under lower average speeds. The energy rates are not significantly impacted by road type under most conditions, if the average speeds of the selected driving cycles are the same. The fuel rates of the two PHEVs exhibit similar patterns for various operation conditions. As the power-split PHEV has much smaller battery pack and AER, the electricity rates from that vehicle is smaller than the series PHEV in general even the motor powers are very similar.

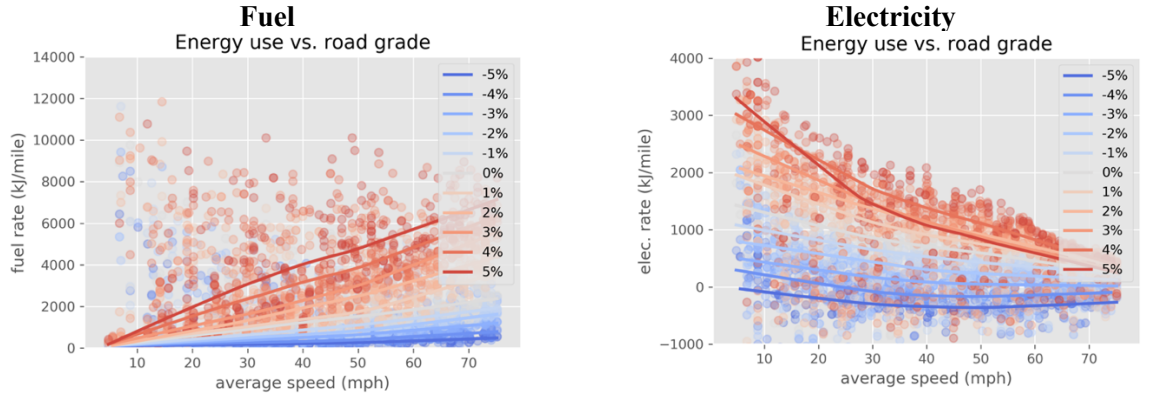

(a) Energy vs. speed vs. road grade

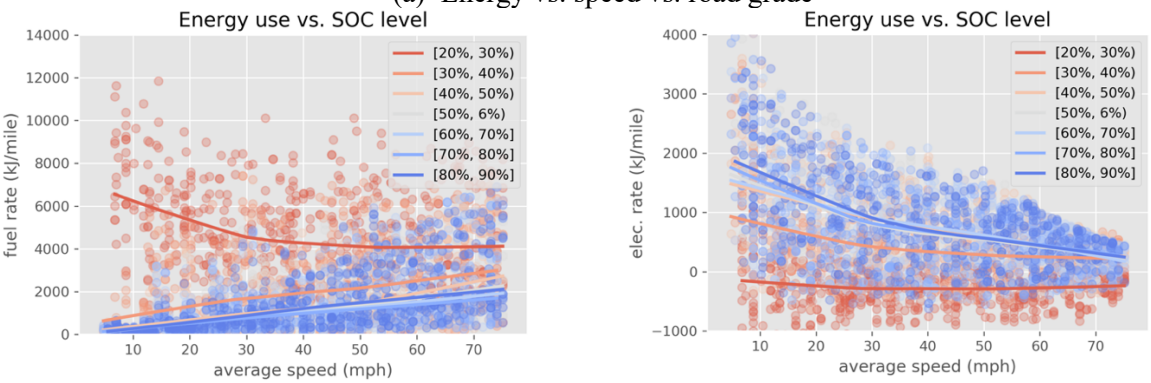

(b) Energy vs. speed vs. SOC

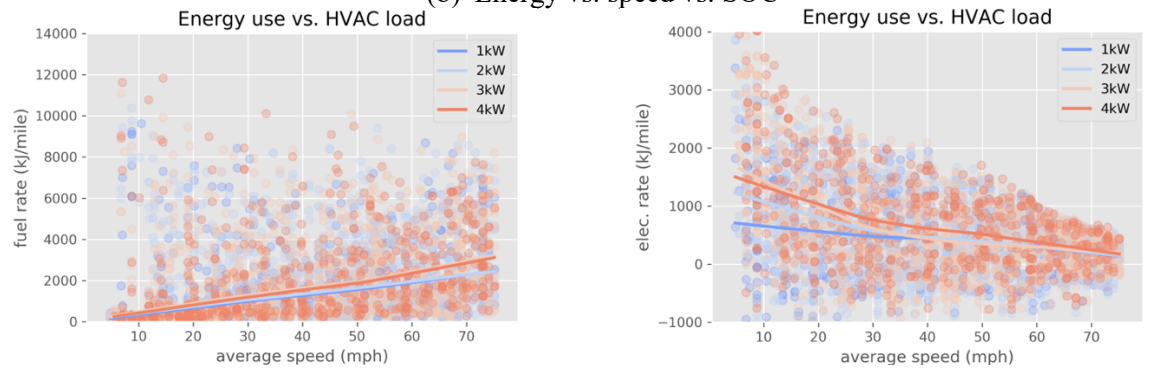

(c) Energy vs. speed vs. HVAC load

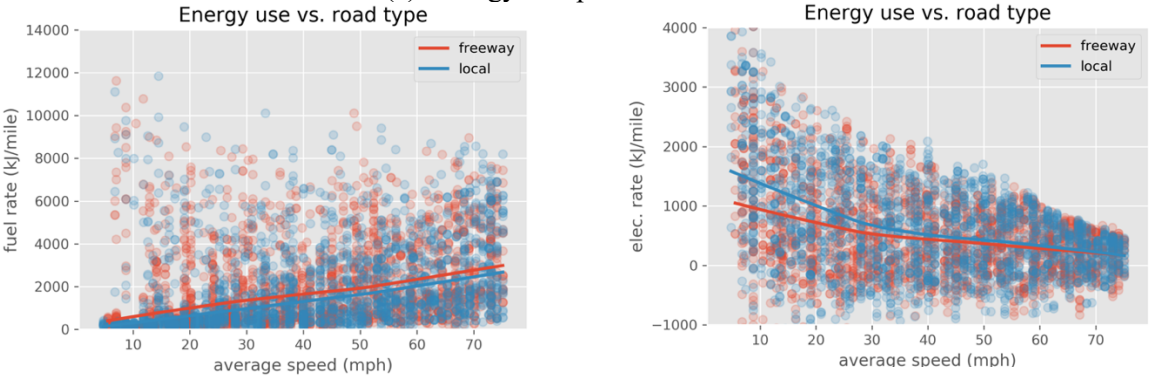

(d) Energy vs. peed vs. road type

Figure 53. Energy rates under various operation conditions for a series PHEV with 50-mile AER (2016 Chevrolet Volt)

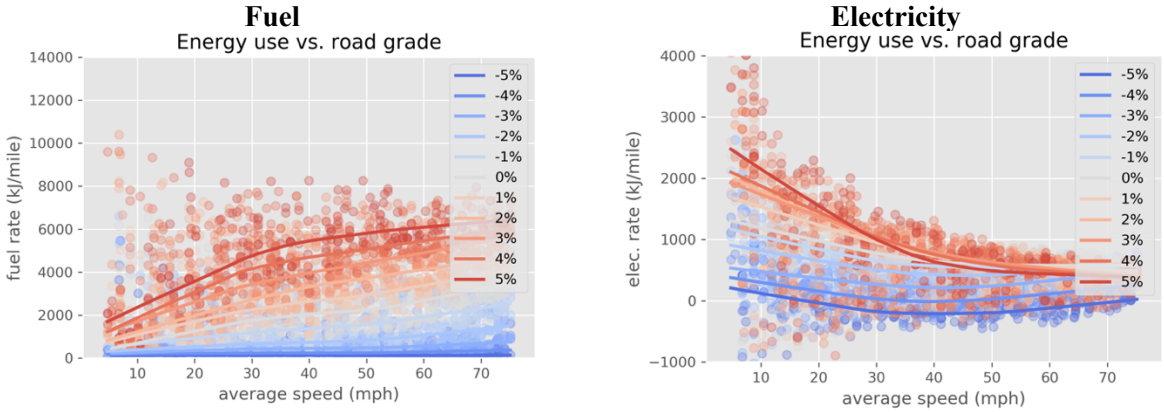

(a) Energy vs. speed vs. road grade

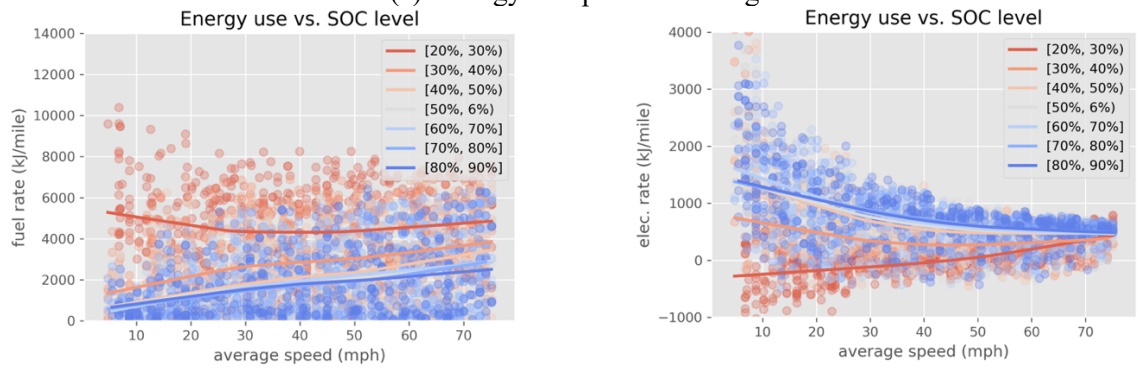

(b) Energy vs. speed vs. SOC

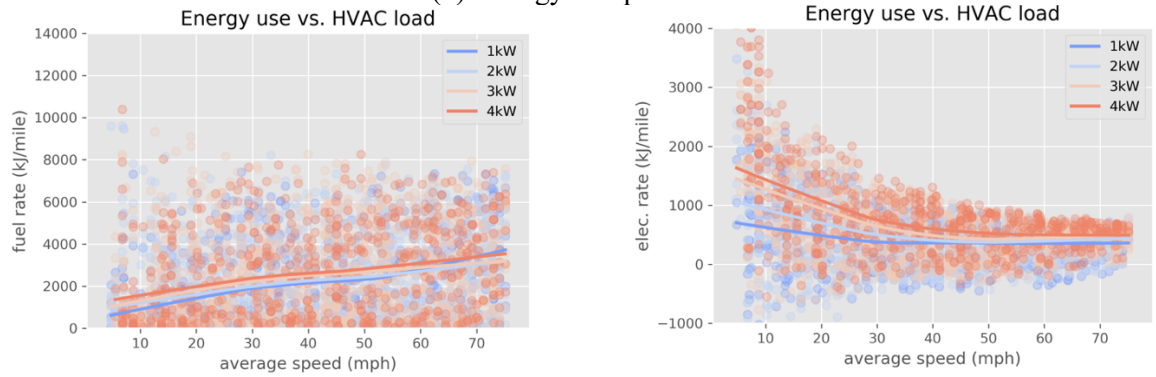

(c) Energy vs. speed vs. HVAC load

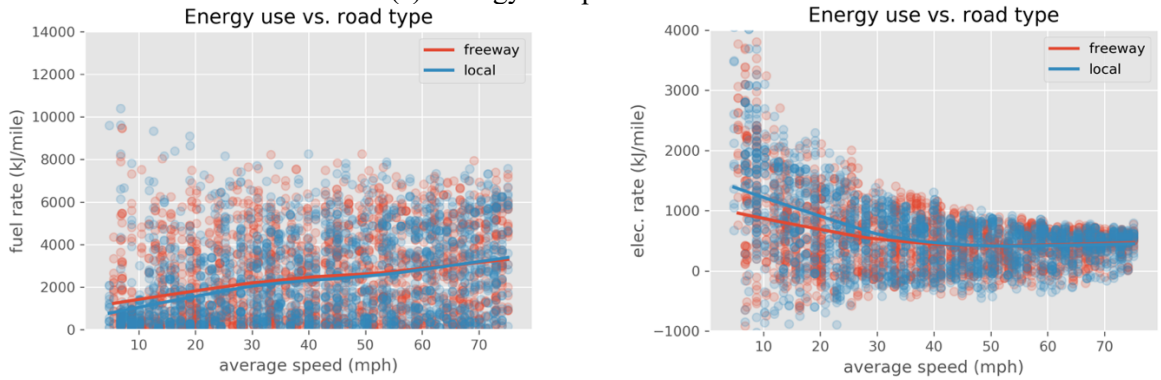

(d) Energy vs. speed vs. road type

Figure 54. Energy rates under various operation conditions for a power-split PHEV with 20-mile AER (2017 Prius Prime)

5.2.3 HEV Results

The sensitivity of the two types of HEVs in Table 11 are investigated using the same approach described earlier for the BEVs and PHEVs. The modeling results are provided in Figure 55 and Figure 56 below. The electricity rates of HEVs are significantly lower than for the PHEVs, likely due to the much smaller batteries installed on HEV than PHEVs. The impacts of road grade, HVAC load and road type seem trivial on electricity rates. The trend of fuel rates under different operating conditions is very similar to PHEVs, with growing fuel rates under higher road grade, higher HVAC load and lower SOC level. The fuel rates are much higher under speed <= 30mph range and slightly higher under speed >= 60 mph. The parallel HEV has higher fuel and electricity rates under most conditions, likely due to the larger battery capacity and larger engine size, as indicated in Table 8.

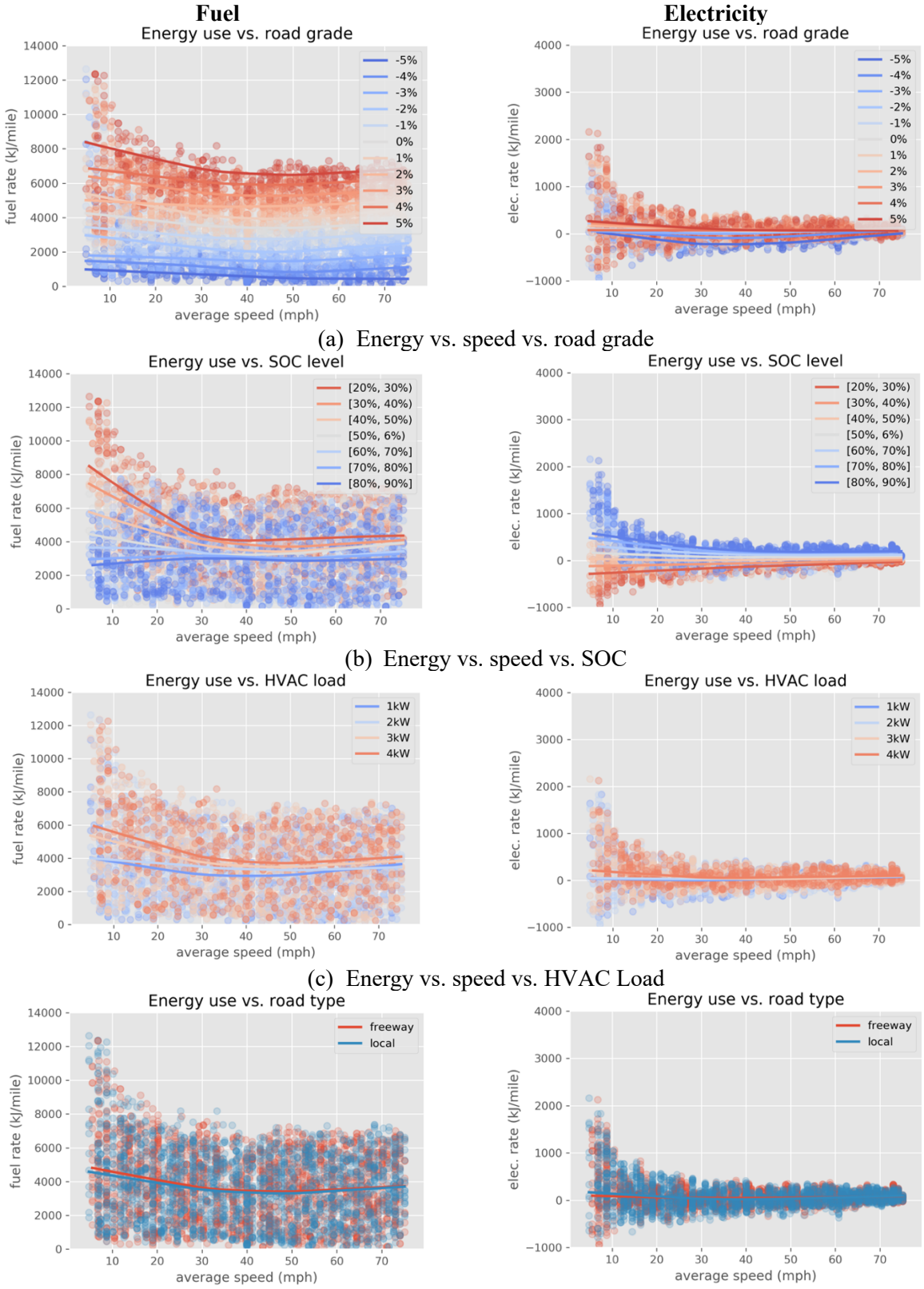

(a) Energy vs. speed vs. road grade

(b) Energy vs. speed vs. SOC

(c) Energy vs. speed vs. HVAC Load

(d) Energy vs. speed vs. road type

Figure 55. Energy rates under various operation conditions for a power-split HEV (2015 Toyota Prius)

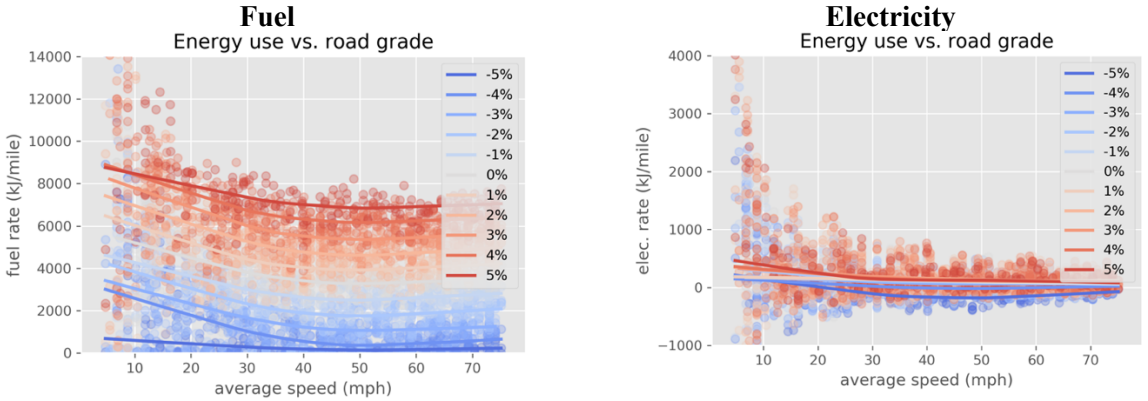

(a) Energy vs. speed vs. road grade

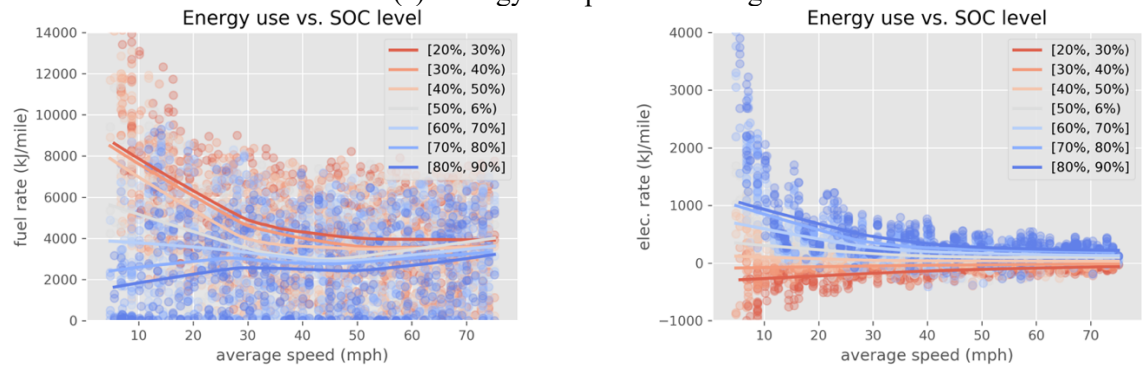

(b) Energy vs. speed vs. SOC

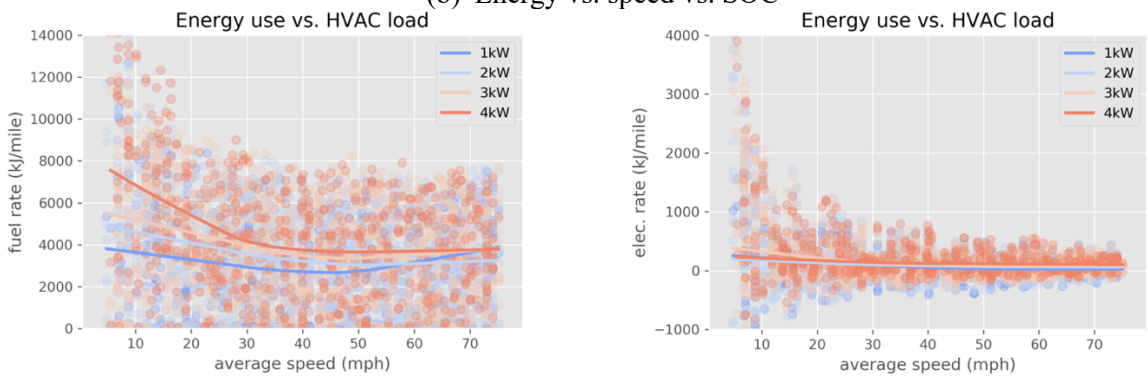

(c) Energy vs. speed vs. HVAC Load

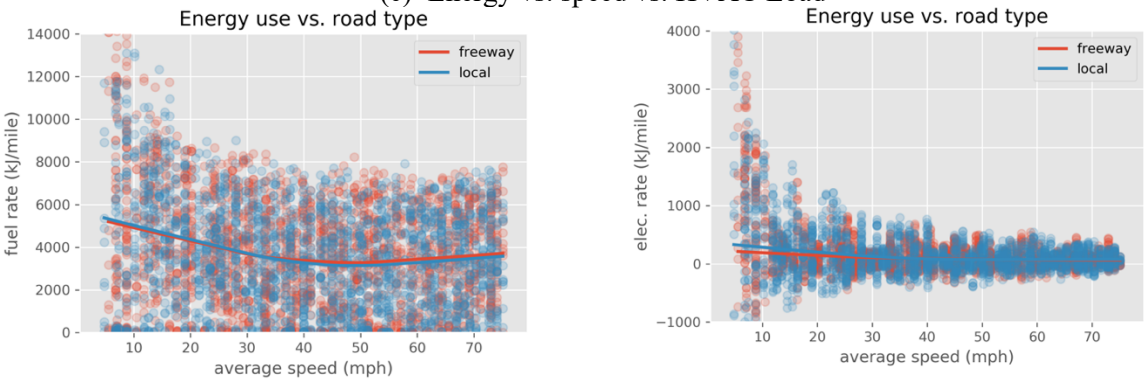

(d) Energy vs. speed vs. road type

Figure 56. Energy rates under various operation conditions for a parallel HEV (2015 Ford Fusion)

The scatter plots above suggest that vehicle speed, road grade, and HVAC load have significant impacts on the energy rates of almost all EVs, while road type shows little impact under the same speeds. For PHEVs and HEVs, the initial SOC also has a significant impact on both fuel use and electricity use rates. The magnitude of impact varies by vehicle type, energy source, and how this factor combined with other operating conditions. However, it is relatively hard to quantify the magnitude of impact from a review of the scatterplots and quantify the potential trade-offs if one of the variables is not available for the analysis. In this case, a quantitative sensitivity analysis needs to be performed to investigate the relative importance of each factors on outcome energy use.

5.3 Variance-based Sensitivity Analysis

In this section, the variance-based sensitivity analysis is performed to help understand how uncertainty in the model output is apportioned to different sources of uncertainty in the model inputs (Saltelli et al., 2002). The objectives of sensitivity analysis in this study can be summarized into following items based on the main features of variance-based SA method (Iooss and Lemaître, 2015):

1. **Verify the developed energy model to ensure it is sensitive to key operation factors.** As discussed in Table 2, the vehicle driving profile, battery level, road grade, and HVAC load significantly impact some of the EVs. The energy model should be sensitive to these factors and this hypothesis needs to be tested in the sensitivity analysis.
2. **Understand the contribution of operation factors on energy use.** This step is designed to identify the most significant factors or factor interactions affecting EV energy use. The differences in energy response from different vehicles and different powertrains is also examined across the variety of operation conditions.

3. **Provide guidance on model simplification and factor prioritization.** By ranking the most influential factors, the model user should be able to prioritize work associated with preparing accurate input factors that are most influential, decide the level of input accuracy, calibrate model inputs, and understand the trade-off of making certain model assumptions.

Many sensitivity analysis techniques have been applied to the assessment of data and variable interactions, including derivative-based approaches, scatter plots, linear regression, analysis of variance (ANOVA), and other variance-based approaches (Iooss and Lemaître, 2015; Saltelli et al., 2007). The key idea of variance-based method is to decompose the variance of the model outputs into fractions that can be attributed to inputs or sets of inputs, without eliminating uncertainty of those inputs. Variance-based methods are generally preferable to other techniques in addressing settings such as factor fixing and factor prioritization for models of unknown *linearity, monotonicity, and additivity* (Saltelli et al., 2007). In previous practice, this method has been widely applied to identify key input factors in transportation modeling (Ciuffo et al., 2013; Ciuffo and Lima Azevedo, 2014; Quaglietta and Punzo, 2013) and vehicle energy/emissions analysis (Asamer et al., 2016; Kioutsioukis et al., 2004; Yao et al., 2014).

In this analysis, the variance-based method is selected based upon its properties and the characteristics demonstrated in the scatter plots above. The variance-based method is model-free (this property will be discussed in following sections), which does not assume linearity, monotonicity, and additivity of the inputs (Iooss and Lemaître, 2015; Saltelli et al., 2007). Based upon the scatter plots presented in Section 5.2, non-linear and non-monotonic relationships appear between energy use and vehicle speed. The variance-based methods are also more practical than common techniques such as factor screening or linear regression. The input factors are composed

of mix of continuous and discrete variables (road type variable is discrete, the SOC level, HVAC load and average speed can be continuous), which makes the derivative based method or ANOVA techniques hard to apply. Because variance-based method calculate the conditional variances (Saltelli et al., 2007), they will not be impacted by the form of the inputs. Furthermore, the combination of input factors may also contribute to the total variance of energy use (e.g., the SOC under lower speeds seem to have an amplified impact on HEV energy use in the scatter plots), where the variance-based method is able to estimate the higher order interaction effect (Iooss and Lemaître, 2015; Saltelli et al., 2007). The drawback of variance-based measures is their computational cost (Iooss and Lemaître, 2015; Saltelli, 2002; Saltelli et al., 2007), which is not a significant concern given the fast computational speed of the proposed energy model. In this case, the variance-based method appears to be the most applicable technique.

5.3.1 Variance-based Sensitivity Analysis Specifications

The basic concepts of model definition and variance decomposition procedure are defined in the literature (Saltelli, 2002; Saltelli et al., 2007, 2002; Sobol, 2001). A model (or a computer program) can be represented as $Y = f(X)$, with D-dimension input vector $X = \{x_1, x_2, \ldots, x_D\}$, output variable Y and projection function f. The total variance of Y can be apportioned to the input vectors using the following equation:

$$\boldsymbol{Var(Y) = \sum_{i=1}^{D} v_i + \sum_{i<j}^{D} v_{ij} + \ldots + V_{12\ldots d}} \quad \textbf{(22)}$$

In the formula above, the variance of the conditional expectation of Y given x_i (denoted by v_i) is represented as:

$$\boldsymbol{v_i = Var_{x_i}(E_{x_{\sim i}}(Y|x_i))} \quad \textbf{(23)}$$

The $x_{\sim i}$ in formula above represent the input combinations except x_i. The v_i is obtained by calculating the expectations of Y across many possible values of x_i and then calculating the variance of all the expectations. The v_i, according to the law of total variance (Blitzstein, 2014), represent the variance of Y explained by x_i and is recognized as a measure of sensitivity (Saltelli et al., 2007). The greater the v_i means the larger the explanatory power from x_i.

The variance of the conditional expectation of Y given x_i and x_j together (denoted by v_{ij}) is represented as:

$$v_{ij} = Var_{x_{ij}}(E_{x_{\sim ij}}(Y|x_i, x_j)) - v_i - v_j \quad \textbf{(24)}$$

The $x_{\sim ij}$ in formula above represent the input combinations except x_i and x_j. The v_{ij} is obtained by calculating the expectations of Y across many possible combinations of x_i and x_j and then calculating the variance of all the expectations. The interpretation of v_{ij} is similar to v_i.

The sensitivity indices (also known as "Sobol indices") are defined as the fraction of variance apportioned to certain factor (or combination of factors) in total variance (Sobol, 2001). The first-order sensitivity index represents the main effect contribution of each input factor to the variance of the output (Saltelli et al., 2007), which is defined as follows::

$$\boldsymbol{S_i = v_i / Var(Y)} \quad \textbf{(25)}$$

The second-order sensitivity index represents the interaction effect from two or more factors jointly, excluding their individual effects. It can be calculated as following:

$$\boldsymbol{S_{ij} = v_{ij} / Var(Y)} \quad \textbf{(26)}$$

The total effect index accounts for the total contribution of factor x_i to the output variation due to its first-order effect plus all higher-order interaction effects. The total effect answers the question about how much variance is lost if a particular factor is fixed. It is calculated as following:

$$\boldsymbol{S_{T_i} = \left[Var(Y) - Var_{x_{\sim i}}\left(E_{x_i}(Y|x_{\sim i})\right)\right] / Var(Y)} \quad \textbf{(27)}$$

By definition, the higher sensitivity indices indicate higher impacts from the input factors, and the sensitivity indices close to zero suggest trivial impacts from these factors (Saltelli et al., 2007, 2002). Theoretically, the summation of the first-order indices and all higher-order indices of all factors should equal one (Saltelli et al., 2007). However, in the real-world implementation, due to the sampling method and sample variance calculated, the summation of first-order and higher-order indices asymptotically equals one. In this study, the variance-based method is implemented using the Python package "SALib" (Herman and Usher, 2017), and the sampling and estimation method is based on a quasi Monte Carlo technique introduced in a forthcoming section.

5.3.2 Quasi Monte Carlo Simulation and Bootstrapping

To compute the sensitivity indices, the Monte Carlo based numerical method is often more applicable than computing the deterministic solution. The Monte Carlo method generates random (pseudo random) input vector, based on pre-defined probability distributions of inputs. The quasi Monte Carlo method is adopted instead. The quasi Monte Carlo method uses a low-discrepancy sequence to generate random samples that are more evenly distributed in the sample space (Sobol, 2001).

In the following discussion, we will assume that any combination of parameter values is equally likely. The quasi Monte Carlo samples were drawn using the Saltelli sampler (Herman and Usher, 2017; Saltelli, 2002) and the specifications in Table 11, with 1,000 * (2D+2) sample link-level

inputs generated for each vehicle type, fuel type, and scenario (D is the number of factors, D=4 for BEVs and D=5 for HEVs and PHEVs). The methodology introduced in Section 5.1 is applied to calculate the link-level energy consumption rate (Y), and the equations 25, 26, and 27 were used to compute the sensitivity indices for main effects, interaction effects, and total effects. The average speeds and road type indicator on each link were sampled during the quasi Monte Carlo experiment, and specific driving cycle from the training set illustrated in Figure 24 were assigned to each link based on average speed and road type. The means and 95% confidence intervals of the sensitivity indices are computed based upon 1,000 Bootstrapping replicas and sub sample size = 1,000. The positive versus negative road grades were considered in separate scenarios, as the contributions of different factors may vary in the two scenarios as demonstrated below. The resulting sensitivity indices are provided in the following section as well as the discussion.

5.3.3 Sensitivity Analysis Results

In this section, the mean and 95% confidence intervals for each vehicle, fuel type, and scenario (uphill/downhill) are provided. The factors or interactions of multiple factors with sensitivity indices smaller than 0.01 were not displayed as their impact on energy use is negligible. The main effects can be interpreted as the contribution on total variance from varying a certain factor alone (Saltelli et al., 2007). The interaction effects can be understood as the contribution on total variance from varying two factors together. The total effects are usually treated as indicators of sensitivity from certain factor in total, in other words, the loss of variance in the output if fixing certain input factors to constant. The final ranking of factor importance is based on the total effect, summing the first-order and all higher order effects from input factors.

First, the sensitivity indices and their 95% confidence intervals of input factors on BEV electricity rates are explored under uphill (road grade>=0%) and downhill (road grade<0%)

scenarios. The results are provided in Figure 57 below. The results from two BEVs are similar, with road grade having the highest impact, followed by average speed, and HVAC load. The impact of road type in this analysis is trivial, which is similar to the conclusions in the scatter plots above. This is probably due to the impact of facility type on energy rates have been reflected in the assigned driving cycle. The interactions between speed and road grade, speed and HVAC load have some contributions to the final variance of energy rates. The road grade has greater impact on 300-mile BEVs, probably due to the greater vehicle mass of the vehicle and larger power demand impact from grade load.

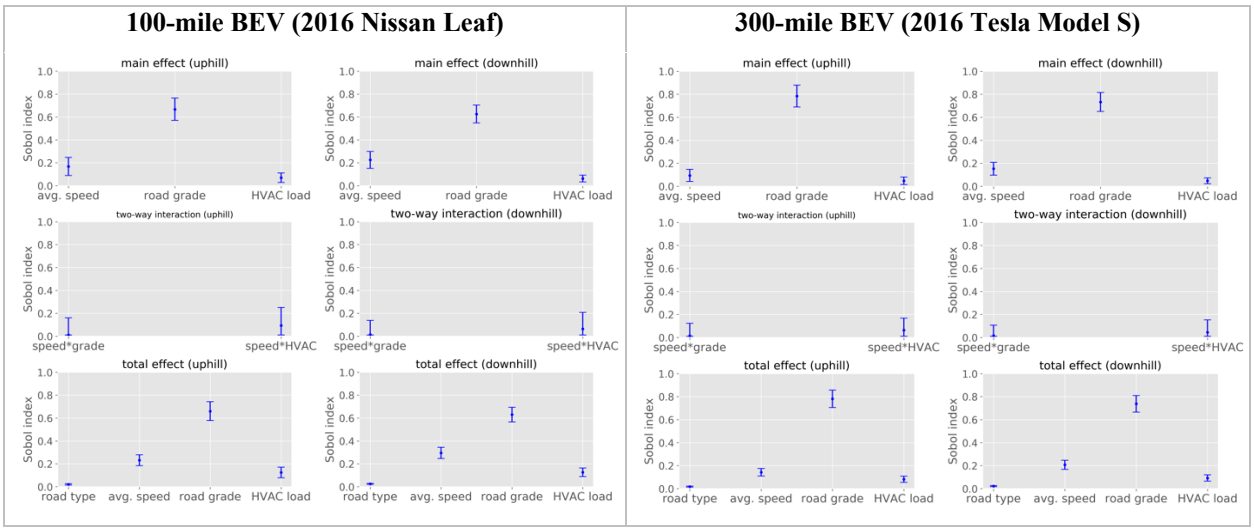

Figure 57. Sobol indices for BEVs

Next, results from two types of PHEVs are provided by fuel types and scenarios in Figure 58. The sensitivity index distribution on electricity use is represented in blue, while fuel use is represented in orange. The sensitivities of different factors vary by uphill and downhill grade and vary by fuel and electricity. The SOC level has the largest impact on fuel rates, followed by speed, and then by road grade. The impact of SOC on fuel variation is greater under downhill operations, probably attributed to regenerative braking and battery recharging when driving downhill. The HVAC load and road type have negligible impact on fuel consumption in all cases. For electricity consumption, average speed usually has the largest impact, followed by SOC and road grade. The road grade impact is greater in any uphill scenario, due to the more load assigned to electric powertrain. The impact of HVAC load is limited for both PHEVs in this model, with slightly larger impact on electricity (the auxiliary system is often connected to the battery). The road type has no significant impact on electricity as well in all cases because the effect of facility type has been represented by assigned driving cycles.

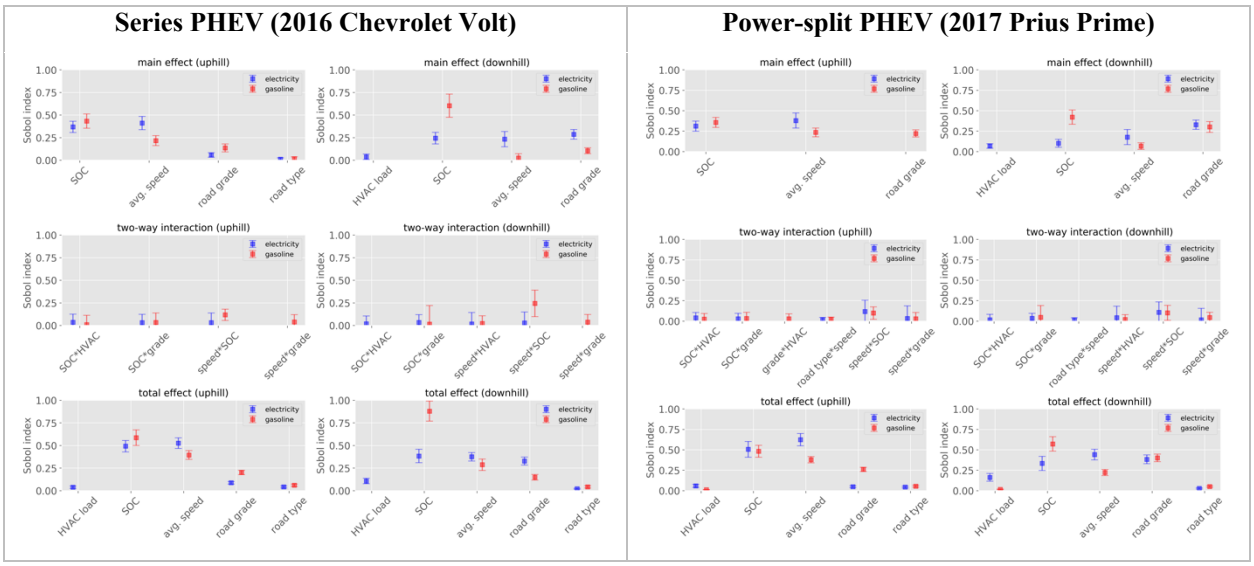

Figure 58. Sobol indices for PHEVs

Finally, results from two types of HEVs are given in Figure 59. Similar to PHEVs, the sensitivities of different factors vary by uphill and downhill and vary by the fuel type. The SOC level, road grade, and average speeds have the largest impacts on fuel rates, with slightly smaller road grade impact in parallel HEVs. The impact of SOC on fuel variation is greater under downhill situation, probably due to the recharging when driving downhill. The HVAC load and road type impacts on fuel consumption are still low in all cases. For electricity consumption, SOC usually has the largest impact, followed by average speed and sometimes road grade. The road grade impact is negligible in downhill scenarios but shows significant impact in uphill scenarios. The impact of HVAC load and road type is limited for both HEVs in this energy model. The impact of HVAC load on electricity use decreased potentially due to smaller power output from electricity, so that more power used for HVAC load comes from engine (which only increase the total engine output by a small margin). The low impact of road type is due to the similar reasons as other vehicle types, which the driving cycle already represent the effect of facility types.

Based on sensitivity results above, the SOC, average speed, and road grade are the three most important factors on both fuel and electricity consumption, regardless of powertrain or

uphill/downhill scenario. The impact of road type is trivial in all cases. The HVAC load impact in this model is limited, but still significant for certain fuel type and powertrain combinations. The priority (ranking) of factor importance depend on the fuel type, powertrain, and road grade conditions, based on the total effects provided.

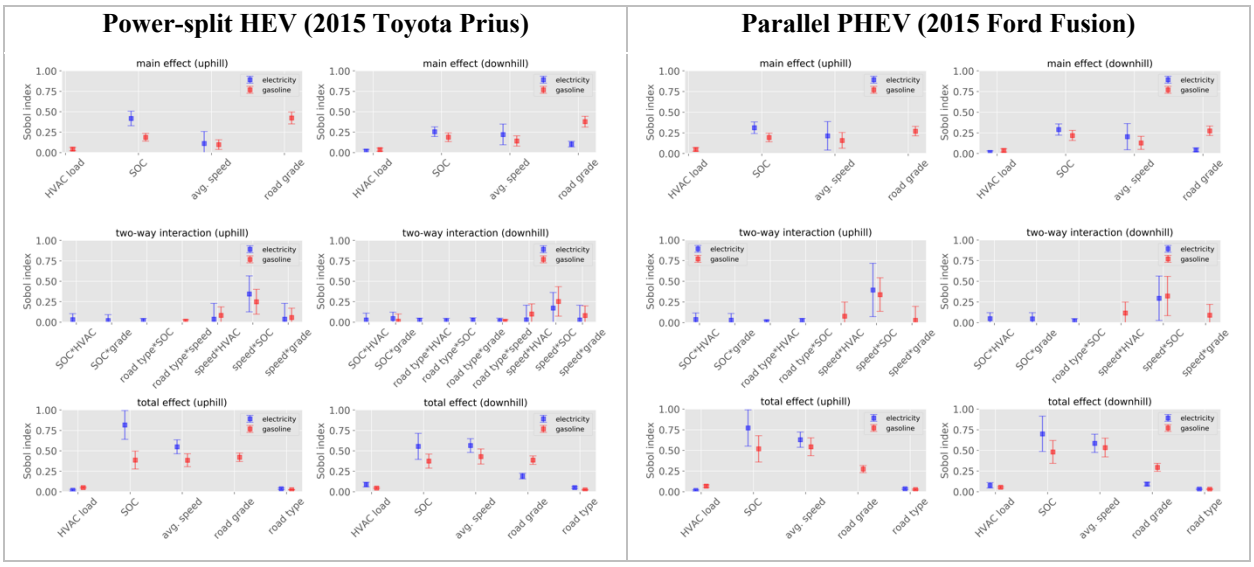

Figure 59. Sobol indices for HEVs

5.4 Methodology of Estimating Network-level EV Energy Use

In this study, the energy consumption with certain fraction of EVs is estimated using the link-level traffic attributes (average speed, road type, link length, and traffic volume), as introduced in Section 5.1, and a randomized distribution of initial SOC. The methodology of preparing fleet composition is introduced in detail in following sections, while the link-level transportation attributes are the same as introduced in Section 3.7, except that an updated calendar year is used (year 2024) with updated travel demand model synthetic population, trip assignment, and traffic assignment. By generating the energy results for EV fleets on each link, the network-level fuel saving as well as electricity demand can be modeled spatially and temporally. The energy saving benefits can also be broken down by link speed and facility type, which provides useful information for transportation improvement planning and implementation.

5.4.1 Fleet Inputs

For each link, and each scenario run, a portion of the on-road fleet is assigned to EV categories, based on EV market penetration rates by 2024. The EV penetration is projected by U.S. Energy Information Administration (US EIA) based on known energy production, delivery, and consumption technology trends (U.S. Energy Information Administration, 2019b, 2017, 2014). The EV penetration by vehicle model year from 2011 to 2024 for the South Atlantic Region is illustrated in Figure 60. Most of the EVs sold before the year 2020 are HEVs and PHEVs, while BEVs start to take about 50% of the market share after 2020. The EV market share is anticipated to reach 12% by 2024, which is clearly more pessimistic than what was assumed in Chapter 3.

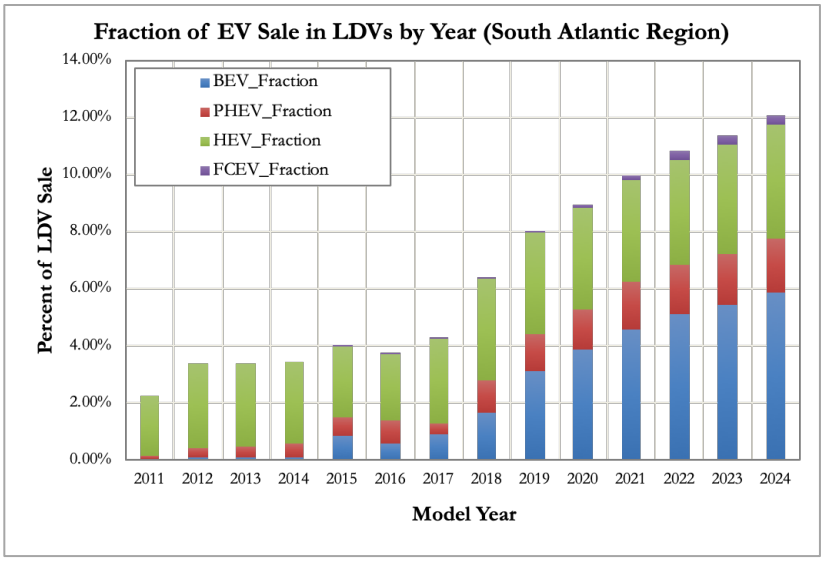

Figure 60. EV fraction input
(U.S. Energy Information Administration, 2019b, 2017, 2014)

The EV penetration rates for model years before 2011 are assumed to be negligible. The adopted EV penetration was applied to different age distributions in rural and urban areas in to obtain the final VMT split by ICEVs and EVs in light-duty vehicle (LDV) fleets, where the baseline model year distributions are provided in Table 12. In urban areas, 6.2% of total VMT was contributed by EVs, and in rural areas, 4.9% of total VMT was contributed by EVs. The VMT

for EVs was then allocated to BEVs, HEVs, PHEVs and FCEVs based upon the fleet composition provided in Figure 60 (mileage accumulation rates were not adjusted by model year in this analysis to reflect that older EVs may be driven less than newer EVs, but this variability can be added in future analyses). The powertrain-specific elements by vehicle types were randomly assigned, given the lack of sufficient vehicle powertrain composition information for the on-road fleet.

Table 12. Regional-level VMT distributions by vehicle type and model year

Area	Age	0-2	3-5	6-8	9-11	12-14	15-17	18-20	21-23	24-26	27-29	>=30
rural	LDV	10.3%	16.6%	18.5%	17.0%	13.9%	10.3%	5.8%	1.9%	1.3%	0.8%	3.7%
	LDT	10.1%	15.3%	13.9%	13.0%	13.7%	15.0%	12.7%	5.7%	0.1%	0.1%	0.5%
	PT	10.7%	15.8%	14.4%	12.6%	12.8%	14.1%	12.6%	5.7%	0.1%	0.1%	1.1%
urban	LDV	16.4%	21.7%	21.1%	16.4%	10.9%	6.5%	2.7%	0.8%	0.5%	0.4%	2.6%
	LDT	14.7%	18.6%	31.4%	10.8%	4.9%	2.9%	3.9%	12.7%	0.0%	0.0%	0.0%
	PT	21.2%	21.2%	15.0%	11.5%	10.3%	10.1%	7.3%	2.9%	0.0%	0.0%	0.5%

5.4.2 Operation Inputs

After quantifying the VMT by EV type on each link by area type (urban vs rural), the next step is to estimate the energy use under given EV VMT. The procedure of estimating link-level energy rates was given in Section 5.1. For each link-level attribute, the data source or data surrogates were introduced as follows:

- **Road type and link average speeds:** the road type and link average speeds are readily available from ABM network assignment results.
- **Road grade:** the road grades are generated from Digital Elevation Model (DEM) and assigned to each link by matching the location information of link end points and elevation from DEM (Liu et al., 2018).

- **Initial SOC:** As the SOC distributions are unknown for the region, the initial SOC for each vehicle on that link is drawn from an assumed uniform distribution between the maximum and minimum SOC values provided in Table 8.
- **HVAC load:** The temperature was assumed to be between 50°F and 70 °F in the baseline assignment. In this case, a 0.5 kW auxiliary load was added to all the EVs.

5.5 Network-level Energy Assessment

After generating energy consumption for the entire network by hour, the spatial and temporal energy use distribution by fuel and electricity was derived from the energy results. First, the spatial distributions of traffic volume, fuel use, electricity use, and percent of fuel (gasoline) savings are compared to the no EV scenario (an EV fleet penetration rate of zero) for a morning peak hour in Figure 61 below. Higher fuel use and electricity use generally occurred in locations with higher traffic volumes, such as Interstate highways and major arterials. The fuel saving benefits are higher in the urban context, compared to the rural context, given that the urban light-duty fleet is newer (average vehicle age = 8.5 years) than the rural fleet (average vehicle age = 10.7 years) and greater regenerative braking occurs in urban areas given the on-road operating characteristics of urban driving conditions (which reduces required battery recharge).

Traffic Volume by Link (veh/hour)

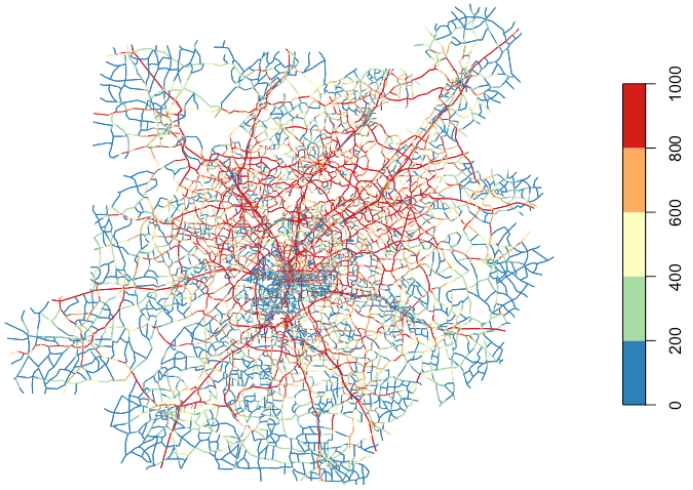

Fuel Use by Link (kJ/mile) Normalized by Link Length

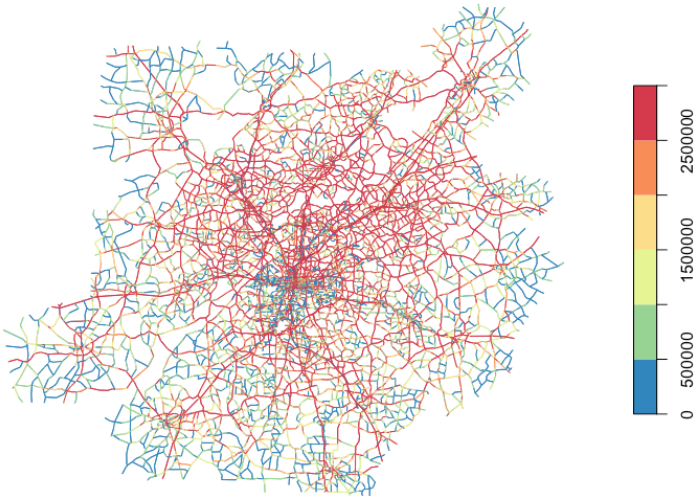

Electricity use by Link (kJ/mile) Normalized by Link Length

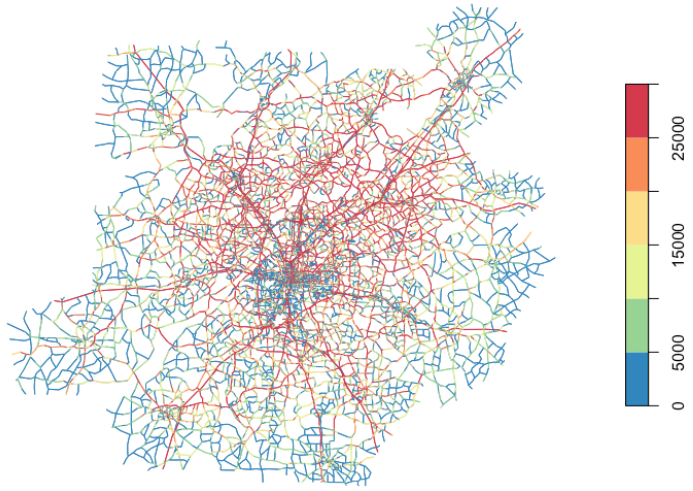

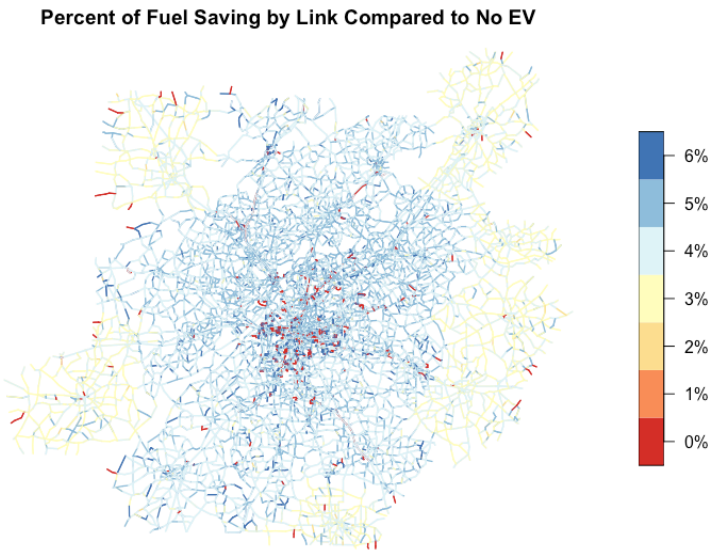

Figure 61. Traffic volume, fuel use, electricity use and percentage of fuel saving

The variation in energy use by time of day is provided in Figure 62 below. For this case study, the 2024 modeling assumed that 6.2% of total VMT in urban areas, and 4.9% of total VMT in rural areas, would be contributed by EVs. The energy benefits provided by EVs, the in terms of hourly fuel savings compared to the 100% ICEV fleet, varied from 4.1% to 4.3%. Furthermore, the electricity use is still much lower than fuel use for the given EV penetration rates. The total daily electricity consumption from EVs are only 1,863 MWh (6,357 MMBtu), compared to a total 370,886 MWh (1,265,462 MMBtu) of fuel use from all vehicles.

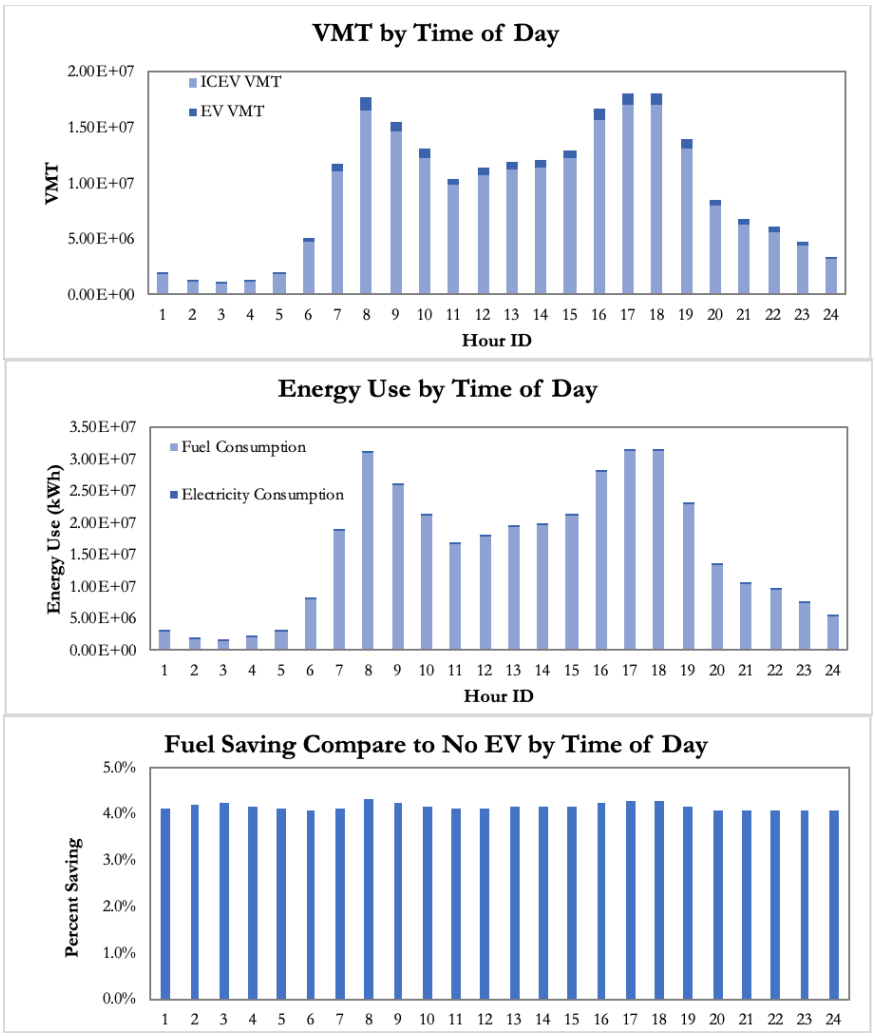

Figure 62. VMT, energy use and percentage of fuel saving by time of day

The network total fuel consumption aggregated by different facility type and different speeds are provided in Figure 63. The fuel consumption of EVs was compared to the energy results under the no EV scenario (i.e., a zero fleet penetration for EVs). For facility type, fuel consumption was aggregated by unrestricted road (arterials) and unrestricted roads (highways), and for rural and urban classes respectively. For link average speeds, fuel consumption was aggregated from 2.5 mph to 65 mph in 5-mph increments. The largest fuel consumption and largest energy savings both occur on urban restricted roads around medium average speeds (20-40 mph). The energy saving benefits are much lower on rural roads and on urban freeways. The higher energy saving

benefits on urban streets comes from high urban VMT, energy recovery from stop-and-go activity on urban roads, and the younger fleet under the assumptions in the urban area.

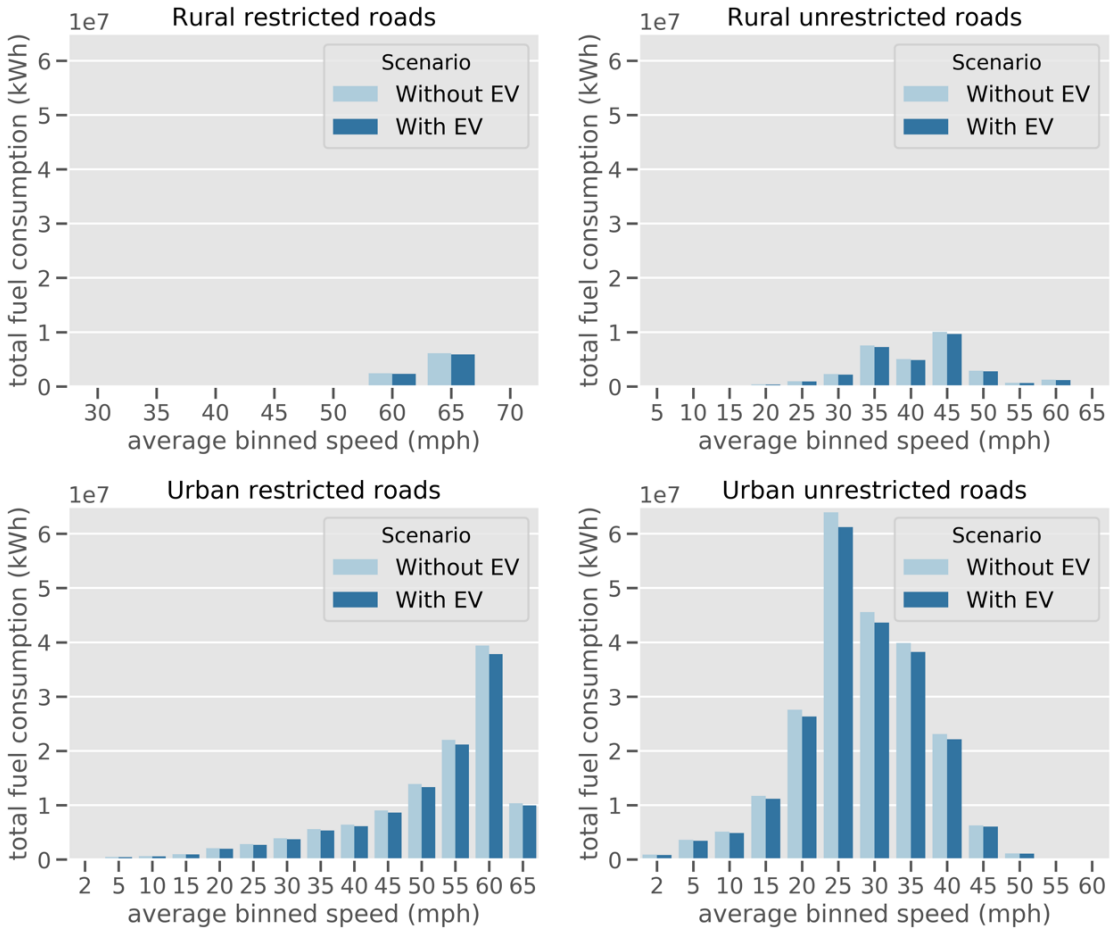

Figure 63. Energy use by facility type and average speeds

5.6 Chapter Summary

In this Chapter, the network-level fuel use and electricity use are estimated using the models derived in Chapter 4. First, the methodology of estimating link-level fuel and electricity are introduced, which provides the guidance on model application setup. Next, the sensitivities of impact factors on energy results are investigated using scatter plot and a variance-based method. The results suggest that SOC, average speed, and road grade have the greatest impact on energy results, with the ranking of importance vary by vehicle types, fuel types, and operation scenarios.

The sensitivity results indicate that the energy model is sensitive to the variables that were previously demonstrated to have impact on EV energy use. Finally, network-level energy use is estimated using the proposed energy model, with the energy for a fraction of EV estimated link by link for 2024 Metro Atlanta network. The spatial and temporal energy savings were provided to show based on the current EV market growth trend, the energy savings at the network level is around 4% for the entire Metro Atlanta area when 6.2% of total VMT in urban areas and 4.9% of total VMT in rural areas is provided by EVs. The induced electricity is also determined to quantify the daily extra electricity load from EV charging. Overall, the results from this chapter demonstrated the accumulative effect of EV adoption at a large scale, which would be helpful for regional-level transportation improvement plans, grid impact assessment and analyzing the potential combination with future mobilities (shared, autonomous, and electric vehicles).

However, the results from this Chapter did not evaluate the costs and benefit of EV adoption at the individual-level, which is critical with respect to EV adoption and reducing system-level energy consumption. Network-level conclusions also may not always be consistent with individual-level results. For instance, even the network-level energy consumption is reduced at around 4%, some EV users may have much less energy saving or higher savings depending on their travel patterns and driving behaviors. Because EV adoption issues and challenges are closely tied to personal attributes and travel patterns, individual-level energy analysis is required to assess the variability of cost-benefits based on personal travel patterns.

Another limitation of current work is the assumption on SOC distribution. Due to the lack of real-world observed SOC distributions (both spatially and temporally) and given the large contribution of SOC on total energy variance, the estimation bias associated with using a randomized initial SOC scheme may be significant. It would be beneficial to collect real-world

SOC distribution for model input calibrations and reduce the estimation bias associated with this factor. However, the models developed within this framework can be readily refined through supplemental data analysis (using the same proposed techniques) once in-use data containing more realistic SOC distributions become available.

CHAPTER 6. HOUSEHOLD-LEVEL EV BENEFIT COSTS ANALYSIS

The research efforts presented in Chapter 5 mainly focused on aggregated-level energy use and applied specific fleet penetration rates across the EVs technologies. To gain a more in-depth understanding of EV adoption barriers, an individual-level analysis is needed to investigate the cost and benefits of different types of EVs based on household travel patterns. In this Chapter, the energy use patterns for 3,943 households, 6,720 persons, and 28,536 driving trips predicted by the regional travel demand model (TDM) were estimated to analyze the c savings associated with using different types of EVs to serve model-predicted daily travel needs. The purpose of this analysis is also to better understand the uncertainty of EV cost savings for a heterogeneous sample of local travelers and to identify the feasible range for EV adoption and operation. The sample of local residents was randomly selected from the synthetic households used in the Atlanta Regional Commissions activity-based model (ABM), which represents a significant fraction of local travelers (Atlanta Regional Commission, 2016a, 2012). The daily travel patterns, including trip departure time, origin-destination (O-D) pairs, mode choice, and number of vehicle occupants were estimated using the activity-based approach within ABM model framework. The departure time for each trip and O-D pairs were post-processed using the Directions Application Programming Interface (API) for Google Maps® ("Google API" in following sections) to estimate the route choice and travel times for each origin-destination pair (Google, 2019). Energy use (fuel and electricity) for each vehicle type was estimated using the energy model developed in Chapter 4 for each household, based on predicted trip, route, distance, and travel time (average speed). The energy use, driving range, and operating cost were analyzed for each household to assess the cost savings of choosing certain types of EVs, and the variability of cost savings of adopting EV is

investigated for EV operation under various travel patterns. Conclusions and recommendations will be provided based on the results as well as the limitations and concerns in EV adoption at the disaggregate household level.

6.1 Household Daily Travel Patterns

The household sociodemographic attributes and household daily travel profiles for a normal weekday were generated by ARC's 2017 ABM model (Atlanta Regional Commission, 2012), with some details already provided in previous chapters. In this section, the sociodemographic attributes, trip patterns, and routes were analyzed as those attributes may directly or indirectly correlated with vehicle energy use.

6.1.1 Household Sociodemographic Attributes

The synthetic households and persons in ABM are generated from population synthesizer embedded in the model using the Public Use Microdata Sample (PUMS) from 2007 to 2011 Census data as model inputs (Atlanta Regional Commission, 2012). The synthetic population include key sociodemographic attributes for households and persons, such as household size, income, vehicle ownership, number of workers, gender, and age distribution.

In this study, the 3,943 sample households were selected randomly to represent the synthetic households, with distributions and mean values of key household/person attributes compared in Figure 64. Among the 3,943 households, the driving trips performed by driving-age household members were kept for further analysis (there is no driver indicator in the trip output, so one of the driving-age persons is randomly selected as the driver), which leads to 6,720 driver samples. The comparison suggested that the sample households, except the age distribution, can relatively represent the distribution in the synthetic households and represent a variety of

household conditions. The range of age distribution is smaller than population age distribution due to only driving age (16-80) persons were selected in the final dataset.

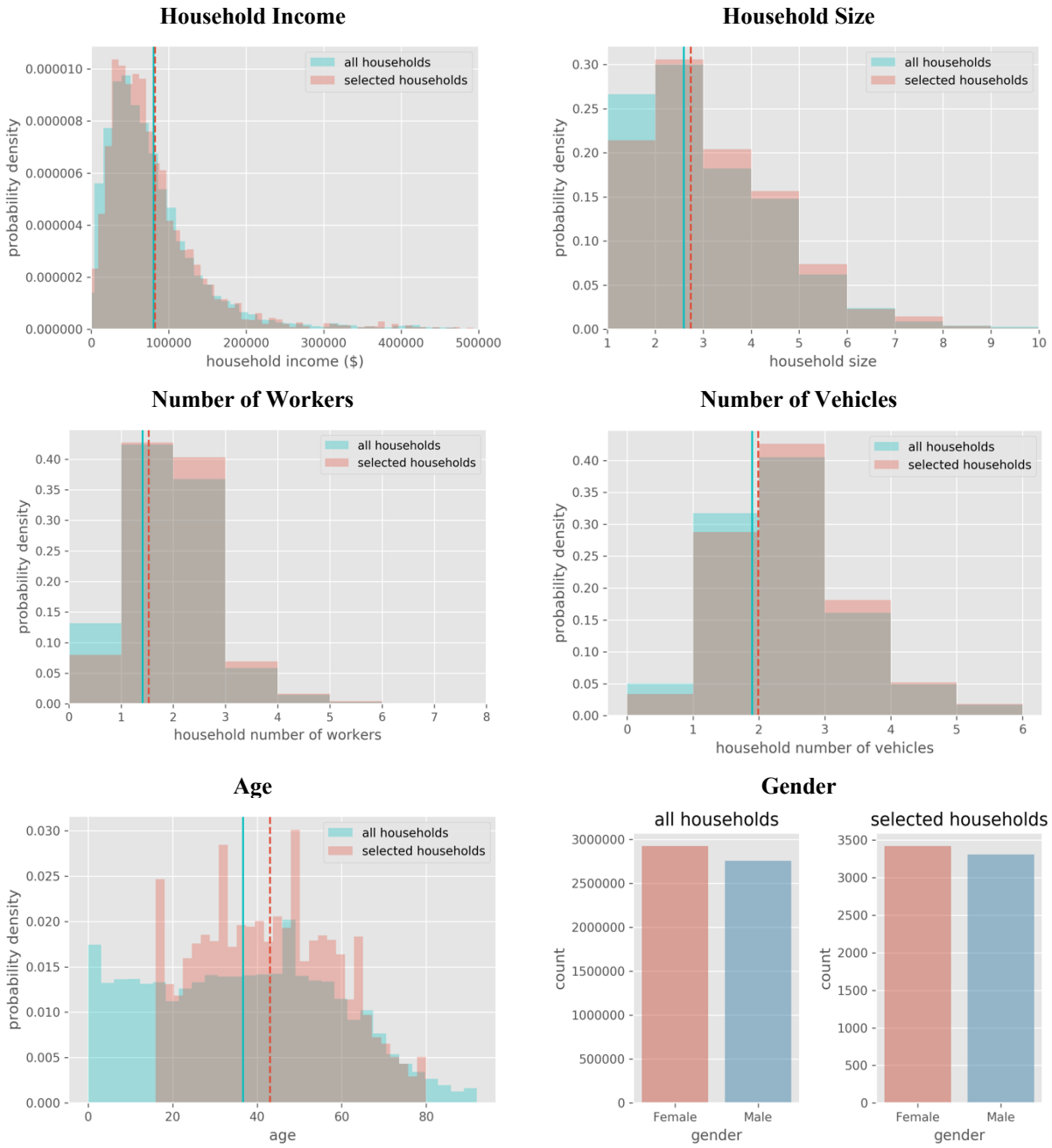

Figure 64. Demographics in overall ABM outputs and household sample subset

6.1.2 Household Travel Patterns

The ARC ABM model is based on the CT-RAMP (Coordinated Travel Regional Activity-Based Modeling Platform) family of Activity-Based Models (Atlanta Regional Commission, 2012, 2016a). This approach models individual travel choices (households and person) as a function of household/person's sociodemographic attributes and surrounding transportation conditions using a series of discrete choice models (multinomial logit model or nested logit model). The parameters in discrete choice models were estimated using 2011 ARC Regional Household Travel Survey (Atlanta Regional Commission, 2016a). The daily tours and trips were predicted with half-hour resolution, incorporating congestion and pricing schemes by time-of-day. The trip generation results were verified and calibrated by comparing to multiple data sources, including the 2010 Census, the 2009-2010 Transit On-Board Survey, 2010 traffic counts, and original household travel survey data.

In this analysis, the 28,536 driving trips (alone or shared) performed by the 3,943 selected households are selected to represent a variety of travel patterns. Each trip record included O-D pairs represented at the TAZ level, departure time in half-an-hour interval, travel group, travel purpose, and mode choice. In this analysis, as only driving modes were selected, the only difference for each mode is the number of passengers. The distribution of travel purpose, number of participants, and trip count by departure time were provided in Figure 65 below. Most of these trips were for a work purpose (including to-work and return from work). The fraction of school and university is relatively low, but still has about 1,000 samples. About 90% of the trips were drive-alone (single occupant vehicle) trips. Most trips depart during rush hours, from 6:30 am to 8:30 am and from 16:30 pm to 18:30 pm, but trips in the sample are conducted throughout the day (see Figure 65).

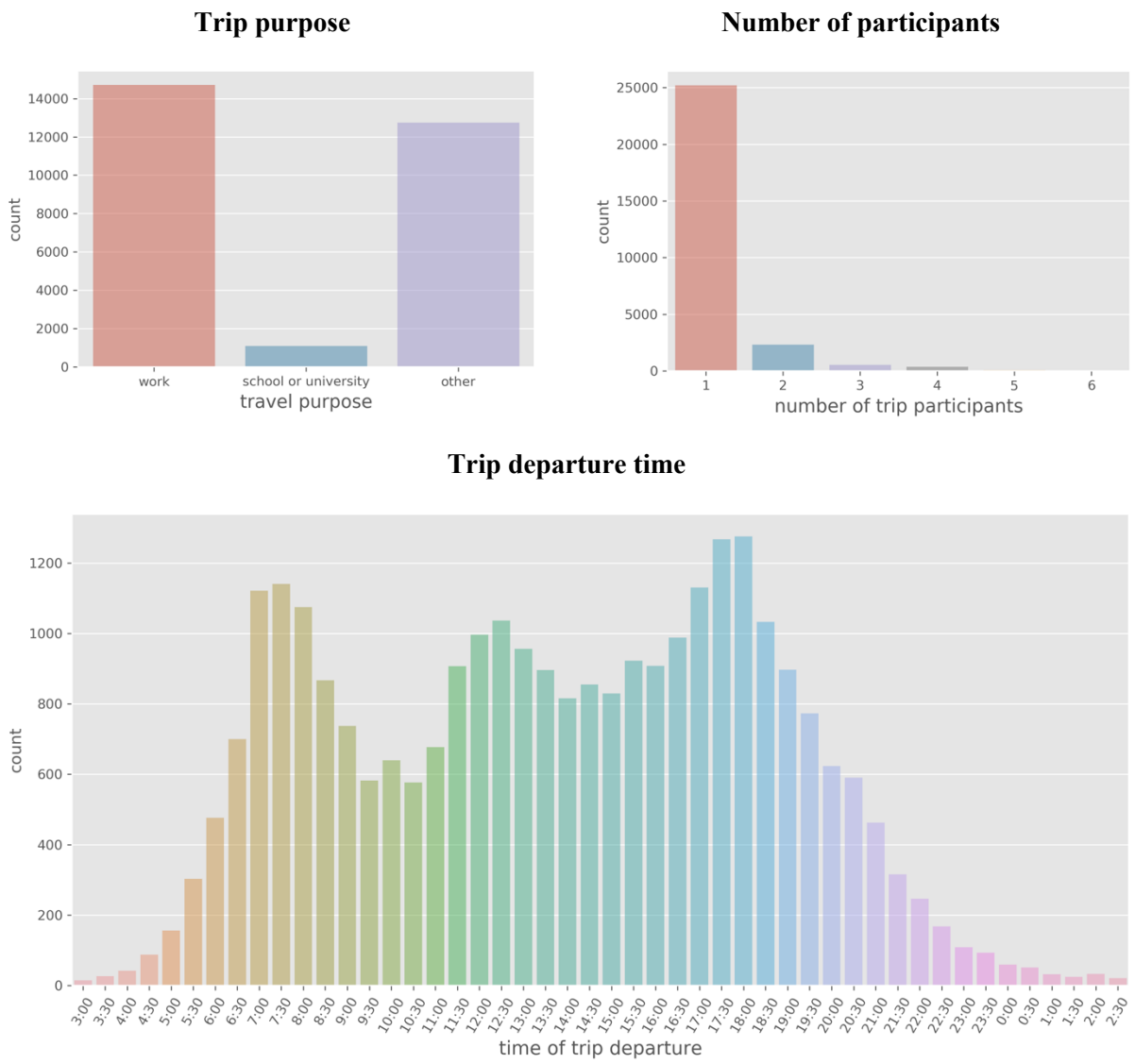

Figure 65. Travel patterns of selected trips

The selected trip origin-destination pairs can be represented by desire lines between each O-D pair (straight line connecting origin and destination). The desire lines for all selected O-Ds were plotted in Figure 66 below. Most trips originated from/arrived at the downtown Atlanta area, with several other high trip attraction/generation frequency area located at Rosewell, Marietta, Decatur, and Union City. Fewer trips were selected from rural areas and locations far from Interstate Highways. In general, the selected trips are dispersed throughout the Metro Atlanta area and represent a variety of operating conditions.

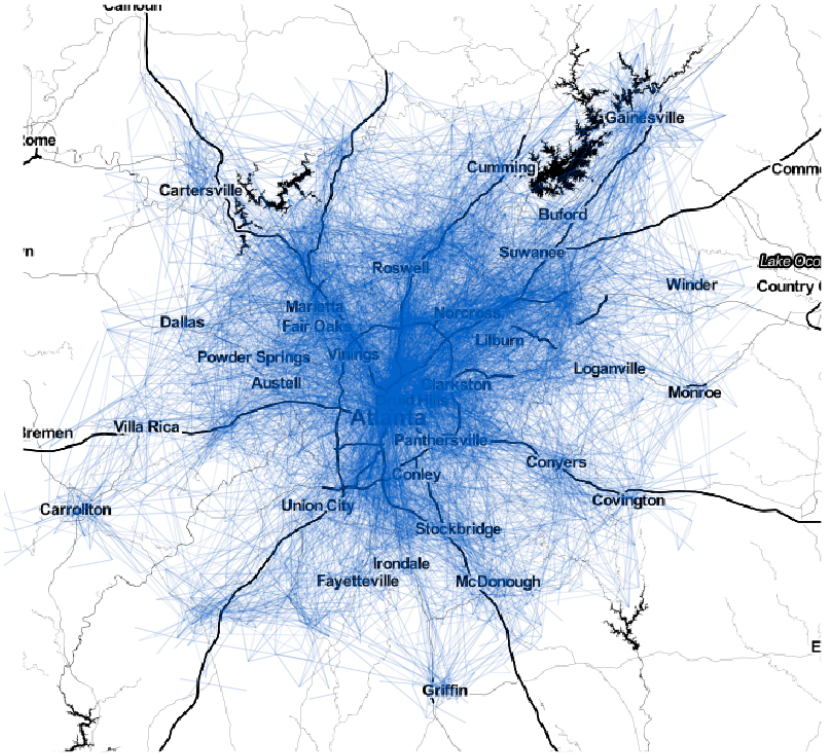

Figure 66. Selected trip origin-destination desire lines

6.1.3 Route Choice Generation

Route assignment in the ABM model to generate traffic volumes and travel speeds on each link employs a bi-conjugate Frank-Wolfe algorithm for five time periods within a day, including early morning, morning peak, mid-of-day, afternoon peak and evening (Atlanta Regional Commission, 2012). However, a major limitation of using Frank-Wolfe algorithms with embedded relationships between traffic volumes and link speeds is that more realistic traffic dynamics (interactions with traffic, traffic signal operations, etc.) are not represented in the algorithms (Wang et al., 2018). Because travel speeds and travel time are key factors in estimating energy use, an enhanced methodology is used to generate travel time and speeds scheme for each trip. This study uses the Google API to compute the route choice and travel times for each origin-destination pair. This

method allows the user to specify the location, mode, and time of day of travel (Hermawan and Regan, 2017) and provide time-specific, high-fidelity travel time and schemes on a detailed network under real-time congestions (Wang and Xu, 2011). The major limitations are the high cost to process large amounts of data in the query, which constraint the sample size in this study as well, and dependence of the response to real-time traffic conditions at the time of the query (which may not reflect typical conditions), and that drivers know and follow the routes with lowest travel times at the time of departure. In this study, the coordinates of origin and destination zone centroids, the mode used ('driving'), the departure time period and fare restrictions (willing or not willing to pay tolls) were used to query the routes via Google API. A sample of estimated routes is provided in Figure 67 below.

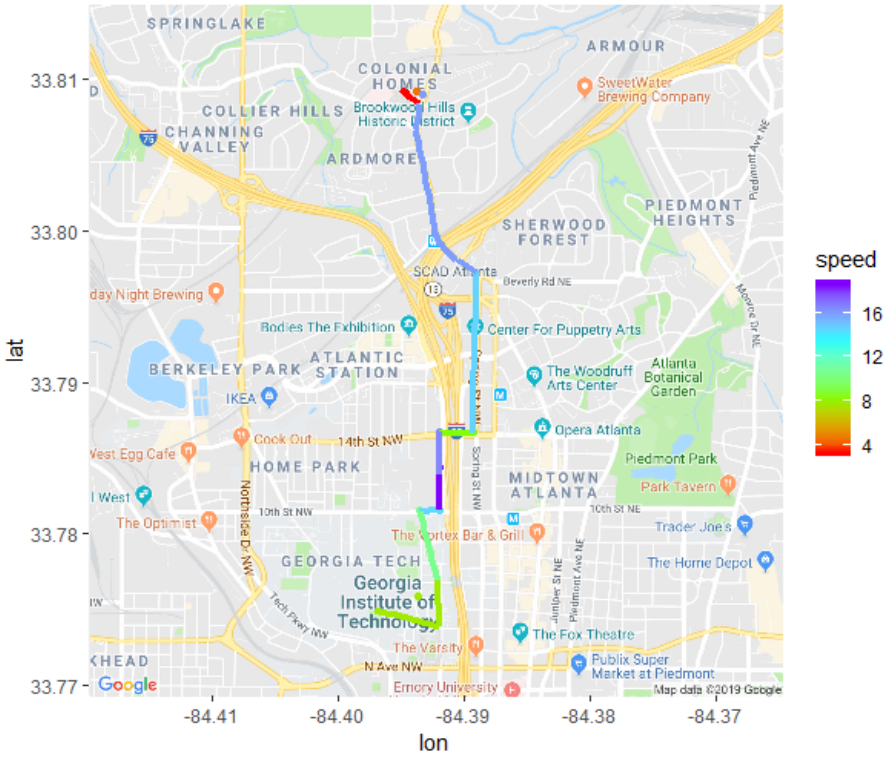

Figure 67. Sample Google API route for a sample O-D pair

The results from Google-predicted travel characteristics and original static traffic assignments were compared for all trips in Figure 68. From the results, the Google API predicts slightly shorter travel distance due to a different network used in the Google Map system (which may include local roads that are not included in the regional travel demand network model that is composed of freeways and arterials). The Google API predicts longer travel times and lower travel speeds than the activity-based model, which suggested more congested conditions compared to the ABM results. There are strong linear relationships between the API results and ABM results, which suggested that the predicted travel trends are likely consistent. Overall, the API results suggest relatively worse travel condition than using the ABM results, which will affect trip-level energy results. Higher energy use, with potentially more regenerative braking, is expected under the more pessimistic traffic conditions provided by the Google API.

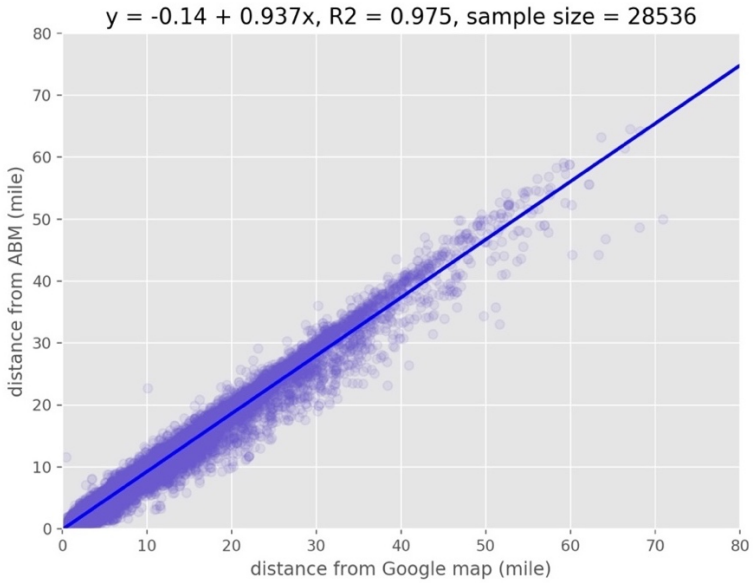

(a) Travel distance

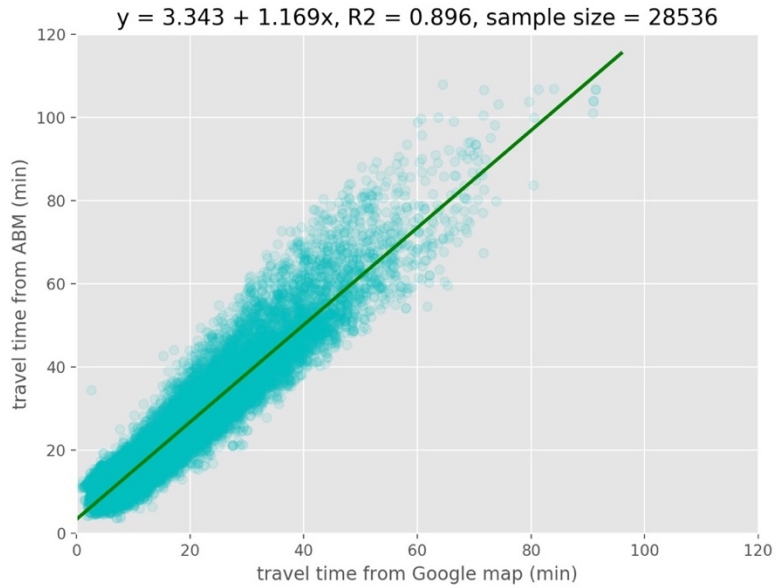

(b) Travel time

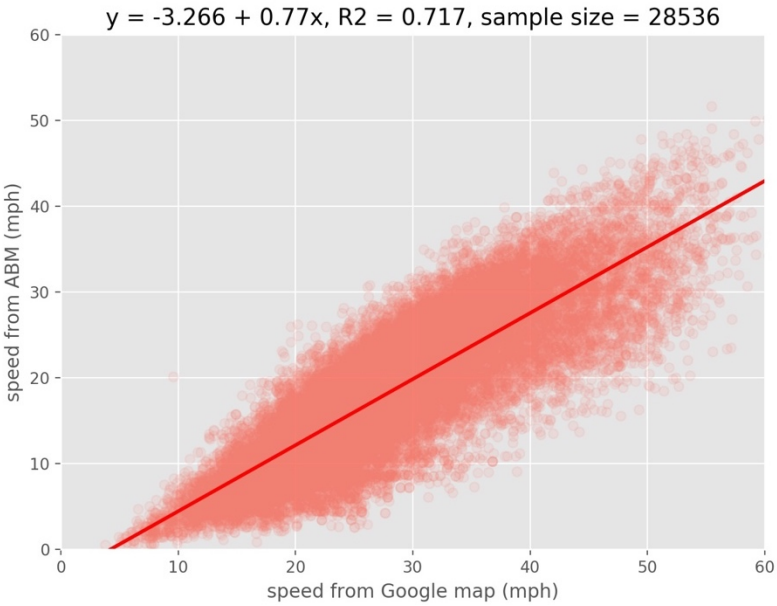

(c) Travel average speed

Figure 68. Comparisons between Google API and ABM assignments results

The relationships between distance, travel time, average speed, and travel purpose are displayed below. The distribution plots, represented by kernel density estimation (KDE), suggested that most trips are within 20 miles, 50 minutes, and with average speeds between 20-40 mph. The travel speeds in general grow with increasing travel distance and travel time. The trips under mandatory tours (to-and-from work, to-and-from school) generally have longer distances

and travel times. The non-mandatory trips (eat out, shopping, leisure, etc.), regardless of by individual or shared by family members, are shorter than trips for mandatory purposes. The at-work tours and trips (lunch break, business, etc.) are the shortest. The variation of each kind of trips is still large and the distributions of all kinds of trips have significant overlaps in terms of travel distance, time, and speeds.

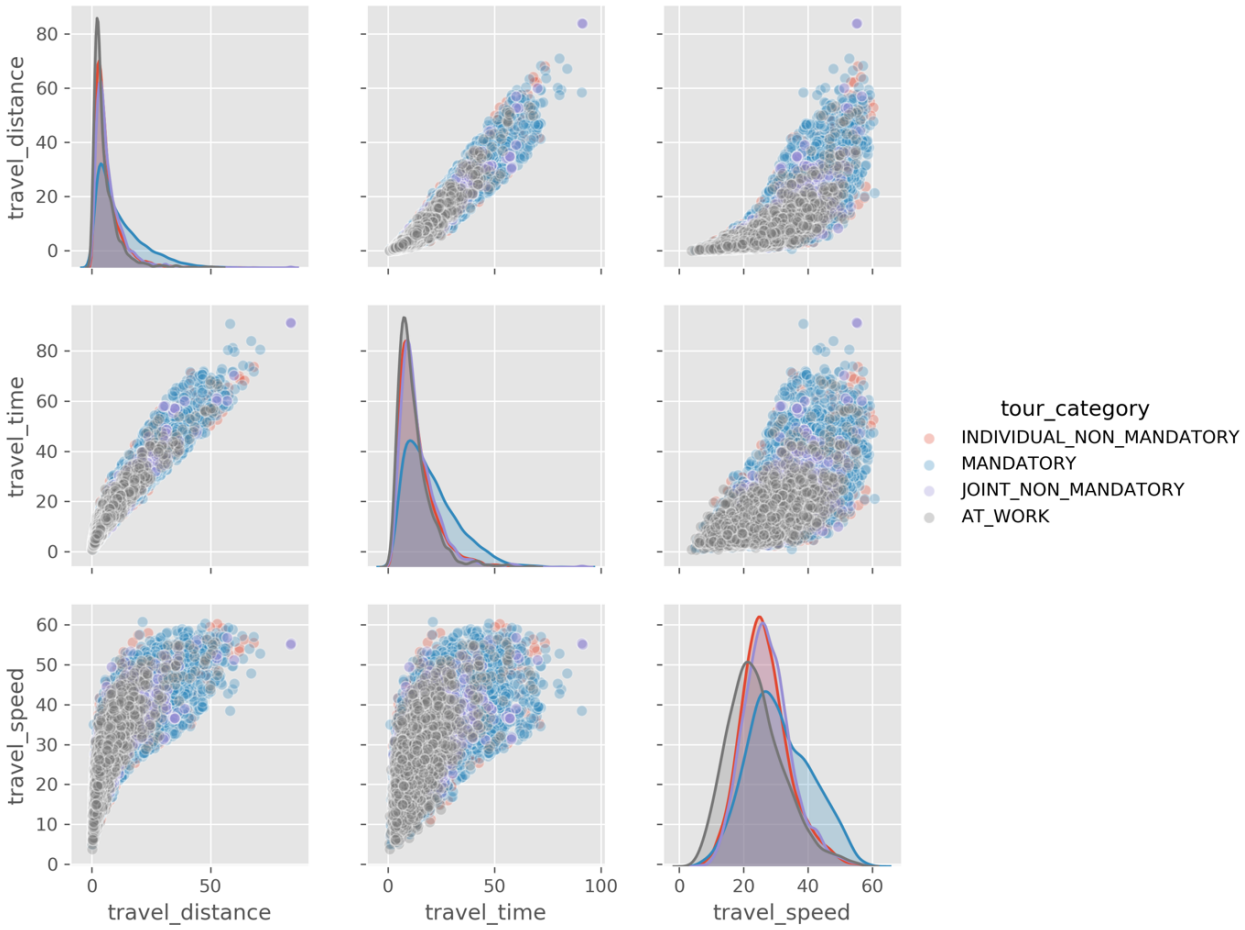

Figure 69. Travel distance, time, and speed distributions by travel purpose

6.2 Household Energy Use Estimation

As suggested in Figure 67 above, household daily travel patterns were ultimately represented by trip routes composed of link-by-link average speed, travel time, and distance. The EV energy analysis is performed using link-level traffic inputs, include road type, link average speed, initial

SOC, and HVAC load, for BEVs, PHEVs, and HEVs. The following sections describe the preparation of each input.

6.2.1 Road Type and Average Speed

Road type is represented by local or freeway for both rural and urban driving conditions. For the purposes of this analysis, flat terrain (road grade = 0%) is assumed for all the trips to simplify the research effort. For each road type and average link speed, a driving cycle is randomly drawn from regional GPS data (Atlanta Regional Commission, 2011; Liu et al., 2018) to simulate the energy rates per mile for the selected link. The total energy use is calculated by multiplying the generated energy rates and the link distance in mile.

6.2.2 Initial SOC

There are several charging scenarios considered for BEVs and PHEVs, which range from reasonably pessimistic conditions to reasonably optimistic conditions. In particular, we considered two charging strategies:

- **Charging at the end of day:** This scenario assumes that households only have access to home charging devices that can fully charge the EVs after the entire day of trips are completed. The vehicle starts from highest battery SOC (90%) at the beginning of the day, and the SOC drops throughout the day as the vehicle is operating.
- **Charging at the end of each trip:** This scenario assumes rapid charge facilities are widely available at most trip ends, and drivers are able to recharge their EVs to full capacity before next trip (the charge rate is assumed to be sufficiently large).

Within each trip, the initial SOC in each link depends on the SOC level at the end of previous link. The initial SOC for HEVs is assumed to be 60%, which is around the control SOC level (Ehsani et al., 2018). For BEVs, if the end-of-link SOC drops below 10%, the electric range is assumed to be depleted and the trip is not fulfilled (in this case the drivers need to use the remaining range looking for a charging location).

6.2.3 HVAC Load

The HVAC load is normally less than 5 kW, peak power may reach 8 kW for some vehicles, and some energy efficient designs may run from 2 kW to 4 kW (Fayazbakhsh and Bahrami, 2013; Kambly and Bradley, 2014; Neubauer and Wood, 2014). In this analysis, we assume two HVAC load scenarios for two common environment conditions:

- **AC on scenario:** This scenario assumes the HVAC load is 3 kW under average high temperature (87°F) in July for Atlanta (U.S. Climate Data, 2019). The impact of humidity on AC use is not considered in this analysis but will need to be integrated into future analyses given the energy use associated with humidity removal.
- **AC off scenario:** This scenario assumes 0.5 kW of HVAC load under average low temperature (70°F) in July for Atlanta (U.S. Climate Data, 2019) and comfort level in the cabin is good. The HVAC load is used for basic ventilation.

The combinations of the charging strategies and HVAC loads form four energy use scenarios (ordered from most pessimistic to most optimistic), include: 1) AC on, charge at end of day, 2) AC off, charge at end of day, 3) AC on, charge at end of each trip, 4) AC off, charge at end of each trip. For HEVs and ICEVs, only the different HVAC load scenarios were investigated. The

energy modelling framework presented in Chapter 4 was adopted to predict the fuel and electricity use for each of EVs presented in Table 8. The ICEV energy consumption was estimated for a new passenger car (age = 0) following a similar procedure with energy rates by VSP bins from MOVES-Matrix (Liu et al., 2019).

6.2.4 EV Energy Use Operating Costs

The energy use operating cost (cents/mile) for each EV type was assessed under various cost schemes. In this analysis, we assume the following price scenarios for fuel and electricity respectively:

- **Electricity price:** The fare rates specified as 1 cent/kWh for non-peak, 7 cent/kWh off-peak, and 20 cent/kWh for peak hours using information from Georgia Power (Georgia Power, 2019). The transition rate as 15 cent/kWh is also added with mixed normal and peak charging, given that the peak period is short (weekday from 2:00 pm to 7:00 pm).
- **Fuel price:** The fuel prices were specified using high ($3/gallon) and low bound ($2/gallon) of Georgia fuel price in 2019 (U.S. Energy Information Administration, 2019c).

The total costs of fuel and electricity consumption were summed and divided by daily VMT to estimate the energy use operating costs of the EVs. The cost analysis was performed combining all the energy use scenarios and cost schemes.

6.3 Household Energy Use Patterns

Using the trip data from previous sections, the energy analysis was performed for each household and each trip for each of the candidate vehicles in the list, including BEVs, HEVs, PHEVs and ICEVs. The disaggregated-level results, including driving range, SOC distribution, energy use, and cost savings, compared to the ICEV baseline, are presented in the following sections.

6.3.1 Electric Range Distribution of BEVs

As discussed above, the driving range of BEVs is a major barrier to EV adoption. In this analysis, the daily VMT driven by vehicles in the sample is first provided in Figure 70, with 99% of daily VMT falling below 150 miles. In this case, the 300-mile Tesla should not raise significant range anxiety issues based on Atlanta driving conditions. The driving ranges of 100-mile BEVs is investigated for the four specified HVAC and recharge scenarios, where its design range covers about 95% of daily VMT. The sample drivers were grouped by their daily VMT in 10-mile increments, and the conditional daily travel survival rate by VMT was estimated as the fraction of "surviving" drivers (daily VMT met by 100-mile BEVs) among all drivers in this VMT range. The conditional daily travel survival rate results are plotted in Figure 70 below.

The results suggested that, under worst case scenarios (AC on, no recharge during the day), the daily travel survival rate drops below one for a 60-mile daily VMT and falls to nearly zero when reaching the 90-mile daily VMT. Keeping the AC off for the same charging conditions increases the daily travel survival rates for the same daily VMT distributions, and a small portion of EV users can actually survive above 100-mile range limit. However, with recharging during the day, the BEVs can sustain most of the daily travel, and maintain the daily travel survival rate higher than 80% even when daily mileage exceeds 150 miles. The availability of mid-day charging can notably address a majority of range issues for the 100-mile BEVs under the assumptions made in this case study.

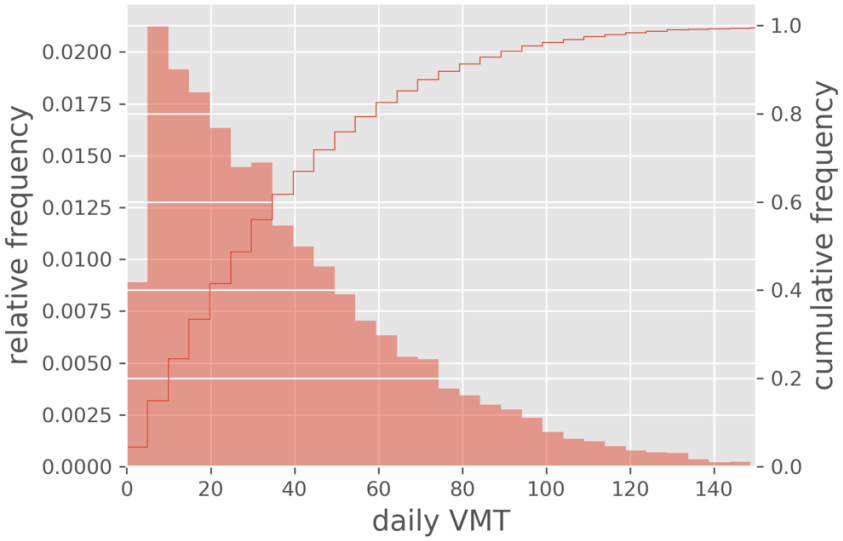

(a) Daily VMT distribution

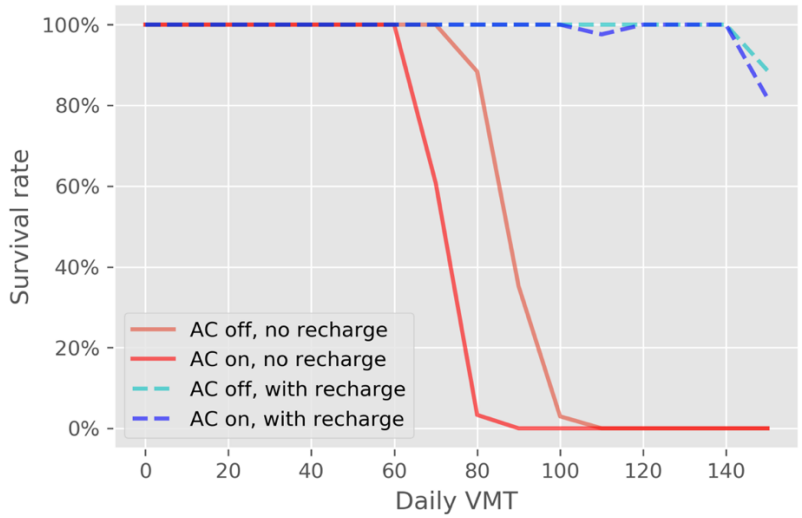

(b) Conditional daily travel survival rate of BEVs by daily VMT

Figure 70. Daily VMT distributions and percentage of personal daily VMT achieved by 100-mile BEV (2016 Nissan Leaf)

The scatter plot of succeed and failed daily travels (Figure 71) suggested that turning AC on at 3kW will significantly reduce the available driving range and increase the percentage of failed daily travel from 7.8% to 13.7% without sufficiently charging during the day. Vehicles that operate at higher speeds have slightly shorter driving ranges versus slower vehicles. Most of the daily travels (>=80%) can be still fulfilled by a 100-mile BEV in a normal workday even under a relatively pessimistic traffic scenario.

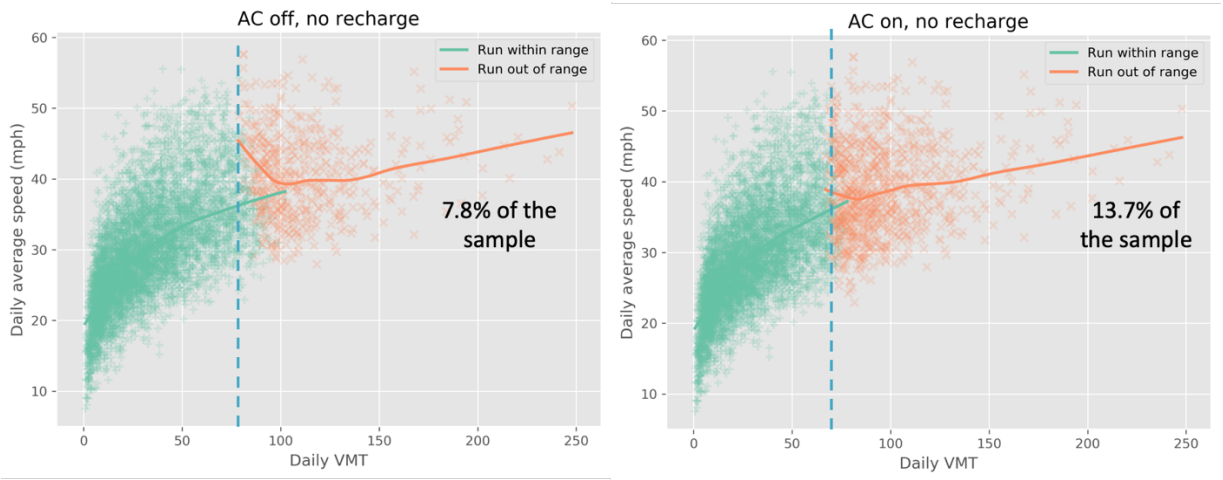

Figure 71. Succeed and failed daily travel suing 100-mile BEVs

6.3.2 Battery SOC Distribution of PEVs

The SOC distributions by time of day are critical for PEVs (PHEVs + BEVs) to assess the potential impacts of charging demand on the electric grid. A higher fraction of low SOC PEVs, infers that demand on electric grid will grow as a consequence of mid-day and end-of-day PEV charging needs.

In this study, using the simulated SOC during the trips, the 24-hour SOC profiles of given PEVs is calculated assuming the PEVs are fully charged at the beginning of the day (90% for the first hour and last hour of the day) except for vehicle travelling across days (through the midnight hour). The SOC level between two consecutive trips were interpolated linearly for a single driver, so when recharge is not available, the SOC curve will be a horizontal line, and when recharge is available, the SOC curve will recover to 90% before next trip start. The SOC distributions for all of the drivers for two types of BEVs under selected time-periods are provided below. The trips that could not be met by BEVs were removed. The results suggested that the SOC levels are generally higher near the beginning of the day (7:30 am in the figure) and shifting towards lower SOC intervals along with time, which may cause higher charging demand in the late afternoon or

early evening. The SOCs of 300-mile BEVs are generally higher than 100-mile BEV, given the larger battery capacities. The SOC drop is limited when AC is off, or recharging is allowed. Many of the BEVs still have sufficient battery SOCs (>=40%) near the end of day. The SOC of 300-mile BEVs should be sufficient for multiple days of travel without any charging in between.

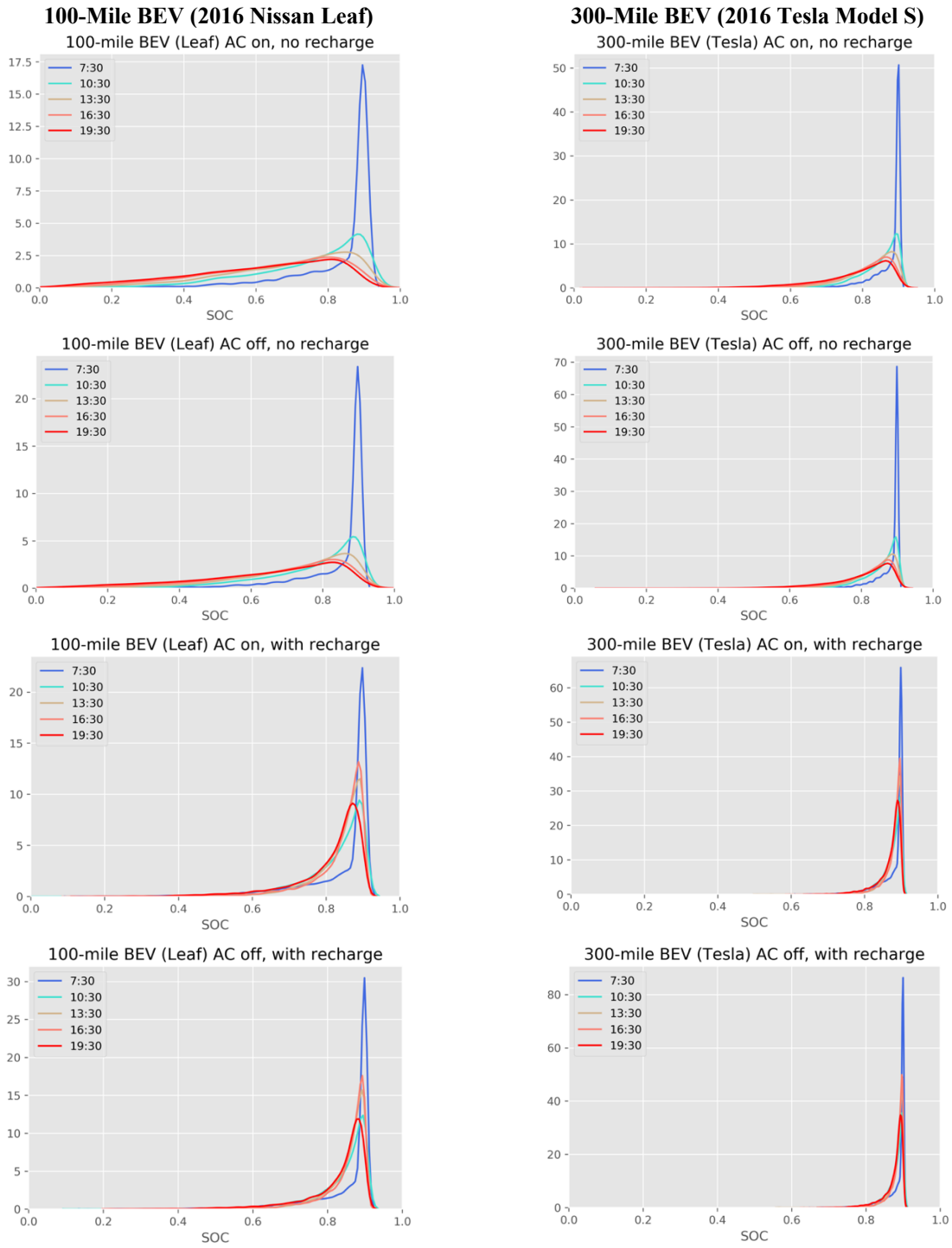

Figure 72. Simulated BEV SOC distributions by time of day

A similar analysis was performed for PHEVs, with no trips removed, because these vehicles can be propelled with gasoline when the battery becomes depleted. The conclusions are quite similar to the results from BEVs, expect that the SOC drops are much more significant for

PHEVs due to the smaller battery size. By the end of day, if no recharge is available during the trip, most of the PHEVs need to be recharged so that all-electric range can be provided for the next trip. Charging between trips can help maintain the SOC at high level, consuming more electricity during daily travel.

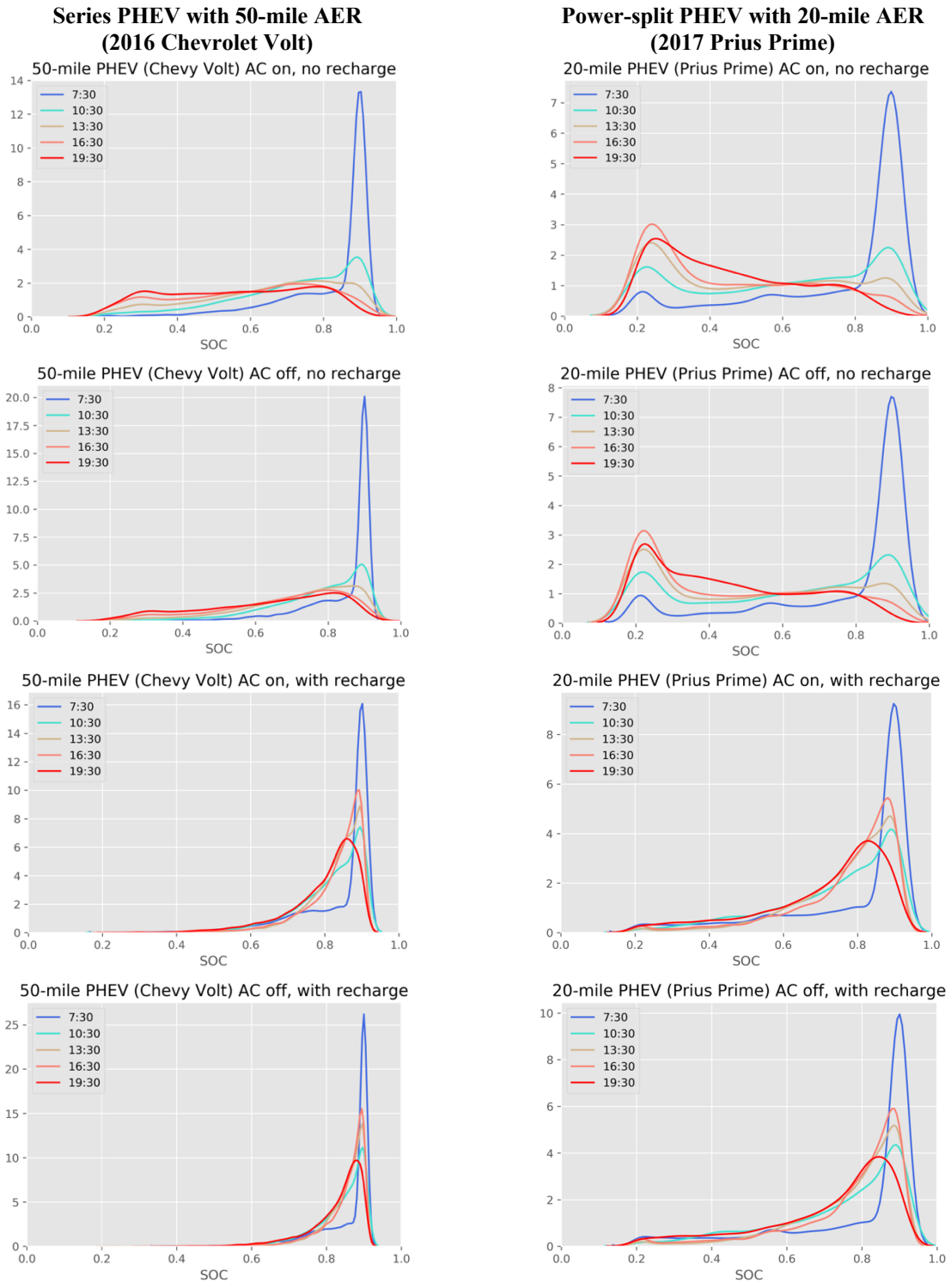

Figure 73. Simulated PHEV SOC distributions by time of day

6.3.3 Energy Consumption of All EVs

The daily energy use results from all vehicles were compared under different daily VMT and daily average travel speeds. The fuel economy in miles per gallon of gasoline equivalent (MPGe), was used to compare all types of vehicle using a consistent metric. The electricity consumption (kWh) was converted to equivalent gasoline using the unit energy content of gasoline (34 kWh/gal). For BEVs, only the recharging scenario is considered so that all trips are included. The fuel economy is calculated by dividing total distance travelled by sum of fuel and electricity use in gallon of gasoline equivalent. The results are provided in Figure 74 and Figure 75 below. The values of MPGe for all kinds of vehicles (EVs and ICEVs) under different operation scenarios (AC on/off, different charging scenarios) and travel patterns (speed of VMT) were plotted and the trendline of MPGe under different travel patterns were plotted using the LOWESS methods. The higher the MPGe values, the suggested energy efficiencies for the specific vehicles.

In terms of daily average speeds, two types of BEVs have the best fuel economy in almost all cases and more efficient under median speeds (20-40 mph), given the high powertrain efficiency and greater potential of regenerative braking in this speed range. The 100-mile BEVs have a lower vehicle mass and a slightly better fuel economy. The fuel economy of the two types of PHEVs varies greatly from low speeds to high speeds, with poor fuel economy under high average speeds. This is probably due to the higher power demand with a heavier vehicle mass and the need to charging battery under the combination of high-power demand and low SOC level. Another possibility is that the underlining Autonomie model and proposed energy model may over-estimate energy use under high speeds, and further calibration of the vehicle simulation model may be necessary when more data become available under extreme driving conditions. Sufficiently charging the PHEVs through the day can be a remedy of fuel economy decrease under

high speeds. Similar to PHEVs, the energy savings for HEVs is also greater under lower speed operation. The high AC demand will reduce fuel economy for all vehicles in all cases, which suggested that energy use will almost certainly increase, regardless of vehicle adopted.

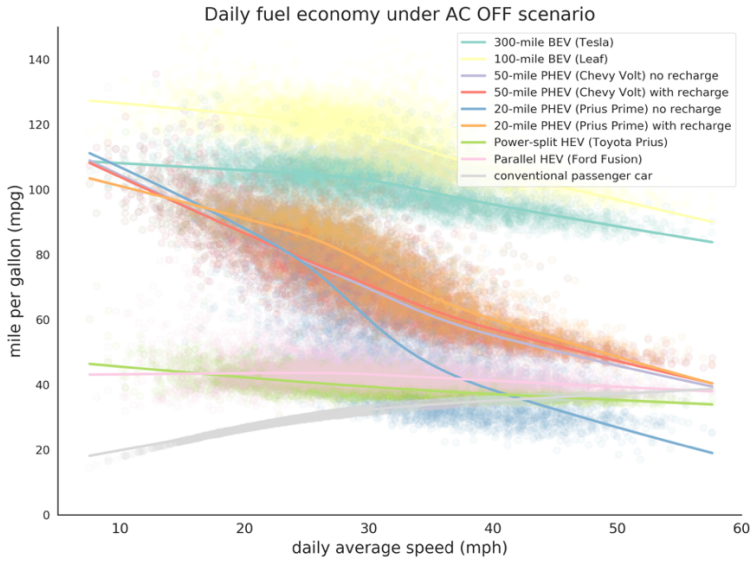

(a) AC off scenario

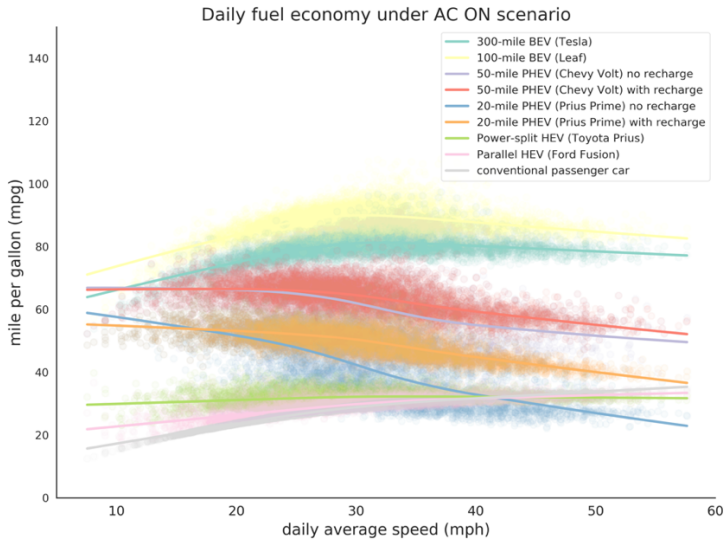

(b) AC on scenario

Figure 74. Vehicle fuel economy by daily average speed

In terms of daily VMT, a similar ranking of fuel economy is observed. As shown earlier in Figure 69, the travel speeds are much higher during long distance trips and the fuel economy of

EVs decreases under high speed operation; hence, the energy saving benefits diminish or even reversed for long-distance daily travel (>= 50 miles). Another possibility is the underlining Autonomie model and proposed energy model may over-estimate energy use under high speed conditions even though the aggregated energy results match with the tested conditions. Further calibration of the vehicle simulation model may be necessary, once additional energy use and operation data become available for more extreme driving conditions.

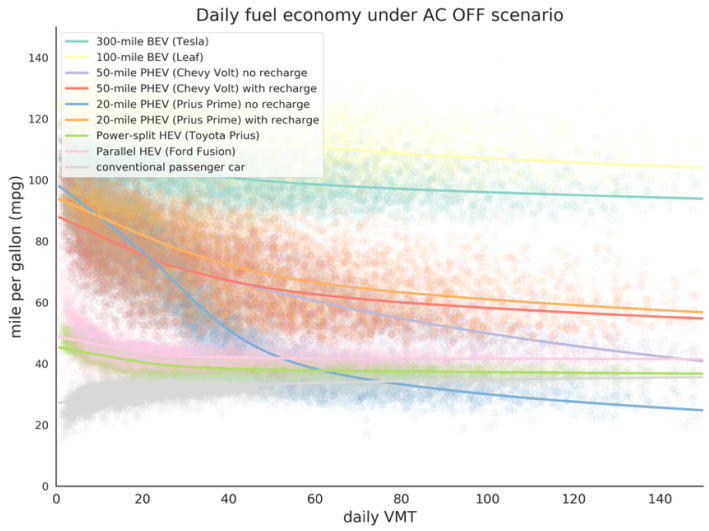

(a) AC off scenario

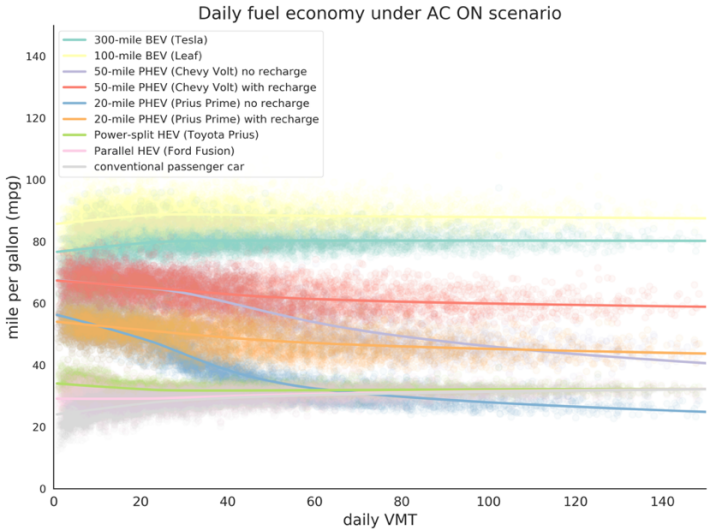

(b) AC on scenario

Figure 75. Vehicle fuel economy by daily VMT

6.3.4 Cost Saving from EV Adoption

Finally, the cost savings of different types of EVs was assessed using unit operating cost per mile under various cost schemes introduced above. The total costs from fuel and electricity consumption were summed and divided by daily VMT to estimate the costs and benefits of EV operation. The Boxen plot (or letter value box plot) shows the distribution of cent/mile cost saving for each vehicle, scenario and cost scheme compared to baseline ICEV (positive value means saving). The median cost saving is highlighted by horizontal line and the area of each box is proportional to the fraction of observations within specified cost/mile range.

The results suggest that, in most cases, the BEVs, PHEVs, and HEVs can help reduce operating costs, except under the high electricity cost with low fuel cost scenario. As expected, cost savings are maximized under the combination of high fuel cost and non-peak charging rates, with BEVs saving about 10 cent/mile, PHEVs saving 5-8 cent/mile, and HEVs saving 0-5 cent/mile. On the other hand, with low fuel price and peak hour charging, the cost saving from BEVs and PHEVs are around 0 cent/mile, while HEVs can still save 1-2 cent/mile under normal weather conditions. The combination of low electricity cost and sufficient charging can increase saving from PHEVs, but cost savings drop as electricity costs increase. The intensive usage of air conditioning can lead to lower cost savings for all EVs under high electricity cost cases, and cost savings of HEVs are almost negligible in the AC on scenarios. The cost savings of the two PHEVs have the largest variance, which implies that the actual savings vary greatly under various combinations of available range and operating conditions. In conclusion, the benefits of using different kinds of EV depending on the adoption scenarios, ambient environment conditions, and energy costs. There is no universal solution for minimizing the operation cost with one kind of vehicle under all cases, and the optimal vehicle selection can be based upon the given a

combination of vehicle, on-road operations, energy costs, and environment conditions. Grade will also significantly influence the performance of these vehicles and will be addressed in future research efforts.

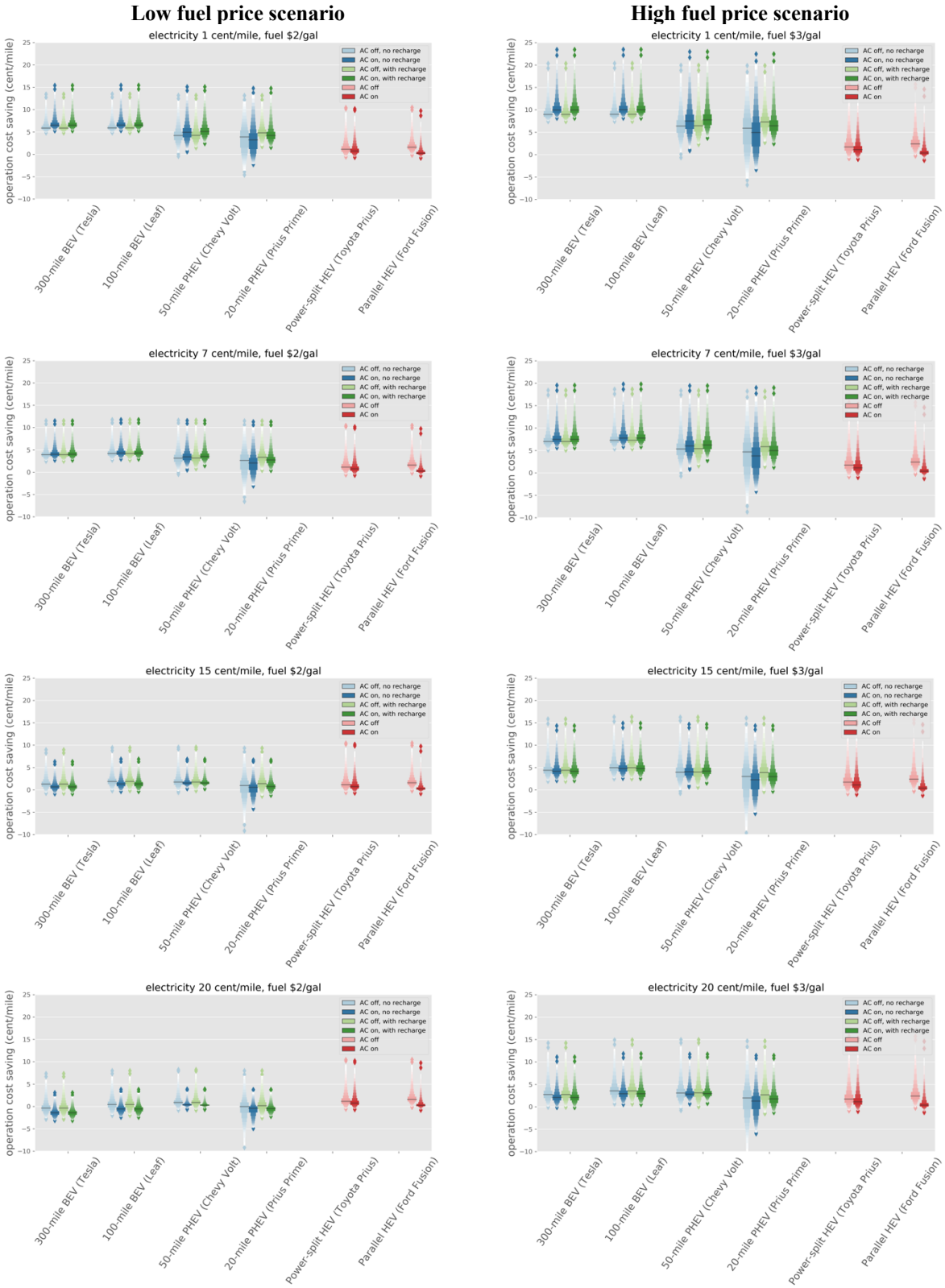

Figure 76. Distribution plots of operating cost per mile by vehicle models, scenarios and fuel/electricity cost schemes

The sensitivities of cost per mile versus different daily VMT for BEVs, PHEVs, HEVs, and ICEVs are provided in Figure 77, Figure 78, and Figure 79. Note that the BEV costs are insensitive to fuel costs (as they use no fuel). HEV (series HEVs) and ICEVs costs are insensitive to electricity costs. In general, the unit operation costs were higher under low VMT for BEVs and ICEVs. The cost savings of PHEVs and HEVs varies by implementation scenarios and environment conditions. For HEVs, the trend of operation cost is close to ICEVs under AC on, but cost tend to increase with higher VMT if for AC off scenarios. For PHEVs, the trend under sufficiently recharged is similar to BEVs. The cost increases with daily VMT, if the PHEV operates without recharging during the day. In conclusion, the final cost effectiveness of using EVs will depend on the vehicle technology, adoption scenario, energy costs, and ambient environmental conditions. In case studies, there is no universal optimal answer that yields the minimum cost; analysts must consider the combined effects of all of these elements.

1 cent/mile **7 cent/mile** **15 cent/mile** **20 cent/mile**

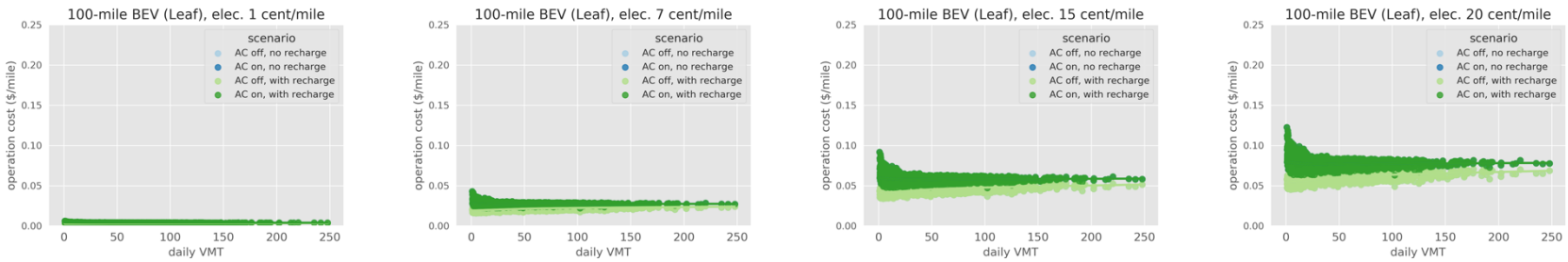

(a) 100-mile BEV (Nissan Leaf)

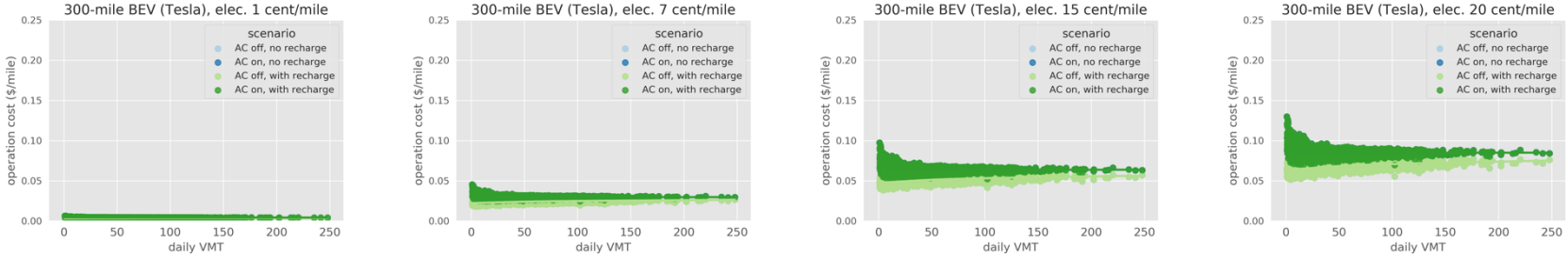

(b) 300-mile BEV (Tesla Model S)

Figure 77. BEV cost/mile by daily VMT

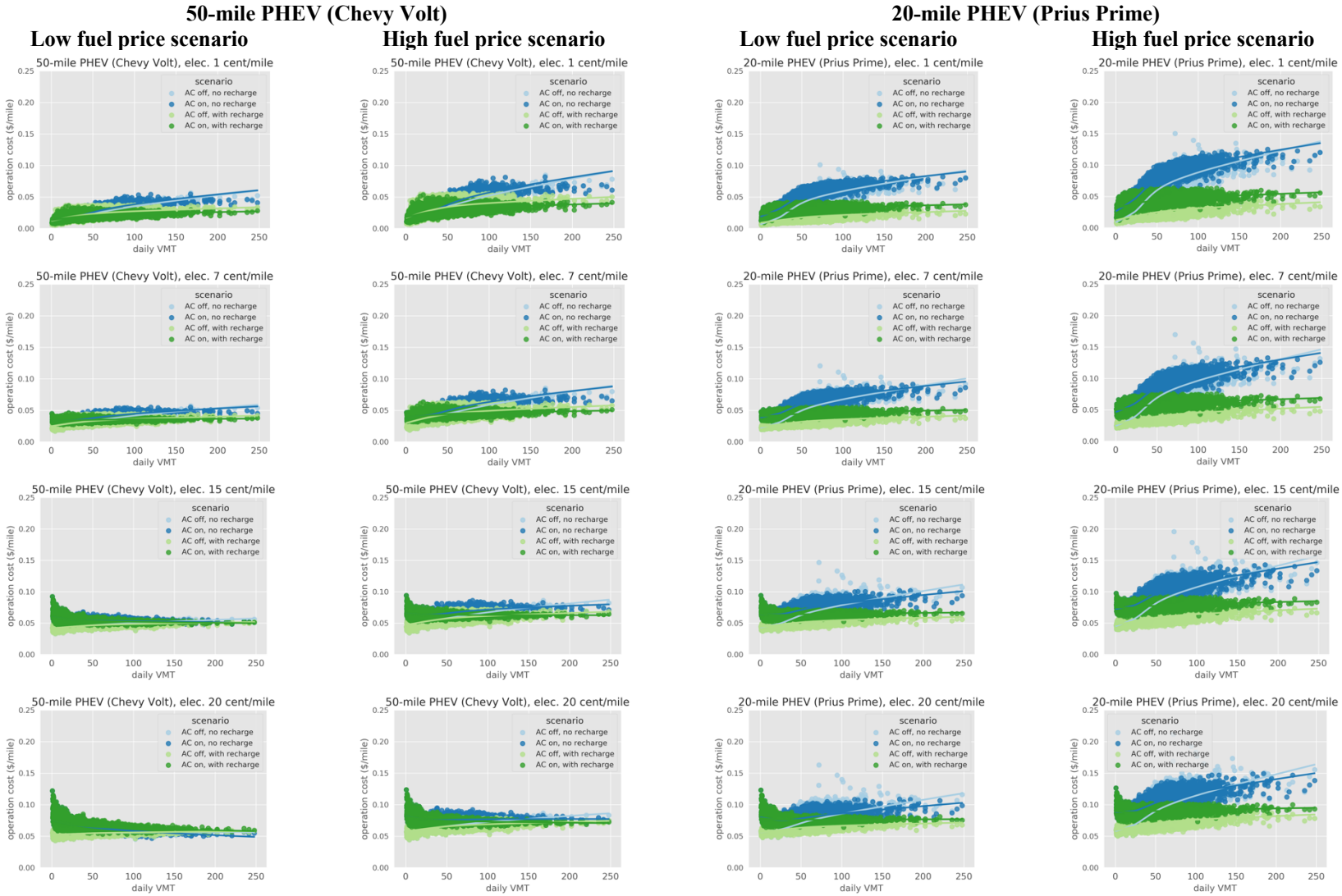

Figure 78. PHEV cost/mile by daily VMT

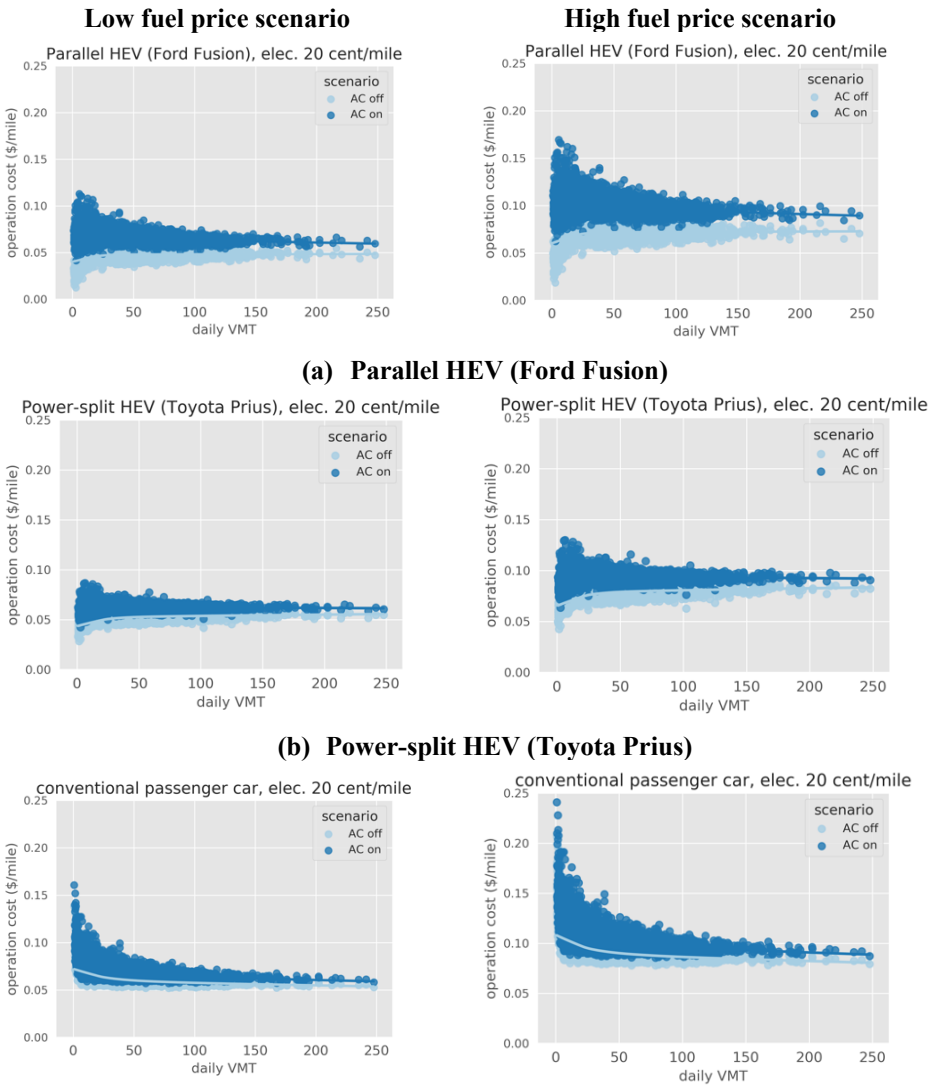

(a) Parallel HEV (Ford Fusion)

(b) Power-split HEV (Toyota Prius)

(c) Conventional passenger car

Figure 79. HEV and ICEV cost/mile by Daily VMT

6.4 Chapter Summary

In this Chapter, the cost savings of different EV types were analyzed for a large sample of household travel predicted by the Atlanta regional travel demand model. The selected sample included 3,943 households, 6,720 persons, and 28,536 driving trips, and represented a wide range of regional travel patterns and on-road operating conditions. The trip-level information was retrieved from the 2017 ABM results, and route choices between predicted O-D pairs were generated using Google Direction API. Energy use (fuel and electricity converted to galls of

gasoline equivalent) for each EV type was estimated for all trips and routes across four implementation scenarios, ranging from relatively pessimistic to relatively optimistic. The results suggested that the driving range, SOC distribution, energy use, and cost savings are sensitive to the specifics of each implementation scenario, and there is no universal best solution that can simultaneously address range, energy use, and cost. The HVAC usage under severe weather conditions in general increases energy use and costs, and sufficient recharging during the day can help reduce energy use and cost in many cases. The conclusions drawn in this Chapter should encourage researchers, engineers, and policy makers to collect more information on EV implementation scenarios and assess how to properly promote various the vehicle technologies given differences in local use contexts. This study can be further improved as follows:

- **Ongoing calibration of the underlining Autonomie simulation and Bayesian Network models.** The energy consumption of EVs is sensitive to operating conditions; hence, it is essential to calibrate both the underlining full-system simulation and the Bayesian simulation inference model, to improve the model goodness-of-fit under a wide range of operating conditions (especially extreme driving conditions). As stated in Section 4.5, the current power-split PHEV may significantly over-estimate fuel consumption under high-speed, low-SOC conditions, which might be addressed with enhanced testing data from on-road vehicles. Further research efforts are needed to to collect relevant data and improve the energy models.
- **Using dynamic traffic assignment for predicting vehicle trajectories and route choices.** The routes generated by the Google API can only reflect current travel trends and lack the ability to predict potential future conditions and to depict microscopic-level vehicle behavior (queuing, ramp spillback, waiting for signals, etc.). A dynamic traffic assignment

model, coupled with the regional travel demand model, may help fill this gap and provide higher-resolution operation data for potential alternative transportation scenarios.

- **Improving the travel pattern estimation from Activity-based Model.** The current regional ABM model does not predict the fleet composition (vehicle make, model and year) at the household-level. In this study, a new vehicle fleet is assumed, with varying fleet penetration rates for the various EV technologies; however, the actual market penetration of various EV technologies may vary significantly across regions as different people and households have different preferences and tastes towards different vehicles. Once a fleet is embedded in the regional travel demand model, further modeling work can be performed to pair vehicle trips with specific vehicles in the ABM modeling process. These changes would allow the ABM to reflect how vehicle choice interacts with tours and trips.

CHAPTER 7. CONCLUSIONS AND FUTURE WORK

The goal of this dissertation was to propose an analytical framework to estimate energy use from electric vehicles that operate within large-scale transportation networks. Activity-based EV energy models were proposed, verified, and applied in multiple case studies. The modeling framework covers several widely-used EV technologies, including BEVs, HEVs, PHEVs, and FCEVs. This modeling framework can be used to assess the energy and cost impacts of adopting EVs at the regional-level and operating these vehicles on dynamic transportation networks. The framework can also be used at the vehicle-level to assess the energy impacts associated with individual vehicle trips and daily household travel on the transportation network.

7.1 Dissertation Contributions

The first accomplishment in this study was the production of a representative EV operation and energy use dataset via full-system vehicle simulation. The Department of Energy's (DOE's) Autonomie model was used to generate energy consumption rates for specific on-road simulations. A total of seven EV models were developed in Autonomie to simulate the energy use (fuel and electricity) under a wide range of operating conditions.

The second accomplishment of this dissertation is the development of a scalable EV energy modeling framework that replicates full-vehicle simulation results with a reasonable level of detail and accuracy. The modeling framework adopts the EV energy and operation data from Autonomie and estimates energy as a function of operating conditions for each type of EV using statistical learning methods. Classification and regression tree (CART) analysis was first applied to the simulation output data to generate energy consumption rates under distinct on-road operating conditions, as represented by combinations of vehicle speed, acceleration rate, and battery state of

charge (SOC). The research then applied the CART-derived energy consumption rates to link-by-link traffic attributes predicted by a large-scale regional travel demand model for the Atlanta, GA metropolitan area, for a variety of EV market share scenarios. The model results suggest that if a 50% PHEV market share can be achieved, more than 30% energy saving can be achieved compared to no PHEV scenario without significantly adding to electricity load.

The energy models were further improved by adopting a statistical-inference model design, using a Bayesian Network approach for various EV models, which combine the physical knowledge about vehicle operation (how the engine, motor, and batteries work together) and data-driven energy inferences. The upper-level vehicle control mode (e.g., engine on and off, electric machine motoring or generating) were modeled as a function of vehicle driving conditions using generalized linear models. The lower-level energy consumption was simulated for distinct control modes from an upper-level linear regression modeling approach. The total energy is the expectation given the probabilities of the control modes and corresponding energy consumption. This proposed EV energy models were verified using a separate testing dataset developed from Autonomie simulation results for another set of driving profiles. The results suggested that the proposed simplified model is able to predict full-vehicle energy simulations at relatively high accuracy. In addition, real-world observed operation and energy use data were collected from select EV models using on-board diagnostic (OBD) devices to verify the energy prediction from the proposed model. The verification results suggested that the proposed model can predict energy use patterns under specific driving conditions. However, the level-of-accuracy highly depends on the representativeness of the underlying Autonomie simulations and the accuracy of collected operation data from OBD devices.

The third contribution of this dissertation is the methodology to estimate the aggregated-level energy consumption (total energy use from all vehicles) for large-scale transportation networks using link-level inputs. The linkage between link-level traffic data and energy models was proposed and tested with a case study and with a sensitivity analysis. The model sensitivity analysis, including the scatter plots and the variance-based sensitivity analysis (also known as "Sobol method"), were performed to identify significant operating factors on energy variation and show potential non-linear relationships between energy use and operating parameters. The network-level energy use was then estimated for 20-county Metropolitan Atlanta area using link-level traffic information include traffic volume and average speed from the network links, vehicle types from current market share and random initial battery state-of-charge. The link-level energy consumption with for EV fleet penetration rates are generated for each roadway link and for each hour of operation and compared to the baseline no-EV scenario (an EV fleet penetration rate of zero) to assess the energy benefits. The spatial and temporal energy savings show, based on the current EV market growth trend, network energy saving are around 4% for the entire Metro Atlanta area. With this approach, the network-level EV energy consumption can be generated and used for various transportation studies. For example, the vehicle-to-grid integration can be analyzed by refining the initial SOC distributions by time-of-day under real-world driving and charging patterns and splitting the energy supply between fuel and electricity with higher accuracy. Eco-driving and eco-routing benefits can also be analyzed using monitored or simulated high-resolution vehicle traces. The life-cycle energy and cost savings can also be performed considering the fuel-cycle, vehicle-cycle energy, emissions, and cost elements for EVs.

The fourth contribution of this dissertation is the methodology to estimate disaggregate-level energy consumption and cost savings for individual households and persons, given their

travel information. In this study, the household travel routines from a typical workday generated by the regional activity-based travel demand model (TDM) were used to estimate the energy use, driving range, and costs of using EVs. The Google Direction API was adopted to generate network-level link speeds for given departure times and origin-destination pairs provided by TDM results. The link-level energy estimation method was applied to each trip performed by each driver in the household to estimate driving range, charging demand, energy use, and operating cost under different EV adoption scenarios, ranging from a relatively pessimistic scenario to a relatively optimistic scenario. The cost savings for the different EV types, compared to conventional ICEVs, can be assessed for a variety of households and diverse travel patterns. The results suggested that the driving range, SOC distribution, energy use, and cost savings are sensitive to implementation scenarios of EVs, and there is no universal best solution that can optimize energy, range, and cost at the same time. The HVAC usage under severe weather conditions will in general increase energy use and costs, and sufficient recharging can help reduce energy use and cost in many cases. The conclusions drawn in this dissertation encourage researchers, engineers, and policy makers to collect more information on EV implementation scenarios and assess vehicle technologies under a local and regional context.

7.2 Limitations and Future Work

The conclusions and findings from this dissertation were subject to limited data sources, assumptions, and current implementation conditions. The works in this dissertation can be further improved by encouraging research efforts on the following aspects:

- **Collecting and refining EV operation and energy use data:** Collecting real-world EV operation data plays a significant role in understanding EV behavior and energy use

patterns. However, the current scope, detail, and accuracy of monitored EV operating data are far from sufficient to fully examine EV use characteristics and obtain highly-confident conclusions. More stakeholders, including vehicle manufacturers, EV owners, transportation planners and engineers, need to be involved in the research efforts to collect high-fidelity on-road performance data (including SOC) and perform analytical work.

- **Incorporating EV degradation rates:** The current analysis on EV energy use does not consider any aging factors (i.e., system deterioration) of the EV throughout the life-cycle and potential energy efficiency drop due to aging of major vehicle components (e.g., engine, motor, transmission). EV deterioration rates affecting energy use (and therefore well-to-pump, and pump-to-wheel emissions) should be explored and incorporated into the modeling system to account for EV aging.
- **Incorporating EV mileage accumulation over time:** Similar to conventional passenger vehicles, the annual mileage of an EV is likely to decrease over time given that households tend to commute and make longer trips with their newest vehicles. Mileage accumulation for the conventional fleet is typically collected in inspection and maintenance (smog-check) programs (EVs are exempt). Data for EV mileage accumulation over time need to be collected through some kind of vehicle registration processes or field measurement to obtain better estimates of the actual model year distribution of the on-road EV fleet. The combination of EV mileage accumulation by time and EV degradation factors will greatly help increase the accuracy of energy estimation of on-road EV fleet.
- **Developing an on-road vehicle fleet synthesizer**: Travel activity and on-road vehicle operations are modeled separately from fleet composition. However, in real-world situations, certain types of vehicles are likely to be assigned to specific activities (e.g., EVs

are often used for home-based short trips with charging availability at home). A fleet synthesizer is needed to generate the proper fleet composition for certain groups of travel, so that the energy use can be accurately predicted using right set of vehicle operation characteristics. Vehicle purchase and household assignment models also need improvement, so that EV owners and modeled travel patterns are properly paired.

- **Calibrating Autonomie simulation with latest observed EV data**: The overall accuracy of the analytical results is constrained by any underlying uncertainty in Autonomie simulations. The current Autonomie simulation model was only calibrated and verified using a subset of EV fleets and may not be representative for other EV vehicles, even those that share the same vehicle type and powertrain design, due to differences over time in computer control strategy software algorithms used in power management. The underlying Autonomie model needs to be calibrated with more EV models available on the market to ensure that the energy model is fully representative of the real-world fleet.
- **Improve the travel pattern predictions using advanced transportation models:** The travel patterns and routes generated in this study mostly rely on modeled travel trends, and the level of detail with respect to on-road operating conditions remains limited. The current travel demand model used in this analysis does not predict high-resolution microscopic-level travel behavior (driving cycles may not be representative of individual vehicle operations). More advanced modeling techniques, such as dynamic traffic assignment or even more detailed simulation models, may provide more accurate representations of on-road operating conditions.

7.3 Dissertation Implications

Given the scalability and sensitivity of developed EV modeling framework, research efforts are beneficial for addressing some of the emerging research questions:

1) **Assessing the effectiveness of EV policy at the aggregate and disaggregate levels:** The modeling framework can be applied to predict changes in energy use and cost associated with any change in vehicle use predicted by modeled analysis of transportation strategies, such as purchase rebates or other EV incentives (e.g., managed lanes access, toll discounts, or free parking). As demonstrated in this study, charging habits, on-road operating conditions, and fuel and electricity prices have significant impact on EV cost savings.
2) **Assessing the impact of infrastructure planning and design on EV utility**: Increasing the availability of home charging and improving the network of charging stations will change EV adoption and use patterns. As demonstrated in Chapter 6, vehicle charging demand varies by time, operating conditions, and ambient environment. Factoring those attributes into infrastructure planning and design will assist in the proper evaluation of infrastructure-side planning efforts.
3) **Assessing the benefits of potential technology application on electric vehicles**: Implementing eco-driving and eco-routing strategies, adopting autonomous systems, and improving drivetrain management (e.g., integration of GPS and driving cycle prediction) can reduce fuel use and operating costs. Given that the EV model can predict energy use for second-by-second vehicle trajectories, the microscopic-level simulation can help policy makers understand the potential benefits of vehicle technology improvements.
4) **Improving criteria pollutant (NOx, VOC, PM, etc.) modeling**: The numbers of engine starts, engine soak time distributions, and potential brake wear during regenerative braking can

be integrated into the modeling system using the same approaches implemented in this research. In its VSP modeling approach, MOVES tool already predicts energy use first and emissions as a function of energy used. The modeling framework can be readily expanded to develop criteria pollutant emissions to accompany the energy use rates developed in this research. Emissions are likely to be a further function of on-road operating conditions, engine/motor related attributes, onboard emissions control systems, etc. Integration of criteria pollutant emissions for these EVs is a promising future research topic, which also linked to air quality, health impact assessment, and climate-related analysis.

APPENDIX A. ESTIMATED ENERGY MODELS FROM BAYESIAN NETWORK APPROACH

1. 100-mile BEV

$$C_1 = 0, C_2 = \begin{cases} 1\ (vsp \geq 0) \\ 0\ (vsp < 0) \end{cases}$$

$$E_{elec} = \begin{cases} 1.95 * vsp + 929.03\ (vsp \geq 0) \\ 1.32 * vsp + 764.41\ (vsp < 0) \end{cases}$$

2. 300-mile BEV

$$C_1 = 0, C_2 = \begin{cases} 1\ (vsp \geq 0) \\ 0\ (vsp < 0) \end{cases}$$

$$E_{elec} = \begin{cases} 2.65 * vsp + 688.61\ (vsp \geq 0) \\ 1.78 * vsp + 624.28\ (vsp < 0) \end{cases}$$

3. FCEV

$$C_1 = 1, C_2 = \begin{cases} 1\ (vsp \geq 0) \\ 0\ (vsp < 0) \end{cases}$$

$$E_{fuel} = \begin{cases} -1.29 * 10^5 * SOC + 4.03 * vsp + 97{,}903.30\ (vsp \geq 0) \\ 3892.00\ (vsp < 0) \end{cases}$$

$$E_{elec} = \begin{cases} 1.07 * 10^4 * SOC + 1.48 * vsp - 0.376 * E_{fuel} - 4848.27\ (vsp \geq 0) \\ 3.81 * 10^3 * SOC + 0.797 * vsp - 0.302 * E_{fuel} - 3029.3\ (vsp < 0) \end{cases}$$

4. Parallel HEV

$$p(C_1 = 1) = \frac{1}{1 + exp\ (-u)}$$

$$u = -2.67 * (SOC \geq 0.5) + 1.55 * (0.45 \leq SOC < 0.5) +$$

$$1.82 * (SOC < 0.45) + 9.46 * 10^{-5} * vsp + 0.691$$

$$p(C_2' = 1) = \begin{cases} 0.699 * (SOC < 0.45) * (Speed < 3.7) * (vsp < 0) \\ 0.371 * (SOC < 0.45) * (Speed < 3.7) * (vsp \geq 0) \\ 0.097 * (SOC < 0.45) * (Speed \geq 3.7) * (vsp < 230) \\ 0.018 * (SOC < 0.45) * (Speed \geq 3.7) * (vsp \geq 230) \\ 0.925 * (SOC \geq 0.45) * (Speed < 3.7) * (vsp < -100) \\ 0.038 * (SOC \geq 0.45) * (Speed \geq 3.7) * (vsp < -100) \\ 0.668 * (SOC \geq 0.45) * (vsp \geq -100) * (vsp < 0) \\ 0.992 * (SOC < 0.45) * (vsp \geq 0) \end{cases}$$

$$C_2" = \begin{cases} 1 \ (vsp \geq 0) \\ 0 \ (vsp < 0) \end{cases}$$

$$E_{fuel} = \begin{cases} 0 \quad (C_1 = 0) \\ -4.21 * 10^4 * SOC + 3.97 * vsp + 25795.59 \quad (C_1 = 1, C_2' = 1) \\ 805.21 * (vsp < 0) + \\ (-2.79 * 10^5 * SOC + 4.36 * vsp + 140{,}439.00) * (vsp \geq 0) \quad (C_1 = 1, C_2' = 0) \end{cases}$$

$$E_{elec} = \begin{cases} 1.27 * vsp + 550.86 \quad (C_1 = 0, C_2" = 0) \\ 1.96 * vsp + 570.97 \quad (C_1 = 0, C_2" = 1) \\ (2.97 * 10^4 * SOC + 0.234 * vsp - 12{,}204.64) * (SOC \geq 0.45) + \\ (0.224 * vsp + 484.24) * (SOC < 0.45) \quad (C_1 = 1, C_2' = 1) \\ (2.32 * 10^3 * SOC + 1.33 * vsp - 385.5) * (vsp < 0) + \\ (8.56 * 10^4 * SOC - 38{,}795.65) * (vsp \geq 0) \quad (C_1 = 1, C_2' = 0) \end{cases}$$

5. Series PHEV

$$p(C_1 = 1) = \frac{1}{1 + exp\ (-u)}$$

$$u = -3.06 * (SOC \geq 0.3) + 8.08 * 10^{-2} * Speed + 3.76 * 10^{-5} * \max\{vsp_t, vsp_{t-1}, vsp_{t-2}\}$$

$$+ 1.66 * 10^{-5} * \min\{vsp_t, vsp_{t-1}, vsp_{t-2}\} - 2.27$$

Where t is the current time step in second.

$$p(C_2' = 1) = \frac{1}{1 + \exp(-v)}$$

$$v = -2.41 * 10^{-4} * vsp + 0.0458$$

$$C_2" = \begin{cases} 1 \ (vsp \geq 0) \\ 0 \ (vsp < 0) \end{cases}$$

$$E_{fuel} = \begin{cases} 0 \ \ (C_1 = 0) \\ -2.75 * 10^5 * (SOC \geq 0.36) - 9.09 * 10^5 * SOC * (SOC < 0.36) + \\ 4.75 * vsp + 288{,}932.84 \ \ (C_1 = 1, C_2' = 1) \\ -1.18 * 10^6 * SOC * (SOC < 0.3) - 3.55 * 10^5 * (SOC > 0.3) + \\ 3.91 * vsp + 385{,}522.62 \ \ (C_1 = 1, C_2' = 0) \end{cases}$$

E_{elec}

$$= \begin{cases} 1.56 * vsp + 538.26 \ \ (C_1 = 0, C_2" = 0) \\ 2.28 * vsp + 476.19 \ \ (C_1 = 0, C_2" = 1) \\ 7.80 * 10^4 * (SOC \geq 0.36) + 2.58 * 10^5 * SOC * (SOC < 0.36) + 0.139 * vsp - 78{,}908.85 \\ (C_1 = 1, C_2' = 1) \\ 2.25 * 10^5 * SOC * (SOC < 0.3) + 6.75 * 10^4 * (SOC > 0.3) - \\ 1.79 * vsp - 75{,}129.88 \ \ (C_1 = 1, C_2' = 0) \end{cases}$$

6. Power-split PHEV

$$p(C_1 = 1) = \frac{1}{1 + exp\ (-u)}$$

$$u = -2.68 * (SOC \geq 0.3) + 4.24 * 10^{-2} * Speed + 9.16 * 10^{-5} * \max\{vsp_t, vsp_{t-1}, vsp_{t-2}\}$$

$$+ 1.65 * 10^{-5} * \min\{vsp_t, vsp_{t-1}, vsp_{t-2}\} - 1.94$$

Where t is the current time step in second.

$$p(C_2' = 1) = \frac{1}{1 + \exp(-v)}$$

$$v = -0.117 * Speed - 2.81 * 10^{-4} * vsp + 0.0420$$

$$C_2" = \begin{cases} 1\ (vsp \geq 0) \\ 0\ (vsp < 0) \end{cases}$$

$$E_{fuel} = \begin{cases} 0 \ \ (C_1 = 0) \\ -3.39 * 10^5 * (SOC \geq 0.36) - 1.17 * 10^6 * SOC * (SOC < 0.36) + \\ 3.36 * vsp + 363{,}839.00\ (C_1 = 1, C_2' = 1) \\ -2.03 * 10^5 * SOC * (SOC < 0.3) - 2.77 * 10^5 * SOC * (0.3 \leq SOC < 0.36) \\ -7.17 * 10^4 * (SOC \geq 0.36) + \\ 4.15 * vsp + 87{,}600.85 \ \ (C_1 = 1, C_2' = 0) \end{cases}$$

E_{elec}

$$= \begin{cases} 1.33 * vsp + 346.42 \quad (C_1 = 0, C_2" = 0) \\ 2.45 * vsp + 144.39 \quad (C_1 = 0, C_2" = 1) \\ 1.70 * 10^5 * (SOC \geq 0.36) + 5.79 * 10^5 * SOC * (SOC < 0.36) + 0.558 * vsp - 173{,}651.62 \\ (C_1 = 1, C_2' = 1) \\ 3.48 * 10^2 * Speed - 6.92 * 10^4 * SOC * (SOC < 0.3) - 3.37 * 10^4 * SOC * (0.3 \leq SOC < 0.36) - \\ 1.47 * 10^4 * (SOC \geq 0.36) - 0.351 * vsp + 3{,}199.50 \quad (C_1 = 1, C_2' = 0) \end{cases}$$

7. Power-split HEV

$$p(C_1 = 1) = \frac{1}{1 + exp\ (-u)}$$

$$u = -1.778 * (\text{SOC} \geq 0.5) - 0.031 * Speed + 4.22 * 10^{-4} * vsp - 0.225$$

$$p(C_2' = 1) = \frac{1}{1 + \exp(-v)}$$

$$v = -0.136 * Speed - 3.11 * 10^{-4} * vsp + 0.325$$

$$C_2" = \begin{cases} 1\ (vsp \geq 0) \\ 0\ (vsp < 0) \end{cases}$$

$$E_{fuel} = \begin{cases} 0 \quad (C_1 = 0) \\ -4.73 * 10^4 * (SOC \geq 0.5) - 9.01 * 10^4 * SOC * (SOC < 0.5) + \\ 4.31 * vsp + 50467.53\ (C_1 = 1, C_2' = 1) \\ -7.19 * 10^4 * SOC * (SOC < 0.4) - 7.64 * 10^4 * SOC * (0.4 \leq SOC < 0.6) \\ -4.38 * 10^4 * (SOC \geq 0.6) + \\ 4.00 * vsp + 48986.67 \ \ (C_1 = 1, C_2' = 0) \end{cases}$$

E_{elec}

$$= \begin{cases} -1.035 * 10^4 * (\text{SOC} \geq 0.5) - 1.851 * 10^4 * SOC * (SOC < 0.5) \\ + 1.28 * vsp + 11660.53\ (C_1 = 0, C_2" = 0) \\ 2.55 * vsp + 609.69 \quad (C_1 = 0, C_2" = 1) \\ 3.06 * 10^4 * SOC * (SOC < 0.4) - 2.93 * 10^4 * SOC * (0.4 \leq SOC < 0.6) \\ +1.78 * 10^4 * (SOC \geq 0.6) + 1062.09 * Acc - 173{,}651.62 \\ (C_1 = 1, C_2' = 1) \\ 1.05 * 10^2 * Speed + 2.28 * 10^4 * SOC * (SOC < 0.4) + 2.48 * 10^4 * SOC * (0.4 \leq SOC < 0.6) \\ +1.56 * 10^4 * (SOC \geq 0.6) - 14753.88 \quad (C_1 = 1, C_2' = 0) \end{cases}$$

APPENDIX B. LIST OF AUTONOMIE SIMULATED ATTRIBUTES

Generic Attributes	Explanation
time(s)	Time series in seconds
SOC	State of charge between 0 and 1
Speed(m/s)	Vehicle speed in m/s
Speed(mph)	Vehicle speed in mph
Acceleration(mph/s)	Vehicle acceleration in mph/s
tracpower(watt)	Vehicle tractive power
VSP	Vehicle specific power = tractive power / vehicle weight in metric tons
cum_elec(J)	Cumulative electricity consumption in Joule
elec_energy(J)	Instantaneous electricity consumption
road_grade(rad)	Road grade
torque_demand(Nm)	Torque demand at the wheel
ess_current	Battery open circuit current in amp
ess_volt	Battery open circuit volt
mot_command	Motor on/off indicator
mot_torque(Nm)	Motor torque output in Nm
mot_speed(rad/s)	Motor rotation speed in rad/s
veh_weight	Vehicle weight in kg
battery_size(Ah)	Battery size in Ah
SOC_max	Maximum SOC

SOC_min	Minimum SOC
auxilliary_power(watt)	Vehicle auxiliary power in Watt

HEV specific	Explanation
fuelrate(kg/s)	gasoline consumption rate
eng_on	Engine on and off status
engine_speed(rad/s)	Engine speed
engine_torque(Nm)	Engine torque
mot2_command	Motor2 on/off indicator
mot2_torque(Nm)	Motor2 torque output in Nm
mot2_speed(rad/s)	Motor2 rotation speed in rad/s

Fuel cell specific	Explanation
fuelrate(kg/s)	Hydrogen consumption rate
fc_command_pwr(watt)	Fuel cell power output required by control system
fc_on	Fuel cell on and off status
fc_temp_coeff	Normalized fuel cell temperature. High temperature is the ideal condition for fuel cell
SOC_target	Target SOC level of control system

REFERENCES

A. Rousseau, 2015. Plug & Play Architecture for System Simulation, in: SIA System Modeling Conference, Paris.

Aasness, M.A., Odeck, J., 2015. The Increase of Electric Vehicle Usage in Norway—Incentives and Adverse Effects. Eur. Transp. Res. Rev. 7, 34. https://doi.org/10.1007/s12544-015-0182-4

Agrawal, S., Zheng, H., Peeta, S., Kumar, A., 2016. Routing Aspects of Electric Vehicle Drivers and Their Effects on Network Performance. Transp. Res. Part D Transp. Environ. 46, 246–266. https://doi.org/10.1016/j.trd.2016.04.002

Alam, A., Ghafghazi, G., Hatzopoulou, M., 2014. Traffic Emissions and Air Quality near Roads in Dense Urban Neighborhood. Transp. Res. Rec. J. Transp. Res. Board 2427, 83–92. https://doi.org/10.3141/2427-09

Argonne National Laboratory., 2014. Autonomie [WWW Document]. URL https://www.autonomie.net/

Asamer, J., Graser, A., Heilmann, B., Ruthmair, M., 2016. Sensitivity analysis for energy demand estimation of electric vehicles. Transp. Res. Part D Transp. Environ. https://doi.org/10.1016/j.trd.2016.03.017

Asher, Z.D., Wifvat, V., Navarro, A., Samuelsen, S., Bradley, T., 2017. The Importance of HEV Fuel Economy and Two Research Gaps Preventing Real World Implementation of Optimal Energy Management. https://doi.org/10.4271/2017-26-0106

Atlanta Regional Commission, 2016a. Activity-Based Model Calibration Report. Atlanta, GA.

Atlanta Regional Commission, 2016b. Activity-Based Model User Guide: Coordinated Travel –

Regional Activity-Based Modeling Platform (CT-RAMP) for Atlanta Regional Commission. Atlanta, GA.

Atlanta Regional Commission, 2012. Activity-Based Travel Model Specifications: Coordinated Travel – Regional Activity Based Modeling Platform (CT-RAMP) for the Atlanta Region [WWW Document]. URL https://atlantaregional.org/transportation-mobility/modeling/modeling/

Atlanta Regional Commission, 2011. Regional Travel Survey - Final Report. Atlanta, GA.

Auld, J., Islam, E., Stephens, T., Driscoll, S., Javanmardi, M., 2018. Modeling the Transportation Energy Impact of Future Population Scenarios for the Detroit Region Using POLARIS and Autonomie, in: Modeling the Transportation Energy Impact of Future Population Scenarios for the Detroit Region Using POLARIS and Autonomie. Transportation Research Board 97th Annual Meeting. Washington DC, United States.

Aziz, H.M.A., Ukkusuri, S. V., 2018. A Novel Approach to Estimate Emissions from Large Transportation Networks: Hierarchical Clustering-based Link-driving-schedules for EPA-MOVES Using Dynamic Time Warping Measures. Int. J. Sustain. Transp. 12, 192–204. https://doi.org/10.1080/15568318.2017.1346732

Bachman, W., Sarasua, W., Hallmark, S., Guensler, R., 2000. Modeling Regional Mobile Source Emissions in a Geographic Information System Framework. Transp. Res. Part C Emerg. Technol. 8, 205–229. https://doi.org/10.1016/S0968-090X(00)00005-X

Barth, M., An, F., Norbeck, J., Ross, M., 1996. Modal Emissions Modeling: A Physical Approach. Transp. Res. Rec. J. Transp. Res. Board 1520, 81–88. https://doi.org/10.1177/0361198196152000110

Blitzstein, J.K., 2014. Introduction to Probability. Chapman and Hall/CRC.

https://doi.org/10.1201/b17221

Bonges, H.A., Lusk, A.C., 2016. Addressing Electric Vehicle (EV) Sales and Range Anxiety through Parking Layout, Policy and Regulation. Transp. Res. Part A Policy Pract. 83, 63–73. https://doi.org/10.1016/j.tra.2015.09.011

Brooker, A., Gonder, J., Wang, L., Wood, E., Lopp, S., Ramroth, L., 2015. FASTSim: A Model to Estimate Vehicle Efficiency, Cost and Performance, in: FASTSim: A Model to Estimate Vehicle Efficiency, Cost and Performance. https://doi.org/10.4271/2015-01-0973

California Air Resources Board, 2018. EMFAC2017 Volume III - Technical Documentation. Sacramento, CA.

Chen, T., 2014. Introduction to Boosted Trees.

Chen, T.D., Kockelman, K.M., Hanna, J.P., 2016. Operations of a shared, autonomous, electric vehicle fleet: Implications of vehicle & charging infrastructure decisions. Transp. Res. Part A Policy Pract. 94, 243–254. https://doi.org/10.1016/j.tra.2016.08.020

Ciuffo, B., Casas, J., Montanino, M., Perarnau, J., Punzo, V., 2013. Gaussian Process Metamodels for Sensitivity Analysis of Traffic Simulation Models. Transp. Res. Rec. J. Transp. Res. Board 2390, 87–98. https://doi.org/10.3141/2390-10

Ciuffo, B., Lima Azevedo, C., 2014. A Sensitivity-Analysis-Based Approach for the Calibration of Traffic Simulation Models. IEEE Trans. Intell. Transp. Syst. 15, 1298–1309. https://doi.org/10.1109/TITS.2014.2302674

Coffman, M., Bernstein, P., Wee, S., 2017. Electric Vehicles Revisited: A Review of Factors that Affect Adoption. Transp. Rev. 37, 79–93. https://doi.org/10.1080/01441647.2016.1217282

Daina, N., Sivakumar, A., Polak, J.W., 2017. Modelling Electric Vehicles Use: A Survey on the Methods. Renew. Sustain. Energy Rev. 68, 447–460.

https://doi.org/10.1016/j.rser.2016.10.005

Davis, S.C., Boundy, R.G., 2019. Transportation Energy Data Book: Edition 37. Oak Ridge, TN (United States). https://doi.org/10.2172/1410917

District Department of Transportation, 2012. Greenhouse Gas Emissions Inventory, Baseline Year 2009 Forecast Year 2040. Washington, D.C.

Doucette, R.T., McCulloch, M.D., 2011. Modeling the prospects of plug-in hybrid electric vehicles to reduce CO2 emissions. Appl. Energy 88, 2315–2323. https://doi.org/10.1016/j.apenergy.2011.01.045

Ehsani, M., Gao, Y., Longo, S., Ebrahimi, K., 2018. Modern Electric, Hybrid Electric, and Fuel Cell Vehicles. CRC press.

Elgowainy, A., Han, J., Poch, L., Wang, M., Vyas, A., Mahalik, M., Rousseau, A., 2010. Well-to-Wheels Analysis of Energy Use and Greenhouse Gas Emissions of Plug-In Hybrid Electric Vehicles.

Elgowainy, A., Rousseau, A., Wang, M., Ruth, M., Andress, D., Ward, J., Joseck, F., Nguyen, T., Das, S., 2013. Cost of Ownership and Well-to-wheels Carbon Emissions/oil use of Alternative Fuels and Advanced Light-duty Vehicle Technologies. Energy Sustain. Dev. 17, 626–641. https://doi.org/10.1016/j.esd.2013.09.001

Emadi, A., Young Joo Lee, Rajashekara, K., 2008. Power Electronics and Motor Drives in Electric, Hybrid Electric, and Plug-In Hybrid Electric Vehicles. IEEE Trans. Ind. Electron. 55, 2237–2245. https://doi.org/10.1109/TIE.2008.922768

Fayazbakhsh, M.A., Bahrami, M., 2013. Comprehensive Modeling of Vehicle Air Conditioning Loads Using Heat Balance Method. https://doi.org/10.4271/2013-01-1507

Fincher, S., Palacios, C., Kishan, S., Preusse, D., Perez, H., 2010. Modifying Link-level Emissions

Modeling Procedures for Applications within the MOVES Framework.

Frey, H., Rouphail, N.M., Zhai, H., 2006. Speed- And Facility-specific Emission Estimates for On-road Light-duty Vehicles on the Basis of Real-world Speed Profiles. Transp. Res. Rec. 6, 128–137. https://doi.org/10.3141/1987-14

Frey, H., Unal, A., Chen, J., Li, S., Xuan, C., 2002. Methodology for Developing Modal Emission Rates for EPA's Multi-scale Motor Vehicle & Equipment Emission System. North Carolina State Univ. US EPA, Ann Arbor, MI 18–20.

Frey, H.C., 2018. Trends in onroad transportation energy and emissions. J. Air Waste Manage. Assoc. 68, 514–563. https://doi.org/10.1080/10962247.2018.1454357

Georgia Power, 2019. Price & Rates Plans - Plug-In Electric Vehicle [WWW Document]. URL https://www.georgiapower.com/residential/billing-and-rate-plans/pricing-and-rate-plans/plug-in-ev.html (accessed 7.17.19).

Gonder, J., Markel, T., Thornton, M., Simpson, A., 2007. Using Global Positioning System Travel Data to Assess Real-World Energy Use of Plug-In Hybrid Electric Vehicles. Transp. Res. Rec. J. Transp. Res. Board 2017, 26–32. https://doi.org/10.3141/2017-04

Google, 2019. Directions API Developers Guide [WWW Document]. URL https://developers.google.com/maps/documentation/directions/intro (accessed 7.29.19).

Guensler, R., Liu, H., Xu, X., Lu, H., Rodgers, M.O., 2018. MOVES-Matrix for High-Performance Emission Rate Model Applications.

Guensler, R., Yoon, S., Feng, C., Li, H., Jun, J., 2005. Heavy-duty Diesel Vehicle Modal Emissions Model (HDDV-MEM): Volume I: Modal Emission Modeling Framework. EPA/600/R-05/090a. Research Triangle Park, NC.

Hardman, S., Jenn, A., Tal, G., Axsen, J., Beard, G., Daina, N., Figenbaum, E., Jakobsson, N.,

Jochem, P., Kinnear, N., Plötz, P., Pontes, J., Refa, N., Sprei, F., Turrentine, T., Witkamp, B., 2018. A Review of Consumer Preferences of and Interactions with Electric Vehicle Charging Infrastructure. Transp. Res. Part D Transp. Environ. 62, 508–523. https://doi.org/10.1016/j.trd.2018.04.002

Hardman, S., Tal, G., 2018. Who are the Early Adopters of Fuel Cell Vehicles? Int. J. Hydrogen Energy 43, 17857–17866. https://doi.org/10.1016/j.ijhydene.2018.08.006

Hastie, T., Tibshirani, R., Friedman, J., 2009. The Elements of Statistical Learning, Springer Series in Statistics. Springer New York, New York, NY. https://doi.org/10.1007/978-0-387-84858-7

He, Y., Rios, J., Chowdhury, M., Pisu, P., Bhavsar, P., 2012. Forward Power-train Energy Management Modeling for Assessing Benefits of Integrating Predictive Traffic Data into Plug-in-hybrid Electric Vehicles. Transp. Res. Part D Transp. Environ. 17, 201–207. https://doi.org/10.1016/j.trd.2011.11.001

Herman, J., Usher, W., 2017. SALib: An open-source Python library for Sensitivity Analysis. J. Open Source Softw. 2, 97. https://doi.org/10.21105/joss.00097

Hermawan, K., Regan, A.C., 2017. On-Demand, App-Based Ride Services: A Study of Emerging Ground Transportation Modes Serving Los Angeles International Airport (LAX). J. Transp. Res. Forum 56, 111–128.

Holdstock, T., Sorniotti, A., Everitt, M., Fracchia, M., Bologna, S., Bertolotto, S., 2012. Energy Consumption Analysis of a Novel Four-speed Dual Motor Drivetrain for Electric Vehicles. 2012 IEEE Veh. Power Propuls. Conf. 295–300. https://doi.org/10.1109/VPPC.2012.6422721

Hu, X., Chang, S., Li, J., Qin, Y., 2010. Energy for sustainable road transportation in China:

Challenges, initiatives and policy implications. Energy. https://doi.org/10.1016/j.energy.2009.05.024

Hu, X., Moura, S.J., Murgovski, N., Egardt, B., Cao, D., 2016. Integrated Optimization of Battery Sizing, Charging, and Power Management in Plug-In Hybrid Electric Vehicles. IEEE Trans. Control Syst. Technol. 24, 1036–1043. https://doi.org/10.1109/TCST.2015.2476799

IEEE-USA, B. of D., 2007. Position Statement: Plug-in Electric Hybrid Vehicles [WWW Document]. URL https://www.engr.uvic.ca/~mech459/Pub_References/PHEV0607.pdf

International Energy Agency, 2018. Global ev outlook 2018.

Iooss, B., Lemaître, P., 2015. A Review on Global Sensitivity Analysis Methods. pp. 101–122. https://doi.org/10.1007/978-1-4899-7547-8_5

IPCC, 2014. Climate Change 2014: Synthesis Report. Geneva, Switzerland.

Jeong, J., Kim, N., Stutenberg, K., Rousseau, A., 2019. Analysis and Model Validation of the Toyota Prius Prime. https://doi.org/10.4271/2019-01-0369

Jimenez-Palacios, J.L., 1999. Understanding and Quantifying Motor Vehicle Emissions with Vehicle Specific Power and TILDAS Remote Sensing. Massachusetts Institute of Technology.

Jun, J., Guensler, R., Ogle, J.H., 2006. Smoothing Methods to Minimize Impact of Global Positioning System Random Error on Travel Distance, Speed, and Acceleration Profile Estimates. Transp. Res. Rec. J. Transp. Res. Board 1972, 141–150. https://doi.org/10.1177/0361198106197200117

Kambly, K.R., Bradley, T.H., 2014. Estimating the HVAC Energy Consumption of Plug-in Electric Vehicles. J. Power Sources 259, 117–124. https://doi.org/10.1016/j.jpowsour.2014.02.033

Karabasoglu, O., Michalek, J., 2013. Influence of Driving Patterns on Life Cycle Cost and Emissions of Hybrid and Plug-in Electric Vehicle Powertrains. Energy Policy 60, 445–461. https://doi.org/10.1016/j.enpol.2013.03.047

Kelly, J.C., Elgowainy, A., 2018. Updating Transmission and Distribution Losses in the GREET Model.

Kelly, J.C., MacDonald, J.S., Keoleian, G.A., 2012. Time-dependent Plug-in Hybrid Electric Vehicle Charging Based on National Driving Patterns and Demographics. Appl. Energy 94, 395–405. https://doi.org/10.1016/j.apenergy.2012.02.001

Khan, M., Kockelman, K.M., 2012. Predicting the Market Potential of Plug-in Electric Vehicles Using Multiday GPS Data. Energy Policy 46, 225–233. https://doi.org/10.1016/j.enpol.2012.03.055

Kim, N., Rousseau, A., Lohse-Busch, H., 2014. Advanced Automatic Transmission Model Validation Using Dynamometer Test Data. https://doi.org/10.4271/2014-01-1778

Kioutsioukis, I., Tarantola, S., Saltelli, A., Gatelli, D., 2004. Uncertainty and global sensitivity analysis of road transport emission estimates. Atmos. Environ. 38, 6609–6620. https://doi.org/10.1016/j.atmosenv.2004.08.006

Kromer, M.A., 2007. Electric powertrains: opportunities and challenges in the US light-duty vehicle fleet. Massachusetts Institute of Technology.

Kvam, P.H., Vidakovic, B., 2007. Nonparametric Statistics with Applications to Science and Engineering, Wiley Series in Probability and Statistics. John Wiley & Sons, Inc., Hoboken, NJ, USA. https://doi.org/10.1002/9780470168707

Lee, T.-K., Adornato, B., Filipi, Z.S., 2011. Synthesis of Real-World Driving Cycles and Their Use for Estimating PHEV Energy Consumption and Charging Opportunities: Case Study for

Midwest/U.S. IEEE Trans. Veh. Technol. 60, 4153–4163. https://doi.org/10.1109/TVT.2011.2168251

Li, J.-M., Lin, Z., LaClair, T., Davidson, D., Xu, A., Guensler, R., Rodgers, M.O., Lee, D.-Y., 2014. Evaluation of GHG emission across transit bus technologies with real-world driving schedules, in: 93rd Annual Meeting of the Transportation Research Board.

Liu, C., Lin, Z., 2017. How Uncertain is the Future of Electric Vehicle Market: Results from Monte Carlo Simulations Using a Nested Logit Model. Int. J. Sustain. Transp. 11, 237–247. https://doi.org/10.1080/15568318.2016.1248583

Liu, H., Guensler, R., Lu, H., Xu, Y., Xu, X., Rodgers, M.O., 2019. MOVES-Matrix for High-Performance On-Road Energy and Running Emission Rate Modeling Applications. J. Air Waste Manage. Assoc. 10962247.2019.1640806. https://doi.org/10.1080/10962247.2019.1640806

Liu, H., Li, H., Rodgers, M.O., Guensler, R., 2018. Development of Road Grade Data Using the United States Geological Survey Digital Elevation Model. Transp. Res. Part C Emerg. Technol. 92, 243–257. https://doi.org/10.1016/j.trc.2018.05.004

Liu, H., Xu, X., Rodgers, M.O., Xu, Y. "Ann", Guensler, R.L., 2017. MOVES-Matrix and Distributed Computing for Microscale Line Source Dispersion Analysis. J. Air Waste Manag. Assoc. 67. https://doi.org/10.1080/10962247.2017.1287788

Liu, K., Yamamoto, T., Morikawa, T., 2017. Impact of Road Gradient on Energy Consumption of Electric Vehicles. Transp. Res. Part D Transp. Environ. 54, 74–81. https://doi.org/10.1016/j.trd.2017.05.005

Lorf, C., Martínez-Botas, R.F., Howey, D.A., Lytton, L., Cussons, B., 2013. Comparative Analysis of the Energy Consumption and CO2 Emissions of 40 Electric, Plug-in Hybrid Electric,

Hybrid Electric and Internal Combustion Engine Vehicles. Transp. Res. Part D Transp. Environ. 23, 12–19. https://doi.org/10.1016/j.trd.2013.03.004

Lv, J., Zhang, Y., 2012. Effect of Signal Coordination on Traffic Emission. Transp. Res. Part D Transp. Environ. 17, 149–153. https://doi.org/10.1016/j.trd.2011.10.005

M. Sabri, M.F., Danapalasingam, K.A., Rahmat, M.F., 2016. A Review on Hybrid Electric Vehicles Architecture and Energy Management Strategies. Renew. Sustain. Energy Rev. 53, 1433–1442. https://doi.org/10.1016/j.rser.2015.09.036

Mi, C., Masrur, M.A., Gao, D.W., 2011. Hybrid Electric Vehicles. John Wiley & Sons, Ltd, Chichester, UK. https://doi.org/10.1002/9781119998914

Mohd Zulkefli, M.A., Zheng, J., Sun, Z., Liu, H.X., 2014. Hybrid Powertrain Optimization with Trajectory Prediction Based on Inter-vehicle-communication and Vehicle-infrastructure-integration. Transp. Res. Part C Emerg. Technol. 45, 41–63. https://doi.org/10.1016/j.trc.2014.04.011

National Renewable Energy Laboratory, 2016. Consumer Views on Plug-in Electric Vehicles – National Benchmark Report (Second Edition).

National Research Council, 2011. Assessment of fuel economy technologies for light-duty vehicles.

Needell, Z.A., McNerney, J., Chang, M.T., Trancik, J.E., 2016. Potential for Widespread Electrification of Personal Vehicle Travel in the United States. Nat. Energy 1, 16112.

Neubauer, J., Wood, E., 2014. Thru-life Impacts of Driver Aggression, Climate, Cabin Thermal Management, and Battery Thermal Management on Battery Electric Vehicle Utility. J. Power Sources 259, 262–275. https://doi.org/10.1016/j.jpowsour.2014.02.083

Nicholas, Michael A., Gil Tal, T.S.T., 2016. Advanced Plug-in Electric Vehicle Travel and

Charging Behavior Interim Report.

Pearre, N.S., Kempton, W., Guensler, R.L., Elango, V. V., 2011. Electric Vehicles: How Much Range is Required for a Day's Driving? Transp. Res. Part C Emerg. Technol. 19, 1171–1184. https://doi.org/10.1016/j.trc.2010.12.010

Propfe, B., Redelbach, M., Santini, D., Friedrich, H., 2012. Cost Analysis of Plug-in Hybrid Electric Vehicles including Maintenance & Repair Costs and Resale Values. World Electr. Veh. J. 5, 886–895. https://doi.org/10.3390/wevj5040886

Qi, X., Wu, G., Boriboonsomsin, K., Barth, M.J., 2018. Data-driven Decomposition Analysis and Estimation of Link-level Electric Vehicle Energy Consumption under Real-world Traffic Conditions. Transp. Res. Part D Transp. Environ. 64, 36–52. https://doi.org/10.1016/j.trd.2017.08.008

Qi, Z., 2014. Advances on Air Conditioning and Heat Pump System in Electric Vehicles – A Review. Renew. Sustain. Energy Rev. 38, 754–764. https://doi.org/10.1016/j.rser.2014.07.038

Quaglietta, E., Punzo, V., 2013. Supporting the design of railway systems by means of a Sobol variance-based sensitivity analysis. Transp. Res. Part C Emerg. Technol. 34, 38–54. https://doi.org/10.1016/j.trc.2013.05.007

Rodier, C., 2017. Simulation of Ridesourcing Using Agent-Based Demand and Supply Regional Models: Potential Market Demand for First-Mile Transit Travel and Reduction in Vehicle Miles Traveled in the San Francisco Bay Area A Research Report from the National Center for Sustainable Transportation Farzad Alemi, Institute of Transportation Studies About the National Center for Sustainable Transportation Disclaimer.

Roger P. Roess, Prassas, E.S., McShane, W.R., 2011. Traffic Engineering, 4th Edition.

Rogers, E.M., 1995. Diffusion of innovations. Simon and Schuster.

Rousseau, A., 2015. Plug&Play Architecture for System Simulation, SIA System Modeling Conference. Paris, France.

S. Fincher, and A.S.P.C.D.K.D.B.R.M.C.S.I.C.J.K., 2015. Input Guidelines for Motor Vehicle Emissions Simulator Model, Volume 1: Practitioners' Handbook: Regional Level Inputs. Transportation Research Board, Washington, D.C. https://doi.org/10.17226/22214

Saleem, M., Västberg, O.B., Karlström, A., 2018. An Activity Based Demand Model for Large Scale Simulations. Procedia Comput. Sci. 130, 920–925. https://doi.org/10.1016/j.procs.2018.04.090

Salmasi, F.R., 2007. Control Strategies for Hybrid Electric Vehicles: Evolution, Classification, Comparison, and Future Trends. IEEE Trans. Veh. Technol. 56, 2393–2404. https://doi.org/10.1109/TVT.2007.899933

Saltelli, A., 2002. Making best use of model evaluations to compute sensitivity indices. Comput. Phys. Commun. 145, 280–297. https://doi.org/10.1016/S0010-4655(02)00280-1

Saltelli, A., Ratto, M., Andres, T., Campolongo, F., Cariboni, J., Gatelli, D., Saisana, M., Tarantola, S., 2007. Global Sensitivity Analysis. The Primer. John Wiley & Sons, Ltd, Chichester, UK. https://doi.org/10.1002/9780470725184

Saltelli, A., Tarantola, S., Campolongo, F., Ratto, M., 2002. Sensitivity Analysis in Practice. John Wiley & Sons, Ltd, Chichester, UK. https://doi.org/10.1002/0470870958

Serov, A., Zenyuk, I. V., Arges, C.G., Chatenet, M., 2018. Hot Topics in Alkaline Exchange Membrane Fuel Cells. J. Power Sources 375, 149–157. https://doi.org/10.1016/j.jpowsour.2017.09.068

Shankar, R., Marco, J., 2013. Method for Estimating the Energy Consumption of Electric Vehicles

and Plug-in Hybrid Electric Vehicles under Real-world Driving Conditions. IET Intell. Transp. Syst. 7, 138–150. https://doi.org/10.1049/iet-its.2012.0114

Shankar, R., Marco, J., Assadian, F., 2012. The Novel Application of Optimization and Charge Blended Energy Management Control for Component Downsizing within a Plug-in Hybrid Electric Vehicle. Energies 5, 4892–4923. https://doi.org/10.3390/en5124892

Sobol, I.., 2001. Global sensitivity indices for nonlinear mathematical models and their Monte Carlo estimates. Math. Comput. Simul. 55, 271–280. https://doi.org/10.1016/S0378-4754(00)00270-6

Song, X., Xie, Z., Xu, Y., Tan, G., Tang, W., Bi, J., Li, X., 2017. Supporting real-world network-oriented mesoscopic traffic simulation on GPU. Simul. Model. Pract. Theory 74, 46–63. https://doi.org/10.1016/j.simpat.2017.02.003

Sperling, D., 2018. Three Revolutions: Steering Automated, Shared, and Electric Vehicles to a Better Future. Island Press.

Thomas, J., Huff, S., West, B., Chambon, P., 2017. Fuel Consumption Sensitivity of Conventional and Hybrid Electric Light-Duty Gasoline Vehicles to Driving Style. SAE Int. J. Fuels Lubr. 10, 2017-01–9379. https://doi.org/10.4271/2017-01-9379

Tukey, J.W., 1977. Exploratory Data Analysis, 1st Editio. ed. Addison-Wesley Publishing Company.

U.S. Climate Data, 2019. Climate Atlanta - Georgia [WWW Document]. URL https://www.usclimatedata.com/climate/atlanta/georgia/united-states/usga0028 (accessed 7.16.19).

U.S. Department of Energy, 2014. Hybrid and Plug-In Electric Vehicles All-Electric Vehicles. Clean Cities.

U.S. Department of Transportation, 2010. Transportation's Role in Reducing U.S. Greenhouse Gas Emissions.

U.S. DOE Alternative Fuels Data Center, 2019a. U.S. Plug-in Electric Vehicle Sales by Model [WWW Document]. URL https://afdc.energy.gov/data/10567 (accessed 8.9.19).

U.S. DOE Alternative Fuels Data Center, 2019b. U.S. HEV Sales by Model [WWW Document]. URL https://afdc.energy.gov/data/10301 (accessed 8.9.19).

U.S. Energy Information Administration, 2019a. Georgia State Profile and Energy Estimates [WWW Document]. URL https://www.eia.gov/state/data.php?sid=GA

U.S. Energy Information Administration, 2019b. Annual Energy Outlook 2019 with Projections to 2050.

U.S. Energy Information Administration, 2019c. Weekly Retail Gasoline and Diesel Prices [WWW Document]. URL https://www.eia.gov/dnav/pet/pet_pri_gnd_dcus_r1z_m.htm (accessed 7.17.19).

U.S. Energy Information Administration, 2017. Annual Energy Outlook 2017 with Projections to 2050.

U.S. Energy Information Administration, 2014. Annual Energy Outlook 2014 with Projections to 2040.

U.S. Environmental Protection Agency, 2018. Emissions & Generation Resource Integrated Database (eGRID).

U.S. Environmental Protection Agency, 2016. Population and Activity of On-road Vehicles in MOVES2014. Washington DC, United States.

U.S. Environmental Protection Agency, 2015a. Exhaust Emission Rates for Light-Duty On-road Vehicles in MOVES2014. Washington, DC.

U.S. Environmental Protection Agency, 2015b. MOVES2014 and MOVES2014a Technical Guidance: Using MOVES to Prepare Emission Inventories for State Implementation Plans and Transportation Conformity. Washington, DC.

U.S Environmental Protection Agency, 2016. Population and Activity of On-road Vehicles in MOVES2014. Washington, D.C.

Wang, F., Xu, Y., 2011. Estimating O–D Travel Time Matrix by Google Maps API: Implementation, Advantages, and Implications. Ann. GIS 17, 199–209. https://doi.org/10.1080/19475683.2011.625977

Wang, M., Elgowainy, A., Benavides, P.T., Burnham, A., Cai, H., Dai, Q., Hawkins, T.R., Kelly, J.C., Kwon, H., Lee, D.-Y. and others, 2018. Summary of Expansions and Updates in GREET® 2018.

Wang, S., Fan, J., Zhao, D., Yang, S., Fu, Y., 2016. Predicting consumers' intention to adopt hybrid electric vehicles: using an extended version of the theory of planned behavior model. Transportation (Amst). 43, 123–143. https://doi.org/10.1007/s11116-014-9567-9

Wang, Y., Szeto, W.Y., Han, K., Friesz, T.L., 2018. Dynamic Traffic Assignment: A Review of the Methodological Advances for Environmentally Sustainable Road Transportation Applications. Transp. Res. Part B Methodol. 111, 370–394. https://doi.org/10.1016/j.trb.2018.03.011

Washington, S., Wolf, J., Guensler, R., 1997. Binary Recursive Partitioning Method for Modeling Hot-Stabilized Emissions From Motor Vehicles. Transp. Res. Rec. J. Transp. Res. Board 1587, 96–105. https://doi.org/10.3141/1587-11

Wasserman, L., 2013. All of Statistics: a Concise Course in Statistical Inference. Springer.

Wikipedia, 2019. Hybrid Synergy Drive [WWW Document]. URL

https://en.wikipedia.org/wiki/Hybrid_Synergy_Drive (accessed 4.9.19).

Wolf, J., Guensler, R., Washington, S., Bachman, W., 1998. High-Emitting Vehicle Characterization Using Regression Tree Analysis. Transp. Res. Rec. J. Transp. Res. Board 1641, 58–65. https://doi.org/10.3141/1641-07

Wu, D., Aliprantis, D.C., 2013. Modeling light-duty plug-in electric vehicles for national energy and transportation planning. Energy Policy 63, 419–432. https://doi.org/10.1016/j.enpol.2013.07.132

Wu, X., Freese, D., Cabrera, A., Kitch, W.A., 2015. Electric Vehicles' Energy Consumption Measurement and Estimation. Transp. Res. Part D Transp. Environ. 34, 52–67. https://doi.org/10.1016/j.trd.2014.10.007

Xie, Y., Chowdhury, M., Bhavsar, P., Zhou, Y., 2012. An Integrated Modeling Approach for Facilitating Emission Estimations of Alternative Fueled Vehicles. Transp. Res. Part D Transp. Environ. 17, 15–20. https://doi.org/10.1016/j.trd.2011.08.009

Xu, X., Aziz, H.M., 2019. An Advanced Modal-Based and Scalable Approach to Estimate Energy Consumption from Electric Vehicles, in: An Advanced Modal-Based and Scalable Approach to Estimate Energy Consumption from Electric Vehicles. Transportation Research Board 98th Annual Meeting, Washington DC, United States, 01.13.2019 - 01.17.2019. Washington DC, United States.

Xu, X., Aziz, H.M.A., Guensler, R., 2019. A modal-based approach for estimating electric vehicle energy consumption in transportation networks. Transp. Res. Part D Transp. Environ. 75, 249–264. https://doi.org/10.1016/j.trd.2019.09.001

Xu, X., Liu, H., Li, H. "Ann," Rodgers, M.O., Guensler, R., 2018a. Integrating Engine Start, Soak, Evaporative, and Truck Hoteling Emissions into MOVES-Matrix. Transp. Res. Rec. J. Transp.

Res. Board 036119811879720. https://doi.org/10.1177/0361198118797208

Xu, X., Liu, H., Passmore, R., Patrick, T., Gbologah, F., Rodgers, M.O., Guensler, R., 2018b. Fuel and Emissions Calculator (FEC), Version 3.0, Summary Report.

Xu, Y., Gbologah, F.E., Lee, D.-Y., Liu, H., Rodgers, M.O., Guensler, R.L., 2015. Assessment of alternative fuel and powertrain transit bus options using real-world operations data: Life-cycle fuel and emissions modeling. Appl. Energy 154, 143–159. https://doi.org/10.1016/j.apenergy.2015.04.112

Yao, Z., Wei, H., Perugu, H., Liu, H., Li, Z., 2014. Sensitivity analysis of project level MOVES running emission rates for light and heavy duty vehicles. J. Traffic Transp. Eng. (English Ed. https://doi.org/10.1016/S2095-7564(15)30092-1

Yoon, S., Li, H., Jun, J., Guensler, R., Rodgers, M., 2005. Transit Bus Engine Power Simulation: Comparison of Speed-acceleration-road grade Matrices to Second-by-second Speed, Acceleration, and Road Grade Data, in: Transit Bus Engine Power Simulation: Comparison of Speed-Acceleration-Road Grade Matrices to Second-by-Second Speed, Acceleration, and Road Grade Data. Conference Proceedings for the 98th Air and Waste Management Association Annual Meeting. Minneapolis, MN.

Yuksel, T., Michalek, J.J., 2015. Effects of Regional Temperature on Electric Vehicle Efficiency, Range, and Emissions in the United States. Environ. Sci. Technol. 49, 3974–3980. https://doi.org/10.1021/es505621s

Zhang, L., Brown, T., Samuelsen, S., 2013. Evaluation of Charging Infrastructure Requirements and Operating Costs for Plug-in Electric Vehicles. J. Power Sources 240, 515–524. https://doi.org/10.1016/j.jpowsour.2013.04.048

Zhang, R., Yao, E., 2015. Electric Vehicles' Energy Consumption Estimation with Real Driving

Condition Data. Transp. Res. Part D Transp. Environ. 41, 177–187. https://doi.org/10.1016/j.trd.2015.10.010

Zhang, X., Mi, C., 2011. Vehicle Power Management, Power Systems. Springer London, London. https://doi.org/10.1007/978-0-85729-736-5

Zhou, X., Tanvir, S., Lei, H., Taylor, J., Liu, B., Rouphail, N.M., Christopher Frey, H., 2015. Integrating a simplified emission estimation model and mesoscopic dynamic traffic simulator to efficiently evaluate emission impacts of traffic management strategies. Transp. Res. Part D Transp. Environ. 37, 123–136. https://doi.org/10.1016/j.trd.2015.04.013